The physicochemical properties and stability of aspalathin in micro- and nanoencapsulated green rooibos extract formulations

Chantelle Human

Dissertation presented for the degree of ***Doctor of Philosophy (Food Science)***

at ***Stellenbosch University*** *Food Science, Faculty of AgriSciences*

The financial assistance of the National Research Foundation (NRF) towards this research is hereby acknowledged. Opinions expressed and conclusions arrived at, are those of the author and not necessarily to be attributed to the NRF.

Supervisor: Prof D. de Beer

Co-supervisors: Prof E. Joubert

Prof G.O. Sigge

April 2019

DECLARATION

By submitting this dissertation electronically, I declare that the entirety of the work contained therein is my own, original work, that I am the sole author thereof (save to the extent explicitly otherwise stated) that reproduction and publication thereof by Stellenbosch University will not infringe any third party rights and that I have not previously in its entirety or in part submitted it for obtaining any qualification.

This dissertation includes 1 original paper published and 1 original paper submitted to peer-reviewed publications. The development and writing of the papers were the principal responsibility of myself and, for each of the cases where this is not the case, a declaration is included in the dissertation indicating the nature and extent of the contributions of co-authors

Date: April 2019

SUMMARY

Green rooibos extracts with high aspalathin content have potential as nutraceutical food ingredients based on their properties relating to the prevention of metabolic syndrome. However, delivery of green rooibos extracts in convenient beverage products is a challenge due to poor stability of aspalathin in the presence of moisture. Thus, the development of alternative ingredients and convenience products is required.

Microencapsulation of a green rooibos extract (GRE) with maltodextrin as control carrier and inulin and chitosan as low kilojoule functional alternatives was achieved by spray-drying. Spray-dried GRE and powders containing maltodextrin or inulin had similar yields (>76%), moisture content (<3.5%) and aspalathin retention (>95%), whereas microencapsulation with chitosan resulted in lower yields (<66%), higher moisture content (>3.4%) and lower aspalathin retention (<83%). Accelerated stability tests (40 °C/75% relative humidity (RH)) revealed similar aspalathin degradation rates (based on fractional conversion model) for GRE, inulin and maltodextrin formulations, but significantly higher degradation rates for chitosan formulations. Given the low incompatibility between GRE and inulin, inulin-microencapsulated GRE (1:1 ratio; IN50) was selected as the most suitable green rooibos nutraceutical beverage ingredient. IN50 was added to iced tea powder formulations, which contained various food grade ingredients (sucrose, xylitol, citric acid and ascorbic acid). Shelf-life trials (30 °C and 40 °C/65% RH for 5–12 months) in different packaging materials (semi-permeable vs impermeable) revealed more aspalathin degradation (based on first order reaction rates), more discolouration and clumping after the addition of crystalline ingredients. These changes were more pronounced at 40 °C and for powders stored in the semi-permeable packaging. The formulation containing IN50, xylitol and citric acid, which showed the most drastic physical and chemical changes during storage, was subjected to descriptive sensory analysis, which confirmed significant changes also in its sensory profile.

Nanoencapsulation of an aspalathin-rich fraction (GRAF) prepared from green rooibos was also investigated. Combinations of natural (chitosan and lecithin) and synthetic [poly(lactide-co-glycolide) and Eudragit S100® (ES100)] polymers with suitable conventional methods and electrospraying were investigated. Overall, ES100 electrosprayed particles had the best combination of properties, i.e. encapsulation efficiency (EE, 55.4%), loading capacity (LC, 11.1%), release rate at pH 7.4 (1.67 h^{-1}) and size (190 nm). Further optimisation of the ES100-GRAF loaded nanoparticles was achieved using a central composite design. Responses included yields between 78.2–78.3%, EE between 73.9–76.4% and LC between 9.9–12.9%. Pure aspalathin was subsequently encapsulated using the optimal conditions, resulting in a similar yield, EE, LC, particle size and particle morphology to that of GRAF loaded nanoparticles. The stability of the aspalathin and GRAF loaded nanoparticles was investigated at fixed pH-time combinations. Nanoencapsulation offered a

more stable environment for aspalathin. Overall, pure aspalathin was less stable than when in GRAF. Even though intestinal permeability could theoretically be improved with nanoencapsulation, the parallel artificial membrane permeability assay and Caco-2 cell model indicated that pure aspalathin and aspalathin nanoparticles both have equally low permeability.

These methods offered an alternative for the production of GRE convenience products and ingredients, whilst providing insight on the effects of encapsulation and ingredients of powder formulations.

OPSOMMING

Groen rooibos ekstrakte met hoë aspalatien inhoud het potentiaal as nutraseutiese voedsel bestandele, gebaseer op eienskappe wat verband hou met voorkoming van die metaboliese sindroom. Die lewering van groen rooibos ekstrakte in gerieflike ys-tee vorm is egter ‘n uitdaging, as gevolg van die lae stabiliteit van aspalatien in die teenwoordigheid van vog. Dus, word die ontwikkeling van alternatiewe bestandele en gerieflikheids produkte benodig.

Mikro-enkapsulering van ‘n groen rooibos ekstrak (GRE) met maltodekstrien as kontrole polimeer en inulien en chitosan as lae kilojoule funksionele alternatiewe is behaal met sproeidroging. Gesproei-droogte GRE en poeiers wat maltodekstrien en inulien bevat het soortgelyke opbrengs (>76%), vog inhoud (<3.5%) en aspalatien retensie (>95%) gehad, terwyl mikro-enkapsulering met chitosan laer opbrengs (<66%), hoër vog inhoud (>3.4%) en laer aspalatien retensie (<83%) gehad het. Versnelde stabiliteits toetse (40 °C/75% relatiewe humiditeit (RH)) het soorgelyke aspalatien degradasie tempo’s (gebaseer op die fraksionele omskakelingsmodel) vir GRE, inulien en maltodekstrien formulasies onthul, maar betekenisvolle hoër degradasie tempo’s vir chitosan formulasies. Aangesien geen interaksies tussen GRE en inulien getoon is nie, is inulien-gemikro-enkapsuleerde GRE (1:1 verhouding, IN50) gekies as mees geskik vir ‘n gepoeierde groen rooibos nutraseutiese bestandeel. IN50 is in ys-tee poeier formulasies gevoeg wat verskeie voedselgraad bestanddele bevat het (sukrose, xylitol, sitroensuur en askorbiensuur). Rakleeftyd proewe (30 °C en 40 °C/65% RH vir 5–12 maande) in verskillende verpakkingsmateriale (semi-deurlaatbaar vs ondeurlaatbaar) het meer aspalatien afbraak (gebaseer op eerste orde reaksie tempo’s), meer verkleuring en klontvorming is onthul na byvoeging van kristallyne bestanddele. Die veranderinge was meer prominent by 40 °C en vir poeiers opgeberg in semi-deurlaatbare verpakking. Die formulasie wat IN50, xylitol en sitroensuur bevat en die mees drastiese fisiese en chemiese veranderinge getoon het tydens opberging, is onderwerp aan beskrywende sensoriese analise, wat betekenisvolle veranderinge in die sensoriese profiel bevestig het.

Nano-enkapsulering van ‘n aspalatien-ryke fraksie (GRAF) voorberei van groen rooibos is ook ondersoek. Kombinasies van natuurlike (chitosan en lesitien) en sintetiese [poli(laktied-ko-glikolied) en Eudgragit S100® (ES100)] polimere met gepaste konvensionele metodes en die elektrosproei tegniek is ondersoek. Algeheel het die ES100 ge-elektrosproeide partikels die beste kombinasie van resultate getoon in terme van enkapsuleeringsdoeltreffenheid (ED, 55.4%), laaikapasiteit (LK, 12.7%), aspalatien vrylatings tempo by pH 7.4 (1.67 h^{-1}) en grootte (190 nm). Verdere optimisering van die ES100-GRAF gelaaide nanopartikels is behaal met ‘n sentrale saamgestelde ontwerp. Die uitkomstes het ingesluit opbrengs tussen 78.2–78.3%, ED tussen 73.9–77.4% en LK tussen 10.4–12.2%. Suiwer aspalatien was daaropvolgend ge-enkapsuleer onder die ge-

optimiseerde kondisies en soortgelyke opbrengs, ED, LK, partikel grootte en partikel argitektuur as die GRAF gelaaide partikels is gevind. Die stabiliteit van die aspalatien en GRAF gelaaide nanopartikels is ondersoek by vaste pH-tyd kombinasies. Nano-enkapsulering het ‘n meer stabiele omgewing vir aspalatien gebied. Algeheel was suiwer aspalatien minder stabiel as in GRAF. Alhoewel dermwand deurdringbaarheid teoreties verbeter kon word met nano-enkapsulering, het die parallel kunsmatige membraan deurdringbaarheidstoets en die Caco-2 sel model getoon dat suiwer aspalatien en aspalatien nanopartikels albei ewe lae deurdringbaarheid het.

Hierdie metodes bied alternatiewe vir die produksie van groen rooibos gerieflikheidsprodukte en bestanddele terwyl insig gegee word op die effekte van enkapsulering en bestanddele van poeier formulasies.

ACKNOWLEDGEMENTS

I wish to express my sincere gratitude and appreciation to the following persons and institutions:

To my supervisor Prof Dalene de Beer and my co-supervisor Prof Lizette Joubert (Post-Harvest and Agro-Processing Technologies, Agricultural Research Council Infruitec-Nietvoorbij), thank you for your guidance, patience and advice offered throughout this study. I am truly grateful for the opportunity to join your research group and where I learned and experienced above and beyond expectations.

Recognition goes to my co-supervisor Prof Gunnar Sigge (Food Science Department, Stellenbosch University) for his kind support and guidance in my crossover to the Food Science Department, as well as various inputs during my doctoral study.

Dr Christiaan Malherbe (Post-Harvest and Agro-Processing Technologies, Agricultural Research Council Infruitec-Nietvoorbij) is thanked for his practical assistance and keen interest throughout my doctoral study.

Recognition to Miss Nina Muller for her patient help and guidance with descriptive sensory analysis.

Mrs Marieta van der Rijst (Biometry Unit, Agricultural Research Council) and Prof Martin Kidd (Centre for Statistical Consultation) for statistical data analyses.

Prof Marique Aucamp (School of Pharmacy, University of the Western Cape) for various physicochemical analyses.

The Department of Chemistry and Polymer Science and the Electron Microscopy unit of the Central Analytical Facilities (Stellenbosch University) for the use of their instrumentation.

Sandra Bowles (Medical Research Council of South Africa) for the Caco-2 cell studies and assistance with calculations.

Rooibos Ltd Clanwilliam for green rooibos plant material.

The Plant Bioactives Research Group (Post-Harvest and Agro-Processing Technologies, Agricultural Research Council Infruitec-Nietvoorbij) is thanked for making me feel welcome and technical assistance when required.

The NRF-DST Professional Development Program is acknowledged for a doctoral scholarship (NRF grant 96711) and financial support for this project provided by the National Research Foundation (NRF grant 93438 to E. Joubert).

TABLE OF CONTENTS

Chapter 3

Effect of carbohydrate microencapsulating polymers on physicochemical properties and aspalathin stability of green rooibos extract powders

Chapter 4

Shelf-life stability of ready-to-use iced tea powder formulations with microencapsulated green rooibos extract – effect of common food ingredients and packaging materials

Chapter 5

Evaluation of conventional methods and electrospraying for nanoencapsulation of an aspalathin-rich fraction prepared from green rooibos with natural and synthetic polymers

NOTES

The dissertation is presented in the format prescribed by the Department of Food Science at Stellenbosch University. The structure is in the form of one or more research chapters (papers prepared for publication) and is prefaced with an introduction chapter with the study objectives, followed by a literature review chapter and culminating with a chapter for elaborating a general discussion and conclusion. The language, style and referencing format used are in accordance with the requirements of the journal of *Food Chemistry*. This dissertation represents a compilation of manuscripts where each chapter is an individual entity and some repetition between chapters, has, therefore, been unavoidable.

Chapter 1

General Introduction

Interest in extracts of *Aspalathus linearis*, an endemic South African fynbos plant, traditionally used for preparation of rooibos herbal tea, has grown in recent years due to their health-promoting properties (Joubert, Gelderblom, Louw & De Beer, 2008; Joubert & De Beer, 2011). Much research has been directed towards aspalathin, a *C*-glucosyl dihydrochalcone very scarcely found in nature, but present in high levels in extracts prepared from green rooibos, the unoxidised plant material. Normally the plant material is oxidised (referred to as "fermented") for production of the conventional rooibos herbal tea (Joubert & De Beer, 2011). Various *in vitro* and *in vivo* studies have shown the relevance of aspalathin in the prevention and management of the metabolic syndrome (Johnson *et al.*, 2018), which is characterised by raised triglycerides, blood pressure and fasting plasma glucose in humans (Han & Lean, 2016). Aspalathin was shown to improve glucose uptake and alleviate insulin resistance, amongst other beneficial health properties (Johnson *et al.*, 2018). Green rooibos extracts with high aspalathin content were demonstrated to have similar beneficial properties to pure aspalathin (Muller *et al.*, 2018), including the ability to inhibit α-glucosidase (Miller, De Beer, Aucamp, Malherbe & Joubert, 2018). α-Glucosidase inhibitors are important to control post-prandial hyperglycaemia, especially since hyperglycaemia contributes significantly to the development of chronic diabetes complications even more than fasting hypoglycaemia (Derosa & Maffioli, 2012). Collectively the various beneficial properties of green rooibos extracts support their use in functional foods and beverages.

The interest in aspalathin-rich green rooibos extracts is driven by the emergence of a substantial global market for nutraceuticals, addressing the need of consumers for "healthier" food (Corbo, Bevilacqua, Petruzzi, Casanova & Sinigaglia, 2014). Globally, a shift in emphasis from "lifespan" to "health span" contributes to the market for functional foods aimed at general health and wellness, in particular disease prevention. Functional beverages offer an excellent means of delivering nutrients and bioactive compounds to the consumer in a convenient format (Corbo *et al.*, 2014).

Delivery of aspalathin in a functional beverage poses a challenge, since it is highly susceptible to oxidation, which is triggered by various environmental factors such as light, oxygen, high pH, high temperature and moisture (Koeppen & Roux, 1965; De Beer *et al.*, 2015). Incorporation of an aspalathin-rich green extract in ready-to-drink (RTD) iced tea formulations in previous studies has highlighted this challenge. Joubert *et al.* (2010) demonstrated the detrimental effect of heat treatment (e.g. sterilisation) of green rooibos iced tea on its aspalathin content. In addition, De Beer, Joubert, Viljoen & Manley (2011) demonstrated that extensive aspalathin losses (<80% remaining) occurred during 3 months storage at 25 °C. This severely limits the shelf-life of rooibos RTD beverages, when delivery of a fixed concentration of aspalathin is the aim. Nanoencapsulation of the green rooibos extract and ascorbic acid by emulsification in a polyoxyethylene

sorbitan monolaurate shell increased aspalathin stability in the same RTD beverage. However, even in the nanoemulsion, only *ca.* 78–88% of aspalathin remained after 3 months storage at 25 °C.

These studies on rooibos iced tea beverages highlight the need for stable rooibos convenience products with high aspalathin content. Instant powdered iced tea formulations, packaged in a single-serve sachet format, could offer both convenience and improved stability. Lower water activity of powdered products are key to increased stability as a variety of unwanted reactions are catalysed by the presence of water (Woo & Bhandari, 2013). An alternative option to the sachet would be a packaging system that prevents access to moisture and delivers the powdered functional ingredient to the beverage directly before consumption, such as the patented 'Gizmo Closure and Delivery System' (Anonymous, 2018). In this system a functional ingredient is released from a modified bottle cap into the solution when the cap is turned.

In powdered product formulations, the effect of individual ingredients on product stability and their possible interactions that could affect aspalathin stability should also be considered. Previous studies by Ortiz, Ferruzzi, Taylor & Mauer (2008) and De Beer *et al.* (2018) observed that the presence of common food ingredients, citric acid and ascorbic acid, in dry powder mixtures containing green tea (*Camellia sinensis*) and green honeybush extract (*Cyclopia subternata*), respectively, increased degradation of phenolic compounds. In addition, physicochemical changes in the mixtures resulted in prominent colour changes, indicating that ingredient compatibility is not a given.

The stability of powdered nutraceutical ingredients added to dry functional foods and beverages could be enhanced by encapsulation with a suitable polymer. Encapsulation has been shown to protect ingredients prone to degradation by environmental factors such as temperature, moisture and pH and control the release of certain compounds in a formulation (Gibbs, Kermasha, Alli & Mulligan, 1999; Augustin & Hemar, 2009; Nedovic, Kalusevic, Manojlovic, Levic & Bugarski, 2011).

Encapsulating materials commonly used for food applications include carbohydrates, gums, proteins and cellulose derivatives, usually produced by spray-drying of mixtures, delivering micro-sized particles >1 µm. Of these, the carbohydrate maltodextrin is most commonly employed, due to its low cost (Murugesan & Orsat, 2012). However, maltodextrin is rapidly metabolised to simple sugars, resulting in an increased glycaemic load (Hofman, Van Buul & Brouns, 2016). The aim to contribute to the prevention of metabolic syndrome by use of aspalathin-rich rooibos extracts, is not compatible with a formulation with a higher glycaemic load and sugar intake (Benade & Essop, 2017). As a result, various studies are investigating more suitable alternative encapsulating polymers such as inulin, pectin, chitosan and alginates (Chiou & Langrish, 2007; Sansone *et al.*, 2011; De Souza *et al.*, 2013; Sun-Waterhouse, Wadhwa & Waterhouse, 2013). Recently, Miller *et al.* (2018)

microencapsulated a green rooibos extract with inulin (1:1, m/m), achieving aspalathin retention >95% during spray-drying. Compared to maltodextrin, inulin improved wettability and lowered the water activity of the microencapsulated extracts (Miller *et al.*, 2018), ideal for dissolution of the powder before consumption and aspalathin stability, respectively. Further advantages of inulin as an encapsulating agent are that it stimulates the growth of beneficial intestinal bacteria as it is not digestible to humans (Kolida & Gibson, 2007), stimulates the immune system and improves the blood lipid profile (Shoaib *et al.*, 2016). It could therefore further improve the functionality of an already functional green rooibos extract. No information is, however, available on the effect of inulin on the stability of aspalathin when it is used to encapsulate a green rooibos extract. Furthermore, the physicochemical characteristics of inulin could also affect the properties of the rooibos powder.

Nanoencapsulation, an alternative and more specialised approach for the production and formulation of nutraceutical ingredients that produces particles <1 µm (McClements & Rao, 2011), has gained popularity in the food industry (Anandharamakrishnan, 2014). Materials and methods used for nanoencapsulation of food ingredients are largely derived from the pharmaceutical industry, whilst taking into account that the polymers used for nanoencapsulation should have Food and Drug Administration (FDA) approval. Rather than just addressing the stability of the bioactive compound, the nanoencapsulation process, as well as the materials, impose properties not inherent to the bioactives (Reis, Neufeld, Ribeiro & Veiga, 2006; Xiao, Cao & Huang, 2017), but potentially required in the product. For instance, nanoencapsulating polymers such as the Eudragit® range are tailored for targeted delivery *in vivo* from pH 7 (McGinity & Felton, 2008). This would potentially be ideal for the addition to RTD iced teas, which usually have a pH of 3–4. In addition to this, a targeted release profile could result in increased intestinal stability after consumption, resulting in more of the bioactive compound reaching its target in the human body. Moreover, nano-sized particles could also increase absorption (Bilia, Isacchi, Righeschi, Guccione & Bergonzi, 2014). However, low loading capacity is usually obtained with nanoencapsulation (Liang *et al.*, 2011; Xie *et al.*, 2011; Fathi, Varshosaz, Mohebbi & Shahidi, 2012), making the methodology more suitable for highly enriched extracts or individual bioactive compounds, rather than conventional extracts, thus, shifting the scope more to high-end nutraceutical ingredients.

The aims of the current study include the optimisation of the microencapsulation of a green rooibos extract with a suitable polymer. Additionally to inulin, chitosan, also a potential functional and indigestible alternative to maltodextrin, will be investigated. For the first time the process will be optimised with regard to the type of polymer and ratio of polymer:extract by investigating the physicochemical properties of the powders. In addition, the stability of aspalathin in the optimum microencapsulated extract will be evaluated individually and in powdered functional iced tea formulations containing a low kilojoule sweetener packaged in a single-serve

format for the first time. The effect of microencapsulation, packaging, storage conditions and individual ingredients on aspalathin stability and physicochemical properties of the final product will be investigated. As an alternative and more targeted approach, nanoencapsulation of an aspalathin-rich extract will be investigated. Different polymers and method for nanoencapsulation are seldom directly compared in the same study, often causing difficulty to select an optimum method/material combination for a specific bioactive. Various polymers and methods will be evaluated based on their suitability for encapsulation of a nutraceutical ingredient, physicochemical properties and their release profiles. Once selection of a suitable polymer and method has been completed, process parameters will be optimised to ensure production of particles with a favourable combination of physicochemical properties. Further investigation will entail the effects of nanoencapsulation on gastrointestinal stability and absorption of aspalathin for the first time.

References

Anandharamakrishnan, C. (2014). Techniques for nanoencapsulation of food ingredients. Pp. 1–89. New York: Springer.

Anonymous (2018). Gizmo packaging: Tea of a kind project. URL https://www.gizmoclosures.com/. Accessed 28.06.18.

Augustin, M. A. & Hemar, Y. (2009). Nano- and micro-structured assemblies for encapsulation of food ingredients. *Chemical Society Reviews,* 38, 902–912.

Benade, J. & Essop, M. F. (2017). Introduction of "sugar tax" in South Africa: Placebo or panacea to curb the onset of cardio-metabolic diseases? *SAHeart,* 3, 148–153.

Bilia, A. R., Isacchi, B., Righeschi, C., Guccione, C. & Bergonzi, M. C. (2014). Flavonoids loaded in nanocarriers: an opportunity to increase oral bioavailability and bioefficacy. *Food and Nutrition Sciences,* 5, 1212–1327.

Chiou, D. & Langrish, T. A. G. (2007). Development and characterisation of novel nutraceuticals with spray drying technology. *Journal of Food Engineering,* 82, 84–91.

Corbo, M. R., Bevilacqua, A., Petruzzi, L., Casanova, F. P. & Sinigaglia, M. (2014). Functional beverages: The emerging side of functional foods. *Comprehensive Reviews in Food Science and Food Safety,* 13, 1192–1206.

De Beer, D., Joubert, E., Viljoen, M. & Manley, M. (2011). Enhancing aspalathin stability in rooibos (*Aspalathus linearis*) ready-to-drink iced teas during storage: the role of nano-emulsification and beverage ingredients, citric and ascorbic acids. *Journal of the Science of Food and Agriculture,* 92, 274–282.

De Beer, D., Malherbe, C. J., Beelders, T., Willenburg, E. L., Brand, D. J. & Joubert, E. (2015). Isolation of aspalathin and nothofagin from rooibos (*Aspalathus linearis*) using high-performance countercurrent chromatography: Sample loading and compound stability considerations. *Journal of Chromatography A,* 1381, 29–36.

De Beer, D., Pauck, C. E., Aucamp, M., Liebenberg, W., Stieger, N., Van der Rijst, M. & Joubert, E. (2018). Phenolic and physicochemical stability of a functional beverage powder mixture during storage: effect of the microencapsulant inulin and food ingredients. *Journal of the Science of Food and Agriculture,* 98, 2925–2934.

De Souza, J. R. R., Feitosa, J. P. A., Ricardo, N. M. P. S., Trevisan, M. T. S., De Paula, H. C. B., Ulrich, C. M. & Owen, R. W. (2013). Spray-drying encapsulation of mangiferin using natural polymers. *Food Hydrocolloids,* 33, 10–18.

Derosa, G. & Maffioli, P. (2012). α-Glucosidase inhibitors and their use in clinical practice. *Archives of Medical Science,* 8, 899–906.

Fathi, M., Varshosaz, J., Mohebbi, M. & Shahidi, F. (2012). Hesperetin-loaded solid lipid nanoparticles and nanostructure lipid carriers for food fortification: Preparation, characterization, and modeling. *Food and Bioprocess Technology,* 6, 1464–1475.

Gibbs, B. F., Kermasha, S., Alli, I. & Mulligan, C. N. (1999). Encapsulation in the food industry: A review. *International Journal of Food Sciences and Nutrition,* 50, 213–224.

Han, T. S. & Lean, M. E. (2016). A clinical perspective of obesity, metabolic syndrome and cardiovascular disease. *Journal of the Royal Society of Medicine Cardiovascular Disease,* 5, 1–13.

Hofman, D. L., Van Buul, V. J. & Brouns, F. J. P. H. (2016). Nutrition, health, and regulatory aspects of digestible maltodextrins. *Critical Reviews in Food Science and Nutrition,* 56, 2091–2100.

Johnson, R., De Beer, D., Dludla, P. V., Ferreira, D., Muller, C. J. F. & Joubert, E. (2018). Aspalathin from rooibos (*Aspalathus linearis*): A bioactive *C*-glucosyl dihydrochalcone with potential to target the metabolic syndrome. *Plant Medica,* 84, 568–583.

Joubert, E. & De Beer, D. (2011). Rooibos (*Aspalathus linearis*) beyond the farm gate: From herbal tea to potential phytopharmaceutical. *South African Journal of Botany,* 77, 869–886.

Joubert, E., Gelderblom, W. C. A., Louw, A. & De Beer, D. (2008). South African herbal teas: *Aspalathus linearis, Cyclopia* spp. and *Athrixia phylicoides*—A review. *Journal of Ethnopharmacology,* 119, 367–412.

Joubert, E., Viljoen, M., De Beer, D., Malherbe, C. J., Brand, D. J. & Manley, M. (2010). Use of green rooibos (*Aspalathus linearis*) extract and water-soluble nanomicelles of green rooibos extract encapsulated with ascorbic acid for enhanced aspalathin content in ready-to-drink iced teas. *Journal of Agricultural and Food Chemistry,* 58, 10965–10971.

Koeppen, B. H. & Roux, D. G. (1965). Aspalathin: a novel *C*-glycosyl flavonoid from *Aspalathus linearis*. *Tetrahedron Letters,* 6, 3497–3503.

Kolida, S. & Gibson, G. R. (2007). Prebiotic capacity of inulin-type fructans. *The Journal of Nutrition,* 137, 2503S–2506S.

Liang, J., Li, F., Fang, Y., Yang, W., An, X., Zhao, L., Xin, Z., Cao, L. & Hu, Q. (2011). Synthesis, characterization and cytotoxicity studies of chitosan-coated tea polyphenols nanoparticles. *Colloids and Surfaces B: Biointerfaces,* 82, 297–301.

McClements, D. J. & Rao, J. (2011). Food-grade nanoemulsions: Formulation, fabrication, properties, performance, biological fate, and potential toxicity. *Critical Reviews in Food Science and Nutrition,* 51, 285–330.

McGinity, J. W. & Felton, L. A. (2008). Aqueous polymeric coatings for pharmaceutical dosage forms. Pp. 1–475. Florida: CRC Press.

Miller, N., De Beer, D., Aucamp, M., Malherbe, C. J. & Joubert, E. (2018). Inulin as microencapsulating agent improves physicochemical properties of spray-dried aspalathin-rich green rooibos (*Aspalathus linearis*) extract with α-glucosidase inhibitory activity. *Journal of Functional Foods,* 48, 400–409.

Muller, C. J. F., Malherbe, C. J., Chellan, N., Yagasaki, K., Miura, Y. & Joubert, E. (2018). Potential of rooibos, its major *C*-glucosyl flavonoids, and *Z*-2-(β-D-glucopyranosyloxy)-3-phenylpropenoic acid in prevention of metabolic syndrome. *Critical Reviews in Food Science and Nutrition,* 58, 227–246.

Murugesan, R. & Orsat, V. (2012). Spray drying for the production of nutraceutical ingredients—A review. *Food and Bioprocess Technology,* 5, 3–14.

Nedovic, V., Kalusevic, A., Manojlovic, V., Levic, S. & Bugarski, B. (2011). An overview of encapsulation technologies for food applications. *Procedia Food Science,* 1, 1806–1815.

Ortiz, J., Ferruzzi, M. G., Taylor, L. S. & Mauer, L. J. (2008). Interaction of environmental moisture with powdered green tea formulations: effect on catechin chemical stability. *Journal of Agricultural and Food Chemistry,* 56, 4068–4077.

Reis, C. P., Neufeld, R. J., Ribeiro, A. J. & Veiga, F. (2006). Nanoencapsulation I. Methods for preparation of drug-loaded polymeric nanoparticles. *Nanomedicine,* 2 8–21.

Sansone, F., Mencherini, T., Picerno, P., d'Amore, M., Aquino, R. P. & Lauro, M. R. (2011). Maltodextrin/pectin microparticles by spray drying as carrier for nutraceutical extracts. *Journal of Food Engineering,* 105, 468–476.

Shoaib, M., Shehzad, A., Omar, M., Rakha, A., Raza, H., Sharif, H. R., Shakeel, A., Ansari, A. & Niazi, S. (2016). Inulin: Properties, health benefits and food applications. *Carbohydrate Polymers,* 147, 444–454.

Sun-Waterhouse, D., Wadhwa, S. S. & Waterhouse, G. I. N. (2013). Spray-drying microencapsulation of polyphenol bioactives: A comparative study using different natural fibre polymers as encapsulants. *Food and Bioprocess Technology,* 6, 2376–2388.

Woo, M. & Bhandari, B. (2013). Spray drying for food powder production. In: *Handbook of Food Powders Processes and Properties*. Pp. 29–56. Cambridge, UK: Woodhead Publishing.

Xiao, J., Cao, Y. & Huang, Q. (2017). Edible nanoencapsulation vehicles for oral delivery of phytochemicals: A perspective paper. *Journal of Agricultural and Food Chemistry,* 65, 6727–6735.

Xie, X., Tao, Q., Zou, Y., Zhang, F., Guo, M., Wang, Y., Wang, H., Zhou, Q. & Yu, S. (2011). PLGA nanoparticles improve the oral bioavailability of curcumin in rats: Characterizations and mechanisms. *Journal of Agricultural and Food Chemistry,* 59, 9280–9289.

Chapter 2

Literature review

2.1 Introduction

The present review will provide a short introduction on rooibos serving as background to a discussion of its phenolic composition with the emphasis on the major flavonoids, their stability, biological significance and bioavailability. Methods employed to assess bioavailability, in particular intestinal adsorption, and degradation of bioactive compounds will be discussed. The second part of the review will focus on different strategies for delivering natural bioactive compounds and include attention to current developments in the nutraceutical and functional food industry to address stability and bioavailability of phenolic compounds. Specific focus will be given to micro- and nanoencapsulation techniques.

2.2 Rooibos

Rooibos is produced from *Aspalathus linearis*, an endemic South African fynbos plant. The use of rooibos herbal tea pre-dates the 1900's and has grown substantially since it has been introduced in the commercial market in 1904 (Joubert, Gelderblom, Louw & De Beer, 2008). The reason for the fast growth in rooibos consumption worldwide can be attributed to its reported high antioxidant activity and caffeine-free status, branding it as a health beverage rather than an ordinary herbal tea (Joubert & De Beer, 2011). These health-promoting properties has led to the use of rooibos extracts in various products including jams, yogurt, ready-to-drink iced teas and "instant cappuccinos" (Joubert & De Beer, 2011).

Traditionally, rooibos products are comprised of the oxidised leaves and stems of the rooibos plant, commercially referred to as "fermented" tea (Joubert & De Beer, 2011). The fermentation process produces the characteristic honey, woody herbal-floral flavour of commercially consumed rooibos tea as known by the consumer (Koch, Muller, Joubert, Rijst & Næs, 2012).

Nevertheless, a small demand for the unfermented product or green rooibos arised in the early 2000's. Unfermented or green rooibos has significantly higher levels of antioxidants, but without the characteristic rooibos flavour, making it suitable for use in health products rather than as a herbal tea (Joubert & Schulz, 2006). Green rooibos can also be used to prepare aspalathin-enriched extracts by extraction with organic solvents and purification (Grüner-Richter, Otto & Weinreich, 2008). In this form the health properties of rooibos are further enhanced and could open the way for pharmaceutical applications.

2.2.1 Phenolic compounds

Phenolic secondary metabolites, identified in the rooibos plant, comprise mostly phenolic acids and monomeric flavonoids belonging to the sub-classes dihydrochalcones, flavones, flavanones and flavonols (Joubert *et al.*, 2008). *Aspalathus linearis* is characterised by and known for high amounts of dihydrochalcones,

specifically aspalathin, a *C*-glucosyl (Koeppen & Roux, 1965) found only in the genus *Aspalathus* to date. The aspalathin content in unprocessed plant material can vary extensively ranging from 3.84 to 9.66% (average 6.62%) (Joubert & De Beer, 2014). Nothofagin, the 3-deoxy analogue of aspalathin is present in much lower quantities (0.20 to 1.24%, average 0.67%) (Joubert & Schulz, 2006) and is not limited to rooibos, although its occurrence is very scarce in nature. Nothofagin has previously only been identified from a few plants including the heartwood of *Nothofagus fusca* (Hillis & Inoue, 1967; Joubert & De Beer, 2011), the bark of *Schoepfia chinensis*, a Chinese medical plant (Huang, Gan, Bai, Ma & Hu, 2008a), and more recently in the peel and flesh of pink guava (Rojas-Garbanzo, Zimmermann, Schulze-Kaysers & Schieber, 2017) and *Leandra dasytricha* (A. Gray) Cogn., a Brazilian medicinal plant (De Almeida *et al.*, 2017).

Furthermore, other significant secondary metabolites present in individual levels of *ca.* 1% or less include the flavone analogues of aspalathin, orientin (luteolin-8-*C*-glucoside) and isoorientin (luteolin-6-*C*-glucoside). The flavone analogues of nothofagin, vitexin (apigenin-8-*C*-glucoside) and isovitexin (apigenin-8-*C*-glucoside) are present at much lower levels (Joubert & De Beer, 2014). Also present are eriodictyol derivatives of aspalathin, luteolin-7-*O*-glucoside, hyperoside (quercetin-3-*O*-galactoside), isoquercitrin (quercetin-3-*O*-glucoside), rutin (quercetin-3-*O*-rutinoside) and quercetin-3-*O*-robinobioside, the major flavonol glycoside (Beelders, Kalili, Joubert, De Beer & De Villiers, 2012). Table 2.1 provides the chemical structures of the major phenolic compounds that have been found to be present in rooibos (Joubert & De Beer, 2014).

Apart from the phenolic compounds present in *A. linearis* the phenolic biosynthetic precursor, phenyl pyruvic acid glucoside (PPAG; *Z*-2-(β-D-glucopyranosyloxy)-3-phenylpropenoic acid), is also of interest as a result of recent studies indicating the anti-diabetic properties of this compound (Muller *et al.*, 2018).

Table 2.1

Chemical structures of the major phenolic compounds present in rooibos (as adapted from Joubert & De Beer (2014))

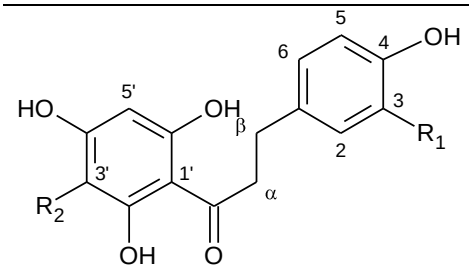	Dihydrochalcones Nothofagin (R_1 = H, R_2 = β-D-glucopyranosyl) Aspalathin (R_1 = OH, R_2 = β-D-glucopyranosyl)
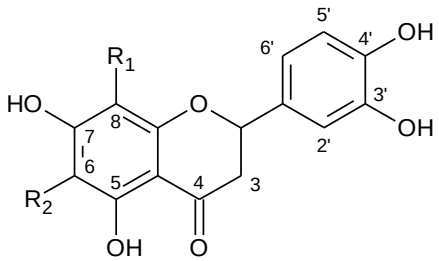	Flavanones (*S*)-Eriodictyol-6-*C*-glucoside (R_1 = H, R_2 = β-D-glucopyranosyl) (*R*)-Eriodictyol-6-*C*-glucoside (R_1 = H, R_2 = β-D-glucopyranosyl) (*S*)-Eriodictyol-8-*C*-glucoside (R_1 = β-D-glucopyranosyl, R_2 = H) (*R*)-Eriodictyol-8-*C*-glucoside (R_1 = β-D-glucopyranosyl, R_2 = H)
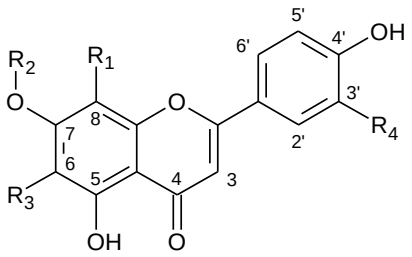	Flavones Orientin (R_1 = β-D-glucopyranosyl, R_4 = OH, R_2 = R_3 = H) Isoorientin (R_1 = R_2 = H, R_4 = OH, R_3 = β-D-glucopyranosyl) Vitexin (R_1 = β-D-glucopyranosyl, R_2 = R_3 = R_4 =H) Isovitexin (R_1 = R_2 = R_4 =H, R_3 = β-D-glucopyranosyl) Luteolin-7-*O*-glucoside (R_1 = R_3 = H, R_2 = β-D-glucopyranosyl, R_4 = OH)
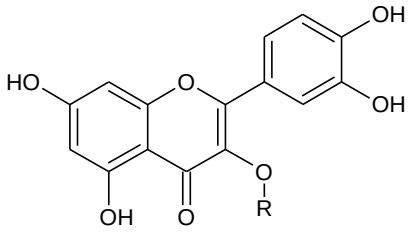	Flavonols Quercetin (R = H) Isoquercitrin (R = β-D-glucopyranosyl) Hyperoside (R = β-D-galactosyl) Rutin (R = β-D-rutinosyl) Quercetin-3-O-robinoside (R = β-D-robinobiosyl)
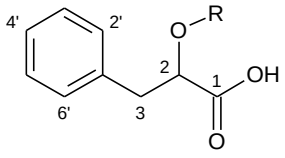	Phenylpropanoid *Z*-2-(β-D-glucopyranosyloxy)-3-phenylpropenoic acid (R = *O*-glucopyranosyl)

2.2.2 Stability of phenolic compounds

Phenolic compounds are generally susceptible to oxidation, causing unwanted changes in food products. However, in the production of traditional rooibos, oxidation ("fermentation") forms an essential element of processing, contributing to the development of the characteristic red-brown colour (Joubert & De Beer, 2014). The fermentation process and heat treatment of rooibos plant material cause quantitative and qualitative changes to the phenolic composition (Joubert, Viljoen, De Beer & Manley, 2009; Joubert *et al.*, 2010; Koch *et al.*, 2012; Walters, De Villiers, Joubert & De Beer, 2017). Qualitative changes associated with heat treatment

include the development of the characteristic flavour and colour of rooibos tea. The main quantitative changes include large decreases in the dihydrochalcones, moderate decreases in the flavonols and increases of the eriodictyol glucoside isomers (Walters *et al.*, 2017).

Aspalathin, considered the characteristic chemical marker for rooibos, is susceptible to oxygen and heat degradation during processing and storage. Photochemical oxidation of aspalathin, investigated by Koeppen & Roux (1965), entailed exposure of an ethanolic solution of aspalathin to sunlight and oxygen over a certain period. Conversion of aspalathin resulted predominantly in the formation of isoorientin and orientin. As the exposure time increased, the concentration of orientin increased further, indicating further conversion of isoorientin to orientin. Higher molecular weight compounds contributing to browning were also formed from aspalathin and nothofagin (Krafczyk, Heinrich, Porzel & Glomb, 2009a). Studies performed by Marais, Janse van Rensburg, Ferreira & Steenkamp (2000) confirmed the reaction products as shown by Koeppen & Roux (1965) and showed the additional formation of a diastereomeric mixture of (S)- and (R)- eriodictyol-6-*C*-glucoside.

Studies performed by Krafczyk *et al.* (2009a) on the oxidation of aspalathin provided better insight into reaction mechanisms that take place during the degradation process when incubated at 37 °C, pH of 7.4. The study found that the eriodictyol glucosides further oxidises to form isoorientin and orientin. It was also revealed that (S)/(R)- eriodictyol-8-*C*-glucoside does not oxidise directly to orientin, but this conversion is postulated to occur via the quinine methide. This mechanism involves the opening of the vinyl ester structure, followed by bond rotation and re-cyclisation. Furthermore, after 10 hours at the above mentioned conditions no isoorientin was detectable, but an increase in a brown unidentified compound was noted (Krafczyk *et al.*, 2009a; Krafczyk, Woyand & Glomb, 2009b). Heinrich, Willenberg & Glomb (2012) identified brown compounds in an oxidised asplatahin solution as dibenzofuran derivatives, (S)- and (R)-3-(7,9-dihydroxy-2,3-dioxo-6-β-D-glucopyranosyl-3,4-dihydrodibenzo[b,d]furan-4a(2H)-yl) propionic acid. Fig. 2.1 shows a basic schematic representation of the oxidative degradation of aspalathin (Krafczyk & Glomb, 2008).

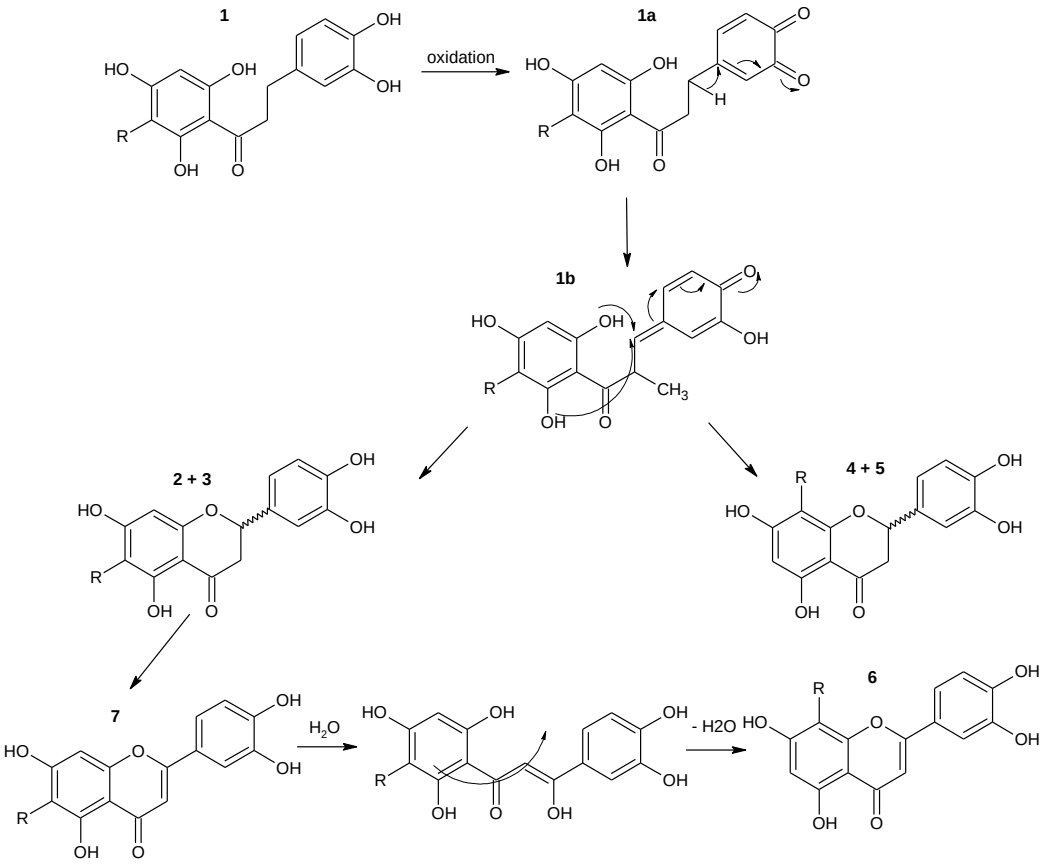

Fig. 2.1 Oxidative degradation of aspalathin (1) proceeds through the formation of flavanones (2-5), (*S*)-eriodictyol-6-*C*-β-D-glucopyranoside, (*S*)-eriodictyol-8-*C*-β-*D*-glucopyranoside, (*R*)-eriodictyol-6-*C*-β-*D*-glucopyranoside and (*R*)-eriodictyol-8-*C*-β-*D*-glucopyranoside which further oxidise to orientin (6) and isoorientin (7) as proposed by (Krafczyk *et al.*, 2009a; Krafczyk *et al.*, 2009b). R represents a β-*D*-glucopyranosyl moiety

2.2.3 Bioactivity of phenolic compounds

Observational studies have shown that individuals and groups that follow diets high in plant-based foods have a lower tendency and risk for chronic diseases including some forms of cancer, diabetes and cardiovascular disease (Hertog *et al.*, 1996; Rimm *et al.*, 1996; Hollman, Feskens & Katan, 1999; Hu, 2003; Riboli & Norat, 2003) leading to interest in polyphenols, amongst others (Scalbert, Johnson & Saltmarsh, 2005). Although polyphenols were believed to act as endogenous antioxidants to help maintain redox homeostasis in the cell, more recent scientific evidence points to the importance of polyphenols in cellular responses that are independent of their antioxidant activity (Williams, Spencer & Rice-Evans, 2004; Virgili & Marino, 2008; Vauzour, Rodriguez-Mateos, Corona, Oruna-Concha & Spencer, 2010; Fraga, Galleano, Verstraeten & Oteiza, 2010; Del Rio *et al.*, 2013).

The antioxidant activity of rooibos tea is widely reported and has been studied using various *in vitro* methods. Through the years, many studies have included rooibos when herbal teas are compared in terms of their relative antioxidant activity (reviewed by Joubert & De Beer (2014)). Schulz, Joubert & Schutze (2003)

correlated the aspalathin content of green rooibos to its total antioxidant capacity. These studies found large variations in the phenolic composition of rooibos plant material harvested from mid-spring to early summer as evidenced by extraction yield and antioxidant assays. Manley, Joubert & Botha (2006) investigated the possible use of near infrared spectroscopy as a method to predict aspalathin and nothofagin content and antioxidant activity in green rooibos plant material and water extracts. NIR spectroscopy showed promising results for the dihydrochalcone determination in the plant materials, however, unacceptable results were obtained for the water extracts as compared to high performance liquid chromatography (HPLC) and antioxidant assays. Von Gadow, Joubert & Hansmann (1997), comparing the antioxidant activity of individual rooibos polyphenols, demonstrated that aspalathin had the highest antioxidant activity based on the (2,2-diphenyl-1-picrylhydrazyl) DPPH radical scavenging and β-carotene bleaching methods. Joubert, Winterton, Britz & Ferreira (2004) also assessed the radical scavenging ability of individual phenolic compounds. In contrast to the previous study, quercetin had the highest antioxidant activity in a DPPH assay followed by aspalathin, orientin, luteolin and isoquercitrin. A more in-depth analysis by Snijman *et al.* (2009) investigated the antioxidant activity of rooibos with various antioxidant assays whilst taking into account the calculated physicochemical parameters. Similar to Von Gadow *et al.* (1997), aspalathin was found to be the most potent antioxidant, followed by quercetin. Quercetin, however, was found to be the most effective inhibitor of the lipid peroxidation assay. The studies showed different relative ranking of compounds, due to different radicals, endpoints, assays, etc., but all confirmed that aspalathin is one of the major antioxidants of rooibos, especially considering its high content compared to that of the other flavonoids. Fermentation of the plant material thus results in a decrease in antioxidant activity of rooibos infusions and extracts due to lower total phenol content and lower radical scavenging ability of the flavanone and flavone conversion products of aspalathin (Snijman *et al.*, 2009; Krafczyk *et al.*, 2009b).

Initial interest in the health-promoting properties of rooibos focused on its anti-mutagenic and anti-cancer properties as reviewed by Joubert *et al.* (2008). Recently, attention was directed towards prevention of metabolic syndrome by rooibos, focusing particularly on contributions by aspalathin and PPAG. The findings of various *in vitro* and *in vivo* studies on rooibos extract, dihydrochalcones and their flavone *C*-glucosides as well as the aglycone, luteolin and apigenin, and PPAG were reviewed by Muller *et al.* (2018). This led to the conclusion that *C*-glucosyl flavonoids and PPAG present in rooibos extracts and infusions play a major role in the health-promoting properties.

The high levels of aspalathin in rooibos and the putative link between aspalathin and many of the bioactive properties of rooibos thus provided impetus for the development of bioactive rooibos extracts (Schulz *et al.*, 2003; Miller, De Beer & Joubert, 2017). Limited adverse effects were observed after administering aspalathin-

enriched green rooibos extracts to rats for 28 and 90 days (Van der Merwe, De Beer, Joubert & Gelderblom, 2015; 2016). The study implied that attention should be given to the effect of the dose and duration of exposure to polyphenol-enriched extracts. These effects should be carefully monitored as subtle disruption of liver function could affect cholesterol metabolism.

2.2.4 Bioavailability of phenolic compounds

Bioavailability can be defined as the relative amount of active compound in a formulation that is available for the human body for physiological functions (Bohn, 2014). From this definition, a detailed description of a 100% bioavailable compound will be given as: The compound is completely released from the dosage form into the gastrointestinal fluid, completely stable under these conditions and the complete administered dose must be able to move through the barrier to the mesenteric circulation system without being metabolised or degraded (Aulton, 1996). Thus, in short, the bioactive compound must be absorbed, distributed, metabolised and excreted.

Various theoretical classification systems are available for bioactive compounds. Lipinski's rule of 5 is often associated with the solubility and permeability of bioactive compounds and a good indication of bioavailability. The number of hydrogen bond donors and acceptors, lipophilicity (Log P) and molecular weight (MW) are parameters associated with this rule, where a MW over 500, Log P over 5 and more than 10 H-bond acceptors relates to poor permeation and absorption (Lipinski, Lombardo, Dominy & Feeney, 2012). Snijman *et al.* (2009) calculated various physicochemical properties related to Lipinski's rule of 5 for flavonoids found in rooibos (Table 2.2). According to the physicochemical properties, all the rooibos flavonoids obey Lipinski's rule of 5 with log P values below 5, however, the glycosides violate the rule in terms of hydrogen bond donors and acceptors. However, apart from this, aspalathin and a few other phenolic compounds in rooibos possess C-C linked glucose moieties, rather than O-glycosides (Muller *et al.*, 2018). These are metabolised by lactase phloridzin hydrolase in the brush order of the small intestine and can only be metabolised by colonic bacterial hydrolases which are related to decreased bioavailability (Bowles *et al.*, 2017).

Other than Lipinski's rule of 5 the "nutraceutical bioavailability classification scheme" known as NuBACS also classifies compounds in 4 different classes according to physicochemical parameters related to bioavailability (McClements, Li & Xiao, 2015) (Table 2.3). The physicochemical properties of aspalathin and other phenolic compounds of rooibos relates to Type III as the compounds are soluble in intestinal fluids, but were shown to have low absorption (0.26% of flavonoids) (Breiter et al., 2011).

Table 2.2

Physicochemical properties of rooibos flavonoids (adapted from Snijman *et al.* (2009))

	HBA[a]	HBD[b]	C.logP[c]
aspalathin	11	9	2.07
nothofagin	10	8	2.68
orientin/iso-orientin	11	8	1.58
vitexin/isovitexin	10	7	1.28
luteolin	6	4	2.40
rutin	6	3	1.81
chrysoeriol	16	10	1.76
isoquercitrin	12	8	1.75
hyperoside	12	8	1.75
quercetin	7	5	3.08
catechin	6	5	0.49

HBA[a] (<10), hydrogen bond acceptors; HBD[b] (<5), hydrogen bond donors; log P[c] (<5), calculated octanol-water partition coefficient.

Table 2.3

Biopharmaceutical classification scheme (adapted from McClements *et al.* (2015))

Type I High solubility, high permeability	Type II Low solubility, high permeability
Type III High solubility, low permeability	Type IV Low solubility, low permeability

Several studies have been performed to assess bioavailability of rooibos and its phenolic compounds by investigating their absorption, distribution, metabolism and excretion as summarised in Table 2.4. *In vitro* absorption studies performed by Huang, Du Plessis, Du Preez, Hamman & Viljoen (2008b) found very low permeation for aspalathin and an aspalathin-enriched green rooibos extract through human skin. Faster, concentration dependent transport and high absorption was evident for the Caco-2 and Franz diffusion cells for both aspalathin and green rooibos extract. To the contrary, Bowles *et al.* (2017) found low absorption and permeation rates with Caco-2 cells for aspalathin. *In vitro* metabolism studies of aspalathin were performed by Van der Merwe *et al.* (2010) and Courts & Williamson (2009) on rat liver fractions and human liver/intestinal fractions, respectively. Results indicated that the main metabolites obtained from human liver/intestinal fractions were methylated forms of aspalathin, whereas the rat liver fractions resulted in sulphated aspalathin metabolites.

Consequent to the *in vitro* studies, *in vivo* studies on the metabolism and absorption of rooibos and its phenolic compounds are also available in literature. Metabolites found in the urine of pigs, following oral

administration of rooibos, included mainly methylated and glucuronidated aspalathin as well as pure aspalathin (Kreuz, Joubert, Waldmann & Ternes, 2008). No metabolites were detected in the plasma. Similar metabolites were found in urine samples of humans, following oral administration of different forms of rooibos extracts and drinks (Courts & Williamson, 2009; Stalmach, Mullen, Pecorari, Serafini & Crozier, 2009; Breiter *et al.*, 2011). Stalmach *et al.* (2009) investigated the regions where aspalathin metabolism takes place with *in vitro* studies. The incubation of aspalathin in gastric juice lead to 100% recovery of aspalathin. This indicates that the polyphenol is not degraded in the stomach, but rather arrives intact at the intestines. Thus, aspalathin must be broken down in the intestines. However, the low levels of metabolites detected indicate that aspalathin cannot be sufficiently absorbed. This is most likely due to incomplete cleaving of the *C*-glucoside moiety by lactase phloridzin hydrolase or by β-glycosidase. Some of the *in vivo* studies also reported on the absorption of rooibos. Compared to the *in vitro* studies, lower levels of absorption between 0.18% (Stalmach *et al.*, 2009) and 0.26% (Breiter *et al.*, 2011) were reported the total administered amount of polyphenols.

Table 2.4

Summary of main findings in literature on rooibos bioavailability

Rooibos sample form	Goal of study	Method	Analytical methods	Main findings	Reference
			In vitro studies		
Aspalathin and green rooibos extracts	Absorption and transport	Franz diffusion cells Caco-2 monolayer cells	HPLC[a]	• Low permeation through skin for aspalathin and green rooibos extracts • High, concentration dependent absorption of aspalathin and extract through Caco-2 cells • High absorption values (79% for aspalathin)	Huang *et al.* (2008b)
Aspalathin	Absorption and transport	Caco-2 monolayer cells	HPLC-DAD[b]	• Low permeation/absorption of aspalathin • Low absorption (5%)	Bowles *et al.* (2017)
Nothofagin and aspalathin	Metabolism	PAPS[5] and UDPGA[6]	HPLC/LC-MS[c] Online radical scavenging LC-MS/MS[d]	• Single sulphated aspalathin metabolite detected • No sulphated nothofagin detected Glucuronidated metabolites found for aspalathin and nothofagin	Van der Merwe *et al.* (2010)
Aspalathin	Metabolism	Human liver and intestine cytosolic fractions	LC-MS/MS	• 3-O-methylaspalathin and 4-O-methylaspalathin were found	Courts & Williamson (2009)
			In vivo studies		
Rooibos extract (16.3 % aspalathin)	Metabolism and excretion	Oral administration to pigs Analysis of urine and plasma	LC/MS	• Methylated aspalathin, aspalathin, aglycone of aspalathin detected in urine • No metabolites detected in plasma	Kreuz *et al.* (2008)
Aspalathin enriched rooibos extract	Absorption, metabolism and excretion	Oral administration to human Analysis of urine and plasma	LC-MS/MS and HPLC	• 3-O-methyl aspalathin and 4-O-methyl aspalathin and intact aspalathin detected in urine	Courts & Williamson (2009)
Ready-to-drink rooibos iced tea: nothofagin and aspalathin	Absorption and metabolism	Oral administration to human Analysis of urine and plasma	HPLC-PDA-MS[e]	• Aspalathin absorbed: 0.18% • Aspalathin absorbed mostly in the intestines • No metabolites detected in plasma • Rapid removal from circulatory system	Stalmach *et al.* (2009)
Unfermented and fermented rooibos drinks. *Aspalathus linearis* fraction	Absorption and metabolism	Oral administration to human Analysis of urine and plasma	HPLC-MS/MS	• Methylated aspalathin, aspalathin, aglycone of aspalathin detected in urine • Unchanged flavonoids detected in plasma • Aspalathin absorbed: 0.26% • Rooibos tea metabolite fraction is higher than that of isolate fraction – indication of synergistic effects	Breiter *et al.* (2011)

[a]HPLC = High performance liquid chromatography
[b]HPLC-DAD = HPLC-diode array detection
[c]HPLC-LC-MS = HPLC-liquid chromatography-mass spectroscopy
[d]LC-MS/MS = Liquid chromatography-tandem mass spectrometry
[e]HPLC-PDA-MS = High performance liquid chromatography - photodiode array- mass spectrometry

2.3 Rooibos functional food/nutraceutical ingredient development opportunity

Current research and findings indicate the usefulness of the polyphenolic compounds, especially aspalathin, present in rooibos, as they possess various health-promoting properties. Beyond basic health improvement, the prevention and progression of the metabolic syndrome are also becoming more realistic, inclining to a nutraceutical application of rooibos. However, factors that should be taken into account include the excessive processing of commercial rooibos products resulting in very low or no aspalathin content, as the compound is sensitive to environmental and storage degradation. Furthermore, its poor absorption limits the exploitation of the health properties. This was highlighted by a study where six cups of rooibos a day only indicated changes to the lipid profile and redox status in adults who were at risk of developing cardiovascular disease (Marnewick *et al.*, 2011). Seen against a background of an agricultural industry under threat due to climate change (Lötter & Le Maitre, 2014), it becomes even more essential to maximise retention and utilisation of the existing available plant bioactive content. From this, the need arises for a stable rooibos product with improved delivery of the functional ingredients containing the bioactive compounds to advance rooibos beyond just a healthy beverage to a product fit for the functional food market. As a step in the right direction, a study on the optimisation of the extraction (Miller *et al.*, 2017) and spray-drying of a green rooibos extract was performed by Miller, De Beer, Aucamp, Malherbe & Joubert (2018), to produce a stable powdered green rooibos nutraceutical extract.

The term nutraceutical was developed by combination of “nutrition”nutrition and “pharmaceutical” by Stephen DeFelice in 1989, the founder of the Foundation for Innovation in Medicine. It can be defined as a part of a food or component found in food products that has the ability to provide health benefits and treatment of disease as a pharmaceutical would (Kalra, 2003). However, in industry the term nutraceutical refers to a concentrated and standardised form of a bioactive compound or mixtures of compounds extracted from a natural product presented as a functional food or delivered as a dietary supplement (Binns, 2009). The aim of nutraceuticals are to exceed and increase the dosages available from the natural source for enhanced health benefits. However, contrary to the original concept of a dietary supplement or functional food, a nutraceutical aims to prevent and/or treat a disease or disorder in addition to supplementing the diet (Kalra, 2003). Nutraceuticals are usually designed in similar delivery forms as pharmaceutical products including that of tablets, pills, extracts and, additionally, as functional food ingredients (Espín, García-Conesa & Tomás-Barberán, 2007). The prerequisites and factors to be considered for nutraceutical formulations are similar to those of pharmaceuticals and include bioavailability, storage stability, degradation kinetics, and physicochemical characteristics (McClements, Decker, Park & Weiss, 2009). These factors are highly dependent on the active compound and the final delivery form. Even though nutraceuticals are generally

assessed using the same methods as for pharmaceuticals, there is a lack of human clinical trials to evaluate the actual physiological effects in humans (Espín *et al.*, 2007).

Wide ranges of nutraceuticals containing phytochemicals are commercially available. Examples include anthocyanins generally derived from berries, proanthocyanidins from pine bark or grape seed (Espín *et al.*, 2007) and resveratrol (Espín *et al.*, 2007).

2.3.1. Bioavailability assessment of nutraceutical/functional food ingredient design forms

The bioavailability of functional ingredients in a dosage design are usually investigated by release studies to assess bioaccessibility, permeability studies to assess absorption and finally, *in vivo* testing. The following section will provide a discussion on merits and limitations of release studies and two commonly used assays that are used by the pharmaceutical industry to predict membrane permeability. Cytotoxicity assessment and *in vivo* testing do not fall within the scope of the current study and will therefore not be discussed.

2.3.1.1 Release studies

The release of active compound can be achieved by three main mechanisms, namely diffusion; swelling and dissolution; and degradation of the capsule/carrier that contains the bioactive compound or mixture (Aulton, 1996). Fig. 2.2 shows the common release mechanism for polymeric delivery systems. The release mechanism can also be a combination of the above mechanisms. Saravanabhavan, Bose, Skylab & Dharmalingam (2013) investigated the release kinetics of chitosan tripolyphosphate (TPP) crosslinked particles loaded with an anti-cancer drug. The particles exhibited an initial burst release followed by a slow sustained release for up to 120 hours. The release kinetics could be attributed to swelling and dissolution of the nanoparticles, followed by degradation of the polymer matrix during the sustained release period. The study also found that the degradation rate and thus the release rate was affected by the degree of acylation and the amount of TPP used in the reaction.

The release mechanism and rate is firstly affected by the polymer properties which include the molar mass, T_g, degradation mechanism, pH sensitivity, crystallinity, and the hydrophobic or hydrophilic nature (Hines & Kaplan, 2013). Secondly, the properties of the bioactive affect its release and include the molar mass, water solubility, degradation kinetics, stability and acid base properties. Furthermore, combined properties such as polymer-bioactive compound interactions, matrix effects, and drug dispersion plays a role (Hines & Kaplan, 2013). In research of functional products containing phenolic compounds, poly(lactide-co-glycolide) (PLGA) is commonly used as a delivery polymer. The release mechanism is a combination of the erosion and diffusion of the polymer, followed by the hydrolytic degradation of the polymer. The degradation of the polymer is greatly

affected by its composition and copolymer ratio. Higher ratios of lactic acid results in a more hydrophobic polymer. This results in less water penetration and slower degradation as water is needed to cleave the ester linkages (Hines & Kaplan, 2013).

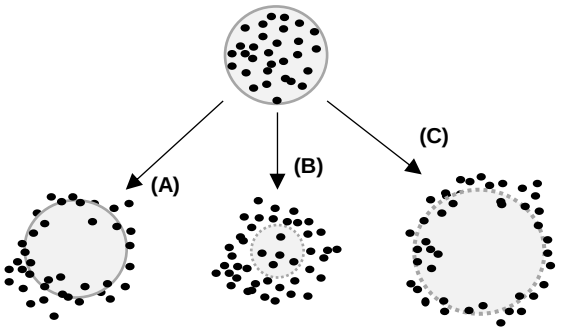

Fig. 2.2 Schematic representation of common release mechanisms of active compounds from encapsulate systems (A) diffusion, (B) polymer degradation, (C) swelling/solvent penetration (Hines & Kaplan, 2013).

The release rate of encapsulated bioactive compounds can be investigated using various methods. The basic concept involves the use of simulated gastric fluid (enzymatic) or conditions (temperature and pH). Example studies include the release of curcumin from PLGA nanoparticles in artificial gastric juice (pH 2.0) and intestinal juice (pH 7.4) without any enzymes. The samples were kept at 37 °C in a shaker. At designated time intervals the pellets were separated by centrifugation and the amount of curcumin present was determined by HPLC (Xie *et al.*, 2011). Other more complicated methods include the use of dialysis bags where the released compound travels through the dialysis bag into the surrounding simulated digestive tract medium. The amount of released compound can be monitored by UV-VIS, HPLC or antioxidant capacity in the case of phenolic compounds (Fathi, Varshosaz, Mohebbi & Shahidi, 2012b; Arulmozhi, Pandian & Mirunalini, 2013). Even more complicated and intricate tests involve the use of gastric intestinal models where the sample spends time in simulated environments for different parts of the intestinal tract including the stomach, duodenum, jejunum, and ileum. These environments are simulated with the correct pH, enzymes and time spent during normal digestion which form part of a continuous system (Madalena *et al.*, 2016).

2.3.1.2 Permeability

In order for a bioactive compound to be metabolised and reach its target area, the compound must be able to permeate the gastrointestinal lining (He, Hu, Yin, Tang & Yin, 2010). Thus, gastrointestinal permeation of bioactive compounds is an integral part of pre-clinical investigations.

The permeation of bioactive compounds across the intestinal epithelium can occur via transcellular or paracellular routes. Transcellular routes take place via facilitated, passive diffusion or active diffusion through

the cell membrane. Paracellular routes involve the movement of small molecules through the tight junctions of the epithelium cells (Bohn, 2014). However, prior to cellular contact and uptake, diffusion through the mucus layers is required. This is a very important prerequisite for cellular uptake and is largely affected by the charge, size, and viscosity of the delivery polymer and bioactive compound (Bohn, 2014).

Two permeability assays have become prevalent in recent years for the pre-screening of new bioactive compounds. Caco-2 models that are derived from human epithelial cells, representing the enterocyte (brush border of the small and large intestine) barrier of the gastrointestinal tract and parallel artificial membrane permeability assays (PAMPA) are employed to predict transcellular passive permeability (Petit *et al.*, 2016). Both these techniques provide valuable information on the rate at which the bioactive compound permeates the intestinal wall in order to reach the blood circulation (Youdim, Avdeef & Abbott, 2003). Table 2.5 shows a general comparison of the techniques with regard to the type of permeability, preparation required and cost.

Table 2.5

General comparison of PAMPA and Caco-2 (as adapted from Chen, 2008)

	Caco-2	PAMPA
Basis	Cell monolayer	Artificial membrane
Permeability measurement	Summative passive and active absorption	Passive absorption
Preparation	Cell culture up to 21 days	Easy, fast preparation
Cost	High	Low

PAMPA and Caco-2 models are often used as complimentary tests in the same study for comparative reasons. A few selected examples in literature include permeation studies of natural products, e.g. *Silybum marianum* extract prepared as a nanoemulsion (Piazzini *et al.*, 2017b), pharmacologically active flavones and flavanones (Serra, Mendes, Bronze & Simplicio, 2008) and *Vitex agnus*-cactus extract (Piazzini *et al.*, 2017a). Table 2.6 summarises the respective permeability (P_{app} and P_{eff}) values obtained for the different methods. Significant discrepancies are seen between permeability as obtained from PAMPA and Caco-2 by Piazzini *et al*. (2017a and b), where PAMPA generally overestimates the permeability of the compounds. Serra *et al.* (2008) showed very good correlation between the two methods. Good correlation between PAMPA and Caco-2 indicate that passive diffusion may be an important mechanism of permeation of the compound in question. However, other factors can also cause discrepancies between the two methods, for instance PAMPA has the tendency to retain 'sticky' compounds that are very common under natural bioactive compounds (Chen, 2008). Furthermore, the type of PAMPA membrane and cell line can also result in differences.

Table 2.6

Comparative permeability x 10^{-6} (cm/s) obtained for PAMPA and Caco-2 (as adapted from Chen (2008))

Bioactive compounds	Pampa[a]	Caco-2	Reference
Nanoemulsion:			Piazzini *et al.* (2017b)
Silymarin	93.5	51.5	
Taxifolin	6.16	66.9	
Aqueous solution:			
Silymarin	44.7	Not applicable	
Taxifolin	21.0	Not applicable	
Diosmin	Not detected	Not detected	Serra *et al.* (2008)
Hesperidin	Not detected	Not detected	
Naringin	Not detected	Not detected	
Diosmetin	76.1 ± 5.6	76.2 ± 3.5	
Hesperetin	35.7 ± 9.4	41.7 ± 1.4	
Naringenin	25.7 ± 7.3	37.8 ± 2.7	
Nanoemulsion:			Piazzini *et al.* (2017a)
Flavonoids	46.5 ± 5.21	25.0 ± 3.4	
Iridoids	41.29 ± 6.45	24.0 ± 1.8	
Aqueous solution:			
Flavonoids	14.05 ± 1.21	8.1 ± 0.9	
Iridoids	29.49 ± 2.35	Not detected	

[a]PAMPA – All PAMPA membranes were lipid based.

2.3.2. Stability assessment

Stability testing, an essential element of functional product development, evaluates the effect of the environment and formulation on the quality of the bioactive compound or formulated product and is utilised for prediction of its shelf-life, determining proper storage conditions and suggesting labelling instructions (Bajaj et al., 2012). Stability studies should be incorporated at all stages of the product development, including early development and late stage follow-up stability testing (Markens, 2009).

In early stages of product development, stability studies are conducted on the active pharmaceutical ingredient (or plant extract) to gather information about physical and chemical properties (solubility profile, hygroscopicity, thermal- and chemical stability) and to determine a preliminary re-test period and storage conditions (Markens, 2009). Kinetic studies form an integral element of stability assessment and can be defined as investigations into the rates at which change occurs in a specific system or formulation and the factors that affect these changes (Aulton, 1996).

The storage conditions during stability testing are usually designed specifically for a product or formulation in order to investigate factors that are significant to the specific product and its end use. However, a general method to ease the stability testing is required for standardisation (Aulton, 1996). The international council for

harmonisation of technical requirements for pharmaceuticals for human use (ICH) guidelines prescribe stability testing conditions according to suitable climatic zone as these will best simulate the conditions that the product will most likely be exposed to during processing and storage. South Africa falls under Zone II (Mediterranean, Subtropical) which prescribes normal testing protocol of 25 °C and 60% relative humidity (RH) for 12 months and accelerated stress testing protocol of 40 °C and 75% RH for 6 months (Markens, 2009; EMEA, 2003). If significant changes occurs (5% from original measured value) in the first three months of accelerated storage, additional short-term stability tests and reports are required. Care should also be taken when selecting the packaging, testing frequency and batch (EMEA, 2003) and the additional applied considerations. For example, a bioactive compound packaged in a semi-permeable container should be monitored for water loss or gain.

Fig. 2.3 shows the use of results obtained from accelerated testing to predict to the amount of change in a product after long storage periods under 'normal' conditions (Aulton, 1996). There are several problems and limitations with accelerated storage testing. Firstly, the reaction order could possibly change over time and the decomposition in formulated products may follow various routes and complex reactions that are difficult to track under accelerated conditions. Secondly, there is a possibility that the accelerated storage conditions result in reactions that do not usually occur under normal conditions. Thirdly, when data is extrapolated by the fitting of kinetic models and regression methods (EMEA, 2003) to 'normal' conditions, care must be taken to define conditions as there is a degree of uncertainty regarding the conditions that the end product will be exposed to (Aulton, 1996). The stipulated normal conditions are usually product specific. In final product evaluations, the extrapolated data is usually confirmed by a retest based on the extrapolated results (EMEA, 2003).

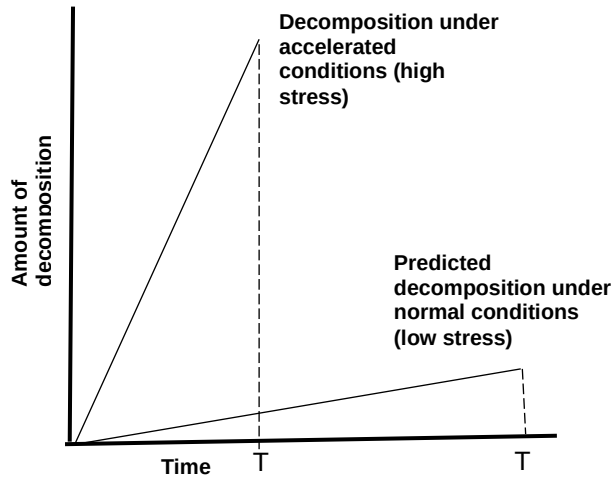

Fig. 2.3 Use of accelerated testing to predict stability under normal stress conditions (adapted from Aulton (1996).

2.3.2.1 Degradation kinetics modelling

The design of products and formulations in the nutraceutical/functional food industry tend to be highly quality orientated. Traditional trial-and-error methods for stability prediction tend to be time consuming and not the preferred due to high demands for product output in the food and pharmaceutical industry (Van Boekel, 2008). Kinetic modelling, a more systematic approach, has found increased application to derive the basic kinetic information of active compounds, formulations or final products. Kinetic information and models can be utilised to predict and understand the chemical degradation during storage (Van Boekel, 1996; 2008).

Chemical reaction kinetics are generally based on homogenous reactions in the gas and liquid phases, however, solid-state kinetics usually cannot be defined as a homogenous system, but rather as heterogeneous. It is important to note that similar kinetics are used with a few assumptions and factors to consider. For example, factors such as particle size, geometric shape, and interfacial area are unique to heterogeneous systems and must be dealt with accordingly (Khawam & Flanagan, 2006).

Consider the following reaction (Eq. 2.1):

$$A \rightarrow B + C \qquad (2.1)$$

The rate of the reaction is often proportional to the concentration of the reactants and products present raised to a fractional power or integer (Khawam & Flanagan, 2006) as shown in Eq. 2.2:

$$(r) \propto [A]^n \text{ or } \propto ([A]_0 - [B])^n \text{ or } \propto ([A]_0 - [C])^n \qquad (2.2)$$

Where (r) is the reaction rate, $[A]_0$ is the initial concentration of A and n is the reaction order. Reaction rates are usually studied as a decrease in concentration of specific compounds of interest. Therefore, the reaction rate becomes (Eq. 2.3):

$$r = \frac{d[A]}{dt} = -\frac{d[B]}{dt} = -\frac{d[C]}{dt} = -k[A]^n \text{ or } = -k([A]_0 - [B])^n \text{ or } = k([A]_0 - [C])^n \qquad (2.3)$$

Where k is the reaction rate constant. In most cases, the compounds of interest are investigated individually and the equation can be simplified to the general rate law for a single reactant at concentration c (Eq.2.4):

$$r = \frac{d[c]}{dt} = k[c]^n \qquad (2.4)$$

The order of the reaction is an important parameter that should be based on the most suitable model for the specific data. The integrated forms of zero order (Eq. 2.5), first order (Eq. 2.6), second order (Eq.2.7) and fractional conversion (Eq.2.8) models are shown below:

Zero order: $c = c_0 - kt$ (2.5)

First order: $lnc = lnc_0 - kt$ (2.6)

Second order: $\frac{1}{c} = \frac{1}{c_0} + kt$ (2.7)

Fractional conversion: $c_\infty + (c_0 - c_\infty) \times \exp(-k \times t)$ (2.8)

Reactions of the third order or higher can be defined as reactions where the rate of change of the reactants and products is proportional to three concentration terms. Such reactions are unlikely to occur and their analysis is very complex (Van Boekel, 1996).

The reaction order is usually determined by means of two methods: The graphical method or the substitution method. The graphical method involves the plotting of the kinetic data in a form that is relevant to the order. If a straight line is obtained with the chosen order and the slope and intercepts are valid for the equation, it can be concluded that the specific reaction follows the chosen reaction order. In the substitution method, a reaction order is initially assumed in the rate equation and the integrated forms are used to obtain a mathematical expression that relates the concentration $[c]$ with time (*t*). The mathematical equation that best fits the changes in the experimental data with the reaction time (best R^2 value) is then selected as representative of the reaction order (Aulton, 1996).

Kinetic modelling can subsequently be used to predict the shelf-life at various storage conditions. The effect of temperature on the rate constant is usually indicated by the Arrhenius equation, Eq. 2.9 (Aulton, 1996):

$$k = Ae^{-E_a RT} \quad (2.9)$$

or the integrated form written as Eq. 2.10:

$$lnk = -\left(\frac{E_a}{R}\right).\frac{1}{T} + \ln[c] \quad (2.10)$$

where A is the so called 'pre-exponential' factor, E_A is the activation energy, R is the gas constant and T is the absolute or thermodynamic temperature (Van Boekel, 2008). The 'pre-exponential' factor can be physically defined as the rate constant where all the molecules have sufficient energy to interact. The Arrhenius equation provides the above information in a quantitative manner and can be practically applied as follows: A graph of *log k* versus*1/T* will result in a straight line. The values for E_A and A can be determined from the slope and intercept of the line, respectively. From this, it is possible to determine the values for rate constants at other temperatures by intra- and extrapolation. The reaction rates obtained from the Arrhenius equation can then be substituted into the appropriate rate equation that applies to the order of the reaction and allow calculation of the predicted amount of degradation after a given time.

2.3.2.2 Stress conditions affecting the storage stability and degradation kinetics

The following section will outline the importance of various stress factors and their effects on the storage stability of polyphenolic compounds. This will be discussed by reviewing selected examples in literature that report on stability testing. The stress factor and its specific effect will be emphasised. Various examples of plant extracts and/or specific phenolic compounds in solid or liquid state are available in literature,

demonstrating the effect of stress factors on degradation or stability of compounds. A few studies were selected and summarised in Table 2.7 to illustrate the relevant effects.

2.3.2.2.1 Temperature

Generally, an increase in the rate of chemical reactions are seen with an increase in temperature. This has been shown for model isoflavone solutions from soybeans (Ungar, Osundahunsi & Shimoni, 2003), 3-*O*-methylquercetin, caffeic acid, quercetin and luteolin from *Achyrocline satureiodes* spray-dried powder (Holzschuh, Silva, Schapoval & Bassani, 2007), anthocyanins from spray-dried black currant polyphenols (Bakowska-Barczak & Kolodziejczyk, 2011) and epigallocatechin gallate (EGCG) powder (Li, Taylor & Mauer, 2014). Additionally this has also been observed for gallic acid, vanillic acid and catechin from vegetal extracts (Volf, Ignat, Neamtu & Popa, 2014), xanthones and benzophenones in honeybush plant material (Beelders, De Beer & Joubert, 2015) and xanthone and benzophenone model solutions (Beelders, De Beer, Ferreira, Kidd & Joubert, 2017). The extent of this rate increase depends on the specific compound. Generally, a 10 °C increase in temperature produces a 2- to 5- fold increase in degradation rates (Aulton, 1996).

It is important to investigate thermal stability, as changes in temperature will occur during processing and storage. Bakowska-Barczak & Kolodziejczyk (2011) investigated the stability of soybean phenolic compounds in solution at 70, 80 and 90 °C during sterilisation, while Beelders *et al.* (2015) investigated the stability of phenolic compounds in honeybush plant material at 80 and 90 °C during oxidation. Furthermore, thermal stability provides an overview of the overall storage stability of a product or a specific phenolic compound. Beelders *et al.* (2017) conducted an in-depth kinetic study on the degradation and conversion of benzophenones and xanthones in aqueous solutions in order to elucidate degradation products. The data was fitted to a first order model which is commonly used for phenolic compounds (Ungar *et al.*, 2003).

Similar to aspalathin found in rooibos, dihydrochalcones from apples are also affected by temperature. A study done by De Paepe *et al.* (2014) ranked the thermostability of the dihydrochalcones in cloudy apple juice in the following order: phloretin-2′-*O*-glucoside > 3-hydroxyphloretin-2′-*O*-xylosylglucoside > 3-hydroxyphloretin-2′-*O*-glucoside according to first order kinetic rates determined over a temperature range of 85 -145 °C.

2.3.2.2.2 pH

The effect of pH on the degradation rates of chemical reactions is strongly dependent on the chemical nature of the active compound in question. The effect of pH comes into play during solubilisation of formulations for delivery or incorporation of functional ingredients into complex food matrices (Aulton, 1996).

Most of the studies found in literature were based on the combination of pH and temperature indicating a significant interaction of the two factors.

Generally, degradation rates for phenolic compounds (based on first order kinetic models) increase at higher pH values as shown for genistein and daidzen solutions (Ungar *et al.*, 2003), caffeic acid, chlorogenic acid and gallic acid solutions (Friedman & Jurgens, 2000) and catechins from green tea infusions (Li, Taylor, Ferruzzi & Mauer, 2012). However, even though all these compounds have an increased degradation rate above a pH of 7, the optimum pH value for the acidic range differ for each compound. Li *et al.* (2012) and Canales, Borrego & Lindley (1993) found optimum pH values of 4 and 5 for catechins and neohesperidin dihydrochalcone, respectively, where an increase in degradation rate was seen below a pH 4.

2.3.2.2.3. Moisture and relative humidity (RH)

Substances that are affected by relative humidity or have the ability to take up water are defined as having a degree of hygroscopicity. The uptake of moisture from atmospheres with high RH could lead to an accelerated rate of decomposition by the process of hydrolysis (Aulton, 1996). However, RH will only have an effect on a substance that is not enclosed in a form of packaging or protective layer. Accelerated storage tests are usually performed on such substances in order to establish the extent of protection that the packaging should provide to ensure the required storage stability.

ICH guidelines prescribed a normal testing protocol of 25 °C and 60% RH and an accelerated stress testing protocol of 40 °C and 75% RH for pharmaceutical products (EMEA, 2003). Many reported studies, however, used temperature/humidity conditions deemed relevant during processing or storage. Examples include the stability of malonylgenistin, acetylgenistin, genistin and genistein in powders (Chien, Hsieh, Kao & Chen, 2005), flavone *C*-glycosides in spray-dried *Passiflora alata* extracts (Bott, Labuza & Oliveira, 2010), green tea powder (Li, Taylor & Mauer, 2011) and EGCG powder (Li *et al.*, 2014) which all showed a decrease in phenolic stability (based on zero and first order kinetic models) when exposed to higher RH values. In addition to chemical changes, Li *et al.* (2014) showed the effect of moisture on physicochemical characteristics such as unwanted crystallisation in the presence of moisture.

2.3.2.2.4 Light

Photochemical degradation is catalysed by light. Generally the effect of light is tested by exposing the sample to a light source with a similar wavelength as that of ultra-visible (UV) light (Aulton, 1996). Such tests are carried out with the purpose to establish the extent of protection that the packaging and pre-formulation of the functional ingredient design should provide to ensure the required storage stability.

Results for UV exposure vary for different phenolic compounds. Extracts containing gallic acid, vanillic acid and catechin (Volf *et al.*, 2014); anthocyanin solutions (Bobbio, Do Nascimento Varella & Bobbio, 1994); *Achyrocline satureiodes* spray-dried powder which contained 3-*O*-methylquercetin, caffeic acid, quercetin and luteolin solutions (Holzschuh *et al.*, 2007) all showed increased degradation when exposed to light, when compared to darkness. No kinetic models were applied to assess the degradation, except for half-life values calculated by Bobbio *et al.* (1994) as very few process parameters were investigated other than light and dark conditions.

2.3.2.2.5 Oxygen

The presence of oxygen can also lead to unfavourable oxidation reactions and products (Aulton, 1996) and usually occurs by the loss of hydrogen. This greatly affects the properties of polyphenolic compounds as these compounds function as antioxidants by providing labile hydrogen cations. The effect of oxygen can be tested by the removal of oxygen in the immediate atmosphere of the formulation or substance. Oxidation, however, can also be catalysed by various other oxidising agents and these must also be taken into account to ensure stability (Aulton, 1996). The effect of oxygen on a functional ingredient product becomes important during processing, as well as in the final packaging.

Varying results were found for the effect of oxygen in selected studies as modelled using mainly first order kinetics. A decrease in the stability of quercetin and rutin buffer solutions were found under oxidative conditions as well as for EGCG solutions tested at different levels of dissolved oxygen (0-100%). However, Van der Sluis, Dekker & Van Boekel (2005) found that phloridzin and quercetin in apple juice were unaffected by changes in oxygen levels between 0.21-100%.

Table 2.7

Summary of a few selected examples found in literature on the effect of different stress conditions on phenolic compounds, including the kinetic model utilised, type of phenolic compound and effect of the stress condition

Active compound and/or formulation	Conditions and Analysis	Kinetic model	Effect of stress condition	Reference
		Stress condition: temperature		
Cyclopia genistoides plant material: xanthones and benzophenones	Temperature: 80 and 90 °C HPLC-DAD[a]	First order Q_{10} values	Decrease in stability with increased temperature Degradation rates increased by 1.40 to 1.72 -fold with 10 °C increase in temperature	Beelders *et al.* (2015)
Spray-dried microencapsulated black currants: anthocyanins	Temperature: 8 and 25 °C HPLC-ESI-MS/MS[b]	No model	Anthocyanins and polyphenols decreased with 24–23% and 8–11% respectively at 25 °C Anthocyanins and polyphenol content unchanged at 8 °C	Bakowska-Barczak & Kolodziejczyk (2011)
Cloudy apple juice: dihydrochalcones and quercetin glucosides	Temperature: 85–145 °C LC-MS[c]	First order Arrhenius	Dihydrochalcones were most heat stable Quercetins were less stable – large difference between degradation rates for different quercetin glucosides	De Paepe *et al.* (2014)
Model solutions: Xanthones and benzophenones	Temperature: 70–130 °C with 10 °C shifts depending on compound UHPLC-DAD[d], LC-ESI-MS/MS	First order Arrhenius	Different compounds had different degree of stability Xanthones had higher stability than benzophenone analogues Cyclisation, isomerisation, dimerisation, acetylation and hydrolysis observed	Beelders *et al.* (2017)
		Stress condition: temperature and/or pH		
Model solutions: Genistein and daidzein isoflavones	Temperature: 70, 80 and 90 °C pH: pH 9 and 7 HPLC analysis	First order Arrhenius	Increased temperature resulted in a decreased genistein and daidzein Increased pH resulted in a decreased genistein and daidzein	Ungar *et al.* (2003)
Model solutions: neohesperidin and dihydrochalcone	Temperature: 30–60 °C pH: 1 - 7	Pseudo first order Arrhenius	Increased pH up to 4 or 5 showed an increased half-life of neohesperidin dihydrochalcone, followed by a decrease up to pH 7 Increased half-life of neohesperidin dihydrochalcone at lower reaction temperatures Neohesperidin dihydrochalcone more temperature sensitive at low pH values	Canales *et al.* (1993)
Model solutions: standards found in green tea infusions	pH: 3–7 Temperature: 25–95 °C HPLC-DAD	First order Arrhenius	Low degradation rates below pH 5, followed by increased rates up to pH of 7 Increased degradation rates at higher temperatures	Komatsu *et al.* (1993)
Model solutions: Caffeic acid, catechin, chlorogenic acid, ferulic acid, gallic acid, EGCG and rutin	pH: 3–11 UV-VIS[e]	No model	Unstable at high pH values: Caffeic acid, chlorogenic acid, and gallic acid Other compounds resisted changes at high pH	Friedman & Jurgens (2000)
Green tea infusion: catechins	pH: 1.5–7.0 Temperature: 25–120 °C	First order Arrhenius	Increased reaction rate constant with increased temperature Catechins were most stable at pH values below 4 and above pH 5 degradation accelerated	Li *et al.* (2012)

Table 2.7 Continued

Active compound and/or formulation	Conditions and Analysis	Kinetic model	Effect of stress condition	Reference
		Stress condition: temperature and/or moisture		
Isoflavones: MG[f], AG[g], G[h] and Ge[i]	Temperature: 100 and 200 °C Moisture: wetting samples	Consecutive reaction First order	More rapid degradation in presence of moisture Increased degradation rate with increased temperature	Chien *et al.* (2005)
Spray and spouted bed dried extracts of *Passiflora alata:* vitexin and *C*-glycoside flavone	Temperature: 34 and 45 °C RH[j]: 52 and 60% HPLC	Zero and first order	Increased degradation rate with increased in humidity and temperature	Bott *et al.* (2010)
Green tea powder: catechins	RH: 1-97% Temperature: 25- 60 °C HPLC	First order Arrhenius	Increased degradation rates increased with increased temperature and RH.	Li *et al.* (2011)
Powder: EGCG[k]	Moisture sorption isotherms (25, 35 and 45 °C) Temperature: 40,60 and 80 °C RH: 75-97% XRD[l], TGA[m] and DSC[n] and colour stability	Arrhenius	Chemical and physical stability significantly affected by moisture XRD showed recrystallisation in presence of moisture Epimerisation and oxidation at higher RH values and temperature	Li *et al.* (2014)
		Stress condition: Temperature and/or light		
Vegetal extracts: gallic acid, vanillic acid and catechin	Temperature: 60, 80 and 100 °C Light: stirred batch photo reactor HPLC and colometric methods	No model	5 hours of UV exposure: 40-83% degradation 4 hours of high temperature treatment: 15-30% degradation Extract was more stable than individual compounds	Volf *et al.* (2014)
Achyrocline satureiodes spray-dried powder: 3-O-methylquercetin, caffeic acid, quercetin and luteolin solutions	Temperature: 50, 80 and 90 °C Light: amber or transparent packaging	No model	Good stability against UV exposure Luteolin and 3-*O*-methylquercetin were most stable Total polyphenol content remained acceptable at normal storage conditions	Holzschuh *et al.* (2007)
DMSO[o] and water solutions: anthocyanins	Light: light and dark conditions UV spectrophotometer	Half-life values	Half-life values of the samples stored in the dark were significantly higher than the samples exposed to light	Bobbio *et al.* (1994)
Model creams: EGCG	Light: Solar radiance source comparable to sunlight Addition of co-antioxidants HPLC-UV and HPLC-ESI-MS/MS *In vitro* antioxidant assay	No model	α-lipoic acid and vitamin C prevented photodegradation Butylated hydroxytoluene had no effect Vitamin E enhanced photolysis	Scalia, Marchetti & Bianchi (2013)

Table 2.7 Continued

Active compound and/or formulation	Conditions and Analysis	Kinetic model	Effect of stress condition	Reference
		Stress condition: Temperature and/or oxygen		
Model solutions: Quercetin and rutin	Oxygen: Oxidative and non-oxidative conditions pH: 8 Temperature: 97 °C HPLC and UV-VIS	Rate constants calculated, but no kinetic model stated	Quercetin and rutin declined with 16% and 22% respectively under non-oxidative conditions quercetin and rutin declined with 98% and 48% respectively under oxidative conditions	Makris & Rossiter (2000)
Model solution: EGCG	Oxygen: 0–100% dissolved	Pseudo first order Arrhenius	Increased degradation rate with increased amount of dissolved oxygen	Zimeri & Tong (1999)
Enriched apple juice: dihydrochalcones and quercetin glucosides	Temperature: 70-100 °C Oxygen: 0, 21 and 100% Antioxidant activity	First order Arrhenius	Phloridzins showed best stability Quercetin compounds found to be more unstable Phloridzin and quercetin compounds were unaffected by oxygen levels	Van der Sluis *et al.* (2005)

[a]HPLC-DAD - High pressure liquid chromatography-diode array detector
[c]LC-MS - Liquid chromatography mass spectroscopy
[d]UHPLC-DAD - Ultra HPLC-DAD
[e]UV-VIS - Ultra Violet visible spectroscopy
[f]MG - malonylgenistin
[g]AG - acetylgenistin
[h]G - genistin
[i]Ge - genistein
[j]RH - Relative humidity
[k]EGCG - epigallocatechin gallate
[l]XRD - X-ray diffraction
[m]TGA - Thermogravimetric analysis
[n]DSC - Differential scanning calorimetry
[o]DMSO - Dimethyl sulfoxide

2.4 Technological strategies for the design of functional ingredients

2.4.1 Microencapsulation

This section will introduce the concept of microencapsulation and provide an overview of the methods and encapsulation materials used for microencapsulation in the food and nutraceutical industry, highlighted by present research concerning the microencapsulation of polyphenols.

Microencapsulation technology has been implemented in the food industry for more than 60 years. The process of microencapsulation can be broadly defined as the encapsulation of materials in the solid, liquid or gaseous phase into micron sized particles or packagings (Desai & Park, 2005b). The capsule material is often referred to as the wall, coating, carrier or shell material, depending on the encapsulation technique and goal of the encapsulation, whereas the encapsulated material is often referred to as the core material (Fang & Bhandari, 2010).

In the microencapsulation process the micron sized particles can be in the form of microcapsules or microparticles, often referred to as microspheres. Microcapsules are utilised most often in the food industry and can be of the matrix or reservoir type (Desai & Park, 2005b). The reservoir type of microcapsule (Fig. 2.4A) consists of the core material surrounded and sealed in by the encapsulating material. The matrix type of microcapsule refers to a system where the core material is embedded in the encapsulating material in the form of individual droplets (Fig. 2.4B) (Ré, 1998). This classification of microcapsules can be further refined to accommodate the addition of a polynuclear system. The latter is ultimately a matrix type, but rather than the core material just being embedded, it exists as numerous smaller cores in the wall material (Fig. 2.4C) (Sri.s, Seethadevi, Prabha, Muthuprasanna & Pavitra, 2012).

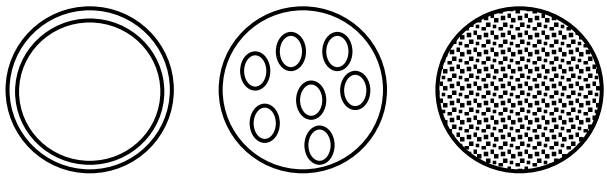

Fig. 2.4 Different types of microcarriers: (A) reservoir type, (B) matrix type, (C) polynuclear type

Microencapsulation technology can be utilised for increased solubility of specific ingredients, addition of bioactive compounds to a food system, protection of bioactive compounds against environmental degradation, masking of unwanted flavours, modification of physical characteristics and to tailor ingredients to a specific release site and thus increase the bioavailability (Desai & Park, 2005a; Fang & Bhandari, 2010). The protection of the core material from adverse environmental conditions including moisture, oxygen and light, is important

to the food industry, as the type of bioactive compounds of interest are usually inherently susceptible to environmental degradation (Desai & Park, 2005b).

In designing an appropriate microencapsulation process and system various factors need to be taken into consideration. It is important to clarify the purpose of the encapsulation, followed by the desired properties of the microcapsules (Desai & Park, 2005b).

The following section will provide an overview of the different microencapsulation methods used in industry with focus on the use of spray-drying.

2.4.1.1 Spray-drying

Spray-drying has been used by the food industry since the 1950's and is still very relevant today as a method for microencapsulation. A liquid feed is transformed into a convenient powdered product in a one-step processing unit operation. Fig. 2.5 shows an image of a typical laboratory-scale spray-drier.

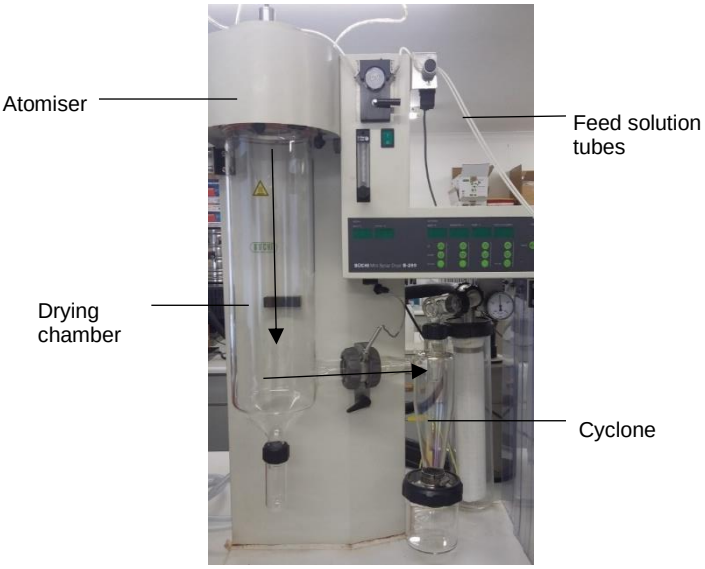

Fig. 2.5 Büchi B-290 mini spray-drier (Büchi Labortechnik AG, Flawil, Switzerland) (air flow is indicated by arrows).

The continuous processing operation involves a series of stages including atomisation, contact of the droplet with hot air, evaporation of the solvent of the droplet and separation of the dry product from the drying air (Ré, 1998). The atomisation process refers to the formation of small liquid droplets suspended in a gas. The smaller and more homogenous the droplets, the larger the surface area to facilitate heat and mass transfer between the liquid and hot dry air (Murugesan & Orsat, 2012). Apart from facilitating heat transfer, small droplets are a pre-requisite for the formation of homogenously dried small powder particles. Atomisers are selected according to the type of feed solution and the targeted properties of the powder. Types of atomisers

used in spray-driers include rotary or centrifugal atomisers, pressure atomisers, pneumatic (two fluid) atomisers and sonic atomisers (Murugesan & Orsat, 2012; Ré, 1998).

After atomisation, the drying process usually proceeds through external and internal mass and heat transfer control, where the external moisture is removed first (Ré, 1998). The heat of the drying medium is transferred to the outer parts of the droplets by convection, followed by conversion to latent heat as evaporation takes place. As the drying process continues and the surface dries out, the moisture must be transported from the internal regions to the external regions of the droplet (Ré, 1998). The removal of the internal moisture depends on the diameter and relative velocity of the particles and drying air (Murugesan & Orsat, 2012). Once the particle is completely dry, the final shape of the particle is set.

After the drying process, the particles fall to the bottom of the drying chamber and travel with the outgoing air to a cyclone or bag filter where the dry product and humid air are separated.

The effect of spray-drying parameters are well known. The inlet air temperature, feed concentration, feed temperature, feed flow rate and drying air flow rate have the most significant effect on the properties of spray-dried powders (Patel, Patel, Chakraborty & Shukla, 2015). The effects of these parameters on the moisture content, particle size, yield and outlet temperature are summarised in Table 2.8. It is important to note that the outputs will affect the properties of the final product. For instance, a product will have higher storage stability and better bulk powder properties if it has a lower final moisture content (Malthlouthi, 2001). To achieve this, higher inlet temperatures, aspirator rates and inlet feed concentrations are required.

Table 2.8

Influence of various spray-drying process parameters on process outputs (Patel *et al.*, 2015)

Input parameters	Outputs			
	Particle size	Moisture content	Outlet temperature	Yield
Increased inlet temperature	No effect	Decrease	Increase	Increase
Increased spray-drying feed solution feed rate	Increased	Increase	Decrease	Increase
Increased aspirator rate	No effect	Decrease	Increase	Increase
Increased drying air flow rate	Decrease	No effect	Decrease	No effect
Increased feed solution concentration or viscosity	Increase	Decrease	Increase	Increase
Increased humidity of drying air	No effect	Increase	Increase	No effect

As the spray-drying parameters affect more than one powder property at a time, it is important to take into account the overall effect of the different parameters to obtain a product with the best set of properties. To achieve this, multivariate statistical method in conjunction with response surface methodology (RSM) is a

viable option. Miller *et al.* (2018) applied RSM methodology to optimise the physicochemical properties of a spray-dried aqueous green rooibos nutraceutical extract. The input parameters included the aspirator rate, inlet air temperature, feed solution concentration, drying air rate, feed solution flow rate where the monitored outputs included the yield, aspalathin retention, moisture content and mean outlet temperature. The data indicated that at the chosen levels, only the inlet air temperature and feed solution concentration had a significant effect on the yield and no significant effects were seen for the moisture content, aspalathin retention and mean outlet temperature. From this, optimum spray-drying conditions were obtained.

2.4.1.1.1 Microencapsulation by spray-drying

Spray-drying is most often considered as a dehydration technique for the drying of liquids and pastes. However, the process can also be used for microencapsulation and is regarded as one of the cheapest microencapsulation methods (Desorby, Netto & Labuza, 1997). The process involves a similar protocol as for conventional spray-drying, but in this case components used to prepare the feed solution are selected with microencapsulation in mind. These components usually include the core material (bioactive compound or functional ingredient), encapsulating material, solvent and depending on the nature of the constituents, an emulsifier. In the latter case, the core material must be dissolved in the encapsulating material to form a stable emulsion (Gharsallaoui, Roudaut, Chambin, Voilley & Saurel, 2007). All the components can affect the properties of the final spray-dried powder.

An important limitation is the limited number of encapsulating materials available for this process. The majority of the spray-drying operations in the food industry are carried out in an aqueous medium, which requires the encapsulating material to be water soluble (Desai & Park, 2005b). Spray-drying encapsulation can be performed with encapsulating materials of low water solubility, but the process becomes tedious and more expensive as much lower feed concentrations are required, impacting negatively on running time and production output.

Apart from the inherent solubility, the consistency of the feed solution must also be considered. It has been found that the particles formed from a suspension feed have better flow properties than these from a solution feed. In the case of suspensions, the active ingredient is usually already encapsulated in the encapsulating material in the feed solutions, resulting in smoother spray-dried particles (Wan, Heng & Chia, 1992). The formation of smooth, flowable particles is also largely affected by the chemical composition of the polymeric encapsulating material and to a lesser extent, the viscosity (Bodmeier & Chen, 1988). The dispersion of the liquid into droplets is governed by the intermolecular bonds between the chains of the wall material and the

interactions present between the solvent, wall material and core material to be encapsulated (Jalil & Nixon, 1990).

Another factor to consider is the ratio of the core material to encapsulating material. This also affects the final properties of the microcapsules, especially the encapsulation efficiency of the core material. Bodmeier & Chen (1988) and Takeuchi, Handa & Kawashima (1989) found that an increased amount of encapsulating material resulted in a higher degree of encapsulation. The higher encapsulation efficiencies can be attributed to the presence of agglomerates of core material at low concentrations of the encapsulating material where the core material is distributed in the encapsulating material at higher concentrations (Ré, 1998). The ratio of the core material to encapsulating material has also been shown to affect the morphology of spray-dried particles (Bodmeier & Chen, 1988; Takeuchi *et al.*, 1989).

2.4.1.1.2 Encapsulating materials used in microencapsulation by spray-drying

Encapsulating material for microencapsulation should be an inert substance with adequate film forming ability and good rheological properties to coat the core material. These materials should also be inert toward or compatible with the core active material, as well as abundantly available and cost effective (Sri.s *et al.*, 2012).

Apart from the inherent properties that an encapsulating material should possess, a range of other properties should also be taken into consideration. These include its coating properties that depend on its density, crystallinity, solubility, and crosslinking abilities. Other properties to be considered are the behaviour of the material in different pH, temperature, solvent and mechanical environments (Murugesan & Orsat, 2012). In addition to the characteristics of the encapsulating material, the desired properties of the final product should also be taken into account. These include the desired particle size, coating thickness, conformity of the particles, colour of the dried powder, flow properties and shelf-life (Murugesan & Orsat, 2012).

Hence, selection of an encapsulation material is a very important step for the production of a successful microencapsulated spray-dried product. The wide variety of suitable encapsulating materials available include carbohydrates (starch, cyclodextrins, maltodextrins, chitosan, xhantan gum and corn syrup solids), gums (gum arabic, agar and sodium alginate), proteins (gelatin, soy protein and whey protein), lipids (oils, paraffin, wax and fats) and cellulose derivatives (carboxy methylcellulose, methylcellulose and ethylcellulose). Of these carbohydrates are used most commonly (Murugesan & Orsat, 2012).

Some of the most common encapsulation materials suitable for spray-drying are summarised in Table 2.9 accompanied by a description of their chemical structure and properties, as well as some of the disadvantages associated with their use.

Table 2.9

Summary of common food grade encapsulation materials suitable for spray-drying accompanied by their chemical structures and properties.

Wall material	Structure	Properties	Disadvantage
Inulin	β(2-1) glycoside bonded fructan containing either terminal β-D-glucose or fructose Degree of polymerisation of 2 to 60 units (Kawai, Fukami, Thanatuksorn, Viriyarattanasak & Kajiwara, 2011)	Prebiotic health benefits Water soluble Natural source of fibre (Ronkart, Paquot, Fougnies, Deroanne & Blecker, 2009; Sun-Waterhouse, 2011)	Contribute to negative sensory attributes if concentration is too high (Sun-Waterhouse, 2011)
Maltodextrin	Saccharide polymer composed of D-glucose, maltose, polysaccharide and oligosaccharides Dextrose equivalent of less than 20 (Cortés-Rojas & Oliveira, 2012)	Cheap, water soluble, easy to use, readily available, versatile (Silva, Stringheta, Teófilo & De Oliveira, 2013) Good oxidative stability (Gharsallaoui *et al.*, 2007)	Highly refined structure (Englyst, Veenstra & Hudson, 1996) Poor emulsifying abilities (Gharsallaoui *et al.*, 2007)
Chitosan	Linear biopolyaminosaccharide Obtained from the deacetylation of chitin Consists of one primary amino group that carriers a positive charge and two hydroxyl groups (Sinha *et al.*, 2004)	Biodegradable, biocompatible, hydrophilic polymer Mucoadhesive properties in the digestive tract Natural source of fibre (Desai & Park, 2005a; Kosaraju, D'Ath & Lawrence, 2006).	Requires a slightly acidic medium to dissolve completely Moderate to poor drug retaining capacity (Desai & Park, 2005a; Kosaraju *et al.*, 2006)
Gum arabic	D-glucoronic acid, L-rhamnose, D-galactose and L-arabinose polymeric material with 2% protein (Gharsallaoui *et al.*, 2007)	Good film forming and emulsion stabilisation properties Stable over a wide pH range (Gharsallaoui *et al.*, 2007)	Costly and limited supply Quality variations were found (Gharsallaoui *et al.*, 2007)
Cyclodextrin	Cyclic derivative of hydrolysed maltodextrins and other starches Common cyclodextrins are made up of 6-8 glucose units (Da Rosa *et al.*, 2013)	Superior protection to volatile and sensitive compounds (Da Rosa *et al.*, 2013) Fast dissolution rate and produces powders with a low a_w[a] (Sun-Waterhouse, Wadhwa & Waterhouse, 2013)	Limited to the encapsulation of compounds that are less polar than water (Desai & Park, 2005b)
Pectins	Complex polysaccharides, mainly α-1,4-linked D-galacturonic acid units. Found in the walls of plant cells (De Souza *et al.*, 2013)	Stable emulsions at very low concentrations Soluble in aqueous medium Natural dietary fibre Readily available and inexpensive (De Souza *et al.*, 2013)	Highly viscous Hygroscopic (Sansone *et al.*, 2011a)
Alginates	Natural occurring polysaccharide Consists of β-D-mannuronic acid and α-L-guluronic acid (Sun-Waterhouse *et al.*, 2013)	Low a_w powders Controlled release delivery (Sun-Waterhouse *et al.*, 2013)	Poor mechanical stability High viscosity when reconstituted (Sun-Waterhouse *et al.*, 2013)

[a]a_w - Water activity

2.4.1.1.3 Microencapsulation of polyphenols by spray-drying

Given that the focus of this study is on the development of a functional rooibos food ingredient with improved stability and increased adsorption of its polyphenols *in vitro*, the next section will discuss relevant examples from literature. Table 2.10 provides a summary of literature on the microencapsulation of phenolic compounds or polyphenol-rich extracts, focusing on the type of carrier used and the main outcomes of the studies.

The spray-drying and microencapsulation of procyanidins and anthocyanins have been widely studied where the focus was mainly on the type of encapsulating material and spray-drying conditions (Zhang, Mou & Du, 2007; Tonon, Brabet & Hubinger, 2008; Robert *et al.*, 2010; Bakowska-Barczak & Kolodziejczyk, 2011;

Chik, Abdullah, Abdullah & Mustapha, 2011; Silva *et al.*, 2013). Of the various factors that play a role during spray-drying microencapsulation, inlet temperature is one of the most investigated. Tonon *et al.* (2008), De Souza, Thomazini, Balieiro & Fávaro-Trindade (2015) and Bakowska-Barczak & Kolodziejczyk (2011) showed a decrease in anthocyanin content as a function of the inlet temperature, indicating that the inlet temperature is a very important parameter to control as it affects the bioactivity of the compounds.

Apart from the spray-drying process, addition of microencapsulating materials can greatly affect the final spray-dried product. Tonon *et al.* (2008), Chik *et al.* (2011), Bakowska-Barczak & Kolodziejczyk (2011) and De Souza *et al.* (2015) found the addition of polymers such as maltodextrin or inulin could improve the yield, stickiness, hygroscopicity and overall properties of the spray-dried powders.

Different types of carriers also have different effects on the powder properties. Silva *et al.* (2013) found pure maltodextrin microcapsules proved to achieve optimum characteristics with regard to the moisture content, anthocyanin content and hygroscopicity whereas mixtures of gum arabic and maltodextrin resulted in more homogenous particles. Robert *et al.* (2010) found that soybean protein isolate formulations had significantly higher encapsulation efficiency, but showed poor protection against degradation when compared to the maltodextrin formulations.

Effects of different microencapsulating materials has been shown for various other phenolic compounds other than anthocyanins as well such as flavonoid-rich *Bidens pilosa* plant extract (Cortés-Rojas & Oliveira, 2012), quercetin, vanillin (Sun-Waterhouse, 2011) and gallic acid (Robert, García, Reyes, Chávez & Santos, 2012).

Rather than investigating the effect of different carriers or polyphenols, Saenz, Tapia, Chavez & Robert (2009) focused on the effect of pre-formulation of the spray-dry feed on the final properties where inclusion of the mucilage and pulp from cactus pear resulted in increased encapsulation of phenolic compounds.

The spray-drying of phenolic compounds found in tea and tea extracts has mainly been studied in terms of the stability of the bioactive compounds as they are very susceptible to oxidation. Spray-drying of green honeybush (Pauck *et al.*, 2017), green rooibos (Miller *et al.*, 2018) and EGCG found in green tea (Gomes *et al.*, 2010; Fu *et al.*, 2011; Peres *et al.*, 2011) all showed good phenolic retention after spray-drying with various conditions with and without the addition of microencapsulating materials.

Table 2.10

Summary of literature on the microencapsulation of phenolic compounds focusing on the type of carrier used and the main outcomes of the studies

Type of polyphenol	Carrier	Phenolic determination method	Outcome	Reference
			Procyanidins and Anthocyanins	
Açai fruit anthocyanin	Maltodextrin	UV-VIS[a]	Reduced hygroscopicity and increased anthocyanin retention Decreased yield and anthocyanin retention with increased inlet temperatures	Tonon *et al.* (2008)
Grape seed procyanidin	Maltodextrin and gum arabic mixture	UV-VIS	Enhanced stability Procyanidin retention not adversely affected	Zhang *et al.* (2007)
Pomegranate anthocyanin	Maltodextrin and soybean protein isolates	Folin-Ciocalteu colorimetric assay	Protected by maltodextrin during storage Higher encapsulation efficiency for the soybean protein isolates	Robert *et al.* (2010)
Black currant cultivar anthocyanin	Maltodextrin and inulin	UV-VIS	Highest polyphenol retention for maltodextrin Overall decrease in polyphenols for spray-drying	Bakowska-Barczak & Kolodziejczyk (2011)
Pitaya fruit anthocyanin	Maltodextrin (10 DE[b], 15 DE and 20 DE)	DPPH[c] colorimetric assay	DE values had no effect Increased retention with ascorbic acid addition No effect for citric acid addition	Chik *et al.* (2011)
Jabotica peel extract anthocyanin	Maltodextrin, gum arabic and mixtures thereof	UV-VIS	Optimum moisture content, anthocyanin retention and hygroscopicity for maltodextrin powders More homogenous particles produced by mixtures of carriers	Silva *et al.* (2013)
Grape waste products	Maltodextrin		Moisture content and anthocyanin retention affected by inlet temperature Hygroscopicity affected by maltodextrin	De Souza *et al.* (2013)
			Herbal teas	
Green rooibos extract	Maltodextrin and inulin	HPLC-DAD[d]	Optimised spray-drying conditions for powder with low moisture content, high yield and high aspalathin retention Increased flowability for inulin encapsulation Increased aspalathin retention with carriers Decreased water activity with carriers	Miller *et al.* (2018)
Green honeybush extract	Maltodextrin and inulin	HPLC-DAD	Inulin is a suitable healthy replacement for maltodextrin Good retention of phenolic compounds Acceptable moisture content and water activity	Pauck *et al.* (2017)
EGCG[e] from green tea	Mixtures of maltodextrin and gum arabic	DPPH colorimetric assay	Spherical particles Good incorporation of the bioactive ingredient	Peres *et al.* (2011)
EGCG from green tea	No carrier	DCFH-DA[f] colorimetric assay	Reasonable EGCG retention at lower inlet temperatures Sufficient particle morphologies and size	Fu *et al.* (2011)
EGCG from green tea	Maltodextrin and gum Arabic mixtures	UV-VIS spectrophotometry	High retention efficiency Controlled release in pH values similar to that of the intestinal tract	Gomes *et al.* (2010)

Table 2.10 Continued

Type of polyphenol	Carrier	Phenolic determination method	Outcome	Reference
			Other phenolic compounds	
Cactus pear extract and pulp polyphenols	Inulin and maltodextrin	Folin-Ciocalteu colorimetric assay	100% recovery of polyphenols of pulp mixtures Lower polyphenol recoveries for ethanolic extracts	Saenz *et al.* (2009)
Badens pilosa plant extract flavonoids	Maltodextrin, colloidal silica, β-cyclodextrin and microcrystalline cellulose	UV-VIS spectrophotometry	Overall better phenolic retention after spray-drying Superior phenolic retention by β-cyclodextrin encapsulation	Cortés-Rojas & Oliveira (2012)
Quercetin and vanillin	Sodium alginate, hydroxypropylmethyl cellulose, β-cyclodextrin and inulin	HPLC spectrophotometry	Powder morphology affected by type of carrier Desired particle morphologies for sodium alginate and hydroxypropylmethyl cellulose Higher encapsulating efficiencies for quercetin than vanillin	Sun-Waterhouse *et al.* (2013)
Gallic acid	Starch, inulin, acetylated starch and acetylated inulin	Folin-Ciocalteu colorimetric assay	Improved encapsulation efficiency by formulations containing acetylated starch Decreased encapsulation for formulations containing acetylated inulin Fast release rates in water, except acetylated inulin formulation	Robert *et al.* (2012)

[a]UV-VIS - Ultraviolet–visible
[b]DE - dextrose equivalent
[c]DPPH - 2,2-diphenyl-1-picrylhydrazyl
[d]HPLC-DAD - High-performance liquid chromatography with photodiode array detection
[e]EGCG - epigallocatechin gallate
[f]DCFH-DA -Dichloro-dihydro-fluorescein diacetate

2.4.1.2 Alternative methods for microencapsulation

Spray-drying is not only a highly productive process to microencapsulate active ingredients, but it entails a simplified approach and use of readily available equipment. In the following sections, alternative methods used for microencapsulation, especially for specific applications, are briefly discussed. The different techniques, their classifications and characteristics of particles are summarised in Table 2.11.

2.4.1.2.1 Spray-cooling and -chilling

Spray-cooling and -chilling involves the solidification of the microencapsulting material around the core material whilst in an atomised mixture exposed to cooled/chilled air. The process makes use of the large surface areas that are created by the atomisation process to allow rapid cooling and solidification. No evaporation of water and solvent takes place. This process is thus suitable for oil based encapsulating materials that are used to encapsulate water-soluble core materials. Microparticles are usually smooth and perfectly spherical. The technique is usually applied to encapsulating water-soluble core materials such as minerals, enzymes, some flavours and water soluble vitamins in a lipid coating (Desai & Park, 2005b).

2.4.1.2.2 Fluidised bed coating

Fluidised bed coating was originally only utilised in the pharmaceutical industry, but is increasingly used in the food industry for functional ingredients where specific properties are required. The technique is limited to the encapsulation of solid core materials. The process involves the suspension of solid core particles in a high velocity chamber. The particles are subsequently coated with an atomised spray of the encapsulating material (Balassa, Fanger & Wurzburg, 1971). The shells of the capsules are solidified by cooling. The process can be repeated until an acceptable level of coating has been accomplished according to a specific application (Zhao, Pan, Li, Chen & Mujumdar, 2004).

2.4.1.2.3 Lyophilisation

Lyophilisation, commonly known as freeze-drying, is generally used as a dehydration process for heat sensitive materials and aromas (Fang & Bhandari, 2010). The process can be used for microencapsulation by homogenisation of the encapsulating material and core material in a matrix solution suitable for both components. The mixture is then co-lyophilised which usually results in uneven microparticles. The process involves freezing the material and reducing the surrounding pressure to sublimate the water matrix (Fang & Bhandari, 2010). The process is regarded to be expensive and time consuming even though the procedure is

rather simplified. This process is used for heat sensitive compounds, for example coffee which is very dependent on volatile aromatic compounds for its flavour (Desai & Park, 2005b).

2.4.1.2.4 Inclusion complexation

Inclusion complexation is one of the few methods for encapsulation that takes place at a molecular level. This technique is mostly limited to β-cyclodextrin, a cyclic derivative of hydrolysed maltodextrin. The internal cavity of the molecule is hydrophobic whereas the external part is hydrophilic (Desai & Park, 2005b). The encapsulation process is governed by hydrophobic interactions between the core material and the cavity presented by the cyclic encapsulating material, usually in a water medium. As a prerequisite, the core material should be less polar than water and should have suitable molecular dimensions to be encapsulated into the cavity. This technique is specifically used for the encapsulation of volatile flavours as it has proved to be the most successful in protecting aroma compounds (Yuliani, Bhandari, Rutgers & D'Arcy, 2004). For example, Teixeira, Ozdemir, Hill & Gomes (2013) encapsulated black pepper oleoresin and Ramírez-Ambrosi, Caldera, Trotta, Berrueta & Gallo (2014) encapsulated various apple polyphenols by inclusion complexation with β-cyclodextrin. This technique resulted in very small particle sizes and high entrapment efficiency.

2.4.1.2.5 Coacervation

Coacervates can be defined as droplets containing colloids rich in organic components that are surrounded by a tight skin of water molecules (Sri.s *et al.*, 2012). The process for coacervate formation involves the formation of three immiscible chemical phases (Desai & Park, 2005b). The three phases includes a liquid manufacturing phase, a core material phase, and a coating material phase. The core material is dispersed in a solution of the encapsulating material and is then coated with the liquid manufacturing phase by the addition of salt, a temperature change or addition of a non-solvent. The liquid coating is deposited on the surface of the already coated core material by adsorption of the encapsulating material to the interface formed between the core material and liquid manufacturing phase (Sri.s *et al.*, 2012). The encapsulating material can be secured by cross-linking or desolvation techniques. The method is considered expensive for encapsulation in the food industry and the microparticles tend to have no definite form.

2.4.1.2.6 Cocrystallisation

Cocrystallisation involves the spontaneous crystallisation of sucrose. The process involves a supersaturated sucrose syrup at a temperature high enough to prevent crystallisation (Desai & Park, 2005b). The core material is added to the syrup and mechanical agitation is used to form nucleus sites for the

crystallisation of the sucrose. During the crystallisation of the sucrose the core material is incorporated in the voids in the micron sized agglomerated crystal structure resulting in incorporation of the core material (Fang & Bhandari, 2010). The microparticles are generally in the form of sugar crystal agglomerates. This method is not suitable for phenolic compounds as these compounds are usually heat-labile.

Table 2.11

Characteristic particles produced by different methods of microencapsulation (Fang & Bhandari, 2010)

Spray-drying	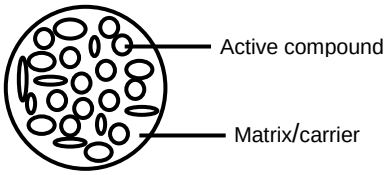
Freeze-drying	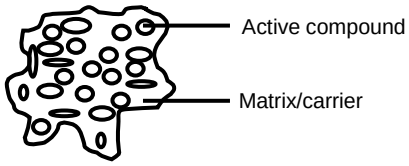
Coacervation	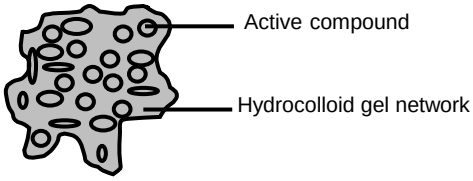
Cocrystallisation	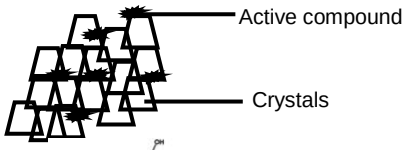
Inclusion complexation	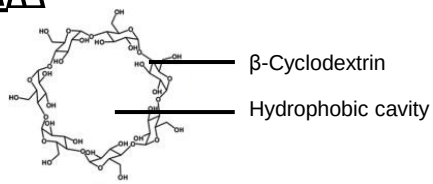

2.4.2 Nanoencapsulation and technology

Nanoscience and technology can be defined as the production, processing, design, and application of materials that have a controllable size scale below 1000 nm (Sanguansri & Augustin, 2006). Generally, a reduction in size to nanoscale results in an increase in the surface to volume ratio. The resulting large surface areas hold various advantages including an increase in reactivity, resulting in drastic improvements in optical, electrical, and mechanical properties (Neethirajan & Jayas, 2011).

The main objective of nanotechnology is not only to improve the existing properties, but also to alter and add properties with the goal of broadening applications of current and new technologies. Nanotechnology has also seen application in food science, however the “generally recognised as safe” status is very important in

this sector (Singh, 2016). In the case of food technology, nanotechnology aims to create products with improved texture, taste, colouring strength, and other sensory attributes. In addition to the physicochemical characteristics of products, nanotechnology also focusses on the improvement of processability, shelf-life stability, thermal stability and solubility (Huang, Yu & Ru, 2010; McClements *et al.*, 2009; Silva, Cerqueira & Vicente, 2011; Ezhilarasi, Karthik, Chhanwal & Anandharamakrishnan, 2013). Moreover, nanotechnology allows the development of 'smart' materials that result in controlled and targeted release of bioactive compounds. Due to the small size of nanodelivery systems and the small size of cellular mucosa pores, a higher intracellular uptake is achieved on nanoscale, regardless of the encapsulation material (Reis, Neufeld, Ribeiro & Veiga, 2006). The encapsulation material itself can also be functional concerning surface charge and other inherent material properties. The intestinal mucosa are dominated by negatively charged compounds, resulting in neutral or cationic compounds passing more efficiently through the pores (Reis *et al.*, 2006). The design of delivery systems with these favourable characteristics could lead to great improvements in the bioavailability of various unstable bioactive compounds, creating opportunities for the nutraceutical and food industry (Roco, 2003). The following sections will provide an overview on the type of encapsulating materials and methods employed for nanoencapsulation focusing on nanoencapsulation of phenolic compounds.

2.4.2.1 Nanodelivery systems

A nanodelivery system can be defined as a system that contains an encapsulating material which entraps a bioactive material on nanoscale and potentially controls the release rate of the bioactive compound (Fathi, Mozafari & Mohebbi, 2012a). The release of the bioactive compound can be controlled by two different mechanisms namely delayed release and sustained release. Delayed release refers to the addition of 'lag time' until release is preferred. As an example, delayed release can be used to protect a nutrient subjected to gastric conditions and promote release in the intestinal region. Sustained release refers to the extended release of a compound over a long period. This type of delivery system is usually employed when a constant concentration of a bioactive compound is desired at a specific target site (Fathi *et al.*, 2012a).

Nanodelivery systems come in various forms, where the type of system is chosen according to the properties of the final product or the properties of a specific food ingredient that needs to be improved. The main types of nanodelivery systems include nanocapsules, nanospheres, micelles, and nanogels (Bilia, Isacchi, Righeschi, Guccione & Bergonzi, 2014; Nuruzzaman, Rahman, Liu & Naidu, 2016). These systems can be further divided into polymeric based or lipid based nanocarriers and molecular complexes. Table 2.12 shows the different types of nanodelivery systems accompanied by a brief description.

Table 2.12

Main types of nanodelivery systems (Nuruzzaman *et al.*, 2016)

Nanosystems		Description
Nanocapsules		Nanocapsules have a core-shell type morphology, where the bioactive compound is encapsulated and sealed inside a protective membrane material.
Nanospheres		Nanospheres have a matrix type morphology, where the bioactive material is embedded in the nanocarrier material as individual droplets.
Micelles	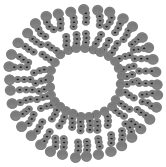	Micellular structures involve the self-assembly of an amphiphilic carrier material. Depending on the type of reaction medium used, micelles with a hydrophobic or hydrophilic core can be obtained. The active compound can reside in the core or outer layers, depending on the solubility of the compound.
Nanogels		Nanogels involve the chemical or physical crosslinking of polymer networks to form aqueous hydrogel particles. Nanogels are able to swell and hold large amounts of water without dissolving.

2.4.2.2 Methods of nanoencapsulation

Nanoencapsulation methodology tends to be more complex than that of microencapsulation (discussed in section 4.1) due to the type of materials, controlled particle morphology and specific particle size range (Chau, Wu & Yen, 2007). Methods that are generally used include that of emulsification, coacervation, inclusion complexation, super critical fluid techniques, emulsion-solvent evaporation, electrospraying and nanoprecipitation. There are various other techniques, but the mentioned techniques are most often used as they produce capsules in the lower nanoscale (Ezhilarasi *et al.*, 2013). The method, encapsulating material, core bioactive material, ratios of components, reaction medium and the interactions thereof are very important considerations when deciding on the desired final properties of the particles. Selected methods will be discussed briefly in the next few sections and summarised in Table 2.13.

2.4.2.2.1 Nanoemulsification

Nanoemulsions can be defined as colloidal dispersions comprised of two immiscible liquids. Oil-in-water emulsions (o/w) are formed when oil droplets are dispersed in an aqueous phase. The technique works well for lipophilic bioactive compounds such as β-carotene, plant sterols, dietary fats, and carotenoids. Water-in-oil emulsions (w/o) are formed when aqueous droplets are dispersed in an oil phase and used for the

encapsulation of hydrophilic compounds (McClements *et al.*, 2009; Ezhilarasi *et al.*, 2013). However, w/o emulsions can be prone to instability and thus water in oil-in-water emulsions (w/o/w) are generally used for the encapsulation of hydrophilic compounds such as polyphenols (Soppimath, Aminabhavi, Kulkarni & Rudzinski, 2001).

Nanoemulsions are in a non-equilibrium state and cannot be formed spontaneously. Various forms of energy input is used to form the above mentioned types of emulsions. Two types of approaches are generally used, namely high energy and low energy. For high-energy emulsification, homogenisers, microfluidisers and ultrasonic homogenisers are utilised. Low energy approaches include self-emulsification methods and phase inversion methods. For both approaches, the disruptive force must be higher than the restoring forces in order to result in droplet dispersion rather than droplet coalescence (Jafari, Assadpoor, Bhandari & He, 2008). Furthermore, the force should also have enough energy to form stable spherical nanosized droplets (Schubert & Engel, 2004). Different approaches of emulsification will be discussed briefly in the next few sections.

Nanoemulsions offer great potential for the encapsulation of bioactive compounds for a wide range of applications, specifically foodstuffs. McClements *et al.* (2009), Neethirajan & Jayas (2011) and Silva *et al.* (2011) have comprehensively reviewed the use of nanoemulsions for the delivery of nutraceuticals and food ingredients. Nanoemulsions hold the advantages of having high kinetic stability due to extremely small droplet sizes which prevents coagulation and creaming (Jafari *et al.*, 2008; Ezhilarasi *et al.*, 2013). However, Ostwald ripening does still occur, where the mean size of the particles increase over time as smaller droplets diffuse through the solvent matrix to form larger droplets (Anandharamakrishnan, 2014).

2.4.2.2.2 Emulsification-solvent evaporation technique

The first step of the emulsification-solvent evaporation technique involves the emulsification of the dissolved encapsulating polymer and bioactive compound into an aqueous phase. A dispersing agent and high pressure homogenisation are used to disperse the water immiscible organic solvent, which contains the polymer and bioactive compound, in the aqueous phase. The water immiscible organic solvent is then evaporated, resulting in the precipitation of nanospheres where the bioactive compound is embedded in the polymer matrix (Soppimath *et al.*, 2001; Reis *et al.*, 2006; Ezhilarasi *et al.*, 2013). Fig. 2.6 shows a schematic representation of this technique. This technique is only applicable to lipophilic bioactive compounds as an oil-in-water (o/w) emulsion is formed. However, this technique can be modified for the formation of a double w/o/w emulsion for water-soluble bioactive compounds. This type of emulsification is done on the same principles as the w/o emulsion, but involves an additional step where the primary w/o emulsion is added to a secondary

aqueous phase containing a stabilising agent (Davda & Labhasetwar, 2002; Xie *et al.*, 2011; Srivastava *et al.*, 2013; Singh *et al.*, 2015).

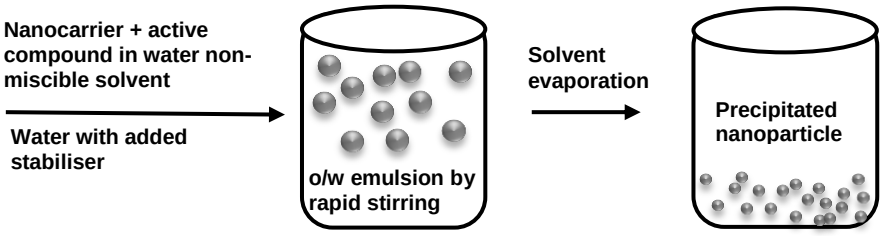

Fig. 2.6 Schematic representation of nanoencapsulation by the emulsification-solvent evaporation technique as adapted from Reis *et al.* (2006)

2.4.2.2.3 Solvent displacement and interfacial deposition

Solvent displacement and interfacial deposition techniques are similar in that both are based on spontaneous emulsification. In these techniques, the polymer and bioactive compound are dissolved in a partially polar, water-soluble organic solvent. This phase is combined with an aqueous solution that contains a stabiliser or surfactant. A colloidal suspension is formed by the deposition of the polymer between the interface of the organic phase and aqueous phase by the fast diffusion of the solvents (Quintanar-Guerrero, Allémann, Fessi & Doelker, 1998). Fig. 2.7 shows a schematic presentation of this technique. It is important that the diffusion rate of the water-miscible organic solvent is fast enough for spontaneous emulsification (Quintanar-Guerrero *et al.*, 1998). This technique has been used to form nanocapsules (with the addition of an oil phase) and nanospheres in the range of 200 nm (Reis *et al.*, 2006).

However, low encapsulation efficiency is achieved for lipophilic and hydrophilic bioactive compounds as it is very difficult to create a system where the solvent and non-solvent of the polymeric material are miscible (Quintanar-Guerrero *et al.*, 1998).

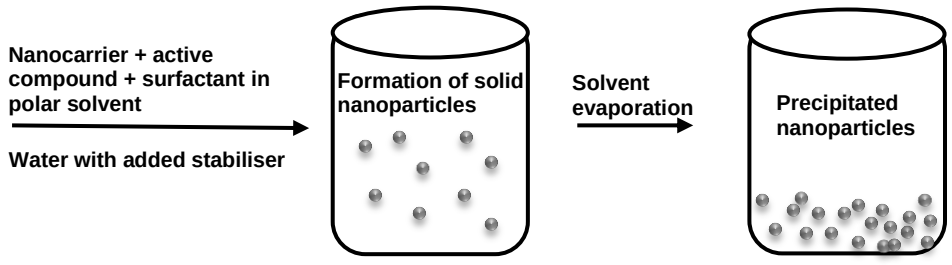

Fig. 2.7 Schematic representation of nanoencapsulation by the solvent displacement and interfacial deposition technique as adapted from Reis *et al.* (2006).

2.4.2.2.4 Emulsification/solvent diffusion technique (salting out/nanoprecipitation)

The emulsification technique was first based on the diffusion of organic solvents. The technique was later adapted to the salting out procedure, which makes use of a water-soluble system. The technique involves the encapsulating polymer dissolved in a water-soluble solvent and saturated with water to create a thermodynamic equilibrium for both solvents. Subsequently, the water saturated phase, which contains the polymer and organic solvent, is emulsified into an aqueous phase which contains a suitable stabiliser (Reis *et al.*, 2006). The emulsification results in diffusion of the solvent containing the encapsulating polymer into the aqueous phase and the formation of nanoparticles by precipitation (Ezhilarasi *et al.*, 2013). A schematic representation of the procedure is shown in Fig. 2.8. Precipitation is followed by removal of the solvent by filtration or evaporation. The technique is advantageous as it was shown to have > 70% encapsulation efficiency with no need for homogenisation or other high-energy inputs. Narrow size distribution has also been reported. In the case of hydrophilic bioactive compounds, leakage into the high volumes of water can occur resulting in a reduction of encapsulation efficiency (Reis *et al.*, 2006). However, this problem could potentially be solved by using solvents that change the polarity of the encapsulating polymers and are suitable for hydrophilic molecules (Bilati, Allémann & Doelker, 2005). The technique has more advantages than emulsion-solvent evaporation for the encapsulation of polar, yet water insoluble bioactive compounds such as cucurbitacin in PLGA (Alshamsan, 2014). Development of this technique has also extended to the encapsulation of water soluble compounds in Eudragit nanoparticles by the use of different solvent combinations (Salatin *et al.*, 2017).

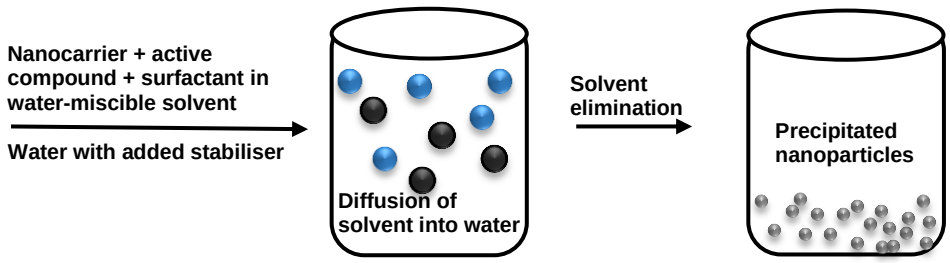

Fig. 2.8 Schematic representation of nanoencapsulation by the emulsification/solvent diffusion technique (salting out/nanoprecipitation) technique as adapted from Reis *et al.* (2006).

2.4.2.2.5 Polymerisation methods

Nanoencapsulation can also be achieved by the direct addition of the bioactive compound to the polymerisation reaction instead of encapsulation with a preformed polymeric material. Two main techniques are used, namely emulsion polymerisation and interfacial polymerisation (Reis *et al.*, 2006). For both these reactions, the monomer is added to the bioactive compound in the presence of a stabiliser. Vigorous stirring

of these mixtures results in initiation of polymerisation. In this process, the bioactive compound is entrapped in the polymer chains as they increase in molecular size (Soppimath *et al.*, 2001). The surfactant surrounds these chains and form a stable emulsion that contains the polymer and bioactive compound. Fig. 2.9 shows a schematic of a typical polymerisation encapsulation process. These are fast, readily scalable one-step reactions without any excess solvent. However, polymerisation methods generally pose problems due to unreacted monomers, initiators, and large amounts of toxic stabilisers in the reaction mixture (Reis *et al.*, 2006).

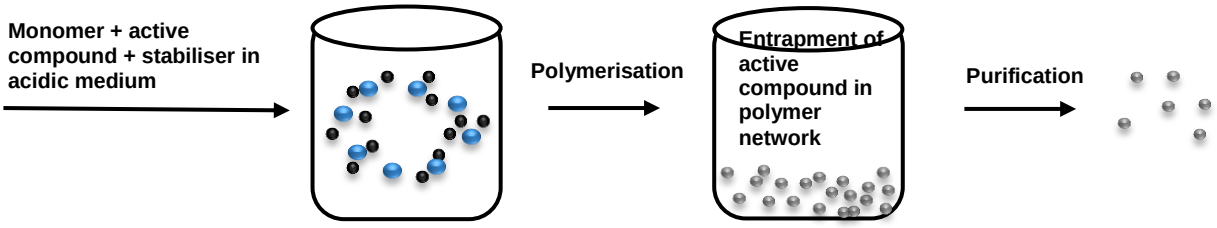

Fig. 2.9 Schematic representation of nanoencapsulation by the polymerisation technique as adapted from Soppimath *et al.* (2001)

2.4.2.2.6 Electrospraying

Electrospraying, sometimes referred to as electrodynamic or electrohydrodynamic processing, is an easy and versatile technique to encapsulate bioactive compounds in polymeric materials (Anandharamakrishnan, 2014; Alehosseini, Ghorani, Sarabi-Jamab & Tucker, 2017). The technique involves a polymer solution (of low viscosity) that is subjected to an electric field mounted opposite a charged collector surface. The electric field results in repulsion between the polymer molecules charged oppositely to that of the surface tension of the polymer solution. This causes the solution at the tip of the capillary to elongate and form a conical shape, i.e. a Taylor cone. At a critical value, when the repulsion caused by the electric field is greater than the surface tension of the polymer, a charged jet of polymer solution will be ejected. The charged jet is attracted to the oppositely charged collector surface where the polymeric particles will collect after complete solvent evaporation has taken place (Reneker & Chun, 1996; Jaworek & Sobczyk, 2008).

Instead of nanoparticles, nanofibers can also be formed if the viscosity of the feed solution is increased. Fig. 2.10 shows a schematic of a basic electrospraying setup. The technique has been shown to give spherical particles with good dipsersibility, size distribution, and encapsulating efficiency. Various process and intrinsic parameters affect the above properties including the voltage, tip-to-collector distance, ratio of the bioactive and the polymer, needle gauge, flow rate, type of solvent and polymer (Drosou, Krokida & Biliaderis, 2017). The parameters show complex behaviour with regard to different polymer and bioactive ingredient systems and need to be assessed for each system (Bock, Woodruff, Hutmacher & Dargaville, 2011).. Examples based

on natural bioactives include the nanoencapsulation of green tea catechins (Bhushani, Kurrey & Anandharamakrishnan, 2017) and *Aloe vera* leaf juice (Torres-Giner, Wilkanowicz, Melendez-Rodriguez & Lagaron, 2017).

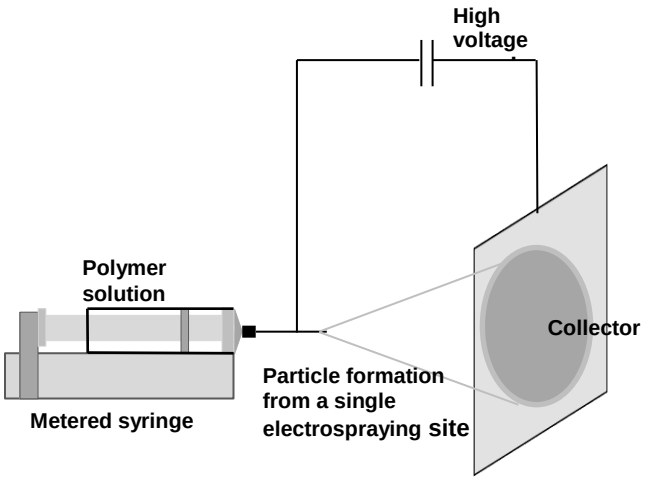

Fig. 2.10 Schematic representation of a basic single needle-electrospraying setup

2.4.2.2.7 Supercritical fluid technique

A supercritical fluid can be defined as any substance that has the ability to adapt to a state where distinct liquid and gas phases do not exist at a temperature and pressure above its critical point. It can act as a gas or a liquid, thus diffusing through solids like a gas or dissolving materials like a liquid. This results in supercritical fluids exhibiting properties of gases and liquids such as low viscosity, low density, high diffusability, and high degrees of mass transfer and high solvating properties (Ezhilarasi *et al.*, 2013).

Examples of these types of compounds include nitrogen, carbon dioxide, water, propane, etc. (Gouin, 2004). For nanoencapsulation, the bioactive compound and the polymeric material are solubilised in the supercritical fluid that expands through the atomising nozzle (Reis *et al.*, 2006). The supercritical fluid is evaporated in the spraying process resulting in precipitation of the solute particles and coating of the bioactive (Ezhilarasi *et al.*, 2013).

2.4.2.2.8 Ionic gelation technique

The ionic gelation technique makes use of charged biopolymers and polyelectrolytes. In short, it involves the dispersion of the bioactive compound in a suitable polyelectrolyte encapsulating material. Coacervation takes place between the bioactive compound and the encapsulating material and the compound is trapped inside or between the encapsulating material to form an insoluble complex (Sri.s *et al.*, 2012). Furthermore, shell formation takes place as more of the encapsulating material is deposited on the surface of the complexes. The complexes can be stabilised by the addition of an ionic crosslinker. The method is strongly affected by the

molar mass, charge of the encapsulating material, as well as the pH, ionic strength and concentration of the reaction medium (Tolstoguzov, 2003; De Kruif, Weinbreck & De Vries, 2004; Turgeon, Schmitt & Sanchez, 2007). These factors can be used advantageously to control particle morphology and result in high encapsulation efficiencies (Gouin, 2004). However, particle sizes tend to be more microscale than nanoscale (Xing, Cheng, Yi & Ma, 2005; Gan & Wang, 2007).

Table 2.13

Summary of selected nanoencapsulation methods

Encapsulation method	Variations	Advantages	Disadvantages
Nanoemulsification	Emulsification-solvent evaporation method Solvent displacement and interfacial deposition method Emulsification-diffusion method	Wide application range Tailored processes	Harsh solvents Multiple step process Stabilisers required
Polymerisation	Emulsion polymerisation Interfacial polymerisation	One step process Ease of upscale	Unreacted monomers, initiators and stabilisers
Electrospraying	Electrospinning Co-axial electrospraying	No solvent waste Ease of upscale Known process parameters One step process	High voltages Not suitable for all materials and solvent systems
Ionic gelation and crosslinking	-	Natural solvents and materials Tailored processes	Multiple step process Not suitable for all materials and solvent systems
Supercritical fluid technique	-	One step process	High cost

2.4.2.3 Nanoencapsulation materials

Encapsulation materials are chosen according to specific properties and the compound to be encapsulated. The biological effect, release kinetics and degradation of the encapsulating materials must also be taken into account in the selection process (Reis *et al.*, 2006). Current encapsulating materials used in the food industry are protein, carbohydrate, or lipid based. However, research is also leaning towards the use of synthetic polymers as they show improved stability when compared to that of natural encapsulating materials (Fathi *et al.*, 2012a). The next section will review the basic properties of various encapsulating materials, including their function, digestion and positive and negative attributes (summarised in Table 2.14).

2.4.2.3.1 Lipid based materials

Lipid based materials are most commonly employed for the formation of liposomes which can be defined as vesicles that consist of a membrane structure made up of one or more phospholipid bilayers surrounding an aqueous core (Fang, Lee, Shen & Huang, 2006). Liposomal structures are based on the amphiphilic nature of most phospholipids where polar groups of the molecules interact with an aqueous medium and hydrophobic

hydrocarbon groups try to minimise contact with the aqueous medium resulting in formation of spherical core shell structures (De Assis, Machado, De Souza Da Motta, Costa & De Souza-Soares, 2014). Depending on the starting materials, the method of formation and product requirements, different types of liposomes can be formed. These include multi-lamellar vesicles (MLV's), large uni-lamellar vesicles (LUV's) and small uni-lamellar vesicles (SUV's) (De Assis *et al.*, 2014). With the variety of formations, tailoring allows for very specific properties such as targeted release of bioactive compounds inside and outside the gastrointestinal tract (Mozafari, Johnson, Hatziantoniou & Demetzos, 2008).

Liposomes are prepared using various starting materials and technologies. Starting materials can include lecithin (Frankel, Huang & Aeschbach, 1997; Lu, Li & Jiang, 2011; Rashidinejad, Birch, Sun-Waterhouse & Everett, 2014), cholesterol (Fang *et al.*, 2006; Lu *et al.*, 2011), 1,2-dimyristoyl-sn-glycero-3-phosphocholine (DMPC) (Li, Braiteh & Kurzrock, 2005), mixtures of lecithin and sunflower oil (Spigno *et al.*, 2013) and various other types of lipid materials. Common technologies include high pressure homogenisation, emulsification, freeze-drying, centrifugation, reverse evaporation (Lu *et al.*, 2011) and the thin film hydration method, which has been reported in various articles (Frankel *et al.*, 1997; Fang *et al.*, 2006; Lu *et al.*, 2011; Rashidinejad *et al.*, 2014).

Liposomes were initially discovered and synthetically prepared by Gregoriadis & Florence (1993) and represented the only nanodelivery vesicle commercially available in 2008. Since the discovery, several companies have invested in research on further commercialisation (Wagner & Vorauer-Uhl, 2011). The interest in the use of liposomes in the food sector is specifically being explored. A few examples of literature on food related bioactive compounds include the encapsulation of compounds of interest found in tea (Huang & Frankel, 1997; Fang *et al.*, 2006; Lu *et al.*, 2011), hesperidin from citrus fruit origin (Fathi *et al.*, 2012b), curcumin (Li *et al.*, 2005) and polyphenolic extracts of grape marc (Sessa *et al.*, 2012; Spigno *et al.*, 2013). From the above examples, the green tea and grape marc liposomes where applied in the solution form, whereas the hesperidin and curcumin liposomes were applied after freeze drying. The reasons for the success of liposomes include their various advantageous properties, i.e. their ability to encapsulate both hydrophilic and hydrophobic compounds (Maurer, Fenske & Cullis, 2001), good entrapment and release efficiencies, targeted release (Huwiler, Kolter, Pfeilschifter & Sandho, 2000; Thompson, Hindmarsh, Haisman, Rades & Singh, 2006; Mozafari *et al.*, 2008), increased stability and bioavailability of bioactive compounds (Mignet, Seguin & Chabot, 2013) and their biodegradable and biocompatible nature. Furthermore, phospholipid liposomes are recognised by human cells and can interact with cells in various ways including binding to cells, release of aqueous compartments to cell cytoplasts and transfer of liposomes into cells. This results in direct delivery of the bioactive compounds to the cells (De Assis *et al.*, 2014). However, further research and

development is required since poor stability during storage poses problems such as leakage of hydrophilic bioactive compounds and rapid elimination from the blood stream after administration (Hans & Lowman, 2002).

In order to improve the properties of liposomes, different lipid carriers are under investigation, namely solid lipid particles and nanostructured lipid carriers. Solid lipid particles can be defined as particles containing a matrix surrounded by a solid lipid shell. Nanostructured lipid carriers are similar, but contain liquid lipids to prevent perfect crystallisation. These carriers have improved controlled release, storage stability due to slower degradation rates and increased possibility of large-scale production (Fathi *et al.*, 2012a).

2.4.2.3.2 Synthetic polymeric materials

Biosorbable polyester polymers used for nanoencapsulation are mainly derived from lactic or glycolic acids that are used in various forms and combinations. The next section will focus on the different types of biodegradable polymers.

Polylactic acid (PLA) is one of the most common degradable polymers and can be produced by condensation polymerisation or addition polymerisation mechanisms. These polymers are hydrophobic, water-insoluble, amorphous, and have a high glass transition temperature making it very suitable for the stabilisation and protection of bioactive ingredients (McGinity & Felton, 2008). The polymers readily undergo scission in the body to produce monomeric units of lactic acid (Kumari, Yadav & Yadav, 2010b). This, in combination with penetration of aqueous medium into the nanoparticle, results in diffusion controlled release of bioactive compounds and is responsible for the initial burst and further delayed release of these types of encapsulation materials (Makadia & Siegel, 2011). Encapsulation is generally achieved by the salting out (Reis *et al.*, 2006), solvent displacement and solvent diffusion methods (Fessi, Puisieux, Devissaguet , Ammoury & Benita, 1989).

Poly-Ɛ-caprolactone (PCL) has also recently received attention as a nanoencapsulating material for the delivery of bioactive compounds due to its biodegradable nature, i.e. breakage of its ester linkages under physiological conditions. In particular, it is used in long term implantable devices, as these polymers take slightly longer to degrade in the human body than other biodegradable delivery polymers (Kumari *et al.*, 2010b).

Furthermore, other combinations of biodegradable polymers as nanodelivery devices for bioactive compounds are being recognised by the functional food industry. PLGA and its derivatives are considered to be some of the most successful current nanodelivery systems and approved by the Food and Drug administration agency in the United States (US FDA) and the European Medicine Agency (EMA) (Danhier *et al.*, 2012). PLGA is a synthetic copolymer of PLA and polyglycolic acid. The ratios of the two polymers and the molecular mass of the copolymer can be varied in order to achieve optimum encapsulation and release rate

of specific bioactive compounds. These variable characteristics also affect the stability and degradation profile as higher molecular mass polymers take longer to degrade (Hans & Lowman, 2002). The copolymer and its constituents are hydrophilic, biocompatible and can be hydrolysed to lactic acid and glycolic acid monomers (Danhier *et al.*, 2012). Examples of hydrophilic compounds include the encapsulation of tea polyphenols (Srivastava *et al.*, 2013), nucleic acids and proteins (De Martimprey, Vauthier, Malvy & Couvreur, 2009; Danhier *et al.*, 2012), EGCG from green tea (Pal & Saha, 2013) and white tea extract (Sanna *et al.*, 2015). Fig. 2.11 shows the typical procedure for the encapsulation of a hydrophilic tea extract. The preparation methods often involve the use of harsh solvents and care should be taken regarding the allowed minimum residual solvent content in nutraceutical/functional food products (Danhier *et al.*, 2012).

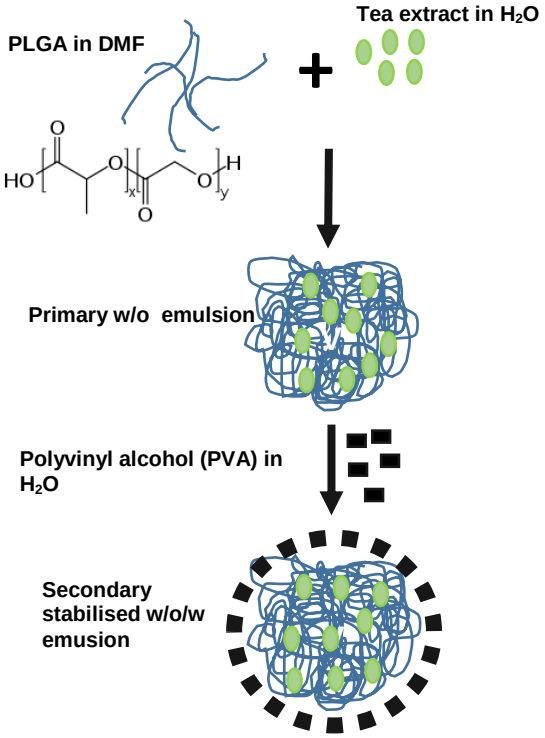

Fig. 2.11 Typical encapsulation procedure for a hydrophilic substance using PLGA as example

Methacrylic polymers include a group of polymers with various esters covalently linked to the carbon-carbon backbone by copolymerisation (commercially grouped under the product name of Eudragit coatings). Studies have shown that methacrylate polymers are not readily degraded in the human body due to the carbon-carbon backbone, and are rapidly excreted in the faeces where it remains chemically unchanged. Studies performed on animals (pigs and dogs) have shown very low levels of oral or dermal toxicity (>2000 mg/kg) (McGinity & Felton, 2008).

Common technologies for encapsulation by methacrylate polymers include compression, granulation, wet extrusion and spray-drying. However, other techniques are usually utilised for the nutraceutical food industry.

These include nanoprecipitation that has been successfully used for the encapsulation of curcumin and quercetin (Moorthi & Kathiresan, 2013) as well as solvent emulsion evaporation used for the encapsulation of curcumin (Jenita, Yathish, Wilson & Premakumari, 2012) and green tea catechins (Singh *et al.*, 2015).

As a result of the number of different esters, these polymers have very unique properties and can be tailored according to a specific end function (McGinity & Felton, 2008). The individual types of polymers, depending on functionalisation, differ in their degree of neutral, acidic or alkaline groups or can have no functional groups (McGinity & Felton, 2008). The next section will focus on a brief overview of the different groups of methacrylate polymers available.

Acid soluble polymers are copolymerised from the cationic monomer dimethylaminoethyl methacrylate (DMAEMA) with methyl- and butyl-methacrylate in a set ratio. These polymers are acid soluble at < pH 5 by salt formation with anions present in the gastric fluid. The polymers are generally used for odour and taste masking as well as protection against moisture (McGinity & Felton, 2008).

Alkali-soluble polymers are copolymerised from the monomer methacrylic acid (MAA) with methyl- and ethyl-methacrylate in different ratios. The ratio of MAA to ethyl-methacrylate in the polymerisation process determines the dissolution properties of the polymer, enabling pH dependent targeting along the gastrointestinal tract. However, methacrylate monomers largely affects the thermal properties and T_g of these polymers (McGinity & Felton, 2008). Both properties should thus be considered when designing the polymeric delivery material.

Insoluble copolymers are obtained by the copolymerisation of neutral esters with MAA that can be derivatised with quaternary ammonium salts, resulting in water insoluble polymers. These polymers have gained interest for time controlled release applications as they have the ability to absorb water from physiological environments to create diffusional barriers independent of pH (McGinity & Felton, 2008).

All of the above mentioned polymers are subject to polymer characterisation and quality control directly after the manufacturing process according to pharmaceutical standards. These procedures include that of purity testing of products and starting materials, identification, isolation of product and functionality testing. The polymers have not yet been approved or investigated for use in the food industry, but have been regarded as safe in the pharmaceutical industry for over 50 years.

2.4.2.3.3 Natural polymers

Natural polymers are extensively used for the encapsulation of food and medical products due to their inexpensive, non-toxic, hydrophilic and biodegradable nature. Different natural polymeric encapsulating

materials have been covered in section 4.1 and will thus not be discussed again. The next section will give selected examples of natural polymers used specifically for nanoencapsulation.

Chitosan is a linear biopolyaminosaccharide and can be obtained by the deacetylation of chitin. The structure consists of one primary amino group, which carriers a positive charge and two hydroxyl groups (Sinha *et al.*, 2004). This natural polymer holds various advantages as it is positively charged, resulting in electrostatic attraction to negatively charged phospholipid head groups in human cells. This is usually reported as mucoadhesive nature or behaviour (Berscht, Nies, Liebendörfer & Kreuter, 1994). This, in combination with hydrolysis and erosion as the polymer swells in the presence of an aqueous medium, results in a slow release mechanism of the bioactive compound (Saravanabhavan *et al.*, 2013). The most common encapsulation mechanism seen in literature is that of ionic gelation, specifically to produce chitosan-tripolyphosphate (Ch-TPP) nanoparticles. Ch-TPP has been used to encapsulate green tea catechins (Hu *et al.*, 2008; Dube, Ng, Nicolazzo & Larson, 2010; Liang *et al.*, 2011), proteins (Wu *et al.*, 2008), ellagic acid (Arulmozhi *et al.*, 2013), yerba mate extract (Harris, Lecumberri, Mateos-Aparicio, Mengíbar & Heras, 2011) and ascorbyl palmitate (Kim, Lee, Kim & Lee, 2013). Fig. 2.12 shows a typical reaction for the nanoencapsulation of ellagic acid in Ch-TPP particles. The conditions of the proposed ionic gelation method for Ch-TPP nanoparticles are very mild and no harsh chemicals are added. However, Ch-TPP nanoparticles have been reported to have poor mechanical stability as it is based on ionic interactions only (Agnihotri, Mallikarjuna & Aminabhavi, 2004).

Gelatine nanoparticles are mainly produced by the desolvation/coacervation (Lu, Yeh, Tsai, Au & Wientjes, 2004) and emulsion methods. These nanoparticles are able to absorb 51-72% water, resulting in the controlled release of bioactive compounds by swelling (Zambaux, Bonneaux, Gref, Dellacherie & Vigneron, 1999). Other examples of natural polymers include carbohydrates such as pectin, gum arabic, alginate and xanthan gum. Proteins include polymers such as albumin, gelatine, soy protein and caseins.

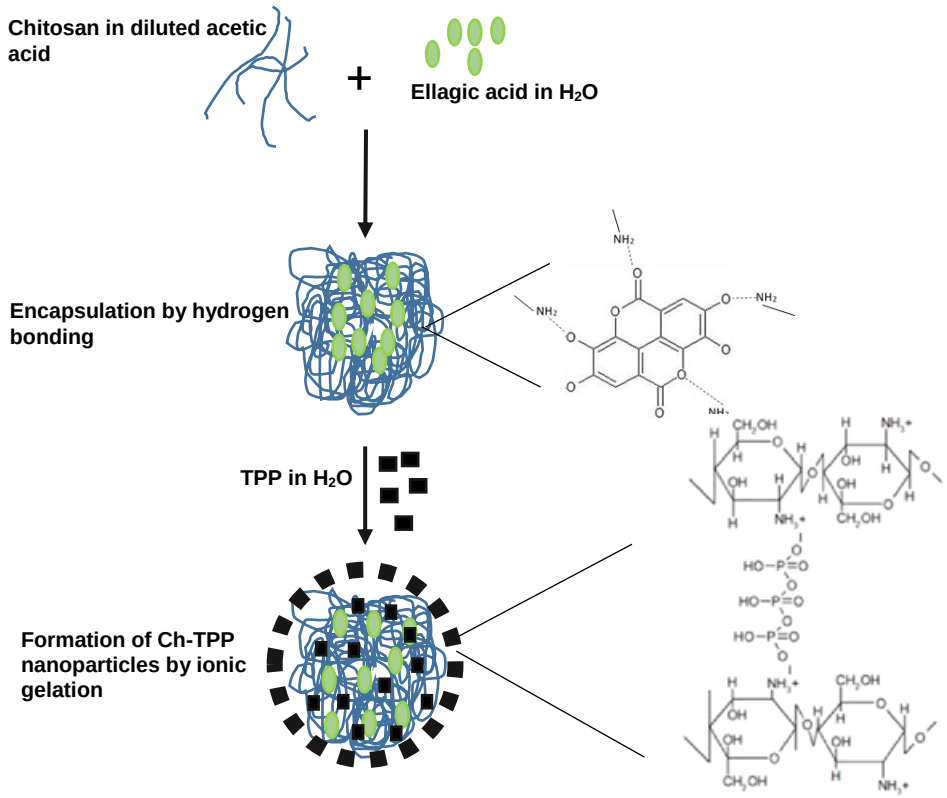

Fig. 2.12 Formation of chitosan-tripolyphosphate particles

Table 2.14

Summary of selected synthetic and natural nanoencapsulation materials

Encapsulation material	Variations	Characteristics	*In vivo* fate
		Synthetic polymers	
Polylactic acid (PLA)	Molecular weight	Hydrophobic, water-insoluble, high T_g and amorphous Controlled release profile	Biodegradable – scission into lactic acid monomers
Poly(lactide-co-glycolide) (PLGA)	Molecular weight Ratio of lactic acid and glycolic acid Polyethylene glycol addition	Hydrophilic Controlled release profile Tailored properties	Biodegradable – scission into lactic acid and glycolic acid monomers
Poly-Ɛ-caprolactone (PCL)	Molecular weight	Longer release and degradation profile Hydrophobic and water-insoluble	Biodegradable – scission of ester linkages
Methacrylate polymers	Alkaline, acidic or neutral functionalities Molecular weight	Targeted release profile Tailored solubility	Non-biodegradable – rapidly excreted chemically unchanged
		Natural polymers	
Chitosan	Molecular weight Degree of deacetylation	Mucoadhesive Anti-microbial Sustained release Hydrophilic	Bioadegradable – scission into digestible amino sugars
Lipids	Type of lipid (lecithin, cholesterol, 1,2-dimyristoyl-sn-glycero-3-phosphocholine and oils) Type of liposome (multi-lamellar vesicles, large uni-lamellar vesicles and small uni-lamellar vesicles)	Ability to encapsulate hydrophilic and hydrophobic compounds Controlled release profile Protection against environmental factors Increased cell absorption	Biodegardable - recognised by human cells (also interaction)

2.4.2.4 Nanoencapsulation of polyphenols

Polyphenolic compounds are known for their health properties as demonstrated by *in vitro* and *in vivo* studies. Lower incidences of cancer, diabetes, cardiovascular disease and other diseases in certain populations have been associated with dietary intake of these compounds (Mignet *et al.*, 2013). However, the absorption and stability of most orally administered polyphenols tend to be poor. This has led to an increased interest in the nanoencapsulation of polyphenolic compounds in order to overcome these caveats by targeted delivery and by protection during storage and digestion (Chen, Lin & Hu, 2003). The next section will review select studies concerning the nanoencapsulation of various phenolic compounds. The overview will give insight into possible techniques suitable for the nanoencapsulation of rooibos polyphenols.

Herbal teas, specifically green tea has been considered as a health-promoting natural product since ancient times (Zhang, Nie & Wang, 2013). However, the absorption of the bioactive compounds found in tea has been found to be less than 5% (Dvorakova, Dorr, Valcic, B. & Alberts, 1999; Catterall, King, Clifford & Ioannides, 2003) and the systematic clearance is rapid (Dvorakova *et al.*, 1999; Cai, Anavy & Chow, 2002). Nanoencapsulation of tea extracts (specifically green tea) and the individual catechins has emerged as a promising technique to overcome these problems.

The nanoencapsulation studies reviewed in this chapter are focused mainly on the encapsulation of pure EGCG, tea extracts (Fang *et al.*, 2006; Peres *et al.*, 2010; Zhang *et al.*, 2013; Hong *et al.*, 2014; Sanna *et al.*, 2015; Ponnuraj *et al.*, 2015) and theaflavins (TF) (Srivastava *et al.*, 2013; Singh *et al.*, 2015) as summarised in Table 2.15. Encapsulation efficiency, particle size and morphology, stability and release studies seemed to be the focus when evaluating the nanoparticulate systems. Pal & Saha (2013), Srivastava *et al.* (2013) and Singh *et al.* (2015) investigated the encapsulation of tea polyphenols in PLGA, Siddiqui *et al.* (2009) in PLGA-PEG and Narayanan *et al.* (2015) in PLGA coated with casein to form core/shell type particles. In the studies reviewed for PLGA and PLGA combinations with other polymers as encapsulation material, particles in the nano-range were obtained with encapsulation efficiencies below 30% and controlled release profiles were observed. Similar encapsulation efficiencies were found for white tea extract encapsulated in PCL and alginate (Sanna *et al.*, 2015). The encapsulation of EGCG with chitosan and an oppositely charged counterpart by ionic gelation showed higher encapsulation efficiencies up to 95% (Ponnuraj *et al.*, 2015). Other studies that encapsulated tea polyphenols in Ch-TPP and chitosan combined with polyaspartic acid also successfully produced smooth spherical particles in the nano-range of 102 to 470 nm with lower encapsulation efficiencies of up to 25% (Hong *et al.*, 2014; Kailaku, Mulyawanti & Alamsyah, 2014). The encapsulation efficiency and loading capacity will ultimately determine the product dose of the nanoparticles, which preferably needs to be minimised for cost and biological implications.

Fang *et al.* (2006) and Zhang *et al.* (2013) investigated the encapsulation of EGCG in liposomes and nanostructured lipid carriers, respectively. These studies also showed higher encapsulation efficiencies than the synthetic polymeric carriers. Krishnaswamy, Orsat & Thangavel (2012) investigated a completely different approach with β-cyclodextrin molecular inclusion. Nano-sized spherical particles were produced and complexation of β-cyclodextrin with EGCG was confirmed by various physicochemical techniques.

In addition to the nanoencapsulation of tea phenolic compounds, resveratrol, curcumin and quercetin has been investigated. Minimal studies on the nanoencapsulation of other phenolic compounds such as grape marc polyphenols (Sessa *et al.*, 2012), hesperetin (Fathi *et al.*, 2012b) etc. are available. A few selected examples of the nanoencapsulation of these compounds are reviewed in Table 2.16. Reported particle sizes varied between 78 and 43000 nm and encapsulation efficiency were between 67 and 91%. These ranges indicate that the nanoencapsulation of phenolic compounds are feasible and that the results are strongly related to the methodology and material utilised.

Advantages of nanoencapsulation for curcumin, resveratrol and quercetin compared to their free/unprocessed counterparts are also noted. Nanoencapsulated curcumin showed increased solubility in aqueous media and increased bioavailability when encapsulated in PLGA (Xie *et al.*, 2011), improved controlled release profiles when encapsulated in Eudragit S100 (Jenita *et al.*, 2012) and increased the cytotoxicity towards carcinoma cells when encapsulated in liposomes (Li *et al.*, 2005).

Nanoencapsulation of resveratrol showed increased cellular uptake and higher cell death in glioma cells when encapsulated in methoxypoly(ethylene glycol) (mPEG) and PCL copolymers (Shao *et al.*, 2009) and higher cytotoxicity of liposomal nanoformulations on H29 cancer cell lines (Soo *et al.*, 2016).

Nanoencapsulation of quercetin showed improved bioaccessibility and prolonged storage stability for encapsulation in Eudragit L30-55 (Pool *et al.*, 2012), while improved controlled release behaviour was shown for encapsulation in PLA (Kumari, Yadav, Pakade, Singh & Yadav, 2010a).

Thus, overall nanoencapsulation has merit for increased bioavailability, controlled release and improving anti-cancer properties of natural bioactive compounds.

Table 2.15

Summary of the nanoencapsulation of green tea and green tea phenolic compounds focusing on the materials, methods, analysis and main findings of the literature

Bioactive	Material	Method	Verification methods	Main findings	Source
			Synthetic encapsulating polymers		
EGCG[a]	PLGA-PEG[b]	Single emulsion dialysis	Cell based assays	Pro-apoptotic and angiogenesis inhibitory effects	Siddiqui *et al.* (2009)
EGCG	PLGA	Single emulsion evaporation	Particle size and morphology (dynamic light scattering and SEM) *In vitro* release kinetics (dissolution in PBS[c]) Cytotoxicity assay (562 cells)	Smooth spherical particles in nanometer range Delayed controlled release Higher cytotoxicity than unencapsulated EGCG	Pal & Saha (2013)
EGCG and TF[d]	PLGA	Solvent evaporation method	Yield, encapsulation efficiency (UV-VIS[e]) and particle size (Zetasizer Nano) *In vitro* release kinetics (incubator shaker) Animal bioassay (DNA alkaline unwinding in mouse skin)	Acceptable yield (70-97%), encapsulation efficiency (18-26%) and particle size (127-129 nm) Biphasic release profiles over 10 day period Protective effect towards DNA break down	Srivastava *et al.* (2013)
EGCG and Paclitaxel	PLGA-casein	Emulsion-precipitation	Particle size and morphology (SEM[f]) Cellular uptake (quantitative flow cytometry) Cytotoxicity (breast cancer cells)	Acceptable particle size (*ca.* 250 nm) Increased cellular uptake Improved cytotoxicity compared to unencapsulated counterpart	Narayanan *et al.* (2015)
White tea extract	PCL and alginate	Nanoprecipitation	Particle size and morphology (SEM and Zetasizer Nano) Encapsulation efficiency (HPLC[g]) Chemical composition (FTIR[h]) Antioxidant activity (DPPH assay[i]) Release kinetics (dialysis bag method) Stability studies	Smooth spherical particles Acceptable particle size (*ca.* 300 nm) and encapsulation efficiency (30-32%) Delayed release profiles Increased stability in solution	Sanna *et al.* (2015)
TF and EGCG in combination with cisplatin (cancer drug)	PLGA	Solvent evaporation method	Particle size (Zetasizer Nano), encapsulation efficiency (spectrophotometrically) and yield In vitro release (dialysis method) Colloidal stability (DLS[j]) *In vitro* studies (cell lines, cytotoxicity , mice bearing carcinomas)	Acceptable encapsulation efficiency (18-26%), yield (79-96%) and particle size (215-239 nm) Initial burst release Increased stability at physiological conditions Increased reduction of tumour size with combination of cisplatin and tea polyphenols when compared to cisplatin	Singh *et al.* (2015)

Table 2.15 Continued

Bioactive	Material	Method	Verification methods	Main findings	Source
			Natural encapsulating polymers		
EGCG	Chitosan and polyaspartic acid	Ionic gelation	Encapsulation efficiency (HPLC) Stability at various pH values Release studies Stability under simulated digestion	Acceptable particle size (102.4 nm) and encapsulation efficiency (25%) Decreased particle stability and release rate at higher pH Higher efficiency against atherosclerosis than free EGCG	Hong *et al.* (2014)
Green tea flavan-3-ols	Chitosan and TPP[k]	Ionic gelation	Particle size (Particle size analyser), structure (SEM and TEM[l]) and encapsulation efficiency (pyrolysis gas chromatography) Emulsion stability (centrifugation) Antioxidant capacity (DPPH)	Acceptable particle sizes (220-470 nm) and encapsulation efficiency (16.8%) Smooth spherical particles Reduced antioxidant activity	Kailaku *et al.* (2014)
Catechin	β-cylodextrin	Molecular inclusion	Physicochemical and thermal characterization (DSC[m], XRD[n], RLS[o], SEM)	Interaction and complexation between β-cyclodextrin and catechin Formed spherical nano-scale inclusion complexes	Krishnaswamy *et al.* (2012)
EGCG	Gum arabic and maltodextrin	Spray-drying	Surface morphology (SEM), particle size (Zetasizer Nano), DSL and AFM[p] and pore size (mercury porosimetry) Antioxidant activity (DPPH) Encapsulation efficiency (UV-VIS spectroscopy)	Indented hollow spherical particles Acceptable particle size (40-400 nm) and high loading efficiency (94%) Antioxidant capacities unchanged when compared to free EGCG	Peres *et al.* (2011)
EGCG	Chitosan and TPP	Ionic gelation	Yield, encapsulation efficiency (HPLC) Particles size (Malverin Zetasizer) and surface morphology (SEM) Thermal (DSC), physical (XRD) and chemical (FTIR) characterization *In vitro* release (USP[q] dissolution apparatus type II)	Acceptable yield (45.9-95.0%), encapsulation efficiency (14.0-91.7%) and particle size (197.8-385.5 nm) Amorphous structure Initial burst release, flowed by plateau	Ponnuraj *et al.* (2015)
EGCG	Liposomes	Thin film hydration	Drug encapsulation efficiency Vesicle size (Zetasizer Nano) *In vitro* release (Franz diffusion cell)	High encapsulation efficiency (100%) Controlled particle size and charge Protection from degradation	Fang *et al.* (2006)
EGCG	NLCE[r] and CSNLCE[s]	Inversion based process	Encapsulation efficiency (HPLC) and particle size (ZetaPalz analyser) Stability study *In vitro* release (dialysis bag method) Cytotoxicity (human THP-1 cell lines)	Acceptable particle size (43-53 nm) and high encapsulation efficiency (99%) Increased stability Delayed in vitro release Lowered levels of toxicity	Zhang *et al.* (2013)

[a]EGCG - Epigallocatechin gallate
[b]PLGA-PEG - Poly(lactide-co-glycolide)- polyethylene glycol
[c]PBS - Phosphate-buffered saline
[d]TF - Theaflavin
[e]UV-VIS - Ultra violet-visible spectroscopy
[f]SEM - Scanning electron microscopy
[g]HPLC - High pressure liquid chromatography
[h]FTIR - Fourier transform Infrared
[i]DPPH assay - 2,2-diphenyl-1-picryl-hydrazyl
[j]DLS - Dynamic light scattering
[k]TPP - Tripolyphosphate
[l]TEM - Transmission electron microscopy
[m]DSC - Differential scanning calorimetry
[n]XRD - X-ray diffraction
[o]RLS - Raman laser spectroscopy
[p]AFM - Atomic force microscopy
[q]USP - Absolute dissolution apparatus
[r]NLCE - Nanostructured lipid carriers
[s]CSNLCE - chitosan coated nanostructured lipid carriers

Table 2.16

Summary of the nanoencapsulation of phenolic compounds focusing on the materials, methods, analysis and main findings of the literature

Bioactive compound	Material	Method	Verification methods	Main findings	Source
Curcumin	PLGA[a]	Solid-in-oil-in-water solvent evaporation technique	Physicochemical characterisation (XRD[b], FTIR[c], DSC[d], HPLC[e] and SEM[f]) Encapsulation efficiency (UV-VIS[g]) Solubility and stability (incubator shaker) Bioavailability (rat model)	Encapsulation by hydrogen bonding Acceptable particle size (200 nm) and high encapsulation efficiency (91.96%) Increased solubility in aqueous media Higher bioavailability (5.6 times) than free curcumin	Xie *et al.* (2011)
	Eudragit S 100	Solvent evaporation technique	Encapsulation efficiency and particle size (optical microscopy and spectrophotometrically) Physical state and interactions (DSC and FTIR)	Acceptable particle size (29–31 µm) and encapsulation efficiency (21–3%) No significant drug-polymer interactions	Jenita *et al.* (2012)
	Liposomes	Lyophilisation	Cell assays (cell proliferation, apoptosis and gene expression) Animal testing (mice)	Increased survival, proliferation and apoptosis than free curcumin Suppression of carcinoma growth *in vivo*	Li *et al.* (2005)
Quercetin	Eudragit L30-55 methacrylate polymers	Solvent displacement method	Encapsulation efficiency and particle size (electrochemical methods) Release profiles (electrochemical methods) Molecular interactions (XRD, DSC and IR) Antioxidant properties (TBARS[h] and fluorescence spectroscopy) Bioaccessibility (in vitro digestion model)	Acceptable encapsulation efficiency (67%) and particle size (370 nm) Encapsulation by hydrogen bonding Improved bioaccessibility Maintained antioxidant ability after 6 month	Pool *et al.* (2012)
	PLA[i]	Solvent evaporation method	Morphological characterisation (SEM and AFM[j]) and encapsulation efficiency (HPLC) Spectroscopic characterisation (fluorescence and FTIR) Antioxidant assay (DPPH[k]) *In vitro* release (stirring under physiological conditions)	Smooth spherical particles Acceptable particle size (136–172 nm) and high encapsulation efficiency (96.7%) Initial burst release followed by sustained release	Kumari *et al.* (2010a)

Table 2.16 Continued

Resveratrol	Peanut-oil and emulsifiers	High pressure homogenisation	Particle size (photo correlation spectroscopy) Florescence spectrum (spectroflurometer) Transport through cells and cytotoxicity (Caco-2 cells) *In vitro* release (dialysis bag method)	Shorter transport time over cell monolayers Preservation of emulsion droplets Protection of resveratrol during cell transport Sustained release profiles	Sessa *et al.* (2012)
	Cyclodextrin and liposomal formulations	Inclusion complexation and thin film hydration methods	Encapsulation efficiency (UV-VIS) Stability study (particle size by light scattering) Drug release (dialysis method) Cytotoxicity (HT-29 cancer cells)	Acceptable particle size (131 nm) and loading capacity (11.6 %) Stabilised particles (up to 7 days) Improved release kinetics Improved cytotoxicity	Soo *et al.* (2016)
	mPEG[l] and PCL[m] copolymers	Nanopre-cipitation technique	Particle size (photo correlation spectroscopy), morphology (SEM and TEM[n]) and encapsulation efficiency (HPLC) *In vitro* release (dialysis bag) Uptake by tumour cells (C6 cells) and cytotoxicity (MTT[o] assay)	Smooth spherical particles Acceptable particle size (78 nm) and high encapsulation efficiency (91%) Initial burst release (50 %) followed by sustained release Higher cellular uptake and glioma cell death than for free resveratrol	(Shao *et al.*, 2009) Shao *et al.* (2009)

[a]PLGA - Poly(lactide-co-glycolide)
[b]XRD - X-ray diffraction
[c]FTIR - Fourier transform Infrared
[d]DSC - Differential scanning calorimetry
[e]HPLC - High pressure liquid chromatography
[f]SEM - Scanning electron microscopy
[g]UV-VIS - Ultra violet-visible spectroscopy
[h]TBARS - Thiobarbituric acid reactive substances
[i]PLA - Poly(lactic acid)
[j]AFM - Atomic force microscopy
[k]DPPH - 2,2-diphenyl-1-picryl-hydrazyl
[l]mPEG - methoxypoly(ethylene glycol)
[m]PCL - Polycaprolactone
[n]TEM - Transmission electron microscopy
[o]MTT - 3-(4,5-dimethylthiazol-2-yl)-2,5-diphenyltetrazolium bromide

2.5 Physicochemical properties and evaluation of encapsulated phenolic compounds

In the process of functional ingredient development, whether as the final product or pre-formulation, study of the physical and chemical characteristics is needed. Various physical properties are important with regard to the encapsulation of bioactive compounds, such as the mean particle size, distribution of particle size, crystallinity, thermal properties, encapsulation and loading efficiency, hygroscopicity and water activity, flow properties of dry product, chemical nature of the coating material, stability over time and bioavailability (Murugesan & Orsat, 2012). The understanding and correct evaluation of these properties is of utmost importance to ensure correct formulation, technical description and stability of encapsulated functional ingredient formulations. The next section will focus on the effect of different physicochemical characteristics on the final product and analytical methods to evaluate these characteristics. Table 2.18 summarises the different types of physicochemical analyses according to importance and main analytical techniques.

2.5.1 Particle size, charge and morphology

Particle size affects the release rate, dissolution rate, stability, visual characteristics and flowability of an ingredient (Aulton, 1996). A decrease in particle size results in an increase in the surface area, leading to increased surface reactivity (Neethirajan & Jayas, 2011). It also enables the uptake of bioactive compounds due to the small size of cellular mucosa pores in the human body (Reis *et al.*, 2006) and increases the free flowing properties of a powdered product (Chiou & Langrish, 2007). The distribution of particle size is also important as a more uniform distribution results in more predictable behaviour in the human body and ease of movement of particles past each other, affecting the physical characteristics (Verma & Stellacci, 2010).

The particle morphology, i.e. shape, texture and charge, affects the flowability, integrity of the structure and absorption. According to Tonon *et al.* (2008) more textured and indented particles tend to cause problems with regard to flowability. Furthermore, textured areas could also act as weak spots in the particle structure, resulting in less protection of the encapsulated compounds against environmental degradation such as oxidation (Tonon *et al.*, 2008). The charges of the particles are important concerning stability and cellular uptake. Charged particles (negative or positive) have been shown to be related to increased colloidal stability due to repulsion between the nanoparticles (Zhang *et al.*, 2008). With regard to cellular uptake, negatively charged compounds dominate the intestinal mucosa, resulting in neutral or cationic carriers passing more efficiently through the pores (Reis *et al.*, 2006). However, studies have shown the effect of charge and related surface chemistry to be more complicated than described above. As an example, Villanueva *et al.* (2009) found increased uptake for anionic iron oxide particles compared to their neutral counterparts. In addition to cellular uptake, the charge density and polarity affects the cytotoxicity. Charged gold nanoparticles are more cytotoxic

than neutral forms and specifically positively charged gold nanoparticles have been shown to have higher toxicity than their negatively charged counterparts. However, this is not applicable to all nanoparticles, as for PLGA and PLGA functionalised nanoparticles, where charge has been shown to play no role (Frohlich, 2012). Thus, comparisons between particulate delivery systems on surface-charge effects can only be deemed feasible when comparing similar chemical, size and shape particles with different charge functionalities.

The particle size, morphology and charge can be investigated using various analytical techniques. Scanning electron microscopy (SEM) allows the imaging of the surface of small particles whereby information on the surface morphology and size can be obtained. Tonon *et al.* (2008), Sansone *et al.* (2011b), Silva *et al.* (2013) and Zhang *et al.* (2013) successfully observed the particle surface morphology and size of microencapsulated phenolic compounds in the form of spray-dried powders with SEM. Other studies described successful application of SEM to view nanoparticles (Peres *et al.*, 2011; Krishnaswamy *et al.*, 2012; Pal & Saha, 2013; Sanna *et al.*, 2015). Transmission electron microscopy (TEM) allows imaging through the particle and provides information on the entire particle morphology, including the distribution of encapsulating material and bioactive compounds as the technique is sensitive to the differences in atomic number. Liang *et al.* (2011), Tsai *et al.* (2011) and Fathi *et al.* (2012a) successfully used TEM to observe the structure and size of nanoparticles. Dynamic light scattering (DLS) can be used to determine the particle size and charge in suspensions. Fang *et al.* (2006), Liang *et al.* (2011), Fathi *et al.* (2012b) and Kim *et al.* (2013) are a few examples where DLS was used to determine the size and charge of different nanoparticles. A detailed study by Bondar, Saifullina, Shakhmaeva, Mavlyutova & Abdullin (2012) proceeded to investigate the effect that polymeric nanoparticles with different charges had on the zeta potential of human cells. Introduction of polycations and amphiphilic Pluronic L121 resulted in neutralisation of negatively charged cells, indicating absorption of the polymers by the cells.

2.5.2 Encapsulation efficiency and loading efficiency

The encapsulation efficiency is a measure of the amount of active compound captured relative to the amount of compound added to the encapsulation reaction. The method and isolation of nanoparticles will vary according to the different encapsulation methods used.

The encapsulation efficiency can be calculated using Eq. 2.11 and 2.12 (Fang *et al.*, 2006; Lu *et al.*, 2011; Fathi *et al.*, 2012b; Zhang *et al.*, 2013):

$$Encapsulation\ efficiency = \frac{total\ mass\ added - total\ mass\ free}{total\ mass\ added} \times 100\% \qquad (2.11)$$

or

$$Encapsulation\ efficiency = \frac{total\ mass\ encapsulated}{total\ mass\ added} \times 100\% \quad (2.12)$$

The loading capacity is similar to that of the encapsulation efficiency, but takes into account the amount of bioactive compound loaded in relation to the nanoparticles. This can be used as an indication of the interaction between the bioactive compound and the nanocapsules. The loading capacity can be calculated using Eq. 2.13 (Fang *et al.*, 2006; Lu *et al.*, 2011; Fathi *et al.*, 2012b; Zhang *et al.*, 2013)

$$Loading\ capacity = \frac{total\ mass\ encapsulated}{total\ mass\ of\ loaded\ particles} \times 100\% \quad (2.13)$$

The amount encapsulated as well as the free and total amount added can be determined by a variety of analytical techniques. The method depends on the nature and solubility of the particles and bioactive ingredients, whether they consist of one compound or a mixture of active components. In the case of a single bioactive compound, UV-VIS spectroscopy is a viable option. For example, the loading and encapsulation efficiency of PLGA nanoparticles loaded with either EGCG or TF were calculated in this manner. A fixed quantity of particles were placed in acetonitrile which dissolves the encapsulating polymer, but precipitates the tea polyphenols. The polyphenols were collected by centrifugation and dissolved in water for UV-VIS analysis (Srivastava *et al.*, 2013). Xie *et al.* (2011) used a similar approach with UV-VIS to determine the amount of curcumin encapsulated in PLGA nanoparticles. However, the curcumin was leached from the particles and the supernatant analysed, instead of dissolving the particles. Other methods for determining the encapsulation efficiency is HPLC or antioxidant assays where the latter gives less specific results. The quantity of white tea extract encapsulated in PCL and alginate was quantified using a colorimetric Folin-Ciocalteu assay as well as HPLC to determine the individual tea polyphenols encapsulated. The results showed slightly higher encapsulation efficiency for the HPLC method than for the Folin-Ciocalteu assay (Sanna *et al.*, 2015).

2.5.3 Flow properties

Several processes in the development of a functional product are affected by the flow characteristics of the bulk solids (granules, powders, dust, single components or blends) including transfer, storage, feeding and blending (Prescott & Barnum, 2000). The flow properties of powders depend on various factors such as the particle size, shape and distribution. Generally, particles below 100 microns tend to be more cohesive due to a high surface area, where particles above 250 microns tend to be free flowing. Particles with uneven shapes and texturing show different flow properties to particles with smooth surfaces due to larger inter-particulate contact areas, causing cohesiveness and poor flow properties (Aulton, 1996). In addition to particle dimensions, the chemical composition of the particles play a role as well as external factors such as

temperature and moisture (Schulze, 2008). Powder flow properties are generally assessed and tested independently from these factors.

Flowability test methods include the angle of repose, Carr's compressibility index (*C.I.*), Hausner ratio (*HR*), dynamic angle of repose, flow funnels and minimum orifice diameter tests as summarised by Prescott & Barnum (2000). The *C.I.* and *HR* can be obtained by pouring the powder into a measuring cylinder and determining the mass (*m*) and the poured volume (V_p) after which the cylinder is tapped until a constant tapped volume (V_t) is obtained.

Poured density, $D_p = \frac{m}{V_p}$ (2.14)

Tapped density, $D_t = \frac{m}{V_t}$ (2.15)

These densities can be used to calculate the *C.I.* and the *HR*:

C.I. = $(D_p - D_t)/D_p$ (2.16)

$HR = D_p/D_t$ (2.17)

As an example, Schüssele & Bauer-Brandl (2003) investigated the flowability of different excipients used for compression in the pharmaceutical industry using compressibility tests as prescribed by the European Pharmacopoeia (Anonymous, 2004). The Carr's compressibility index and the Hausner ratio were also calculated as an indicator of flowability. Pauck *et al.* (2017) and Miller *et al.* (2018) determined the flowability of microencapsulated spray-dried honeybush and rooibos powders, respectively, in order to determine the effect of the microencapsulation agent on the powder properties. The powders were classified as ranging from free flowing to cohesive according to Table 2.17:

Table 2.17

Powder flow characteristics based on Carr's compresibility index and Hausner ratio (Carr, 1965; Fitzpatrick, 2013)

Flow character	Carr compressibility index	Hausner ratio
Very, very poor	>38	>1.60
Very poor	32–37	1.46–1.59
Poor	26–31	1.35–1.45
Passable	21–25	1.26–1.34
Fair	16–20	1.19–1.25
Good	11–15	1.12–1.18
Excellent	0–10	1.00–1.11

2.5.4 Compatibility and interaction between active compounds and excipients

All functional food ingredients and products are required to show a degree of physical and chemical stability during storage and production in order to be considered viable. Shelf-life testing of products can be laborious, costly and time consuming. As an alternative, the thermal properties are determined as heat transfer accompanies chemical and physical degradation processes (Oliyai & Lindenbaum, 1991). One of these

methods includes the screening of excipient compatibility with the bioactive compound. The incompatibility between excipients and active ingredients implies that reactions could take place resulting in physical and/or chemical changes in the final formulation.

Traditionally techniques used include differential scanning calorimetry (DSC) and differential thermal analysis (DTA) which requires small amounts of sample, short analysis time and minimal experimental work. Generally it is assumed that if the components are compatible with each other the thermal properties, including the melting point, change in enthalpy, glass transition and recrystallisation, appear as the sum of the components in a single transition (Chadha & Bhandari, 2004). Thus, if thermal transitions shift significantly or new peaks appear which do not form part of the individual ingredients, it can be an indication of an interaction between components and subsequent possible instability. However, DSC has poor sensitivity and high temperatures are needed to observe chemical changes (Schmitt, Peck, Sun & Geoffroy, 2001).

Isothermal microcalorimetry allows the measurement of these reactions at much lower and more relevant temperatures due to increased detection sensitivity (Schmitt *et al.*, 2001). The reactions that take place in mixtures containing active compounds and excipients are generally complicated and difficult to identify. Isothermal microcalorimetry has the ability to detect enthalpy changes from several chemical processes including evaporation, phase transitions, chemical reactions, crystallisation, and dissolution. The technique is used to detect any changes that might cause instability during storage, rather than predict what the instability is, owing to the non-specific nature of the analysis. The different processes taking place in isothermal microcalorimetry can be mathematically defined in Eq.2.18:

$$\frac{dq}{dt} = -\sum_{i=1}^{n} \Delta H_i \frac{dn_i}{dt} \qquad (2.18)$$

where $\frac{dq}{dt}$ is the measured signal or outcome, ΔH_i the reaction enthalpy and $\frac{dn_i}{dt}$ the rate of the reaction or process.

In order to establish the compatibility of a mixture, the heat flow of the individual components are measured. These curves are used to construct a non-interaction curve that is compared to that of the actual mixture. Any significant differences in heat flow curves are indicators of possible interactions and thus possible problems during storage (Schmitt *et al.*, 2001). As an demonstration of this, Pauck *et al.* (2017) and Miller *et al.* (2018) respectively investigated the compatibility of honeybush and rooibos spray-dried powders with the microencapsulation agents by constructing non-interaction curves. The results were used to indicate which formulations might have poor storage stability and were used to eliminate certain carriers and formulations.

The interaction of different components in a mixture can also be determined by investigation of the crystal structure and the characteristic chemical nature. Wu *et al.* (2008) investigated the encapsulation of quercetin

in Eudragit with PVA as stabiliser. X-ray diffractograms showed a disappearance of the crystal structure of quercetin after encapsulation owing to the amorphous intermolecular interactions in the matrix of the carrier. The study also relied on FTIR to investigate any interactions in the nanoparticulate systems. This technique gave contradicting results as no evidence of interactions between the encapsulating polymer, stabiliser and active component were seen.

2.5.5 Glass transition (T_g), crystallinity, water activity, moisture content and hygroscopicity

The interactions that takes place between functional food formulations and water in environments with different RH's during development and storage are of great interest in the product development process. It is important to determine the physical properties of the components beforehand to ensure correct handling and storage. Factors that affect the hygroscopicity of a formulation include the T_g and crystallinity. Apart from the properties that might cause physical changes when in contact with moisture vapour, the inherent water activity and moisture content of the formulation and components should also be considered.

2.5.5.1 Glass transition temperature (T_g)

The glass transition temperature can be defined as the temperature where an amorphous material transitions from a hard glassy substance to a rubbery substance as molecules have enough energy to move more freely (Jaya & Das, 2009). The T_g is also often called the sticky point temperature since foodstuffs generally become sticky and difficult to handle above this temperature (Jaya & Das, 2009). Generally, natural bioactive products, such as extracts from fruits contain low molecular sugars and have low glass transition temperatures. Furthermore, moisture acts as a plasticiser and continues to decrease the T_g, resulting in undesirable properties up to a point of deliquescence. Deliquescence is defined as a first order phase transition where a solid absorbs enough water in combination with condensation of water on the surface of the material, resulting in dissolution (Mauer & Taylor, 2010). DSC is generally used to determine the T_g, where the transition is usually detected as a shift in the baseline as a result of change in the heat capacity (Jaya & Das, 2009).

2.5.5.2 Crystallinity

Natural substances, due to complex mixtures and matrices, are generally amorphous, which is directly associated with T_g. The degree of crystallinity has an effect on the stickiness, flowability and solubility of powdered products (Cortés-Rojas & Oliveira, 2012). Amorphous structures are considered more unstable than their crystalline counterparts, especially in the presence of moisture. Water can penetrate into the amorphous regions of the material, acting as a plasticiser. This results in increased molecular mobility, leading to an

increase in reaction rates and possible crystallisation (Bott *et al.*, 2010). These types of transitions are undesirable when designing a functional food product as it will result in a decrease in the activity of the bioactive ingredients and undesirable physical attributes.

X-ray diffraction is a popular technique to obtain information on the crystal structure of functional food formulations. Fathi *et al.* (2012b) investigated the physical state of hesperetin-loaded lipid based nanoparticles. The unloaded nanoparticles showed a crystalline structure with distinct peaks with a decrease in the crystallinity, as shown by broad peaks, noted for the hesperetin-loaded nanoparticles. The results were confirmed by investigating the DSC of the nanostructures where smaller melting endotherms were seen after loading of hesperetin. The crystallinity of the different encapsulating lipids investigated also directly affected the encapsulation efficiency of hesperetin.

Shaikh, Ankola, Beniwal, Singh & Kumar (2009) investigated the crystal structure of PLGA encapsulated curcumin. In this case, the results were in contrast to those observed by Fathi *et al.* (2012b) for hesperetin. The encapsulating material showed an amorphous structure, whereas the active molecule showed a highly crystalline structure which disappeared after encapsulation. Transitions in the crystal structure can also be quantified and investigated with isothermal calorimetry (Andrade, Lemus & Perez, 2011). Briggner, Buckton, Bystrom & Darcy (1994) investigated the crystallisation of amorphous lactose monohydrate powders in the presence of moisture. This technique gave quantitative information on the crystal structure of the powders allowing predictions to be made on the possible transitions the material will undergo over time under certain storage conditions.

2.5.5.3 Moisture content and water activity

Apart from the possible changes that might occur due to the T_g and crystallinity of functional food products, properties such as moisture content of the product must also be considered. Most of the reactions that take place during storage of phenolic-rich products are related to moisture already present in the products. Thus in order to increase the shelf-life, the availability of water for biochemical degradation reactions must be minimised (Malthlouthi, 2001).

The measurement of moisture content and water activity (a_w) are the most frequent analyses performed in the food industry (Malthlouthi, 2001). The most common method for moisture content measurement is the desiccation method where the total amount of moisture present is expressed as a percentage of the total weight of the product. The sample is heated until no further water loss is observed. As a guideline, powders produced by spray-drying must have a moisture content below 5% to ensure good handleability and shelf-life stability (Sinija, Mishra & Bal, 2007; Şahin-Nadeem, Dinçer, Torun, Topuz & Özdemir, 2013).

However, the moisture content is not a sufficient indication of the stability as it does not provide any information on the nature of the water within the product (Malthlouthi, 2001). Therefore, the water activity must also be determined to give a better indication of the effect that the water will have on the stability of a product. Water activity can be defined as the amount of water available for chemical, biochemical and microbiological reactions to take place (Andrade *et al.*, 2011) and thus the degree to which the water is bound within a system (Al-Muhtaseb, McMinn & Magee, 2002). A_w values are classified on a scale of zero to 1, where 1 corresponds to pure water and zero indicates the absence of water. To ensure minimal microbial growth and biochemical degradation, a value below 0.5 is recommended for shelf stable food products (Woo & Bhandari, 2013).

2.5.5.4 Hygroscopicity

Hygroscopicity can be defined as the interaction of water with a material (Murikipudi, Gupta & Sihorkar, 2013). Knowledge on hygroscopicity is vital for functional food ingredients, based on natural bioactive ingredients with an amorphous nature and low T_g, in order to establish correct storage conditions and packaging. Hygroscopicity can be determined by various analytical techniques, including determination of the equilibrium moisture content where samples are equilibrated in specific RH environments created by saturated salt solutions. However, this method requires long time periods before equilibrium is reached and large sample sizes (Murikipudi *et al.*, 2013).

These draw backs can be overcome by the dynamic vapour sorption analysis method used to obtained moisture sorption isotherms (MSI's). MSI's provide a complete behavioural overview of a product over a large range of humidity. Vapour sorption analysis involves the recording of gravimetric differences as a function of RH under isothermal conditions (Murikipudi *et al.*, 2013). The RH could be increased or decreased resulting in absorption and desorption data, respectively. This provides insight not only into the hygroscopicity, but the nature of the interaction of water with the material as it describes the relationship between moisture content and water activity (Andrade *et al.*, 2011). Fig. 2.13 shows a typical MSI absorption and desorption cycle for a food product.

The shape of the isotherm provides insight into the binding mechanism of the water to the material in question. Three distinct regions are usually visible, namely strongly bound water (a), structural and monolayer water bonded by hydrogen (b) and water that is trapped between voids, but is not bound to the material (c). Furthermore, differences in the absorption and desorption curves is defined as hysteresis, which is an indication of permanent structural changes that takes place with water uptake (Andrade *et al.*, 2011). These types of changes are usually associated with shorter shelf-life of products.

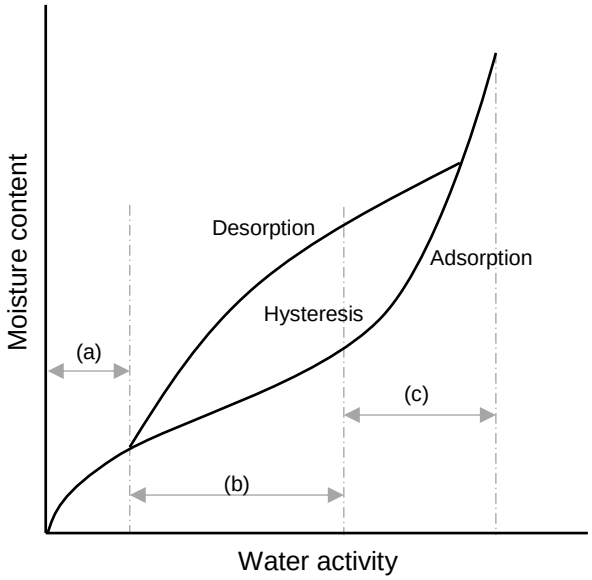

Fig. 2.13 Example of a typical MSI absorption and desorption cycle for a food product (a) strongly bound water, (b) capillary water and (c) free water (Andrade *et al.*, 2011)

The isotherms as a whole are also classified according to their shape and processes (Brunauer, Deming & Teller, 1940). Langmuir isotherms (type 1) are recognised by convex upwards curves and takes into account the filling of a single layer at the internal surface layer of a material with moisture. Sigmoidal (type 2) isotherms are recognised by concave upwards curves and take into account filling of multiple layers at the internal surface of a material with moisture. Flory-Huggins isotherms (type 3) take into account the plasticising effect of moisture. Type 4 isotherms take into account swellable hydrophilic materials up to a point of maximum absorption and Brunauer-Emmett-Teller (BET) multilayer adsorption isotherms (type 5) specifically indicate the interaction of water vapour with charcoal. Types 2 and 4 are most generally seen for food products (Andrade *et al.*, 2011).

Different mathematical models have been developed to describe the relation between water activity and moisture content of materials. The Guggenheim-Anderson-de Boer (GAB) and BET models are most commonly used in the food industry (Andrade *et al.*, 2011). The BET model is suitable for isotherms type 2 and 3 and is based on the principle of multi-layer water sorption up until a_w values < 0.4. The GAB model is a refined form of the BET and other models. It's based on the principle that water molecules in the sorbed layers are identical, but different to water molecules in the liquid state.

From these models the monolayer moisture content can be calculated, as a measure of the amount of water that is strongly absorbed to the surface of a material and as a rule, at any RH above this value, water is more available for chemical reactions (De Souza *et al.*, 2013). As an example of application of the MSI, Fabra, Márquez, Castro & Chiralt (2011) investigated the effect of maltodextrin as an excipient on the water sorption

behaviour of moni *(Morinda citifolia* L.*)* pulp powder. The sorption data was found to fit well to the GAB model and the curves were sigmoidal in shape indicating the filling of multiple layers with moisture. The latter type of isotherm is common for food stuff and herbal products as found for a *Passiflora alata* bed- and spray-dried extract (Bott *et al.*, 2010).

Table 2.18

Summary of the different types of physicochemical analysis according to importance and main analytical techniques utilised

Physicochemical factor	Importance	Main Analysis techniques
Particle size, morphology and charge	Affect flow properties and bioavailability (Reis *et al.*, 2006; Chiou & Langrish, 2007; Tonon *et al.*, 2008).	SEM[a] TEM[b] DLS[c]
Flow properties	Affect transfer, storage, feeding and blending of powder (Prescott & Barnum, 2000).	Carr's compressibility index Hausner ratio Angle of repose
Compatibility between active compounds and excipients	Affect stability - Interactions between excipients and active compounds bring about unwanted physical and chemical changes (Chadha & Bhandari, 2004).	Isothermal calorimetry DSC[d] XRD[e] FTIR[f]
Crystallinity	Affect the stability – amorphous materials can crystallise during storage and in the presence of moisture (Bott *et al.*, 2010).	XRD Isothermal calorimetry
Glass transition temperature	Affects the stability – Storage above T_g[g] results in stickiness and phase transitions (Jaya & Das, 2009).	DSC XRD
Water activity, moisture content and hygroscopicity	Affect the degradation, microbial spoilage, lowering of the T_g and crystallisation (Cortés-Rojas & Oliveira, 2012).	Water activity analyser Vapour sorption analysis- (MSI) Equilibrium moisture content analyser Desiccation
Encapsulation and loading efficiency	Affects the dose required and efficiency of the process (Fang et al., 2006, Lu et al., 2011, Fathi et al., 2012b, Zhang et al., 2013).	UV-VIS[h] HPLC[i] FTIR

[a]SEM - Scanning electron microscopy
[b]TEM - Transmission electron microscopy
[c]DLS - Dynamic light scattering
[d]DSC - Differential scanning calorimetry
[e]XRD - X-ray diffraction
[f]FTIR - Fourier transform infrared
[g]T_g - Glass transition temperature
[h]UV-VIS - Ultra violet visible spectroscopy
[i]HPLC - High pressure liquid chromatography

2.6 General conclusion

Rooibos tea consumption is fast growing as a result of its high reported antioxidant activity and caffeine-free status, branding it as a health product rather than an ordinary tea (Joubert & De Beer, 2011). Despite all the health-promoting properties of rooibos, and specifically, aspalathin which has been shown to be useful in the prevention of metabolic syndrome (Muller *et al.*, 2018; Johnson *et al.*, 2018), the benefits cannot be utilised due to poor stability during storage in conventional ready-to-drink beverages. Thus, there is a need for alternative functional rooibos products with high aspalalthin content and better stability.

Recent literature on functional food and nutraceutical products containing phenolic compounds has focused on micro- and nanoencapsulation as an efficient method to improve the qualities of the bioactive compounds, aiming to produce market viable functional products. Limited studies are available on the micro- or

nanoencapsulation of rooibos. Miller *et al.* (2018) optimised the spray-drying of green rooibos nutraceutical extract with different microencapsulation materials. To date, only one study reported the use of a nanoencapsulated rooibos extract (De Beer, Joubert, Viljoen & Manley, 2011). A green rooibos extract encapsulated with ascorbic acid in a polyoxyethylene sorbitan monolaurate (Tween 20 emulsifier) shell improved the thermal stability of aspalathin compared to the un-encapsulated extract. There are various methods and materials for the encapsulation of phenolic compounds applicable to rooibos; however, the research on rooibos encapsulation is currently limited to a few select studies.

Furthermore, routine testing methods and analysis of natural remedies and functional food ingredients and products are needed. For further growth in this market, consumers need sufficient evidence that natural products can live up to the claims made regarding their health benefits. During development of a green rooibos functional ingredient product, various encapsulation formulations and methods will be investigated and types of analysis required for functional foods and nutraceutical products will be addressed.

This research on functional food product development will aim to fill a gap in the market for successful and properly evaluated, standardised natural health remedies. This will also advance aspalathin as a health-promoting substance by reclassifying it in the minds of the consumers as a standerdised nutraceutical product.

2.7 References

Agnihotri, S. A., Mallikarjuna, N. N. & Aminabhavi, T. M. (2004). Recent advances on chitosan-based micro- and nanoparticles in drug delivery. *Journal of Controlled Release,* 100, 5–28.

Al-Muhtaseb, A. H., McMinn, W. A. M. & Magee, T. R. A. (2002). Moisture sorption isotherm characteristics of food products: A review. *Food and Bioproducts Processing,* 80, 118–128.

Alehosseini, A., Ghorani, B., Sarabi-Jamab, M. & Tucker, N. (2017). Principles of electrospraying: A new approach in protection of bioactive compounds in foods. *Critical Reviews in Food Science and Nutrition*, DOI: 10.1080/10408398.2017.1323723.

Alshamsan, A. (2014). Nanoprecipitation is more efficient than emulsion solvent evaporation method to encapsulate cucurbitacin I in PLGA nanoparticles. *Saudi Pharmaceutical Journal,* 22, 219–222.

Anandharamakrishnan, C. (2014). Techniques for nanoencapsulation of food ingredients. Pp. 1–89. New York: Springer.

Andrade, R. D., Lemus, R. & Perez, C. E. (2011). Models of sorption isotherms for food. *Vitae Revista de la Facultad de Quimica Farmaceutica,* 18, 325–334.

Anonymous (2004). Towards a European strategy for nanotechnology. Pp. 4–21. Luxembourg: Office for official Publications of the European Communities.

Arulmozhi, V., Pandian, K. & Mirunalini, S. (2013). Ellagic acid encapsulated chitosan nanoparticles for drug delivery system in human oral cancer cell line (KB). *Colloids and Surfaces B: Biointerfaces,* 110, 313–320.

Aulton, M. E. (1996). Pharmaceutics: The science of dosage form design. Pp. 1–725. New York: Churchill Livingstone.

Bakowska-Barczak, A. M. & Kolodziejczyk, P. P. (2011). Black currant polyphenols: Their storage stability and microencapsulation. *Industrial Crops and Products,* 34, 1301–1309.

Balassa, L. L., Fanger, G. O. & Wurzburg, O. B. (1971). Microencapsulation in the food industry. *Critical Reviews in Food Science & Nutrition,* 2, 245–265.

Beelders, T., De Beer, D., Ferreira, D., Kidd, M. & Joubert, E. (2017). Thermal stability of the functional ingredients, glucosylated benzophenones and xanthones of honeybush (*Cyclopia genistoides*), in an aqueous model solution. *Food Chemistry,* 233, 412–421.

Beelders, T., De Beer, D. & Joubert, E. (2015). Thermal degradation kinetics modeling of benzophenones and xanthones during high-temperature oxidation of *Cyclopia genistoides* (L.) Vent. plant material. *Journal of Agricultural and Food Chemistry,* 63, 5518–5527.

Beelders, T., Kalili, K. M., Joubert, E., De Beer, D. & De Villiers, A. (2012). Comprehensive two-dimensional liquid chromatographic analysis of rooibos (*Aspalathus linearis*) phenolics. *Journal of Seperation Science,* 35, 1808–1820.

Berscht, P. C., Nies, B., Liebendörfer, A. & Kreuter, J. (1994). Incorporation of basic fibroblast growth factor into kethylpyrrolidinone chitosan fleeces and determination of the in vitro release characteristics. *Biomaterials,* 15, 593–600.

Bhushani, J. A., Kurrey, N. K. & Anandharamakrishnan, C. (2017). Nanoencapsulation of green tea catechins by electrospraying technique and its effect on controlled release and *in-vitro* permeability. *Journal of Food Engineering,* 199, 82–92.

Bilati, U., Allémann, E. & Doelker, E. (2005). Development of a nanoprecipitation method intended for the entrapment of hydrophilic drugs into nanoparticles. *European Journal of Pharmaceutical Sciences,* 24, 67–75.

Bilia, A. R., Isacchi, B., Righeschi, C., Guccione, C. & Bergonzi, M. C. (2014). Flavonoids loaded in nanocarriers: an opportunity to increase oral bioavailability and bioefficacy. *Food and Nutrition Sciences,* 5, 1212–1327.

Binns, N. (2009). Perspective on ILSI's international activities on functional foods. *ILSI Europe Functional Foods Task Force*, 1-57.

Bobbio, F. O., Do Nascimento Varella, M. T. & Bobbio, P. A. (1994). Effect of light and tannic acid on the stability of anthocyanin in DMSO and in water. *Food Chemistry,* 51, 183–185.

Bock, N., Woodruff, M. A., Hutmacher, D. W. & Dargaville, T. R. (2011). Electrospraying, a reproducible method for production of polymeric microspheres for biomedical applications. *Polymers,* 3, 131–149.

Bodmeier, R. & Chen, H. (1988). Preparation of biodegradable poly (±) lactide microparticles using a spray-drying technique. *Journal of Pharmacy and Pharmacology,* 40, 754–757.

Bohn, T. (2014). Dietary factors affecting polyphenol bioavailability. *Nutrition Reviews,* 72, 429–452.

Bondar, O. V., Saifullina, D. V., Shakhmaeva, I. I., Mavlyutova, I. I. & Abdullin, T. I. (2012). Monitoring of the zeta potential of human cells upon reduction in their viability and interaction with polymers. *Acta naturae,* 4, 78–81.

Bott, R. F., Labuza, T. P. & Oliveira, W. P. (2010). Stability testing of spray- and spouted bed-dried extracts of *Passiflora alata*. *Drying Technology,* 28, 1255–1265.

Bowles, S., Joubert, E., De Beer, D., Louw, J., Brunschwig, C., Njoroge, M., Lawrence, N., Wiesner, L., Chibale, K. & Muller, C. (2017). Intestinal transport characteristics and metabolism of *C*-glucosyl dihydrochalcone, aspalathin. *Molecules,* 22, 554–569.

Breiter, T., Laue, C., Kressel, G., Gröll, S., Engelhardt, U. H. & Hahn, A. (2011). Bioavailability and antioxidant potential of rooibos flavonoids in humans following the consumption of different rooibos formulations. *Food Chemistry,* 128 338–347.

Briggner, L., Buckton, G., Bystrom, K. & Darcy, P. (1994). The use of isothermal microcalorimetry in the study of changes in crystallinity induced during the processing of powders. *International Journal of Pharmaceutics,* 105, 125–135.

Brunauer, S., Deming, L. S. & Teller, E. (1940). On a theory of Van der Waals adsorption of gases. *Journal of the American Chemical Society,* 62, 1723–1732.

Cai, Y., Anavy, N. D. & Chow, H. S. (2002). Contribution of presystemic hepatic extraction to low oral bioavailability of green tea catechins in rats. *Drug and Metabolism Disposition,* 30, 1246–1249.

Canales, I., Borrego, F. & Lindley, M. G. (1993). Neohesperidin dihydrochalcone stability in aqueous buffer solutions. *Journal of Food Science,* 57, 589–591.

Carr, R. L. (1965). Classifying flow properties of solids. *Chemical Engineering,* 72, 69–72.

Catterall, F., King, L., Clifford, M. & Ioannides, C. (2003). Bioavailability of dietary doses of ^{3}H-labelled tea antioxidants (+)-catechin and (-)-epicatechin in rat. *Xenobiotica,* 33, 743–753.

Chadha, R. & Bhandari, S. (2004). Drug–excipient compatibility screening — Role of thermoanalytical and spectroscopic techniques. *Journal of Pharmaceutical and Biomedical Analysis,* 87, 82–97.

Chau, C., Wu, S. & Yen, G. (2007). The development of regulations for food nanotechnology. *Trends in Food Science & Technology,* 18, 269–280.

Chen, J., Lin, H. & Hu, M. (2003). Metabolism of flavonoids via enteric recycling: Role of intestinal disposition. *Journal of Pharmacology and Experimental Therapeutics,* 304, 1228–1235.

Chen, X. K. (2008). PAMPA: Novel BD Gentest™ pre-coated PAMPA plate system with high Caco-2 and human absorption predictability. URL: https://www.bdbiosciences.com/documents/webinar_2008_08_PAMPA101.pdf. Accessed 17.10.17.

Chien, J. T., Hsieh, H. C., Kao, T. H. & Chen, B. H. (2005). Kinetic model for studying the conversion and degradation of isoflavones during heating. *Food Chemistry,* 91 425–434.

Chik, C. T., Abdullah, A., Abdullah, N. & Mustapha, W. A. W. (2011). The effect of maltodextrin and additive added towards pitaya juice powder total phenolic content and antioxidant activity. *International Proceedings of Chemical, Biological and Environmental Engineering,* 9, 224–228.

Chiou, D. & Langrish, T. A. G. (2007). Development and characterisation of novel nutraceuticals with spray drying technology. *Journal of Food Engineering,* 82, 84–91.

Cortés-Rojas, D. F. & Oliveira, W. P. (2012). Physicochemical properties of phytopharmaceutical preparations as affected by drying methods and carriers. *Drying Technology,* 30, 921–934.

Courts, F. L. & Williamson, G. (2009). The *C*-glycosyl flavonoid, aspalathin, is absorbed, methylated and glucuronidated intact in humans. *Molecular Nutrition and Food Research,* 53, 1104–1111.

Da Rosa, C. G., Borges, D. B., Zambiazi, R. C., Nunes, M. R., Benvenutti, E. V., Da Luz, S. R., D'Avila, R. F. & Rutz, J. K. (2013). Microencapsulation of gallic acid in chitosan, β-cyclodextrin and xanthan. *Industrial Crops and Products,* 46, 138–146.

Danhier, F., Ansorena, E., Silva, J. M., Coco, R., Le Breton, A. & Préat, v. (2012). PLGA-based nanoparticles: An overview of biomedical applications. *Journal of Controlled Release,* 161, 505–522.

Davda, J. & Labhasetwar, V. (2002). Characterization of nanoparticle uptake by endothelial cells. *International Journal of Pharmaceutics,* 233, 51–59.

De Almeida, C. L. B., Boeing, T., Somensi, L. B., Steimbach, V. M. B., Da Silva, L. M., De Andrade, S. F., Delle Monache, F., Cechinel-Filho, V. & De Souza, P. (2017). Diuretic, natriuretic and potassium-sparing effect of nothofagin isolated from *Leandra dasytricha* (A. Gray) Cogn. leaves in normotensive and hypertensive rats. *Chemico-Biological Interactions,* 268, 103–110.

De Assis, L. M., Machado, A. R., De Souza Da Motta, A., Costa, J. A. V. & De Souza-Soares, L. A. (2014). Development and characterization of nanovesicles containing phenolic compounds of microalgae *spirulina* strain LEB-18 and *Chlorella pyrenoidosa*. *Advances in Materials Physics and Chemistry,* 04, 6–12.

De Beer, D., Joubert, E., Viljoen, M. & Manley, M. (2011). Enhancing aspalathin stability in rooibos (*Aspalathus linearis*) ready-to-drink iced teas during storage: the role of nano-emulsification and beverage ingredients, citric and ascorbic acids. *Journal of the Science of Food and Agriculture,* 92, 274–282.

De Kruif, C. G., Weinbreck, F. & De Vries, R. (2004). Complex coacervation of proteins and anionic polysaccharides. *Current Opinion in Colloid & Interface Science,* 9, 340–349.

De Martimprey, H., Vauthier, C., Malvy, C. & Couvreur, P. (2009). Polymer nanocarriers for the delivery of small fragments of nucleic acids: oligonucleotides and siRNA. *European Journal of Pharmaceutics,* 71, 490–504.

De Paepe, D., Valkenborg, D., Coudijzer, K., Noten, B., Servaes, K., De Loose, M., Voorspoels, S., Diels, L. & Van Droogenbroeck, B. (2014). Thermal degradation of cloudy apple juice phenolic constituents. *Food Chemistry,* 162, 176–185.

De Souza, J. R. R., Feitosa, J. P. A., Ricardo, N. M. P. S., Trevisan, M. T. S., De Paula, H. C. B., Ulrich, C. M. & Owen, R. W. (2013). Spray-drying encapsulation of mangiferin using natural polymers. *Food Hydrocolloids,* 33, 10–18.

De Souza, V. B., Thomazini, M., Balieiro, J. C. & Fávaro-Trindade, C. S. (2015). Effect of spray drying on the physicochemical properties and color stability of the powdered pigment obtained from vinification byproducts of the Bordo grape (*Vitis labrusca*). *Food and Bioproducts Processing,* 93, 39–50.

Del Rio, D., Rodriguez-Mateos, A., Spencer, J. P., Tognolini, M., Borges, G. & Crozier, A. (2013). Dietary (poly)phenolics in human health: structures, bioavailability, and evidence of protective effects against chronic diseases. *Antioxidants & Redox Signaling,* 18, 1818–1892.

Desai, K. G. & Park, H. J. (2005a). Encapsulation of vitamin C in tripolyphosphate cross-linked chitosan microspheres by spray drying. *Journal of Microencapsulation,* 22, 179–192.

Desai, K. G. H. & Park, H. J. (2005b). Recent developments in microencapsulation of food ingredients. *Drying Technology,* 23, 1361–1394.

Desorby, S. A., Netto, F. M. & Labuza, T. P. (1997). Comparison of spray-drying, drum-drying and freeze-drying for β-carotene encapsulation and preservation *Journal of Food Science,* 62, 1159–1162.

Drosou, C. G., Krokida, M. K. & Biliaderis, C. G. (2017). Encapsulation of bioactive compounds through electrospinning/electrospraying and spray drying: A comparative assessment of food-related applications. *Drying Technology,* 35, 139–162.

Dube, A., Ng, K., Nicolazzo, J. A. & Larson, I. (2010). Effective use of reducing agents and nanoparticle encapsulation in stabilizing catechins in alkaline solution. *Food Chemistry,* 122, 662–667.

Dvorakova, K., Dorr, R. T., Valcic, S., B., T. & Alberts, D. S. (1999). Pharmacokinetics of the green tea derivative, EGCG, by the topical route of administration in mouse and human skin. *Cancer Chemotherapy and Pharmacology,* 43, 331–335.

EMEA (2003). ICH Q1A Stability testing guidelines: Stability testing of new drug substances and products. URL http://www.ich.org/fileadmin/Public_Web_Site/ICH_Products/Guidelines/Quality/Q1A_R2/Step4/Q1A_R2__Guideline.pdf. Accessed 13.10.17.

Englyst, N. H., Veenstra, J. & Hudson, J. G. (1996). Measurement of rapidly available glucose (RAG) in plant foods: a potential in vitro predictor of the glycaemic response. *British Journal of Nutrition,* 75, 327–337.

Espín, J. C., García-Conesa, M. T. & Tomás-Barberán, F. A. (2007). Nutraceuticals: Facts and fiction. *Phytochemistry,* 86, 2986–3008.

Ezhilarasi, P. N., Karthik, P., Chhanwal, N. & Anandharamakrishnan, C. (2013). Nanoencapsulation techniques for food bioactive components: A review. *Food and Bioprocess Technology,* 6, 628–647.

Fabra, M. J., Márquez, E., Castro, D. & Chiralt, A. (2011). Effect of maltodextrins in the water-content–water activity–glass transition relationships of noni (*Morinda citrifolia* L.) pulp powder. *Journal of Food Engineering,* 103, 47–51.

Fang, J. Y., Lee, W. R., Shen, S. C. & Huang, Y. L. (2006). Effect of liposome encapsulation of tea catechins on their accumulation in basal cell carcinomas. *Journal of Dermatological Science,* 42, 101–109.

Fang, Z. & Bhandari, B. (2010). Encapsulation of polyphenols - A review. *Trends in Food Science & Technology,* 21, 510–523.

Fathi, M., Mozafari, M. R. & Mohebbi, M. (2012a). Nanoencapsulation of food ingredients using lipid based delivery systems. *Trends in Food Science & Technology,* 23, 13–27.

Fathi, M., Varshosaz, J., Mohebbi, M. & Shahidi, F. (2012b). Hesperetin-loaded solid lipid nanoparticles and nanostructure lipid carriers for food fortification: Preparation, characterization, and modeling. *Food and Bioprocess Technology,* 6, 1464–1475.

Fessi, H., Puisieux, F., Devissaguet , J. P., Ammoury, N. & Benita, S. (1989). Nanocapsule formation by interfacial polymer deposition following solvent displacement. *International Journal of Pharmaceutics,* 55, R1–R4.

Fitzpatrick, J. (2013). Powder properties in food production systems In: *Handbook of Food Powders: Processes and Properties*. Cambridge: Woodhead Publishing: Elsevier.

Fraga, C. G., Galleano, M., Verstraeten, S. V. & Oteiza, P. I. (2010). Basic biochemical mechanisms behind the health benefits of polyphenols. *Molecular Aspects of Medicine,* 31, 435–445.

Frankel, E. N., Huang, S. & Aeschbach, R. (1997). Antioxidant activity of green teas in different lipid systems. *Journal of the American Oil Chemists' Society,* 74, 1309–1315.

Friedman, M. & Jurgens, H. S. (2000). Effect of pH on the stability of plant phenolic compounds. *Journal of Agricultural and Food Chemistry,* 48, 2101–2110.

Frohlich, E. (2012). The role of surface charge in cellular uptake and cytotoxicity of medical nanoparticles. *International Journal of Nanomedicine,* 7, 5577–5591.

Fu, N., Zhou, Z., Jones, T. B., Tan, T. T., Wu, W. D., Lin, S. X., Chen, X. D. & Chan, P. P. (2011). Production of monodisperse epigallocatechin gallate (EGCG) microparticles by spray drying for high antioxidant activity retention. *International Journal of Pharmaceutics,* 413, 155–166.

Gan, Q. & Wang, T. (2007). Chitosan nanoparticle as protein delivery carrier-systematic examination of fabrication conditions for efficient loading and release. *Colloids and Surfaces B: Biointerfaces,* 59, 24–34.

Gharsallaoui, A., Roudaut, G., Chambin, O., Voilley, A. & Saurel, R. (2007). Applications of spray-drying in microencapsulation of food ingredients: An overview. *Food Research International,* 40, 1107–1121.

Gomes, J. F., Rocha, S., Do Carmo Pereira, M., Peres, I., Moreno, S., Toca-Herrera, J. & Coelho, M. A. (2010). Lipid/particle assemblies based on maltodextrin-gum arabic core as bio-carriers. *Colloids and Surfaces B: Biointerfaces,* 76, 449–455.

Gouin, S. (2004). Microencapsulation: Industrial appraisal of existing technologies and trends. *Trends in Food Science & Technology,* 15, 330–347.

Gregoriadis, G. & Florence, A. T. (1993). Liposomes in drug delivery. *Drugs,* 45, 15–28.

Grüner-Richter, S., Otto, F. & Weinreich, B. (2008). Rooibos extract with an increased aspalathin content, method for producing one such rooibos extract, and cosmetic agent containing the same. US Patent 0247974.

Hans, M. L. & Lowman, A. M. (2002). Biodegradable nanoparticles for drug delivery and targeting. *Current Opinion in Solid State and Materials Science,* 6, 319–327.

Harris, R., Lecumberri, E., Mateos-Aparicio, I., Mengíbar, M. & Heras, A. (2011). Chitosan nanoparticles and microspheres for the encapsulation of natural antioxidants extracted from *Ilex paraguariensis*. *Carbohydrate Polymers,* 84, 803–806.

He, C., Hu, Y., Yin, L., Tang, C. & Yin, C. (2010). Effects of particle size and surface charge on cellular uptake and biodistribution of polymeric nanoparticles. *Biomaterials,* 31, 3657–3666.

Heinrich, T., Willenberg, I. & Glomb, M. A. (2012). Chemistry of color formation during rooibos fermentation. *Journal of Agricultural and Food Chemistry,* 60, 5221–5228.

Hertog, M. G. L., Bueno-de-Mesquita, H. B., Fehily, A. M., Sweetnam, P. M., Peter C. Elwood & Kromhout, D. (1996). Fruit and vegetable consumption and cancer mortality in the Caerphilly Study. *Cancer Epidemiology, Biomarkers & Prevention,* 5, 673–677.

Hillis, W. E. & Inoue, T. (1967). The polyphenols of *Nothofagus* species-II. The heartwood of *Nothofagus fusca*. *Phytochemistry,* 6, 59–67.

Hines, D. J. & Kaplan, D. L. (2013). Poly (lactic-co-glycolic acid) controlled release systems: Experimental and modeling insights. *Critical Reviews in Food Science & Nutrition,* 30, 257–276.

Hollman, P. C., Feskens, E. J. & Katan, M. B. (1999). Tea flavonols in cardiovascular disease and cancer epidemiology. *Proceedings of the Society for Experimental Biology and Medicine,* 220, 198–202.

Holzschuh, M. H., Silva, D. M., Schapoval, E. E. E. S. & Bassani, V. L. (2007). Thermal and photo stability of phenolic constituents of an *Achyrocline satureioides* spray-dried powder. *Pharmazie,* 62, 902–906.

Hong, Z., Xu, Y., Yin, J. F., Jin, J., Jiang, Y. & Du, Q. (2014). Improving the effectiveness of (-)-epigallocatechin gallate (EGCG) against rabbit atherosclerosis by EGCG-loaded nanoparticles prepared from chitosan and polyaspartic acid. *Journal of Agricultural and Food Chemistry,* 62, 12603–12609.

Hu, B., Pan, C., Sun, Y., Hou, Z., Ye, H., Hu, B. & Zeng, X. (2008). Optimization of fabrication parameters to produce chitosan-tripolyphosphate nanoparticles for delivery of tea catechins. *Journal of Agricultural and Food Chemistry,* 56, 7451–7458.

Hu, F. B. (2003). Plant-based foods and prevention of cardiovascular disease: An overview. *The American Journal of Clinical Nutrition,* 78, 544–551.

Huang, C. F., Gan, X. W., Bai, H. Y., Ma, L. & Hu, L. H. (2008a). Schoepfin A, B, C: Three new chalcone *C*-glycosides from *Schoepfia chinensis*. *Natural Product Research,* 22, 623–627.

Huang, M., Du Plessis, J., Du Preez, J., Hamman, J. & Viljoen, A. (2008b). Transport of aspalathin, a rooibos tea flavonoid, across the skin and intestinal epithelium. *Phytotherapy Research,* 22, 699–704.

Huang, Q., Yu, H. & Ru, Q. (2010). Bioavailability and delivery of nutraceuticals using nanotechnology. *Journal of Food Science,* 75, R50–57.

Huang, S. & Frankel, E. N. (1997). Antioxidant activity of tea catechins in different lipid systems. *Journal of Agricultural and Food Chemistry,* 45, 3033–3038.

Huwiler, A., Kolter, T., Pfeilschifter, J. & Sandho, K. (2000). Physiology and pathophysiology of sphingolipid metabolism and signaling. *Biochimica et Biophysica Acta,* 1485, 63–99.

Jafari, S. M., Assadpoor, E., Bhandari, B. & He, Y. (2008). Nano-particle encapsulation of fish oil by spray drying. *Food Research International,* 41, 172–183.

Jalil, R. & Nixon, J. (1990). Biodegradable poly (lactic acid) and poly (lactide-co-glycolide) microcapsules: Problems associated with preparative techniques and release properties. *Journal of Microencapsulation,* 7, 297–325.

Jaworek, A. & Sobczyk, A. T. (2008). Electrospraying route to nanotechnology: An overview. *Journal of Electrostatics,* 66, 197–219.

Jaya, S. & Das, H. (2009). Glass transition and sticky point temperatures and stability/mobility diagram of fruit powders. *Food Bioprocess Technology,* 2, 89–95.

Jenita, J., Yathish, M., Wilson, B. & Premakumari, K. B. (2012). Formulation and evaluation of microparticles containing curcumin for colorectal cancer. *Journal of Drug Delivery & Therapeutics,* 3, 125–128.

Johnson, R., De Beer, D., Dludla, P. V., Ferreira, D., Muller, C. J. F. & Joubert, E. (2018). Aspalathin from rooibos (*Aspalathus linearis*): A bioactive *C*-glucosyl dihydrochalcone with potential to target the metabolic syndrome. *Plant Medica,* 84, 568–583.

Joubert, E. & De Beer, D. (2011). Rooibos (*Aspalathus linearis*) beyond the farm gate: From herbal tea to potential phytopharmaceutical. *South African Journal of Botany,* 77, 869–886.

Joubert, E. & De Beer, D. (2014). Antioxidants of rooibos beverages: Role of plant composition and processing. In: *Processing and Impact on Antioxidants in Beverages* (edited by Preedy, V. R.). Pp. 131–144. USA: Academic Press.

Joubert, E., Gelderblom, W. C. A., Louw, A. & De Beer, D. (2008). South African herbal teas: *Aspalathus linearis, Cyclopia* spp. and *Athrixia phylicoides*—A review. *Journal of Ethnopharmacology,* 119, 367–412.

Joubert, E. & Schulz, H. (2006). Production and quality aspects of rooibos tea and related products. A review. *Journal of Applied Botany and Food Quality,* 80, 138–144.

Joubert, E., Viljoen, M., De Beer, D., Malherbe, C. J., Brand, D. J. & Manley, M. (2010). Use of green rooibos (*Aspalathus linearis*) extract and water-soluble nanomicelles of green rooibos extract encapsulated with ascorbic acid for enhanced aspalathin content in ready-to-drink iced teas. *Journal of Agricultural and Food Chemistry,* 58, 10965–10971.

Joubert, E., Viljoen, M., De Beer, D. & Manley, M. (2009). Effect of heat on aspalathin, iso-orientin, and orientin contents and color of fermented rooibos (*Aspalathus linearis*) iced tea. *Journal of Agricultural and Food Chemistry,* 57, 4204–4211.

Joubert, E., Winterton, P., Britz, T. J. & Ferreira, D. (2004). Superoxide anion and α, α-diphenyl-β-picrylhydrazyl radical scavenging capacity of rooibos (*Aspalathus linearis)* aqueous extracts, crude phenolic fractions, tannin and flavonoids. *Food Research International,* 37, 133–138.

Kailaku, S. I., Mulyawanti, I. & Alamsyah, A. N. (2014). Formulation of nanoencapsulated catechin with chitosan as encapsulation material. *Procedia Chemistry,* 9, 235–241.

Kalra, E. K. (2003). Nutraceutical - definition and introduction. *Official Journal of the American Association of Pharmaceutical Scientists,* 5, 1–2.

Kawai, K., Fukami, K., Thanatuksorn, P., Viriyarattanasak, C. & Kajiwara, K. (2011). Effects of moisture content, molecular weight, and crystallinity on the glass transition temperature of inulin. *Carbohydrate Polymers,* 83, 934–939.

Khawam, A. & Flanagan, D. R. (2006). Basics and applications of solid-state kinetics: A pharmaceutical perspective. *Journal of Pharmaceutical Sciences,* 95, 472–498.

Kim, M. K., Lee, J. S., Kim, K. Y. & Lee, H. G. (2013). Ascorbyl palmitate-loaded chitosan nanoparticles: Characteristic and polyphenol oxidase inhibitory activity. *Colloids and Surfaces B: Biointerfaces,* 103, 391–394.

Koch, I. S., Muller, M., Joubert, E., Rijst, M. V. d. & Næs, T. (2012). Sensory characterization of rooibos tea and the development of a rooibos sensory wheel and lexicon. *Food Research International,* 46, 217–228.

Koeppen, B. H. & Roux, D. G. (1965). Aspalathin: a novel *C*-glycosyl flavonoid from *Aspalathus linearis*. *Tetrahedron Letters,* 6, 3497–3503.

Komatsu, Y., Suematsu, S., Hisanobu, Y., Saigo, H., Matsuda, R. & Hara, K. (1993). Effects of pH and temperature on reaction kinetics of catechins in green tea infusion. *Bioscience, Biotechnology, and Biochemistry,* 57, 907–910.

Kosaraju, S. L., D'Ath, L. & Lawrence, A. (2006). Preparation and characterisation of chitosan microspheres for antioxidant delivery. *Carbohydrate Polymers,* 64, 163–167.

Krafczyk, N. & Glomb, A. A. (2008). Characterization of phenolic compounds in rooibos tea. *Journal of Agricultural and Food Chemistry,* 56, 3368–3376.

Krafczyk, N., Heinrich, T., Porzel, A. & Glomb, A. A. (2009a). Oxidation of the dihydrochalcone aspalathin leads to dimerization. *Journal of Agricultural and Food Chemistry,* 57, 6838–6843.

Krafczyk, N., Woyand, F. & Glomb, M. A. (2009b). Structure–antioxidant relationship of flavonoids from fermented rooibos. *Molecular Nutrition & Food Research,* 53, 635–642.

Kreuz, S., Joubert, E., Waldmann, K. & Ternes, W. (2008). Aspalathin, a flavonoid in *Aspalathus linearis* (rooibos), is absorbed by pig intestine as a *C*-glycoside. *Nutrition Research,* 28, 690–701.

Krishnaswamy, K., Orsat, V. & Thangavel, K. (2012). Synthesis and characterization of nano-encapsulated catechin by molecular inclusion with beta-cyclodextrin. *Journal of Food Engineering,* 111, 255–264.

Kumari, A., Yadav, S. K., Pakade, Y. B., Singh, B. & Yadav, S. C. (2010a). Development of biodegradable nanoparticles for delivery of quercetin. *Colloids and Surfaces B: Biointerfaces,* 80, 184–192.

Kumari, A., Yadav, S. K. & Yadav, S. C. (2010b). Biodegradable polymeric nanoparticles based drug delivery systems. *Colloids and Surfaces B: Biointerfaces,* 75, 1–18.

Li, L., Braiteh, F. S. & Kurzrock, R. (2005). Liposome-encapsulated curcumin: in vitro and in vivo effects on proliferation, apoptosis, signaling, and angiogenesis. *American Cancer Society,* 104, 1322–1331.

Li, N., Taylor, L. S., Ferruzzi, M. G. & Mauer, L. J. (2012). Kinetic study of catechin stability: Effects of pH, concentration, and temperature. *Journal of Agricultural and Food Chemistry,* 60, 12531–12539.

Li, N., Taylor, L. S. & Mauer, L. J. (2011). Degradation kinetics of catechins in green tea powder: Effects of temperature and relative humidity. *Journal of Agricultural and Food Chemistry,* 59, 6082–6090.

Li, N., Taylor, L. S. & Mauer, L. J. (2014). The physical and chemical stability of amorphous (−)-epi-gallocatechin gallate: Effects of water vapor sorption and storage temperature. *Food Research International,* 58, 112–123.

Liang, J., Li, F., Fang, Y., Yang, W., An, X., Zhao, L., Xin, Z., Cao, L. & Hu, Q. (2011). Synthesis, characterization and cytotoxicity studies of chitosan-coated tea polyphenols nanoparticles. *Colloids and Surfaces B: Biointerfaces,* 82, 297–301.

Lipinski, C. A., Lombardo, F., Dominy, B. W. & Feeney, P. J. (2012). Experimental and computational approaches to estimate solubility and permeability in drug discovery and development settings. *Advanced Drug Delivery Reviews,* 64, 4–17.

Lötter, D. & Le Maitre, D. (2014). Modelling the distribution of *Aspalathus linearis* (Rooibos tea): implications of climate change for livelihoods dependent on both cultivation and harvesting from the wild. *Ecology and Evolution,* 4, 1209–1221.

Lu, Q., Li, D. C. & Jiang, J. G. (2011). Preparation of a tea polyphenol nanoliposome system and its physicochemical properties. *Journal of Agricultural and Food Chemistry,* 59, 13004–13011.

Lu, Z., Yeh, T., Tsai, M., Au, J. L. S. & Wientjes, M. G. (2004). Paclitaxel-loaded gelatin nanoparticles for intravesical bladder cancer therapy. *Clinical Cancer Research,* 10, 7677–7684.

Madalena, D. A., Ramos, O. L., Pereira, R. N., Bourbon, A. I., Pinheiro, A. C., Malcata, F. X., Teixeira, J. A. & Vicente, A. A. (2016). In vitro digestion and stability assessment of β-lactoglobulin/riboflavin nanostructures. *Food Hydrocolloids,* 58, 89–97.

Makadia, K. H. & Siegel, S. J. (2011). Polylactic-co-glycolic acid (PLGA) as biodegradable controlled drug delivery carrier. *Polymers,* 3, 1377–1397.

Makris, D. P. & Rossiter, J. T. (2000). Heat-induced, metal-catalyzed oxidative degradation of quercetin and rutin (quercetin 3-*O*-rhamnosylglucoside) in aqueous model systems. *Journal of Agricultural and Food Chemistry,* 48, 3830–3838.

Malthlouthi, M. (2001). Water content, water activity, water structure and the stability of foodstuffs. *Food Control,* 12, 409–417.

Manley, M., Joubert, E. & Botha, M. (2006). Quantification of the major phenolic compounds, soluble solids content and total antioxidant activity of green rooibos *(Aspalathus linearis*) by means of infrared spectroscopy. *Journal of Near Infrared Spectroscopy,* 14, 213–222.

Marais, C., Janse van Rensburg, W., Ferreira, D. & Steenkamp, J. A. (2000). (*S*)- and (*R*)-Eriodictyol-*6*-*C*-β-D-glucopyranoside, novel keys to the fermentation of rooibos (*Aspalathus linearis*). *Phytochemistry,* 55, 43–49.

Markens, U. (2009). Stability studies-recent changes to climatic zone IV. URL http://www.sgs.com/~/media/Global/Documents/Technical%20Documents/SGS%20Stability%20Studies-EN-09.pdf. Accessed 13.10.17.

Marnewick, J. L., Rautenbach, F., Venter, I., Neethling, H., Blackhurst, D. M., Wolmarans, P. & Macharia, M. (2011). Effects of rooibos (*Aspalathus linearis*) on oxidative stress and biochemical parameters in adults at risk for cardiovascular disease. *Journal of Ethnopharmacology,* 133, 46–52.

Mauer, L. J. & Taylor, L. S. (2010). Water-solids interactions: deliquescence. *Annual Review of Food Science and Technology,* 1, 41–63.

Maurer, N., Fenske, D. B. & Cullis, P. R. (2001). Developments in liposomal drug delivery systems. *Emerging Biotherapeutic Technologies,* 6, 1–25.

McClements, D. J., Decker, E. A., Park, Y. & Weiss, J. (2009). Structural design principles for delivery of bioactive components in nutraceuticals and functional foods. *Critical Reviews in Food Science and Nutrition,* 49, 577–606.

McClements, D. J., Li, F. & Xiao, H. (2015). The nutraceutical bioavailability classification scheme: classifying nutraceuticals according to factors limiting their oral bioavailability. *Annual Review of Food Science and Technology,* 6, 299–327.

McGinity, J. W. & Felton, L. A. (2008). Aqueous polymeric coatings for pharmaceutical dosage forms. Pp. 1–475. Florida: CRC Press.

Mignet, N., Seguin, J. & Chabot, G. G. (2013). Bioavailability of polyphenol liposomes: A challenge ahead. *Pharmaceutics,* 5, 457–471.

Miller, N., De Beer, D., Aucamp, M., Malherbe, C. J. & Joubert, E. (2018). Inulin as microencapsulating agent improves physicochemical properties of spray-dried aspalathin-rich green rooibos (*Aspalathus linearis*) extract with α-glucosidase inhibitory activity. *Journal of Functional Foods,* 48, 400–409.

Miller, N., De Beer, D. & Joubert, E. (2017). Minimising variation in aspalathin content of aqueous green rooibos extract: optimising extraction and identifying critical material attributes. *Journal of the Science of Food and Agriculture,* 97, 4937–4942.

Moorthi, C. & Kathiresan, K. (2013). Reversed phase high performance liquid chromatographic method for simultaneous estimation of curcumin and quercetin in pharmaceutical nanoformulation. *International Journal of Pharmacy and Pharmaceutical Sciences,* 5, 622–625.

Mozafari, M. R., Johnson, C., Hatziantoniou, S. & Demetzos, C. (2008). Nanoliposomes and their applications in food nanotechnology. *Journal of Liposome Research,* 18, 309–327.

Muller, C. J. F., Malherbe, C. J., Chellan, N., Yagasaki, K., Miura, Y. & Joubert, E. (2018). Potential of rooibos, its major *C*-glucosyl flavonoids, and *Z*-2-(β-D-glucopyranosyloxy)-3-phenylpropenoic acid in prevention of metabolic syndrome. *Critical Reviews in Food Science and Nutrition,* 58, 227–246.

Murikipudi, V., Gupta, P. & Sihorkar, V. (2013). Efficient throughput method for hygroscopicity classification of active and inactive pharmaceutical ingredients by water vapor sorption analysis. *Pharmaceutical Development and Technology,* 18, 348–58.

Murugesan, R. & Orsat, V. (2012). Spray drying for the production of nutraceutical ingredients—A review. *Food and Bioprocess Technology,* 5, 3–14.

Narayanan, S., Mony, U., Vijaykumar, D. K., Koyakutty, M., Paul-Prasanth, B. & Menon, D. (2015). Sequential release of epigallocatechin gallate and paclitaxel from PLGA-casein core/shell nanoparticles sensitizes drug-resistant breast cancer cells. *Nanomedicine,* 11, 1399–13406.

Neethirajan, S. & Jayas, D. S. (2011). Nanotechnology for the food and bioprocessing industries. *Food and Bioprocess Technology,* 4, 39–47.

Nuruzzaman, M., Rahman, M. M., Liu, Y. & Naidu, R. (2016). Nanoencapsulation, nano-guard for pesticides: A new window for safe application. *Journal of Agricultural and Food Chemistry,* 64, 1447–1483.

Oliyai, R. & Lindenbaum, S. (1991). Stability testing of pharmaceuticals by isothermal heat conduction calorimetry: Ampicillin in aqueous solution. *International Journal of Pharmaceutics,* 73, 33–36.

Pal, S. & Saha, C. (2013). Preparation and physicochemical characterization of poly(*D, L*-lactide-co-glycolide) nanoparticles for controlled release of EGCG. *International Journal of Science and Research,* 4, 862–865.

Patel, B. B., Patel, J. K., Chakraborty, S. & Shukla, D. (2015). Revealing facts behind spray dried solid dispersion technology used for solubility enhancement. *Saudi Pharmaceutical Journal,* 23, 352–365.

Pauck, C., De Beer, D., Aucamp, M., Liebenberg, W., Stieger, N., Human, C. & Joubert, E. (2017). Inulin suitable as reduced-kilojoule carrier for production of microencapsulated spray-dried green *Cyclopia subternata* (honeybush) extract. *LWT-Food Science and Technology,* 75, 631–639.

Peres, I., Rocha, S., Gomes, J., Morais, S., Pereira, M. C. & Coelho, M. (2011). Preservation of catechin antioxidant properties loaded in carbohydrate nanoparticles. *Carbohydrate Polymers,* 86, 147–153.

Peres, I., Rocha, S., Pereira, M. d. C., Coelho, M., Rangel, M. & Ivanova, G. (2010). NMR structural analysis of epigallocatechin gallate loaded polysaccharide nanoparticles. *Carbohydrate Polymers,* 82, 861–866.

Petit, C., Bujard, A., Skalicka-Wozniak, K., Cretton, S., Houriet, J., Christen, P., Carrupt, P. A. & Wolfender, J. L. (2016). Prediction of the passive intestinal absorption of medicinal plant extract constituents with the parallel artificial membrane permeability assay (PAMPA). *Planta Medica,* 82, 424–431.

Piazzini, V., Monteforte, E., Luceri, C., Bigagli, E., Bilia, A. R. & Bergonzi, M. C. (2017a). Nanoemulsion for improving solubility and permeability of *Vitex agnus-castus* extract: formulation and in vitro evaluation using PAMPA and Caco-2 approaches. *Drug Delivery,* 24, 380–390.

Piazzini, V., Rosseti, C., Bigagli, E., Luceri, C., Bilia, A. R. & Bergonzi, M. C. (2017b). Prediction of permeation and cellular transport of *Silybum marianum* extract formulated in a nanoemulsion by using PAMPA and Caco-2 cell models. *Planta Medica,* 83, 1184–1193.

Ponnuraj, R., Janakiraman, K., Gopalakrishnan, S., Senthilnathan, K., Meganathan, V. & Saravanan, P. (2015). Formulation and characterization of epigallocatechin gallate nanoparticles. *Indo American Journal of Pharmaceutical Research,* 5, 387–398.

Pool, H., Quintanar, D., De dios Figueroa, J., Bechara, J. E. H., McClements, D. J. & Mendoza, S. (2012). Polymeric nanoparticles as oral delivery systems for encapsulation and release of polyphenolic compounds: Impact on quercetin antioxidant activity & bioaccessibility. *Food Biophysics,* 7, 276–288.

Prescott, J. K. & Barnum, R. A. (2000). On powder flowability. *Pharmaceutical Technology,* 10, 60–84.

Quintanar-Guerrero, D., Allémann, E., Fessi, H. & Doelker, E. (1998). Preparation techniques and mechanisms of formation of biodegradable nanoparticles from preformed polymers. *Drug Development and Industrial Pharmacy,* 24, 1113–1128.

Ramírez-Ambrosi, M., Caldera, F., Trotta, F., Berrueta, L. Á. & Gallo, B. (2014). Encapsulation of apple polyphenols in β-CD nanosponges. *Journal of Inclusion Phenomena and Macrocyclic Chemistry,* 80, 85–92.

Rashidinejad, A., Birch, E. J., Sun-Waterhouse, D. & Everett, D. W. (2014). Delivery of green tea catechin and epigallocatechin gallate in liposomes incorporated into low-fat hard cheese. *Food Chemistry,* 156, 176–183.

Ré, M. I. (1998). Microencapsulation by spray drying. *Drying Technology,* 16, 1195–1236.

Reis, C. P., Neufeld, R. J., Ribeiro, A. J. & Veiga, F. (2006). Nanoencapsulation I. Methods for preparation of drug-loaded polymeric nanoparticles. *Nanomedicine,* 2 8–21.

Reneker, D. H. & Chun, I. (1996). Nanometre diameter fibres of polymer, produced by electrospinning. *Nanotechnology,* 7, 216–223.

Riboli, E. & Norat, T. (2003). Epidemiologic evidence of the protective effect of fruit and vegetables on cancer risk. *American Society for Clinical Nutrition,* 78, 559S–569S.

Rimm, E. B., Ascherio, A., Giovannucci, E., Spiegelman, D., Stampfer, M. J. & Willett, W. C. (1996). Vegetable, fruit, and cereal fiber intake and risk of coronary heart disease among men. *Journal of the American Medical Association,* 275, 447–451.

Robert, P., García, P., Reyes, N., Chávez, J. & Santos, J. (2012). Acetylated starch and inulin as encapsulating agents of gallic acid and their release behaviour in a hydrophilic system. *Food Chemistry,* 134, 1–8.

Robert, P., Gorena, T., Romero, N., Sepulveda, E., J., C. & C., S. (2010). Encapsulation of polyphenols and anthocyanins from pomegranate (*Punica granatum*) by spray drying. *International Journal of Food Science and Technology,* 45, 1386–1394.

Roco, M. C. (2003). Nanotechnology: Convergence with modern biology and medicine. *Current Opinion in Biotechnology,* 14, 337–346.

Rojas-Garbanzo, C., Zimmermann, B. F., Schulze-Kaysers, N. & Schieber, A. (2017). Characterization of phenolic and other polar compounds in peel and flesh of pink guava (*Psidium guajava L. cv. 'Criolla*') by ultra-high performance liquid chromatography with diode array and mass spectrometric detection. *Food Research International,* 100, 445– 453.

Ronkart, S. N., Paquot, M., Fougnies, C., Deroanne, C. & Blecker, C. S. (2009). Effect of water uptake on amorphous inulin properties. *Food Hydrocolloids,* 23, 922–927.

Saenz, C., Tapia, S., Chavez, J. & Robert, P. (2009). Microencapsulation by spray drying of bioactive compounds from cactus pear (*Opuntia ficus-indica*). *Food Chemistry,* 114, 616–622.

Şahin-Nadeem, H., Dinçer, C., Torun, M., Topuz, A. & Özdemir, F. (2013). Influence of inlet air temperature and carrier material on the production of instant soluble sage (*Salvia fruticosa Miller*) by spray drying. *LWT-Food Science and Technology,* 52, 31–38.

Salatin, S., Barar, J., M., B.-J., Adibkia, K., Kiafar, F. & Jelvehgari, M. (2017). Development of a nanoprecipitation method for the entrapment of a very water soluble drug into Eudragit RL nanoparticles. *Research in Pharmaceutical Sciences,* 12, 1–14.

Sanguansri, P. & Augustin, M. A. (2006). Nanoscale materials development – a food industry perspective. *Trends in Food Science & Technology,* 17, 547–556.

Sanna, V., Lubinu, G., Madau, P., Pala, N., Nurra, S., Mariani, A. & Sechi, M. (2015). Polymeric nanoparticles encapsulating white tea extract for nutraceutical application. *Journal of Agricultural and Food Chemistry,* 63, 2026–2032.

Sansone, F., Mencherini, T., Picerno, P., d'Amore, M., Aquino, R. P. & Lauro, M. R. (2011a). Maltodextrin/pectin microparticles by spray drying as carrier for nutraceutical extracts. *Journal of Food Engineering,* 105, 468–476.

Sansone, F., Picerno, P., Mencherini, T., Villecco, F., D'Ursi, A. M., Aquino, R. P. & Lauro, M. R. (2011b). Flavonoid microparticles by spray-drying: Influence of enhancers of the dissolution rate on properties and stability. *Journal of Food Engineering,* 103, 188–196.

Saravanabhavan, S. S., Bose, R., Skylab, S. & Dharmalingam, S. (2013). Fabrication of chitosan/TPP nanoparticles as a carrier towards the treatment of cancer. *International Journal of Drug Delivery,* 5, 35–42.

Scalbert, A., Johnson, I. T. & Saltmarsh, M. (2005). Polyphenols: antioxidants and beyond. *The American Journal of Clinical Nutrition,* 81, 215–217.

Scalia, S., Marchetti, N. & Bianchi, A. (2013). Comparative evaluation of different co-antioxidants on the photochemical- and functional-stability of epigallocatechin-3-gallate in topical creams exposed to simulated sunlight. *Molecules,* 18, 574–587.

Schmitt, E. A., Peck, K., Sun, Y. & Geoffroy, J. (2001). Rapid, practical and predictive excipient compatibility screening using isothermal microcalorimetry. *Thermochimica Acta,* 380, 175–183.

Schubert, H. & Engel, R. (2004). Product and formulation engineering of emulsions. *Chemical Engineering Research and Design,* 82, 1137–1143.

Schulz, H., Joubert, E. & Schutze, W. (2003). Quantification of quality parameters for reliable evaluation of green rooibos (*Aspalathus linearis*). *European Food Research and Technology,* 216, 539–543.

Schulze, D. (2008). Powders and bulk solids. Pp. 1–503. New York: Springer-Verlag Berlin Heidelberg.

Schüssele, A. & Bauer-Brandl, A. (2003). Note on the measurement of flowability according to the European Pharmacopoeia. *International Journal of Pharmaceutics,* 257, 301–304.

Serra, H., Mendes, T., Bronze, M. R. & Simplicio, A. L. (2008). Prediction of intestinal absorption and metabolism of pharmacologically active flavones and flavanones. *Bioorganic & Medicinal Chemistry,* 16, 4009–4018.

Sessa, M., Casazza, A. A., Perego, P., Tsao, R., Ferrari, G. & Donsì, F. (2012). Exploitation of polyphenolic extracts from grape marc as natural antioxidants by encapsulation in lipid-based nanodelivery systems. *Food and Bioprocess Technology,* 6, 2609–2620.

Shaikh, J., Ankola, D. D., Beniwal, V., Singh, D. & Kumar, M. N. (2009). Nanoparticle encapsulation improves oral bioavailability of curcumin by at least 9-fold when compared to curcumin administered with piperine as absorption enhancer. *The European Journal of Pharmaceutical Sciences,* 37, 223–230.

Shao, J., Li, X., Lu, X., Jiang, C., Hu, Y., Li, Q., You, Y. & Fu, Z. (2009). Enhanced growth inhibition effect of resveratrol incorporated into biodegradable nanoparticles against glioma cells is mediated by the induction of intracellular reactive oxygen species levels. *Colloids and Surfaces B: Biointerfaces,* 72, 40–47.

Siddiqui, I. A., Adhami, V. M., Bharali, D. J., Hafeez, B. B., Asim, M., Khwaja, S. I., Ahmad, N., Cui, H., Mousa, S. A. & Mukhtar, H. (2009). Introducing nanochemoprevention as a novel approach for cancer control: Proof of principle with green tea polyphenol epigallocatechin-3-gallate. *Cancer Research,* 69, 1712–1716.

Silva, H. D., Cerqueira, M. Â. & Vicente, A. A. (2011). Nanoemulsions for food applications: Development and characterization. *Food and Bioprocess Technology,* 5, 854–867.

Silva, P. I., Stringheta, P. C., Teófilo, R. F. & De Oliveira, I. R. N. (2013). Parameter optimization for spray-drying microencapsulation of Jaboticaba (*Myrciaria jaboticaba*) peel extracts using simultaneous analysis of responses. *Journal of Food Engineering,* 117, 538–544.

Singh, H. (2016). Nanotechnology applications in functional foods; opportunities and challenges. *Preventive Nutrition and Food Science,* 21, 1–8.

Singh, M., Bhatnagar, P., Mishra, S., Kumar, P., Shukla, Y. & Gupta, K. C. (2015). PLGA-encapsulated tea polyphenols enhance the chemotherapeutic efficacy of cisplatin against human cancer cells and mice bearing Ehrlich ascites carcinoma. *International Journal of Nanomedicine,* 10, 6789–809.

Sinha, V. R., Singla, A. K., Wadhawan, S., Kaushik, R., Kumria, R., Bansal, K. & Dhawan, S. (2004). Chitosan microspheres as a potential carrier for drugs. *International Journal of Pharmaceutics,* 274, 1–33.

Sinija, V. R., Mishra, H. N. & Bal, S. (2007). Process technology for production of soluble tea powder. *Journal of Food Engineering,* 82, 276–283.

Snijman, P. W., Joubert, E., Ferreira, D., Li, X. C., Ding, Y., Green, I. R. & Gelderblom, W. C. (2009). Antioxidant activity of the dihydrochalcones aspalathin and nothofagin and their corresponding flavones in relation to other rooibos (*Aspalathus linearis*) flavonoids, epigallocatechin gallate, and trolox. *Journal of Agricultural and Food Chemistry,* 57, 6678–6684.

Soo, E., Thakur, S., Qu, Z., Jambhrunkar, S., Parekh, H. S. & Popat, A. (2016). Enhancing delivery and cytotoxicity of resveratrol through a dual nanoencapsulation approach. *Journal of Colloid and Interface Science,* 462, 368–374.

Soppimath, K. S., Aminabhavi, T. M., Kulkarni, A. R. & Rudzinski, W. E. (2001). Biodegradable polymeric nanoparticles as drug delivery devices. *Journal of Controlled Release,* 70, 1–20.

Spigno, G., Donsì, F., Amendola, D., Sessa, M., Ferrari, G. & De Faveri, D. M. (2013). Nanoencapsulation systems to improve solubility and antioxidant efficiency of a grape marc extract into hazelnut paste. *Journal of Food Engineering,* 114, 207–214.

Sri.s, J., Seethadevi, A., Prabha, K. S., Muthuprasanna, P. & Pavitra, P. (2012). Microencapsulation: A review. *International Journal of Pharma and Bio Sciences,* 3, 509–531.

Srivastava, A. K., Bhatnagar, P., Singh, M., Mishra, S., Kumar, P., Shukla, Y. & Gupta, K. C. (2013). Synthesis of PLGA nanoparticles of tea polyphenols and their strong in vivo protective effect against chemically induced DNA damage. *International Journal of Nanomedicine,* 8, 1451–1462.

Stalmach, A., Mullen, W., Pecorari, M., Serafini, M. & Crozier, A. (2009). Bioavailability of *C*-linked dihydrochalcone and flavanone glucosides in humans following ingestion of unfermented and fermented rooibos teas. *Journal of Agricultural and Food Chemistry,* 57, 7104–7111.

Sun-Waterhouse, D. (2011). The development of fruit-based functional foods targeting the health and wellness market: A review. *International Journal of Food Science & Technology,* 46, 899–920.

Sun-Waterhouse, D., Wadhwa, S. S. & Waterhouse, G. I. N. (2013). Spray-drying microencapsulation of polyphenol bioactives: A comparative study using different natural fibre polymers as encapsulants. *Food and Bioprocess Technology,* 6, 2376–2388.

Takeuchi, H., Handa, T. & Kawashima, Y. (1989). Controlled release theophylline tablet with acrylic polymers prepared by spray-drying technique in aqueous system. *Drug Development and Industrial Pharmacy,* 15, 1999–2016.

Teixeira, B. N., Ozdemir, N., Hill, L. E. & Gomes, C. L. (2013). Synthesis and characterization of nano-encapsulated black pepper oleoresin using hydroxypropyl β-cyclodextrin for antioxidant and antimicrobial applications. *Journal of Food Science,* 78, 1913–1920.

Thompson, A. K., Hindmarsh, J. P., Haisman, D., Rades, T. & Singh, H. (2006). Comparison of the structure and properties of liposomes prepared from milk fat globule membrane and soy phospholipids. *Journal of Agricultural and Food Chemistry,* 54, 3704–3711.

Tolstoguzov, V. (2003). Some thermodynamic considerations in food formulation. *Food Hydrocolloids,* 17, 1–23.

Tonon, R. V., Brabet, C. & Hubinger, M. D. (2008). Influence of process conditions on the physicochemical properties of açai (*Euterpe oleraceae* Mart.) powder produced by spray drying. *Journal of Food Engineering,* 88, 411–418.

Torres-Giner, S., Wilkanowicz, S., Melendez-Rodriguez, B. & Lagaron, J. M. (2017). Nanoencapsulation of *Aloe vera* in synthetic and naturally occurring polymers by electrohydrodynamic processing of interest in food technology and bioactive packaging. *Journal of Agricultural and Food Chemistry,* 65, 4439–4448.

Tsai, Y. M., Jan, W. C., Chien, C. F., Lee, W. C., Lin, L. C. & Tsai, T. H. (2011). Optimised nano-formulation on the bioavailability of hydrophobic polyphenol, curcumin, in freely-moving rats. *Food Chemistry,* 127, 918–925.

Turgeon, S. L., Schmitt, C. & Sanchez, C. (2007). Protein–polysaccharide complexes and coacervates. *Current Opinion in Colloid & Interface Science,* 12, 166–178.

Ungar, Y., Osundahunsi, O. F. & Shimoni, E. (2003). Thermal stability of genistein and daidzein and its effect on their antioxidant activity. *Journal of Agricultural and Food Chemistry,* 51, 4394–4399.

Van Boekel, M. A. J. S. (1996). Statistical aspects of kinetic modeling for food science problems. *Journal of Food Science,* 61, 477–486.

Van Boekel, M. A. J. S. (2008). Kinetic modeling of food quality: A critical review. *Comprehensive Reviews in Food Science and Food Safety,* 7, 144–158.

Van der Merwe, J. D., De Beer, D., Joubert, E. & Gelderblom, W. C. (2015). Short-term and sub-chronic dietary exposure to aspalathin-enriched green rooibos (*Aspalathus linearis*) extract affects rat liver function and antioxidant status. *Molecules,* 20, 22674–22690.

Van der Merwe, J. D., De Beer, D., Joubert, E. & Gelderblom, W. C. (2016). Correction: Van der Merwe, J.D., et al. Short-term and sub-chronic dietary exposure to aspalathin-enriched green rooibos (*Aspalathus linearis*) extract affects rat liver function and antioxidant status. *Molecules,* 20, 22674–22690.

Van der Merwe, J. D., Joubert, E., Manley, M., De Beer, D., Malherbe, C. J. & Gelderblom, W. C. A. (2010). *In vitro* hepatic biotransformation of aspalathin and nothofagin, dihydrochalcones of rooibos (*Aspalathus linearis*), and assessment of metabolite antioxidant activity. *Journal of Agricultural and Food Chemistry,* 58, 2214–2220.

Van der Sluis, A. A., Dekker, M. & Van Boekel, M. A. (2005). Activity and concentration of polyphenolic antioxidants in apple juice. 3. Stability during storage. *Journal of Agricultural and Food Chemistry,* 53, 1073–1080.

Vauzour, D., Rodriguez-Mateos, A., Corona, G., Oruna-Concha, M. J. & Spencer, J. P. (2010). Polyphenols and human health: prevention of disease and mechanisms of action. *Nutrients*, 1106–1131.

Verma, A. & Stellacci, F. (2010). Effect of surface properties on nanoparticle-cell interactions. *Small,* 6, 12–21.

Villanueva, A., Canete, M., Roca, A. G., Calero, M., Veintemillas-Verdaguer, S., Serna, C. J., Morales Mdel, P. & Miranda, R. (2009). The influence of surface functionalization on the enhanced internalization of magnetic nanoparticles in cancer cells. *Nanotechnology,* 20, 1–9.

Virgili, F. & Marino, M. (2008). Regulation of cellular signals from nutritional molecules: a specific role for phytochemicals, beyond antioxidant activity. *Free Radical Biology and Medicine,* 45, 1205–1216.

Volf, I., Ignat, I., Neamtu, M. & Popa, V. (2014). Thermal stability, antioxidant activity, and photo-oxidation of natural polyphenols. *Chemical Papers,* 68, 121–129.

Von Gadow, A., Joubert, E. & Hansmann, C. F. (1997). Effect of extraction time and additional heating on the antioxidant activity of rooibos tea (*Aspalathus linearis*) extracts. *Journal of Agricultural and Food Chemistry,* 45, 1370–1374.

Wagner, A. & Vorauer-Uhl, K. (2011). Liposome technology for industrial purposes. *Journal of Drug Delivery,* 2011, doi:10.1155/2011/591325.

Walters, N. A., De Villiers, A., Joubert, E. & De Beer, D. (2017). Improved HPLC method for rooibos phenolics targeting changes due to fermentation. *Journal of Food Composition and Analysis,* 55, 20–29.

Wan, L. S. C., Heng, P. W. S. & Chia, C. G. H. (1992). Spray drying as a process for microencapsulation and the effect of different coating polymers. *Drug Development and Industrial Pharmacy,* 18, 997–1011.

Williams, R. J., Spencer, J. P. & Rice-Evans, C. (2004). Flavonoids: antioxidants or signalling molecules? *Free Radical Biology and Medicine,* 36, 838–849.

Woo, M. & Bhandari, B. (2013). Spray drying for food powder production. In: *Handbook of Food Powders Processes and Properties*. Pp. 29–56. Cambridge, UK: Woodhead Publishing.

Wu, T. H., Yen, F. L., Lin, L. T., Tsai, T. R., Lin, C. C. & Cham, T. M. (2008). Preparation, physicochemical characterization, and antioxidant effects of quercetin nanoparticles. *International Journal of Pharmaceutics,* 346, 160-8.

Xie, X., Tao, Q., Zou, Y., Zhang, F., Guo, M., Wang, Y., Wang, H., Zhou, Q. & Yu, S. (2011). PLGA nanoparticles improve the oral bioavailability of curcumin in rats: Characterizations and mechanisms. *Journal of Agricultural and Food Chemistry,* 59, 9280–9289.

Xing, F., Cheng, G., Yi, K. & Ma, L. (2005). Nanoencapsulation of capsaicin by complex coacervation of gelatin, acacia, and tannins. *Journal of Applied Polymer Science,* 96, 2225–2229.

Youdim, K. A., Avdeef, A. & Abbott, N. J. (2003). *In vitro* trans-monolayer permeability calculations: often forgotten assumptions. *Drug Discovery Today,* 8, 997–1003.

Yuliani, S., Bhandari, B., Rutgers, R. & D'Arcy, B. (2004). Application of microencapsulated flavor to extrusion product. *Food Reviews International,* 20, 163–185.

Zambaux, M. F., Bonneaux, F., Gref, R., Dellacherie, E. & Vigneron, C. (1999). Preparation and characterization of protein C-loaded PLA nanoparticles. *Journal of Controlled Release,* 60, 179–188.

Zhang, J., Nie, S. & Wang, S. (2013). Nanoencapsulation enhances epigallocatechin-3-gallate stability and its antiatherogenic bioactivities in macrophages. *Journal of Agricultural and Food Chemistry,* 61, 9200–9209.

Zhang, L., Mou, D. & Du, Y. (2007). Procyanidins: extraction and micro-encapsulation. *Journal of the Science of Food and Agriculture,* 87, 2192–2197.

Zhang, Y., Yang, M., Portney, N. G., Cui, D., Budak, G., Ozbay, E., Ozkan, M. & Ozkan, C. S. (2008). Zeta potential: a surface electrical characteristic to probe the interaction of nanoparticles with normal and cancer human breast epithelial cells. *Biomedical Microdevices,* 10, 321–328.

Zhao, L., Pan, Y., Li, J., Chen, G. & Mujumdar, A. S. (2004). Drying of a dilute suspension in a revolving flow fluidized bed of inert particles. *Drying Technology,* 22, 363–376.

Zimeri, J. & Tong, C. H. (1999). Degradation kinetics of *(-*)-epigallocatechin gallate as a function of pH and dissolved oxygen in a liquid model system. *Journal of Food Science,* 64, 753–758.

Chapter 3

Effect of carbohydrate microencapsulating polymers on physicochemical properties and aspalathin stability of green rooibos extract powders

*Submitted for publication in *Journal of Science of Food and Agriculture*

DECLARATION BY THE CANDIDATE

With regard to *Chapter 3 (Pp. 91–124)*, the nature and scope of my contribution were as follows:

Nature of contribution	Extent of contribution (%)
Conducted all experimental work and data interpretation. Wrote the entire manuscript and edited the document in its entirety.	70%

The following co-authors have contributed to *Chapter 3 (Pp. 91–124)*:

Name	e-mail address	Nature of contribution	Extent of contribution (%)
Prof Dalene de Beer	DBeerD@arc.agric.za	Assisted in editing the document in its entirety	10%
Ms Marieta van der Rijst	VanDerRijstM@arc.agric.za	Advice and assistance with statistical analysis	5%
Prof Marique Aucamp	maucamp@uwc.ac.za	Isothermal microcalorimetry analyses and assistance with data interpretation	5%
Prof Elizabeth Joubert	JoubertL@arc.agric.za	Assisted in editing and contextualisation of the document in its entirety	10%

Signature of candidate: **Declaration with signature in possession of candidate and supervisor*	**Date**

DECLARATION BY CO-AUTHORS

The undersigned hereby confirm that:

1. the declaration above accurately reflects the nature and extent of the contributions of the candidate and the co-authors to *Chapter 3 (Pp. 91–124)*,
2. no other authors contributed to *Chapter 3 (Pp. 91–124)*, besides those specified above, and
3. potential conflicts of interest have been revealed to all interested parties and that the necessary arrangements have been made to use the material in *Chapter 3 (Pp. 91–124)* of this dissertation.

Signature	Institutional affiliation	Date
**Declaration with signature in possession of candidate and supervisor* *Prof Dalene de Beer*	Plant Bioactives Group, Post-Harvest & Agro-Processing Technologies, Agricultural Research Council (ARC), Infruitec-Nietvoorbij	
Ms Marieta van der Rijst	Biometry Unit, Agricultural Research Council (ARC), Infruitec-Nietvoorbij	
Prof Marique Aucamp	School of Pharmacy, University of the Western Cape, Bellville, 7535, South Africa	
Prof Elizabeth Joubert	Plant Bioactives Group, Post-Harvest & Agro-Processing Technologies, Agricultural Research Council (ARC), Infruitec-Nietvoorbij	

ABSTRACT

Carbohydrate polymers (maltodextrin, inulin and chitosan) were assessed as microencapsulating agents of a green rooibos extract (GRE) with high aspalathin content, aimed at use as a food ingredient. Minimal aspalathin degradation was observed after microencapsulation by spray-drying with either inulin or maltodextrin (< 5%), irrespective of ratio, while the chitosan formulations (10 and 15%, m/m) showed a significant decrease in aspalathin content (> 17%). The yield (> 76%) and moisture content (< 3.5%) of spray-dried GRE, and GRE microencapsulated with inulin were similar to those of the maltodextrin formulations, whereas the chitosan formulations resulted in lower yields (< 66%) and higher moisture content (> 3.4%). All the formulations produced amorphous and hygroscopic powders with high deliquescence at > 65% relative humidity (RH). Aspalathin degradation followed fractional conversion kinetics when subjected to accelerated stability testing (40 °C/75% RH) for 96 h. Aspalathin degradation > 10% was observed for GRE and the formulations containing carbohydrate polymers. Microencapsulation of GRE with chitosan decreased stability of aspalathin during storage, while inulin and maltodextrin had no effect.

3.1 Introduction

Nutraceutical plant extracts are increasingly applied as food ingredients to enhance the bioactive content of various food products, including beverages and bakery products. Factors to be considered in their manufacture and storage include physicochemical characteristics of the powders and stability of bioactive compounds (McClements, Decker, Park & Weiss, 2009). Bioactive compounds of interest are usually inherently susceptible to degradation so that protection from adverse environmental conditions including moisture, oxygen and light is important for stability. Microencapsulation with carbohydrate polymers by spray-drying is commonly used to improve handling and stability of nutraceutical ingredients for use in functional foods (Desai & Park, 2005). Spray-drying results in conveniently free-flowing microencapsulated powders with sufficiently low moisture content (MC) and water activity (a_w) for prolonged shelf-life and easier handling (Murugesan & Orsat, 2012).

Food grade nutraceutical extracts, prepared from "unfermented" *Aspalathus linearis*, have demonstrated their potential in the prevention of the metabolic syndrome (Muller *et al.*, 2018), a condition characterised by reduced high density lipoprotein-cholesterol, raised triglycerides, blood pressure and fasting plasma glucose in humans (Han & Lean, 2016). The beneficial effects of green rooibos extracts are largely attributed to the *C*-glucosyl dihydrochalcone, aspalathin, due to its ability to target relevant cellular pathways (Johnson *et al.*, 2018). Delivery of aspalathin as part of the diet poses a challenge due to its instability under oxidative conditions (Joubert & De Beer, 2014). Aspalathin was demonstrated to degrade during storage of ready-to-drink green rooibos iced teas at 25 °C (De Beer, Joubert, Viljoen & Manley, 2011), however, its stability in powdered green rooibos extract during storage is not known. Recently, Miller, De Beer, Aucamp, Malherbe & Joubert (2018) optimised spray-drying process parameters for a green rooibos extract-inulin mixture (1:1, m/m) to obtain maximum powder yield. More than 95% of aspalathin was retained under these conditions. Compared to maltodextrin, inulin improved wettability and lowered the water activity of the microencapsulated extract (Miller *et al.*, 2018). Maltodextrin, produced by partial hydrolysis of starch, is commonly used by industry for microencapsulation of plant extracts, including rooibos extract, due to low cost. A disadvantage of maltodextrin is that it is metabolised as glucose in the human digestive tract, resulting in an increased glycaemic load and therefore post meal glycaemia (Hofman, Van Buul & Brouns, 2016). Inulin, a fructan-type polysaccharide, is not only indigestible to humans, but it stimulates growth of beneficial intestinal bacteria (Kolida & Gibson, 2007), stimulates the immune system and improves the blood lipid profile (Shoaib *et al.*, 2016). In the present study, chitosan, a polyaminosaccharide, has been compared with inulin and maltodextrin as microencapsulating agents of green rooibos extract. An advantage of chitosan is its ability to bind fat and cholesterol in the digestive tract, thus increasing their excretion (Yao & Chiang, 2006). Both inulin and chitosan

thus offer healthier alternatives to maltodextrin in the production of microencapsulated spray-dried green rooibos extract powder for use as the nutraceutical ingredient in functional food products aimed at the management of obesity and type 2 diabetes.

In the present study different concentrations of these carbohydrate polymers were used in the formulation of microencapsulated green rooibos extract (GRE) powder with high aspalathin content. The physicochemical properties of the powders and the protection offered to aspalathin against degradation were evaluated under accelerated storage conditions to provide an additional criteria to guide selection of a suitable polymer. Different kinetic models were tested to determine the most suitable model describing aspalathin degradation under accelerated storage conditions.

3.2 Material and methods

3.2.1 Chemicals

Analytical grade ascorbic acid, high performance liquid chromatography (HPLC)-grade acetonitrile and dimethyl sulfoxide (DMSO) were obtained from Sigma Aldrich (St Louis, MO, USA). Formic acid (purity > 95%) and sodium chloride (NaCl) were obtained from Merck (Darmstadt, Germany). Deionised water prepared using an Elix water purification system was further purified to HPLC grade using a Milli-Q Academic water purification system from Merck. Isoorientin, orientin, isovitexin, hyperoside, eriodictyol-7-*O*-glucoside and luteolin-7-*O*-glucoside were supplied by Extrasynthese (Genay, France), isoquercitrin, ribitol and pinitol by Sigma-Aldrich (St Louis, MO, USA), rutin by Transmit (Gießen, Germany) and aspalathin by the South African Medical Research Council of South Africa (SAMRC, Cape Town, South Africa). All phenolic reference standards were of high purity (> 95% purity, HPLC-mass spectroscopy and -diode array detection (DAD)).

3.2.2 Green rooibos extract and carbohydrate polymers

Green rooibos extract (GRE; 14.64% aspalathin, dry basis) was obtained from a commercial extract manufacturer. Inulin (21–26 degree of polymerisation, extracted from chicory root (*Cichorium intybus* var. sativum)), maltodextrin (dextrose equivalent 9, derived from maize starch) and chitosan (medium molecular mass) were supplied by Savannah Fine Chemicals Ltd (Cape Town, South Africa), Tongaat Hulett Starch (Gauteng, South Africa) and Sigma-Aldrich (St Louis, MO, USA), respectively.

3.2.3 Microencapsulation by spray-drying

GRE and the carbohydrate polymers were mixed in three predefined ratios to obtain a feed solution (350 g) with a concentration of 10% soluble solids (m/m) for each spray-drying operation. Formulations included GRE (0% carbohydrate polymer) and GRE-polymer mixtures (25% inulin (IN25), 50% inulin (IN50), 75% inulin (IN75), 25% maltodextrin (MA25), 50% maltodextrin (MA50), 75% maltodextrin (MA75), 5% chitosan (CH5), 10% chitosan (CH10) and 15% chitosan (CH15)). The addition of chitosan was restricted by the high viscosity of the solution, necessitating the use of lower amounts than that used for maltodextrin and inulin. Maltodextrin and inulin were added to deionised water and after complete dissolution by sonication, GRE was added. Chitosan was added to 1% (m/v) acetic acid at 60 °C and stirred until a clear, viscous solution was obtained. The GRE was added when the solution was cooled to room temperature (*ca.* 22 °C). Each mixture were prepared in triplicate.

Spray-drying was conducted on a Büchi B-290 mini spray-drier (Büchi Labortechnik AG, Flawil, Switzerland) fitted with a 1.5 mm nozzle and B-296 dehumidifier. The operating conditions, previously optimised by Miller *et al.* (2018) for a GRE-inulin mixture (1:1, m/m), were as follows: inlet temperature, 220 °C; peristaltic pump speed, 35% (equalling *ca.* 1744 L/h); atomisation air rotameter, 60 mm; aspirator rate, 100%; nozzle cleaner, 4 strikes/min. The outlet temperature varied, depending on the composition of the feed solution (*ca.* 90–110 °C). After completion of the spray-drying process, the powders collected after the cyclone were weighed to determine powder yield (%, g powder obtained per 100 g solids in the feed solution). The powders were sealed in glass vials for temporary storage at ambient temperatures before analyses and accelerated storage.

3.2.4. Characterisation of powders

3.2.4.1 Bulk properties

The poured bulk density (D_p) of all the powders was calculated as a ratio of the powder mass and the volume occupied in a 100 mL measuring cylinder. The tapped bulk density (D_t) was calculated as the ratio between the powder mass and volume after tapping the cylinder until no change in the volume was observed (*ca.* 100 times). Measurements were performed in triplicate and the values employed to calculate Carr's compressibility index (*C.I.,* Eq. 3.1) and the Hausner ratio (*HR,* Eq. 3.2) (Schüssele & Bauer-Brandl, 2003):

$$C.I. = (D_p - D_t)/\, D_p \qquad (3.1)$$

$$HR = (D_p/\, D_t) \qquad (3.2)$$

3.2.4.2 Particle size and morphology

Scanning electron microscopy (SEM) imaging of the powders was accomplished using a Zeiss MERLIN field emission scanning electron microscope (Zürich, Switzerland). Powder samples, placed on aluminum stubs, were coated with a 10 nm gold layer (Edwards S150A Gold Sputter Coater from Perkin Elmer, USA). The beam conditions during the image analysis were 5 kV acceleration voltage, 250 pA beam current (I-Probe) and 3 to 5.5 mm working distance (WD). Images were captured using a Zeiss inlens (secondary electron type 1) detector.

In addition to SEM, scanning transmission electron microscopy (STEM) images were captured with a STEM detector sensitive to differences in atomic number, indicating different regions inside the microparticles. The powder samples were mounted onto carbon-coated copper STEM grids prior to imaging in dark field mode. The beam conditions during the image analysis were 25 kV acceleration voltage (Extra-High Tension target), 250 pA beam current (I-Probe), 3 to 5.5 mm WD and analytic column configuration (Column Mode).

3.2.4.3 Polyphenol content

Quantification of the major phenolic compounds in samples before and after spray-drying, as well as during the accelerated stability tests was achieved with HPLC-DAD analysis on an Agilent 1200 HPLC system (Waldbronn, Germany), using a validated method for rooibos (Walters, De Villiers, Joubert & De Beer, 2017). Prior to analysis 10% (m/v) ascorbic acid solution was added to the samples to prevent oxidation of phenolic compounds during sample analysis. The compound concentration was expressed as g compound/100 g of extract (recalculated to a dry basis (d.b.)) in order to directly compare the phenolic content of powders, irrespective of different formulations and moisture content.

3.2.4.4 Pinitol and glucose content

Prior to derivatisation GRE was dissolved with 60% (v/v) methanol at 70°C for 120 min and subsequently dried under vacuum, using centrifugal vacuum equipment (Labconco Centrivap Concentrator, Kansas City, USA). Ribitol was added as an internal standard at a final concentration of 10 ppm. The dried sample were reconstituted in 2.5% (v/v) methoxyamine in pyridine (100 µL), whereafter 100 µL *N,O*-bis(trimethylsilyl)trifluoroacetamide was added. The mixture was derivatised by incubating for 30 min in an oven maintained at 60°C.

Quantification of glucose and pinitol was achieved on an Agilent 6890 N gas chromatograph coupled to a Agilent 5975 MS mass spectrometer detector, using a Zebron AB-MultiResidue column (30 m, 0.25 mm

internal diameter, 0.25 µm film thickness). The injector was operated in the splitless mode at 200 °C and the oven temperature maintained at 80 °C for 1 min and ramped at 7 °C/min to 250 °C, held for 2 min. Helium was used as carrier gas with a flow rate of 1.2 mL/min. Data were recorded in full scan mode (35–600 *m/z*) at temperatures of 240 °C and 150 °C for the ion source and quadrupole, respectively.

3.2.4.5 X-ray powder diffraction (XRPD)

A Bruker AXS D2 Phaser desktop diffractometer, equipped with a LYNXEYE™ detector (Billerica, USA), was used to determine the solid state nature of the carbohydrate polymers and microencapsulated products. Samples were spread evenly on a zero-background sample holder and diffractograms were recorded at ambient temperature. The radiation source was Cu in a standard ceramic sealed tube with X-ray generation at 30 kV/10 mA.

3.2.4.6 Differential scanning calorimetry (DSC)

A Q Series™ Differential Scanning Calorimeter (Q100) (TA Instruments, New Castle, USA) in conjunction with TA Universal Analysis software was used to record and analyse thermograms of green rooibos powders and carbohydrate polymers. Samples were accurately weighed (*ca.* 5 mg) in closed aluminium pans and heated from 40–350 °C (heating rate 10 °C/min; nitrogen gas purge rate 35 mL/min).

3.2.4.7 Moisture content (MC), water activity (a_w) and moisture sorption analysis

The MC of the spray-dried powders was determined gravimetrically, using a HR73 Halogen Moisture Analyser (Mettler Toledo, Greifensee, Switzerland). A pre-zeroed aluminium dish with *ca.* 2 g of thinly spread powder was dried at 100 °C for 60 min. The moisture content was expressed on a d.b. The a_w was measured at 25 °C, using a Novasina LabMaster-a_w electric hydrometer (Lachen, Switzerland).

Moisture sorption analysis of the spray-dried powders was performed, using a VTI-SA Vapour Sorption Analyser (TA Instruments). The spray-dried powders were subjected to a pre-drying step at 40 °C until the mass fluctuation was less than 1.0 mg. The analyses were performed at 25 °C and the relative humidity (RH) was increased from 5% to 65% to obtain the adsorption curve. The upper RH was limited to prevent deliquescence. This was followed by a decrease in the RH from 65% to 5% in order to obtain the desorption curve. For both curves, the RH was changed after the mass remained stable for 2 min. The data were fitted to Brunauer-Emmet-Teller (BET) and Guggenheim-Anderson-de Boer (GAB) models (Labuza & Altunakar, 2007).

3.2.4.8 Compatibility of GRE and carbohydrate polymers

A 2277 Thermal Activity Monitor (TAM III) calorimeter (TA Instruments, New Castle, USA) was used to obtain the heat flow curves of GRE, microencapsulated GRE and carbohydrate polymers at 40 °C. The thermograms of GRE and the specific polymer used for microencapsulation were used to construct a non-interaction curve. The difference between the theoretical (calculated) thermogram and the experimental thermogram recorded for the microencapsulated powder was expressed as the interaction average heat flow error (µW/g). This was determined for each polymer and its corresponding microencapsulated GRE.

3.2.5 Accelerated storage stability testing

Stability testing of GRE and the different microencapsulated GREs was performed in triplicate under accelerated storage conditions (40 °C/75% RH) in a stability cabinet (SMC Scientific Manufacturing cc., Table View, South Africa) over a period of 96 h. Samples were removed from storage at predetermined sampling intervals. Mini-hygrostats (75% RH) were created by inserting a glass conical insert containing 250 µL of a saturated NaCl solution (3.6 g/mL) into each 24 mL vial. The glass insert was mounted in a stainless steel compression spring to avoid contact of the insert with the powder (*ca.* 100 mg; mass accurately recorded on a 5-decimal balance) (Fig. 3.1). The vials were sealed with PTFE screw caps after all the components were added.

Directly after sampling, the glass conical insert containing the saturated salt solution was removed and the increase in the powder mass, due to moisture adsorption, determined gravimetrically. After weighing, the complete sample was dissolved in aqueous DMSO (10%, m/v) to a concentration of *ca.* 0.55 mg/mL of GRE with the spring still in situ to avoid any powder loss. Aliquots were stored at −20 °C until HPLC-DAD analysis.

Various regression models were fitted on the data and the fractional conversion model (Van Boekel, 2008; Wibowo, Grauwet, Gedefa, Hendrickx & Van Loey, 2015) was selected (highest adjusted coefficient of determination (R^2_{adj})) to quantify the effect of storage on the aspalathin content in terms of degradation rate and final content in the formulation (Eq. 3.3):

$$C = C_\infty + (C_0 - C_\infty)e^{-Kt} \quad (3.3)$$

where C, C_0 and is C_∞ is the aspalathin content (g/100 g extract, dry basis (d.b.) at time t, at time 0 and equilibrium conditions, respectively, t is the time in months and K is the reaction rate constant.

Isothermal microcalorimetry analysis at 40 °C/75% RH was also performed to view any changes in heat flow under these conditions that could affect the storage stability. The RH was adjusted by placing micro-hygrostats, containing a saturated NaCl solution, inside crimp-top glass ampoules containing the samples.

Fig. 3.1 Hygrostat system for accelerated stability tests (40 °C/75% RH) with stainless steel spring, glass conical insert with saturated NaCl solution and clear 24 ml vial (in actual experiments amber vials were used) sealed with PTFE caps

3.2.6 Statistical analysis

The experimental design was completely randomised with three independently replicated experiments for each of the ten powder formulations (GRE, IN25, IN50, IN75, MA25, MA50, MA75, CH5, CH10 and CH15). Analysis of Variance (ANOVA) was performed on variables assessed to test for formulation as a main effect using the GLM (General Linear Models) procedure of SAS software (Version 9.4; SAS Institute Inc, Cary, USA).

For the accelerated storage stability testing, the aspalathin content of the powders, sampled at different time intervals, was determined for each experimental replicate (n = 3). Non-linear regression analysis with time as independent variable was performed to describe aspalathin degradation over time, using the NLIN procedure of SAS. Zero, first, second order and fractional conversion regression models were fitted for each experimental replicate. The regression parameters obtained for the fractional conversion regression model (highest R^2_{adj}) were used as input for ANOVA to test for the effect of formulation on the model parameters.

The Shapiro-Wilk test was performed on the data to test for deviation from normality. Fisher's least significant difference (LSD) was calculated at the 5% level to compare treatment means where $P < 0.05$ were considered significant.

3.3 Results and discussion

3.3.1 Retention of aspalathin during spray-drying

Spray-drying had little effect on the aspalathin content of GRE and GRE microencapsulated with maltodextrin or inulin, irrespective of their levels, where MA25 and inulin containing formulations showed slightly less loss of aspalathin compared to GRE (Table 3.1). The aspalathin content of the powder decreased by less than 5%, similar to the findings of Miller *et al.* (2018) for a green rooibos extract microencapsulated in

a 1:1 ratio with inulin or maltodextrin. Significantly lower aspalathin levels were obtained when chitosan was used as microencapsulating agent at the 10 and 15% polymer levels (17.6 and 19.3% decrease, respectively, Table 3.1). Due to the poor aspalathin retention, chitosan was deemed unsuitable as a microencapsulating polymer for the rooibos extract.

The content of other major flavonoids in GRE, as well as the phenylpropenoid acid glucoside, *Z*-2-(β-D-glucopyranosyloxy)-3-phenylpropenoic acid, is provided in Supplementary material (Table A.1). No clear patterns were evident, except the consistently lower content values for the powders, CH10 and CH15. Exposure of GRE to the high inlet temperature of the spray-drying process is very short, and while the dry powder exited the spraying chamber at *ca.* 90°C and did not cool immediately to room temperature, the a_w of the powder is low (Table 3.2), limiting chemical reactions. The consistently lower phenolic content values for powders containing chitosan suggest that degradation is most likely not the cause.

3.3.2 General powder characteristics

Powder yield ranged from 65.2% to 82.0% (Table 3.1) with the highest yields obtained for formulations containing maltodextrin. Encapsulation with inulin delivered the same or slightly lower product yields. Chitosan produced significantly lower yields compared to the other formulations ($P < 0.05$), also evident from the deposit on the wall of the chamber. Given these practical limitations of chitosan, inulin could be a suitable alternative to maltodextrin. Previously, Miller *et al.* (2018) found both maltodextrin and inulin to have no effect on powder yield when used in a 1:1 ratio with a green rooibos extract.

The flowability of microencapsulated GRE, based on Carr's compressibility index (Table 3.1), can be mostly classified as poor (26.03–37.26) with no clear relationship shown for the different levels of polymer. The use of polymers decreased the flowability compared to GRE (13.18), classified as having good flowability. The Hausner ratio of microencapsulated GRE exceeded 1.4, indicating cohesiveness. A value of 1.16 was obtained for GRE (Supplementary material; Table A.2), indicating free flowing powder, confirming the assessment of powder flowability based on Carr's compressibility index. The flow properties of powders, important for handling and application, are dependent on various factors including the temperature, MC, particle morphology and size and the chemical composition (Schulze, 2008), proving difficult to predict.

Average particle sizes ranged from 0.89–2.99 µm with large dispersity based on standard deviations (Table 3.1). This is not unusual for microencapsulation by spray-drying as the particle formation process is largely uncontrolled. The formulations containing chitosan showed the smallest particle diameter and distributions (0.89–1.32 µm), followed by inulin (1.22–2.43 µm) and maltodextrin (1.70–2.99 µm). The particle morphologies

also differed for the different polymers (Fig. 3.2). GRE appeared to be mostly smooth spherical particles, but broken particles were also present. Microencapsulation with maltodextrin produced much more irregular shaped particles with characteristic indented surfaces. Indentation was observed to a lesser extent for GRE microencapsulated with inulin. These basic particle morphologies agreed with findings of Miller *et al.* (2018). At the lower concentration (5%) chitosan produced spherical microencapsulated particles, but as the chitosan concentration was increased to 15%, the particles had a progressively finely wrinkled appearance. Indentation of particles would decrease flowability. The indented surfaces and irregular shapes can be rationalised by a more rapid loss of water from the microencapsulating material than the extract (Robert, García, Reyes, Chávez & Santos, 2012). However, various other factors, including differences in chemical structure, charge and inter-molecular forces (Banerjee & Bhattacharya, 2012), hydrophobicity, and hydrophilicity and solubility, affect the size of atomised particles and final particle characteristics (Sun-Waterhouse, Wadhwa & Waterhouse, 2013).

STEM images (Fig. 3.3) provide information on the different internal architectures of the particles, based on the different colouration of the regions. As expected, GRE produced powder particles are made up of a uniform chemical phase, while the microencapsulated GRE particles exhibited core-shell architecture, matrix architectures and particles that appeared to consist of a single phase, confirming a degree of immobilisation of GRE within/on the encapsulating polymers (Desai & Park, 2005).

All the spray-dried powders and their feed constituents showed the typical ‘halo’ XRPD pattern of an amorphous state with no distinct crystalline peaks (Fig. 3.4), typical of the spray-dried plant powders (Bhandari & Howes, 1999). Amorphous powders exist in a state of thermodynamic instability (Franks, 1994) and are less stable than their crystalline counterparts where unfavourable storage conditions are associated with crystallisation and other state transformations (Bott, Labuza & Oliveira, 2010).

Table 3.1

Summary of yield, particle size, Carr's compressibility index (C.I.) and aspalathin loss during spray-drying for the green rooibos extract (GRE), and GRE microencapsulated with maltodextrin (MA25, MA50, MA75), inulin (IN25, IN50 and IN75) and chitosan (CH5, CH10, CH15)

Formulation	Yield (%)[a]	Size (µm)[b]	C.I.	Aspalathin loss after spray-drying (%)[c]
GRE	73.14 ± 1.10 c[d]	2.03 ± 1.48	13.80 ± 0.32 d	−4.8 ± 0.4 d
MA25[e]	79.82 ± 0.58 b	1.70 ± 1.25	34.85 ± 3.45 ab	1.0 ± 0.6 a
MA50	79.47 ± 0.52 b	2.89 ± 2.04	31.15 ± 0.56 bc	−4.0 ± 0.5 d
MA75	82.04 ± 1.49 a	2.99 ± 2.22	27.84 ± 1.79 c	−4.8 ± 0.3 d
IN25	78.92 ± 0.60 b	2.43 ± 1.60	37.26 ± 1.58 a	−0.5 ± 0.8 b
IN50	75.78 ± 0.69 c	1.22 ± 0.76	30.82 ± 1.65 bc	−2.1 ± 1.8 c
IN75	79.24 ± 1.24 b	2.23 ± 1.12	26.57 ± 4.16 c	−1.3 ± 0.3 bc
CH5	66.20 ± 0.21 d	0.95 ± 0.91	31.09 ± 2.99 bc	−3.6 ± 0.3 d
CH10	65.70 ± 0.21 d	0.89 ± 0.62	31.53 ± 2.95 bc	−17.6 ± 0.3 e
CH15	65.24 ± 0.15 d	1.32 ± 0.94	26.03 ± 7.54 c	−19.3 ± 0.8 f

[a]Calculated as a percentage of the recovered powder and solids in the feed solution (%, m/m); [b]Particle size as measured from 3 scanning electron microscopy images, 30 measurements per image; [c]Change in aspalathin calculated as difference in aspalathin (g/100 g, d.b.) before spray-drying and after spray-drying where a negative value indicate loss; [d]Means in the same column with the same letter are not significantly different (P ≥ 0.05); [e]Values indicate the percentage (m/m) of polymer in the formulation

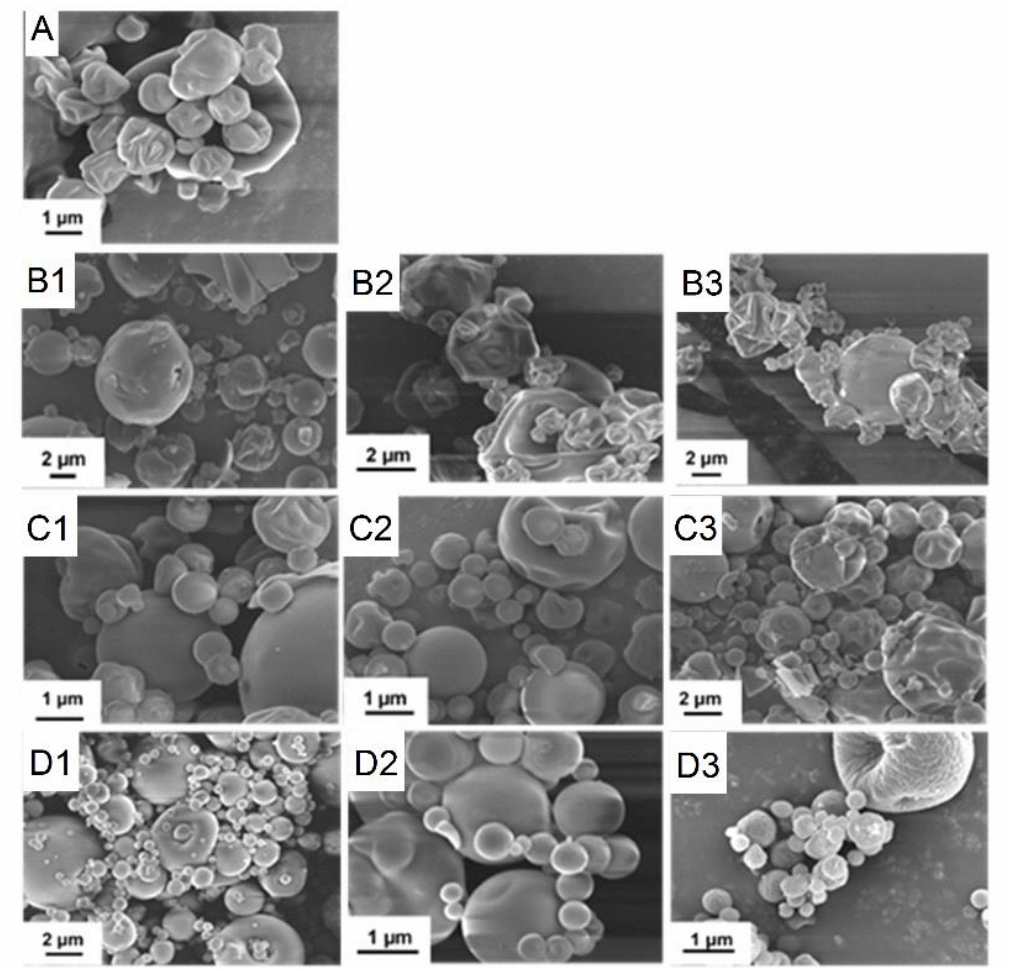

Fig. 3.2 SEM images for: (A) green rooibos extract (GRE), GRE microencapsulated with maltodextrin (B1) MA25, (B2) MA50 and (B3) MA75; inulin (C1) IN25, (C2) IN50 and (C3) IN75 and chitosan (D1) CH5, (D2) CH10 and (D3) CH15. Values indicate the percentage (m/m) of polymer in the formulation.

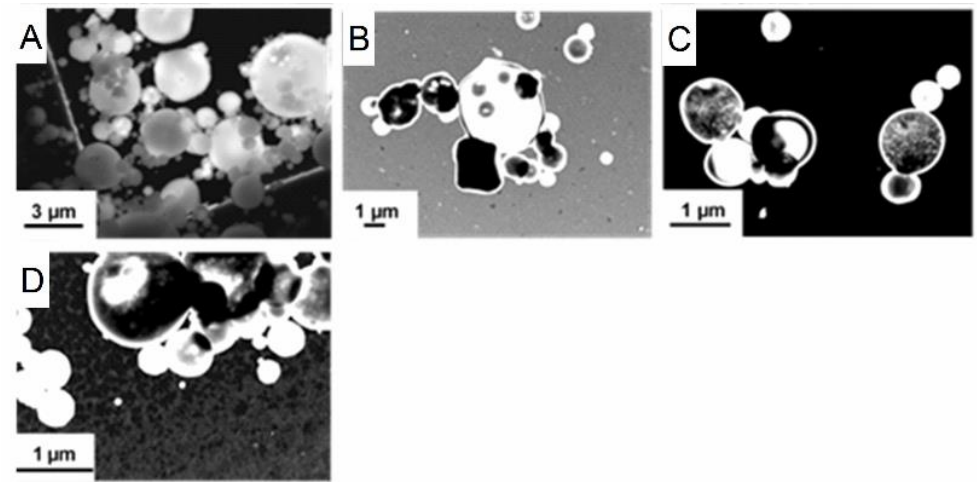

Fig. 3.3 STEM images for: (A) green rooibos extract (GRE), GRE microencapsulated with (B) maltodextrin (MA50), (C) inulin (IN50) and (D) chitosan (CH10). Values indicate the percentage (m/m) of polymer in the formulation.

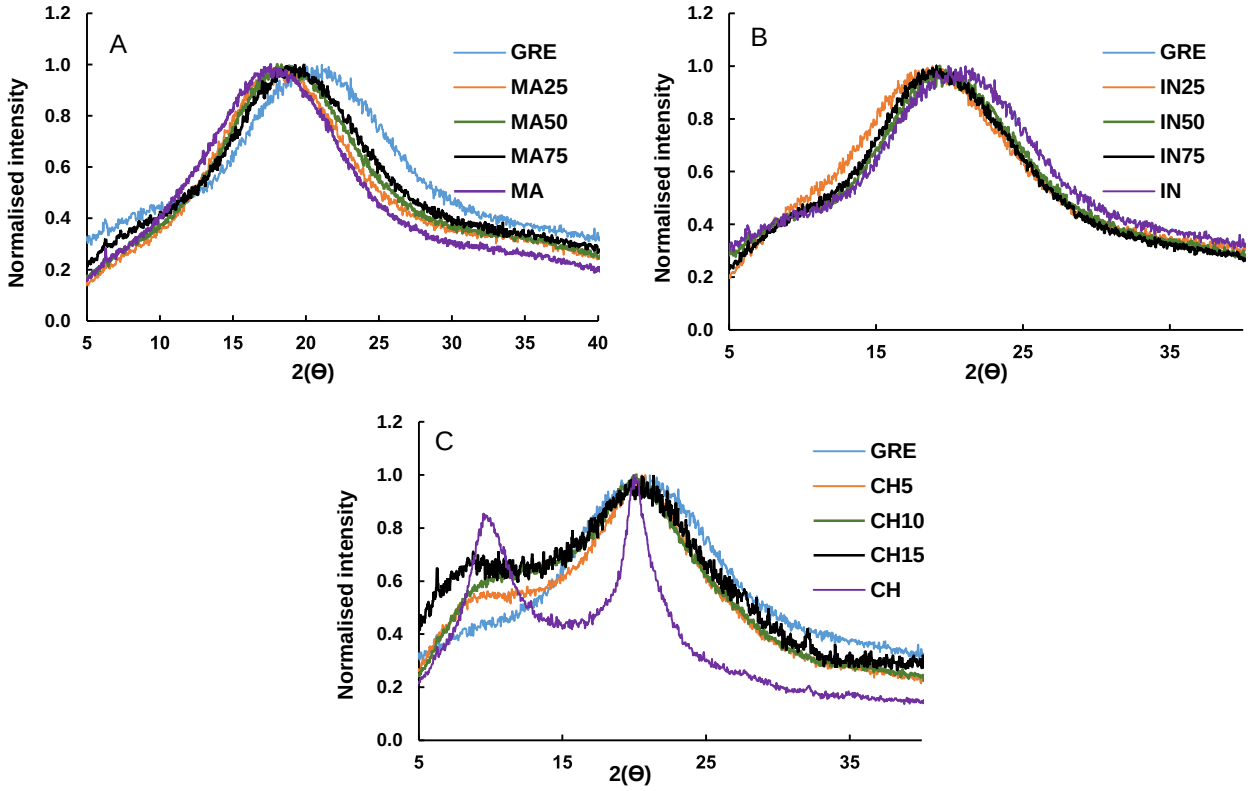

Fig. 3.4 X-ray powder diffraction for the green rooibos extract (GRE), encapsulating polymers and GRE microencapsulated with: (A) maltodextrin (MA, MA25, MA50, MA75), (B) inulin (IN, IN25, IN50, IN75) and (C) chitosan (CH, CH5, CH10, CH15). Values in brackets indicate the percentage (m/m) of polymer in the formulation.

3.3.3 Thermal phase transition

Following confirmation of the amorphous state of the powders, further investigating was required to identify possible phase transitions that might occur when stored. The DSC thermograms of GRE and

microencapsulated GREs showed a broad thermal event between 50 and 100 °C (Fig. 3.5), indicative of water loss (Ronkart, Paquot, Fougnies, Deroanne & Blecker, 2009). A distorted exothermic peak (174 ºC) was observed for GRE, which could be attributed to the thermal degradation of the extract (Fig. 3.5). The peak decreased or completely disappeared after microencapsulation, indicating that microencapsulation might prevent the thermal degradation of GRE to a certain extent, however, the peak could also decrease due to the 'dilution' of GRE with the addition of microencapsulating polymer. The thermal degradation peaks (> 200 °C) (Guinesi & Cavalheiro, 2006; Ronkart *et al.*, 2009) of maltodextrin and inulin became more distorted and undefined, in combination with a shift to lower temperatures, as the amount of encapsulating polymer in the powder decreased.

No glass transitions were observed in the thermograms of the polymers or spray-dried powders (Fig.3.5). Previously, Pauck *et al.* (2017), using other equipment, reported glass transition between 50–59 °C for the same inulin used in the present study. Nurhadi, Roos & Maidannyk (2016) reported T_g values for maltodextrin with DE10 and $a_w \geq 0.23$ at 75 °C and higher. Ratto & Hatakeyamat (1995) reported T_g values for chitosan at 30 ºC, whereas Sakurai, Maegawa & Takahashi (2000) reported T_g at 203 ºC, depending on crystallinity of chitosan. Amorphous material below its T_g is in a glassy state and slow physical aging will take place as a result of changes in physical properties such as free volume, water permeation and density (Abdul-Fattah, Dellerman, Bogner & Pikal, 2007). At temperatures > T_g, there is an increase in free molecular volume, an increase in thermal expansion and heat capacity, accelerating the rate of movement on a molecular level and phase transformations (Bhandari & Howes, 1999), resulting in sticky and difficult to handle powders (Jaya & Das, 2009). It is unlikely that the powders will be exposed to temperatures above these reported T_g values during storage. However, moisture (external RH conditions and a_w of powder) acts as a lubricant for molecular movement and would result in a lower T_g (Bott *et al.*, 2010). Practically, a_w and environmental RH together with the T_g should be considered when optimum storage conditions for amorphous powders are decided.

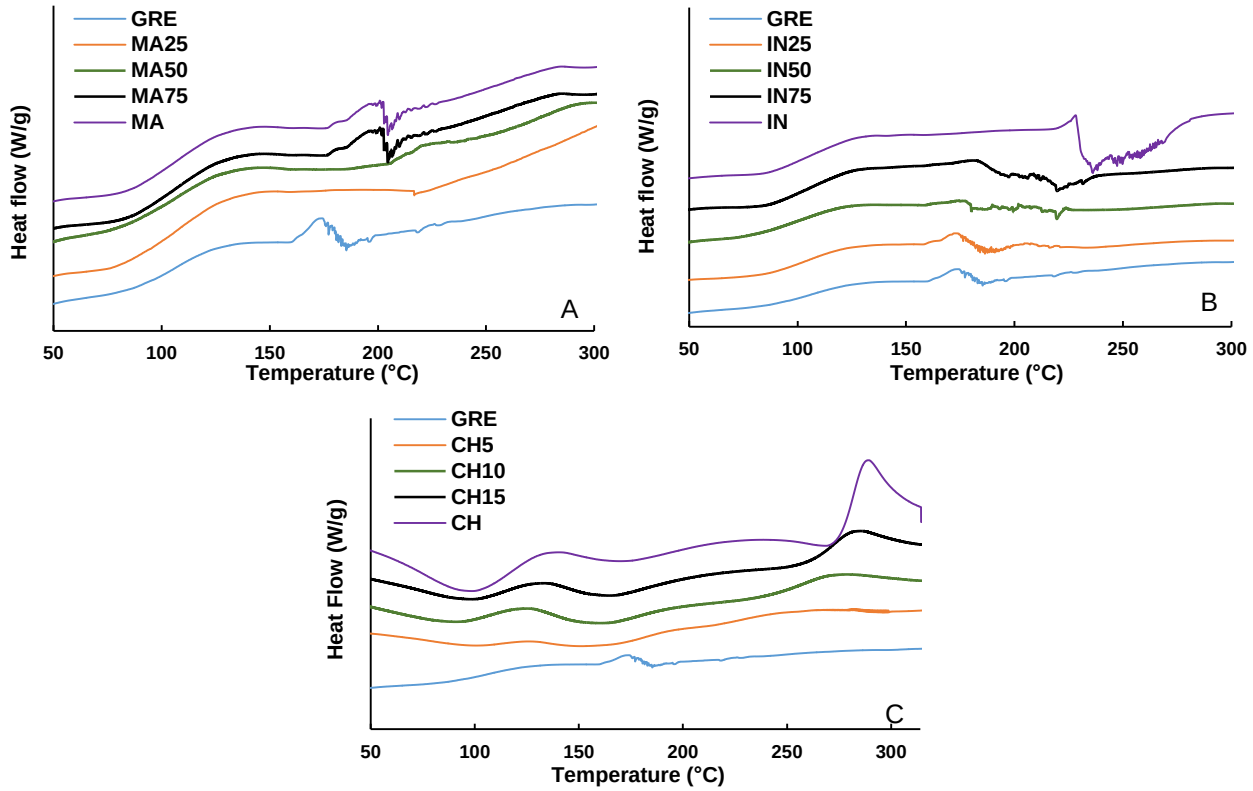

Fig. 3.5 Differential scanning calorimetry thermograms for the green rooibos extract (GRE), encapsulating polymers and GRE microencapsulated with: (A) maltodextrin (MA, MA25, MA50, MA75), (B) inulin (IN, IN25, IN50, IN75) and (C) chitosan (CH, CH5, CH10, CH15). Values in brackets indicate the percentage (m/m) of polymer in the formulation.

3.3.4 Relationship between equilibrium moisture content and water activity

Moisture sorption isotherms (MSI's) were used to describe the thermodynamic relationship between the equilibrium MC and a_w of spray-dried powders (Al-Muhtaseb, McMinn & Magee, 2002). All the formulations showed significant moisture uptake, consistent with their amorphous nature and the low molecular mass sugar/inositol content, which are often associated with hygroscopicity of natural extracts (Bott *et al.*, 2010). GRE contained 0.50% and 1.92% glucose and pinitol, respectively. The MSI's of GRE and GRE-inulin microcapsules show the typical sigmoidal type II curve and hysteresis loop (Fig. 3.6) of a carbohydrate polymer such as starch (Al-Muhtaseb *et al.*, 2002) and deliquescence at *ca.* 65% RH. The powders containing maltodextrin showed similar sigmoidal curves and hysteresis loops, but for chitosan the sigmoidal curve was less pronounced and the hysteresis loop smaller (Supplementary material; Fig. A.1–2). The MSI's for GRE microencapsulated with chitosan (CH10 and CH15) were distinctive in that the adsorption and desorption curves showed a crossover point at *ca.* 15 and 45% RH, respectively, indicating changes in water binding.

Hysteresis indicates permanent physical changes (Al-Muhtaseb *et al.*, 2002). The effect is likely an indication that the powders transitioned from the glassy to rubbery state as the T_g is lowered by the plasticising

effect of increased moisture at high RH conditions (Bott *et al.*, 2010). Amorphous powders are predisposed to moisture sorption due to their lack of crystallinity (Chu & Chow, 2000). In practical terms, GRE and microencapsulated GRE should be stored in low humidity environments as they are very susceptible to moisture absorption, which would result in caking, stickiness, and potentially loss of aspalathin.

The moisture sorption data were fitted to the BET and GAB sorption models. The BET model is only valid for a_w between 0.05 and 0.35 (Al-Muhtaseb *et al.*, 2002) and was therefore only fitted for a_w levels ≤ 0.3 (Table 3.2 and Supplementary material Fig. A.3–6). At these low a_w levels the BET model provided a better fit than the GAB model. The monolayer moisture content values (M_0), calculated with the BET model, ranged between 3.57–5.04%. The M_0 values increased as the amount of inulin and maltodextrin in the powders increased, likely due to the hydrophilic nature of the polymers. Similar trends were observed for the C values obtained from the BET model. The values were similar or slightly higher compared to M_0 values for GRE, IN50 and MA50 powders produced by Miller *et al.* (2018). In all cases the MC values fell well within the range of M_0 values (Table 3.2). The M_0 values provide an indication of strongly bound surface water (Gabas, Telis, Sobral & Telis-Romero, 2007). Water above this layer is more available for chemical reactions and will most likely adversely affect the stability of the product (De Souza, Thomazini, Balieiro & Fávaro-Trindade, 2015).

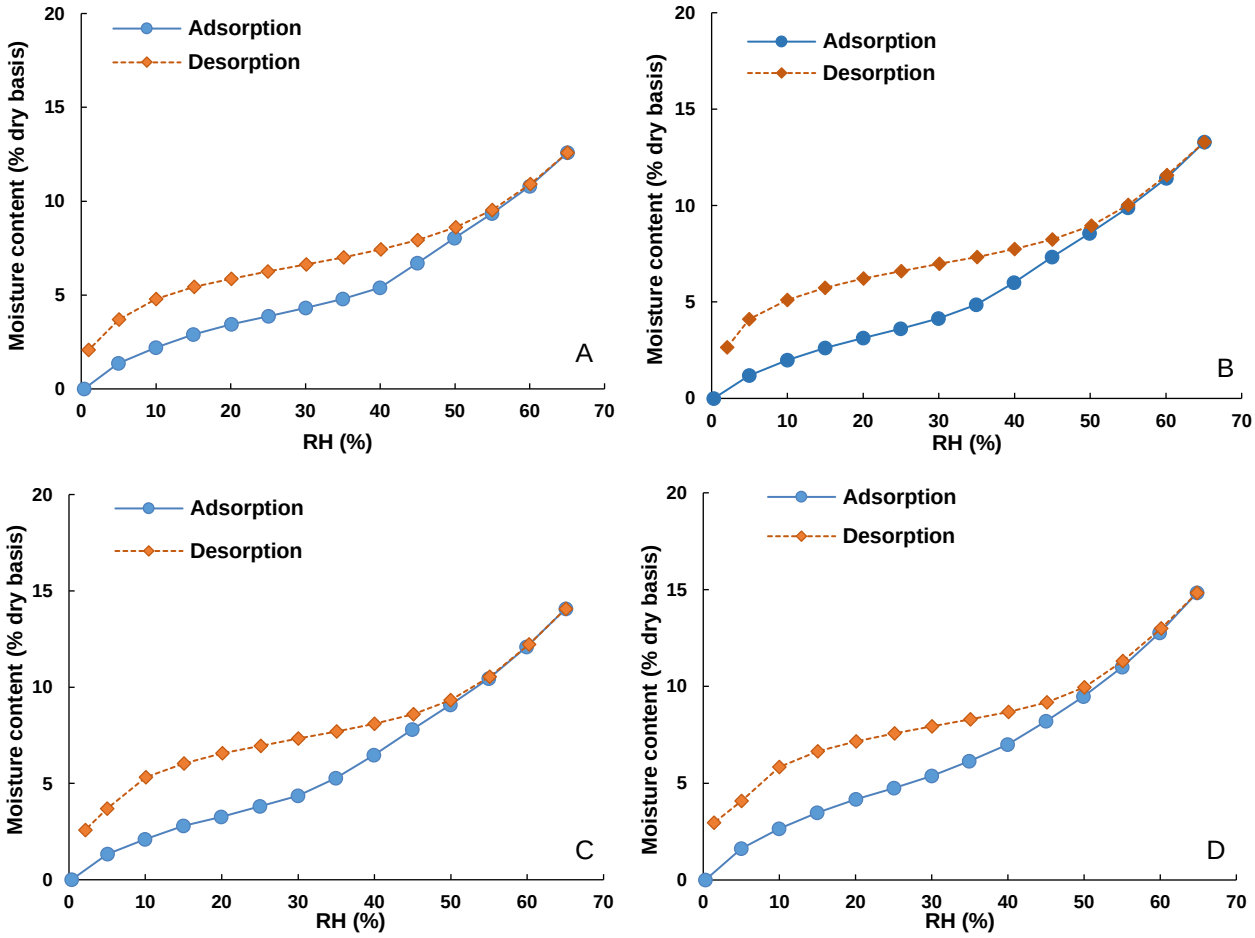

Fig. 3.6 Moisture sorption and desorption isotherms obtained at 25 °C for: (A) green rooibos extract (GRE) and GRE microencapsulated with inulin (B) IN25, (C) IN50 and (D) IN75. Values indicate the percentage (m/m) of polymer in the formulation.

Table 3.2

Moisture content (MC), water activity (a_w) and Guggenheim-Anderson-de Boer (GAB) and Brunauer-Emmet-Teller (BET)) model parameters from moisture sorption isotherm data obtained at 25°C for green rooibos extract (GRE), and GRE microencapsulated with maltodextrin (MA25, MA50, MA75), inulin (IN25, IN50 and IN75) and chitosan (CH5, CH10, CH15)

Formulation	MC (%)[a]	a_w[b]	GAB model				BET model		
			M_0[c]	C[d]	K[e]	R^2	M_0	C	R^2
GRE	2.40 ± 0.14 d[f]	0.176 ± 0.006 c	3.41	10.09	1.16	0.9503	3.73	10.43	0.9981
MA25[g]	3.00 ± 0.09 c	0.152 ± 0.004 d	3.42	9.81	1.15	0.9457	3.58	11.22	0.9999
MA50	3.48 ± 0.07 b	0.189 ± 0.007 b	3.76	10.08	1.10	0.9638	3.84	11.41	1.0000
MA75	2.96 ± 0.05 c	0.219 ± 0.005 a	4.57	11.98	1.00	0.9906	4.43	13.27	0.9999
IN25	2.85 ± 0.17 c	0.119 ± 0.005 e	3.65	6.68	1.17	0.8852	3.70	8.45	0.9998
IN50	2.98 ± 0.10 c	0.145 ± 0.004 d	3.83	6.95	1.18	0.8690	3.80	9.21	0.9986
IN75	2.24 ± 0.17 d	0.123 ± 0,006 e	4.50	8.78	1.11	0.9877	4.72	9.34	0.9996
CH5	3.39 ± 0.04 b	0.119 ± 0.003 e	3.86	5.28	1.01	0.8964	3.57	6.22	0.9948
CH10	3.48 ± 0.09 b	0.185 ± 0.004 b	5.12	6.67	1.04	0.9781	5.04	7.38	0.9998
CH15	3.75 ± 0.04 a	0.146 ± 0.004 d	3.81	6.51	1.10	0.9240	3.77	7.79	0.9999

[a]Moisture content (% dry basis); [b]Water activity measured at 25°C; [c]M_0 = monolayer moisture content (% dry basis); [d]C = Constant in BET and GAB sorption model; [e]K = constant of GAB model; [f]Means in the same column with the same letter are not significantly different (P ≥ 0.05); [g]Values in brackets indicate the percentage (m/m) of polymer in the formulation

3.3.5 Compatibility of GRE and carbohydrate polymers

Isothermal microcalorimetry was utilised to detect possible incompatibility between GRE and the carbohydrate polymers. The difference between the experimental interaction heat flow curve obtained from the microencapsulated GRE and its theoretical non-interaction curve as calculated from the heat flow curves of the individual components (GRE and polymer) is used to indicate their possible incompatibility (Table 3.3). The average interaction heat flow error values for the different powders, with IN50 and MA50 showing the smallest (0.76 µW/g) and largest (10.13 µW/g) values, respectively, are very small, implying a very low degree of incompatibility. In light of this, IN50 could be considered the most suitable formulation for the further development of a microencapsulated GRE powder.

Table 3.3

Interaction average heat flow values and errors obtained from isothermal microcalorimetry of green rooibos extract microencapsulated with maltodextrin (MA25, MA50, MA75), inulin (IN25, IN50 and IN75) and chitosan (CH5, CH10, CH15)

Formulation	Interaction average heat flow (µW/g) (absolute values)[a]	Interaction average heat flow error (µW/g) (absolute values)[b]
MA25	1.13	2.71
MA50	8.99	10.13
MA75	0.93	2.92
IN25	7.81	8.94
IN50	0.66	0.76
IN75	0.71	8.14
CH5	4.54	7.70
CH10	1.37	5.36
CH15	0.93	5.44

[a]Heat flow of actual microencapsulated spray-dried rooibos powders measured at 40°C; [b]Difference between the heat flow of actual microencapsulated spray-dried rooibos powders and the theoretical zero interaction curve of the ingredients; [c]Values in brackets indicate the percentage (m/m) of polymer in the formulation

3.3.6 Accelerated stability testing

The stability of the powders was first assessed at accelerated conditions (40 °C/75% RH) by measuring heat flow, which is proportional to the rate at which a given chemical or physical process takes place. The thermograms for GRE and the powders containing inulin showed two large peaks before 5 h, while pure inulin showed one distinct peak (Fig. 3.7). For powders containing maltodextrin or chitosan, only a single large peak was visible between 0–1 h (Fig. 3.7). The peaks indicated physicochemical change, which can be attributed to water absorption when the powders were exposed to 75% RH. Under these conditions, the absorbed water acts as plasticiser, allowing sufficient mobility of the molecules and conversion of materials to their thermodynamically stable state (Bott *et al.*, 2010). The carbohydrate polymers will most likely crystallise (Ronkart *et al.*, 2006), whereas GRE, a complex mixture, will rather start to dissolve instead of crystallise. In the case of the powders containing inulin, water adsorption and phase transformation are not kinetically

synchronised, giving rise to two separate thermal events (Briggner, Buckton, Bystrom & Darcy, 1994). The powders containing maltodextrin or chitosan can be regarded as less stable since the peaks were observed after less than 1 h compared to 5 h for inulin.

Given that deliquescence of the powders will take place at RH > 65%, chemical instability will be enhanced beyond the deliquescence point (Hiatt, Taylor & Mauer, 2011). Chemical stability of samples stored at 40 °C/75% RH for 96 h was subsequently assessed in terms of aspalathin. Aspalathin degradation was accompanied by substantial moisture uptake (Fig. 3.8), where visual deliquescence was observed between 16 and 24 h. The increase in moisture content and aspalathin degradation both show biphasic curves, with a rapid increase in moisture and decrease in aspalathin up to 36 h, followed by a gradual decrease and plateau. This indicates that aspalathin degradation is most likely due to a combination of factors, including storage temperature and physicochemical changes brought on by water adsorption. The fractional conversion model, based on first order kinetics, was found to predict aspalathin degradation the best as shown by the adjusted coefficient of determination ($R^2_{adj} > 0.96$) (Supplementary material, Fig. A.7 and Table A.3).

Aspalathin degraded by more than 10% in all the spray-dried powders, including GRE, over 96 h (Table 3.4). Significantly ($P < 0.05$) higher reaction rate constants were observed for GRE microencapsulated with chitosan (2.23–2.71 min^{-1}) and significantly higher aspalathin degradation was observed for chitosan at higher levels (CH10, 19.73% and CH15, 19.05%) compared to GRE (1.48 min^{-1}; 17.14%). Thus, chitosan proved to be not suited as encapsulating polymer as it resulted in lower levels of aspalathin after storage. However, due to the high viscosity of reconstituted chitosan solutions and possible interactions between chitosan and polyphenols (Popa, Aelenei, Popa & Andrei, 2000), the apparent decrease in aspalathin stability could possibly be due to experimental loss rather than increased degradation.

Even though significantly ($P < 0.05$) less aspalathin degradation for MA75 and IN50 compared to GRE and significantly higher aspalathin equilibrium contents for all the inulin formulations and MA75 was observed, no significant differences were observed between the reaction rates of any of the GRE formulations microencapsulated with inulin or maltodextrin compared to that of GRE (Table 3.4), prompting that further testing is required under normal storage conditions. Only slight differences were also observed between the aspalathin degradation rate in the inulin and maltodextrin formulations, and no clear pattern is evident with regard to the different levels of the polymers in the powders.

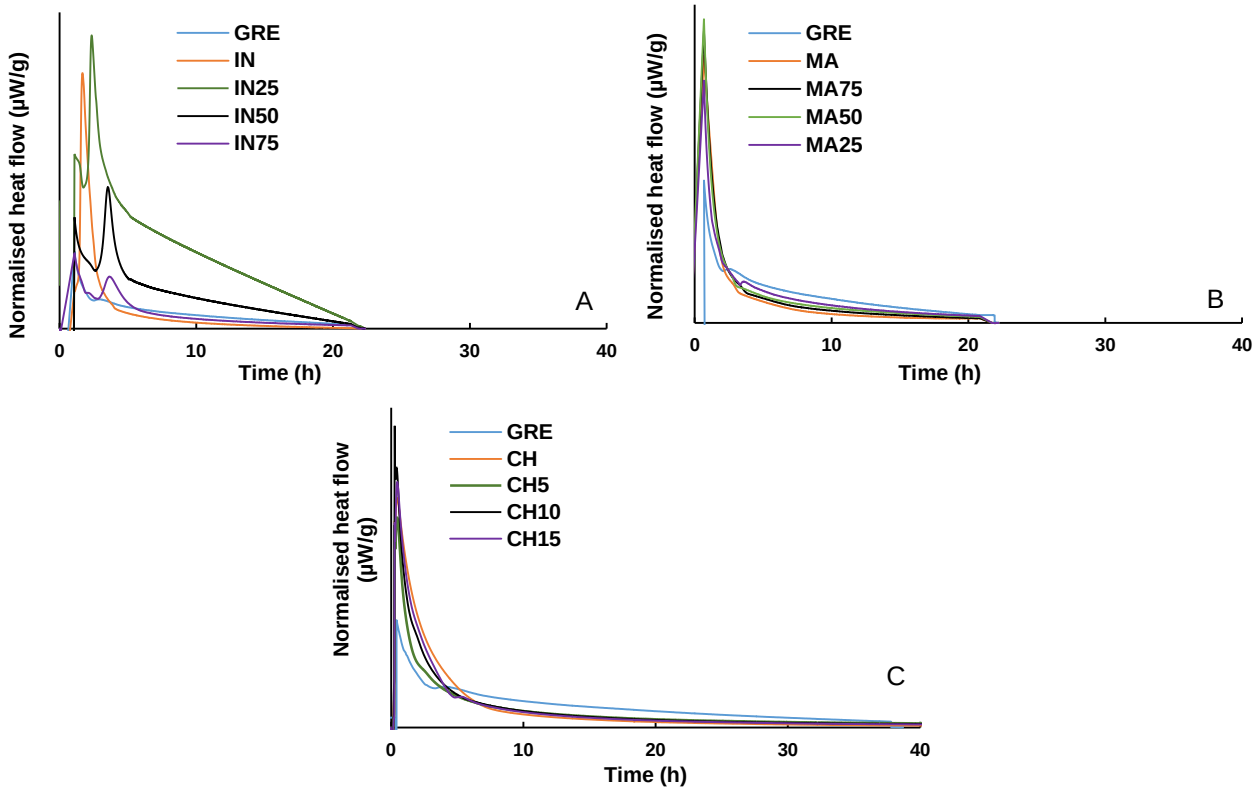

Fig. 3.7 Heat flow measurements (isothermal microcalorimetry) for the green rooibos extract (GRE), encapsulating polymers and GRE microencapsulated with: (A) inulin (IN25, IN50, IN75), (B) maltodextrin (MA25, MA50, MA75) and (C) chitosan (CH5, CH10 and CH15) at accelerated stress conditions (40 °C/75% RH). Values in brackets indicate the percentage (m/m) of polymer in the formulation.

Table 3.4
Percentage aspalathin change and fractional conversion kinetic parameters (equilibrium concentration, C_∞, initial concentration, C_0 and reaction rate constant, K) for the degradation of aspalathin at 40 °C/75% RH in green rooibos extract (GRE), and GRE microencapsulated with maltodextrin (MA25, MA50, MA75), inulin (IN25, IN50 and IN75) and chitosan (CH5, CH10, CH15)

Formulation	Change (%) after 96 h	Fractional conversion model[a]			
		C_0 (g/100 g, d.b.)	C_∞ (g/100 g, d.b.)	K (min^{-1})	R^2_{adj}
GRE	−17.14 ± 1.06 bcd[b]	13.93 ± 0.06 e	11.23 ± 0.21 cd	1.48 ± 0.22 cd	0.9877
MA25[c]	− 16.58 ± 0.40 cde	14.83 ± 0.08 a	12.17 ± 0.03 a	1.83 ± 0.09 bc	0.9360
MA50	− 15.26 ± 1.59 def	14.08 ± 0.02 d	11.68 ± 0.17 abc	1.48 ± 0.25 cd	0.8917
MA75	− 14.51 ± 0.56 ef	14.09 ± 0.01 d	10.96 ± 0.48 d	0.87 ± 0.22 d	0.9436
IN25	− 15.19 ± 2.29 def	14.63 ± 0.07 b	11.99 ± 0.66 ab	1.48 ± 0.22 cd	0.9930
IN50	− 11.96 ± 1.74 f	14.32 ± 0.10 c	12.08 ± 0.71 ab	1.60 ± 0.69 bcd	0.9815
IN75	− 15.26 ± 0.50 def	14.64 ± 0.03 b	12.05 ± 0.06 ab	2.08 ± 0.09 abc	0.9348
CH5	− 18.73 ± 0.81 abc	14.18 ± 0.14 d	11.50 ± 0.15 bcd	2.71 ± 0.58 a	0.9754
CH10	− 19.73 ± 0.57 a	12.16 ± 0.083 f	9.58 ± 0.14 e	2.23 ± 0.32 ab	0.9661
CH15	− 19.05 ± 2.24 a	11.93 ± 0.04 g	9.51 ± 0.17 e	2.40 ± 0.45 ab	0.9647

[a]Fractional conversion model: $C = C_\infty + (C_0-C_\infty)*\exp(-K*t)$ where C is aspalathin content (g/100 g extract, d.b.); [b]Means in the same column with the same letter are not significantly different $P \geq 0.05$; [c]Values indicate the percentage of polymer in the formulation

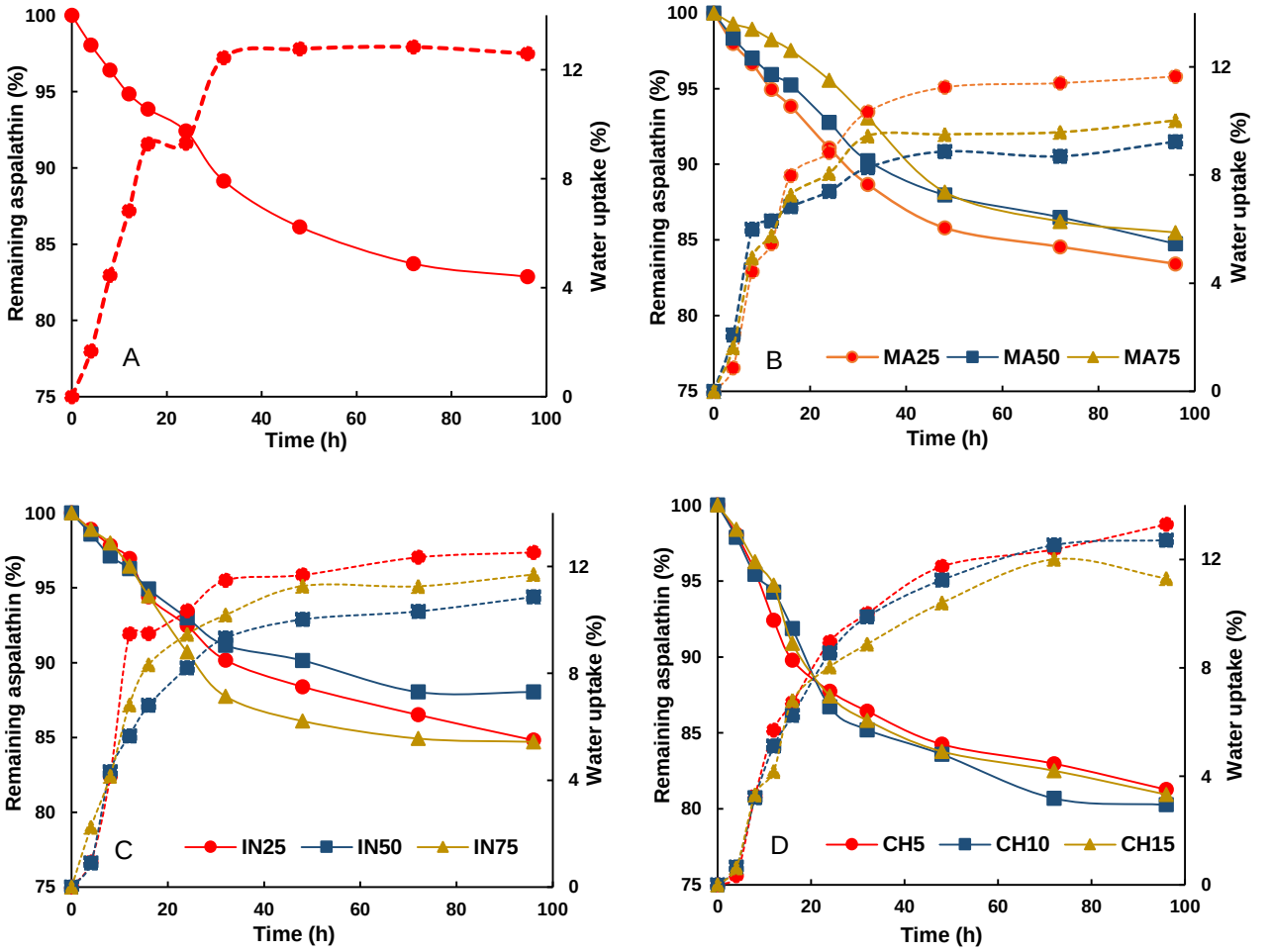

Fig. 3.8 Remaining aspalathin (%, dry basis) (solid lines) and water uptake (%) (broken lines) at 40°C/75% RH for: (A) green rooibos extract (GRE) and GRE microencapsulated with (B) maltodextrin (MA25, MA50, MA75); inulin (IN25, IN50,IN75) and (D) chitosan (CH5, CH10, CH15). Values in brackets indicate the percentage (m/m) of polymer in the formulation.

3.4. Conclusions

Microencapsulation of an aspalathin-rich green rooibos extract improved handling of the powder. Inulin, but not chitosan, proved to be a suitable alternative for maltodextrin. Not only were powder yields lower and powder moisture content and water activity higher when chitosan was used, but aspalathin was less stable in comparison to inulin and maltodextrin during accelerated storage. A lower ratio of chitosan to green rooibos extract had to be used, limiting 'bulking' with polymer. This has a negative implication for a single serve convenience product. Green rooibos extract mixed in a 1:1 ratio with inulin showed the lowest interaction between extract and polymer with aspalathin degradation rates comparable to a 1:1 mixture of extract and maltodextrin. Taking into consideration the low glycaemic load of inulin and its prebiotic effect, inulin is the best option for microencapsulated green rooibos extract for use as nutraceutical ingredient in functional food products aimed at management of metabolic syndrome.

3.5 References

Abdul-Fattah, A. M., Dellerman, K. M., Bogner, R. H. & Pikal, M. J. (2007). The effect of annealing on the stability of amorphous solids: chemical stability of freeze-dried moxalactam. *Journal of Pharmaceutical Sciences,* 96, 1237–1250.

Al-Muhtaseb, A. H., McMinn, W. A. M. & Magee, T. R. A. (2002). Moisture sorption isotherm characteristics of food products: A review. *Food and Bioproducts Processing,* 80, 118–128.

Banerjee, S. & Bhattacharya, S. (2012). Food gels: gelling process and new applications. *Critical Reviews in Food Science & Nutrition,* 52, 334–46.

Bhandari, B. R. & Howes, T. (1999). Implication of glass transition for the drying and stability of dried foods *Journal of Food Engineering,* 40, 71–79.

Bott, R. F., Labuza, T. P. & Oliveira, W. P. (2010). Stability testing of spray- and spouted bed-dried extracts of *Passiflora alata*. *Drying Technology,* 28, 1255–1265.

Briggner, L., Buckton, G., Bystrom, K. & Darcy, P. (1994). The use of isothermal microcalorimetry in the study of changes in crystallinity induced during the processing of powders. *International Journal of Pharmaceutics,* 105, 125–135.

Chu, K. K. W. & Chow, A. H. L. (2000). Impact of carbohydrate constituents on moisture sorption of herbal extracts. *Pharmaceutical Research,* 17, 1133–1137.

De Beer, D., Joubert, E., Viljoen, M. & Manley, M. (2011). Enhancing aspalathin stability in rooibos (*Aspalathus linearis*) ready-to-drink iced teas during storage: the role of nano-emulsification and beverage ingredients, citric and ascorbic acids. *Journal of the Science of Food and Agriculture,* 92, 274–282.

De Souza, V. B., Thomazini, M., Balieiro, J. C. & Fávaro-Trindade, C. S. (2015). Effect of spray drying on the physicochemical properties and color stability of the powdered pigment obtained from vinification byproducts of the Bordo grape (*Vitis labrusca*). *Food and Bioproducts Processing,* 93, 39–50.

Desai, K. G. H. & Park, H. J. (2005). Recent developments in microencapsulation of food ingredients. *Drying Technology,* 23, 1361–1394.

Franks, F. (1994). Accelerated stability testing of bioproducts: attractions and pitfalls. *Trends in Biotechnology,* 12, 114–117.

Gabas, A. L., Telis, V. R. N., Sobral, P. J. A. & Telis-Romero, J. (2007). Effect of maltodextrin and arabic gum in water vapor sorption thermodynamic properties of vacuum dried pineapple pulp powder. *Journal of Food Engineering,* 82, 246–252.

Guinesi, L. S. & Cavalheiro, É. T. G. (2006). The use of DSC curves to determine the acetylation degree of chitin/chitosan samples. *Thermochimica Acta,* 444, 128–133.

Han, T. S. & Lean, M. E. (2016). A clinical perspective of obesity, metabolic syndrome and cardiovascular disease. *Journal of the Royal Society of Medicine Cardiovascular Disease,* 5, 1–13.

Hiatt, A. N., Taylor, L. S. & Mauer, L. J. (2011). Effects of co-formulation of amorphous maltodextrin and deliquescent sodium ascorbate on moisture sorption and stability. *International Journal of Food Properties,* 14, 726–740.

Hofman, D. L., Van Buul, V. J. & Brouns, F. J. P. H. (2016). Nutrition, health, and regulatory aspects of digestible maltodextrins. *Critical Reviews in Food Science and Nutrition,* 56, 2091–2100.

Jaya, S. & Das, H. (2009). Glass transition and sticky point temperatures and stability/mobility diagram of fruit powders. *Food Bioprocess Technology,* 2, 89–95.

Johnson, R., De Beer, D., Dludla, P. V., Ferreira, D., Muller, C. J. F. & Joubert, E. (2018). Aspalathin from rooibos (*Aspalathus linearis*): A bioactive *C*-glucosyl dihydrochalcone with potential to target the metabolic syndrome. *Plant Medica,* 84, 568–583.

Joubert, E. & De Beer, D. (2014). Antioxidants of rooibos beverages: Role of plant composition and processing. In: *Processing and Impact on Antioxidants in Beverages* (edited by Preedy, V. R.). Pp. 131–144. USA: Academic Press.

Kolida, S. & Gibson, G. R. (2007). Prebiotic capacity of inulin-type fructans. *The Journal of Nutrition,* 137, 2503S–2506S.

Labuza, T. P. & Altunakar, L. (2007). Water activity prediction and moisture sorption isotherms. In: *Water Activity in Foods*. Pp. 109–154. Ames, Iowa: Blackwell Publishing Ltd.

McClements, D. J., Decker, E. A., Park, Y. & Weiss, J. (2009). Structural design principles for delivery of bioactive components in nutraceuticals and functional foods. *Critical Reviews in Food Science and Nutrition,* 49, 577–606.

Miller, N., De Beer, D., Aucamp, M., Malherbe, C. J. & Joubert, E. (2018). Inulin as microencapsulating agent improves physicochemical properties of spray-dried aspalathin-rich green rooibos (*Aspalathus linearis*) extract with α-glucosidase inhibitory activity. *Journal of Functional Foods,* 48, 400–409.

Muller, C. J. F., Malherbe, C. J., Chellan, N., Yagasaki, K., Miura, Y. & Joubert, E. (2018). Potential of rooibos, its major *C*-glucosyl flavonoids, and *Z*-2-(β-D-glucopyranosyloxy)-3-phenylpropenoic acid in prevention of metabolic syndrome. *Critical Reviews in Food Science and Nutrition,* 58, 227–246.

Murugesan, R. & Orsat, V. (2012). Spray drying for the production of nutraceutical ingredients—A review. *Food and Bioprocess Technology,* 5, 3–14.

Nurhadi, B., Roos, Y. H. & Maidannyk, V. (2016). Physical properties of maltodextrin DE 10: Water sorption, water plasticization and enthalpy relaxation. *Journal of Food Engineering,* 174, 68–74.

Pauck, C., De Beer, D., Aucamp, M., Liebenberg, W., Stieger, N., Human, C. & Joubert, E. (2017). Inulin suitable as reduced-kilojoule carrier for production of microencapsulated spray-dried green *Cyclopia subternata* (honeybush) extract. *LWT-Food Science and Technology,* 75, 631–639.

Popa, M.-I., Aelenei, N., Popa, V. I. & Andrei, D. (2000). Study of the interactions between polyphenolic compounds and chitosan. *Reactive & Functional Polymers,* 45, 35–43.

Ratto, J. & Hatakeyamat, T. (1995). Differential scanning calorimetry investigation of phase transitions in water/chitosan systems. *Polymer,* 36, 2915-2919.

Robert, P., García, P., Reyes, N., Chávez, J. & Santos, J. (2012). Acetylated starch and inulin as encapsulating agents of gallic acid and their release behaviour in a hydrophilic system. *Food Chemistry,* 134, 1–8.

Ronkart, S., Blecker, C., Fougnies, C., Van Herck, J. C., Wouters, J. & Paquot, M. (2006). Determination of physical changes of inulin related to sorption isotherms: An X-ray diffraction, modulated differential scanning calorimetry and environmental scanning electron microscopy study. *Carbohydrate Polymers,* 63, 210–217.

Ronkart, S. N., Paquot, M., Fougnies, C., Deroanne, C. & Blecker, C. S. (2009). Effect of water uptake on amorphous inulin properties. *Food Hydrocolloids,* 23, 922–927.

Sakurai, K., Maegawa, T. & Takahashi, T. (2000). Glass transition temperature of chitosan and miscibility of chitosan/poly(N-vinyl pyrrolidone) blends. *Polymer,* 41, 7051–7056.

Schulze, D. (2008). Powders and bulk solids. Pp. 1–503. New York: Springer-Verlag Berlin Heidelberg.

Schüssele, A. & Bauer-Brandl, A. (2003). Note on the measurement of flowability according to the European Pharmacopoeia. *International Journal of Pharmaceutics,* 257, 301–304.

Shoaib, M., Shehzad, A., Omar, M., Rakha, A., Raza, H., Sharif, H. R., Shakeel, A., Ansari, A. & Niazi, S. (2016). Inulin: Properties, health benefits and food applications. *Carbohydrate Polymers,* 147, 444–454.

Sun-Waterhouse, D., Wadhwa, S. S. & Waterhouse, G. I. N. (2013). Spray-drying microencapsulation of polyphenol bioactives: A comparative study using different natural fibre polymers as encapsulants. *Food and Bioprocess Technology,* 6, 2376–2388.

Van Boekel, M. A. J. S. (2008). Kinetic modeling of reactions in foods. Boca Raton: CRC Press.

Walters, N. A., De Villiers, A., Joubert, E. & De Beer, D. (2017). Improved HPLC method for rooibos phenolics targeting changes due to fermentation. *Journal of Food Composition and Analysis,* 55, 20–29.

Wibowo, S., Grauwet, T., Gedefa, G. B., Hendrickx, M. & Van Loey, A. (2015). Quality changes of pasteurised mango juice during storage. Part II: Kinetic modelling of the shelf-life markers. *Food Research International,* 78, 410–423.

Yao, H.-T. & Chiang, M.-T. (2006). Effect of chitosan on plasma lipids, hepatic lipids, and fecal bile acid in hamsters. *Journal of Food and Drug Analysis,* 14, 183–189.

SUPPLEMENTARY MATERIAL CHAPTER 3_ADDENDUM A

Table A.1

Concentration of PPAG[a] and phenolic compounds for the green rooibos extract (GRE) before and after spray-drying, and GRE microencapsulated with maltodextrin (MA25, MA50, MA75), inulin (IN25, IN50 and IN75) and chitosan (CH5, CH10, CH15) after spray-drying

	Phenolic compounds (g/100g, d.b.)[b]										
	PPAG	Aspalathin	Nothofagin	Isoorientin	Orientin	Isoquercitrin	Vitexin	Hyperoside	Rutin	Isovitexin	Isoquercitrin
GRE (before)	0.51	14.64	1.42	1.51	1.30	1.42	0.25	0.54	0.64	0.40	0.62
GRE (after)	0.45 ± 0.01 f[c]	13.94 ± 0.06 d	1.27 ± 0.01 d	1.41 ± 0.02 b	1.54 bc ± 0.02	1.31 ± 0.01 c	0.24 ± 0.01 bc	0.48 ± 0.0 bc	0.56 ± 0.01 b	0.23 ± 0.00 b	0.75 ± 0.01 b
MA25[d]	0.51 ± 0.02 d	14.79 ± 0.09 a	1.35 ± 0.01 b	1.50 ± 0.02 a	1.62 a ± 0.02	1.39 ± 0.01 a	0.25 ± 0.01 a	0.50 ± 0.01 a	0.60 ± 0.01 a	0.29 ± 0.01 a	0.78 ± 0.02 a
MA50	0.49 ± 0.01 de	14.06 ± 0.08 d	1.35 ± 0.01 b	1.38 ± 0.04 b	1.53 bcd ± 0.04	1.31 ± 0.01 c	0.24 ± 0.00 b	0.48 ± 0.00 bc	0.56 ± 0.00 b	0.27 ± 0.001 b	0.74 ± 0.01 bc
MA75	0.49 ± 0.01 de	13.95 ± 0.04 d	1.33 ± 0.02 c	1.40 ± 0.01 b	1.52 cd ± 0.002	1.30 ± 0.01 c	0.24 ± 0.00 b	0.47 ± 0.01 c	0.56 ± 0.01 b	0.27 ± 0.00 b	0.73 ± 0.01 c
IN25	0.56 ± 0.01 c	14.57 ± 0.11 b	1.40 ± 0.02 a	1.41 ± 0.04 b	1.37 e ± 0.02	1.30 ± 0.00 c	0.23 ± 0.01 c	0.48 ± 0.01 b	0.54 ± 0.01 cd	0.26 ± 0.01 c	0.64 ± 0.01 e
IN50	0.58 ± 0.01 bc	14.33 ± 0.26 c	1.38 ± 0.01 a	1.37 ± 0.03 b	1.38 e ± 0.02	1.26 ± 0.02 d	0.23 ± 0.00 c	0.49 ± 0.01 b	0.53 ± 0.01 d	0.25 ± 0.02 d	0.66 ± 0.01 e
IN75	0.62 ± 0.02 a	14.45 ± 0.04 bc	1.39 ± 0.02 a	1.37 ± 0.01 b	1.56 b ± 0.02	1.35 ± 0.01 b	0.21 ± 0.01 d	0.44 ± 0.01 d	0.54 ± 0.02 c	0.24 ± 0.01 d	0.69 ± 0.01 d
CH5	0.61 ± 0.03 ab	14.11 ± 0.04 d	1.35 ± 0.02 b	1.28 ± 0.01 c	1.50 d ± 0.02	1.35 ± 0.02 b	0.21 ± 0.01 d	0.44 ± 0.01 d	0.57 ± 0.02 b	0.21 ± 0.01 e	0.66 ± 0.01 e
CH10	0.51 ± 0.01 de	12.07 ± 0.05 e	1.12 ± 0.02 e	1.08 ± 0.03 d	1.14 f ± 0.02	0.81 ± 0.01 e	0.17 ± 0.01 e	0.37 ± 0.01 e	0.33 ± 0.01 e	0.19 ± 0.00 f	0.53 ± 0.01 g
CH15	0.48 ± 0.03 e	11.82 ± 0.12 f	1.11 ± 0.02 e	1.12 ± 0.02 d	1.13 f ± 0.01	0.80 ± 0.02 e	0.17 ± 0.00 e	0.35 ± 0.00 f	0.32 ± 0.01 e	0.16 ± 0.01 g	0.56 ± 0.03 f

[a]Z-2-(β-D-glucopyranosyloxy)-3-phenylpropenoic acid; [b]Phenolic compounds quantified with HPLC-DAD; [c]Means in the same column with the same letter are not significantly different ($P \geq 0.05$); [d]Values in brackets indicate the percentage (m/m) of polymer in the formulation

Table A.2

Flowability according to bulk powder properties as derived from the Hausner ratio (HR) and Carr's compressibility index (C.I.) for green rooibos extract (GRE), and GRE microencapsulated with maltodextrin (MA25, MA50, MA75), inulin (IN25, IN50 and IN75) and chitosan (CH5, CH10, CH15)

Formulation	HR	Value > 1.4 = cohesive Value < 1.25 = free flowing	C.I.	Value < 20 = good flowability Value > 20 = poor flowability
GRE	1.16 ± 0.00 d[a]	free flowing	13.80 ± 0.32 d	good flowability
MA25[b]	1.54 ± 0.08 ab	cohesive	34.85 ± 3.45 ab	poor flowability
MA50	1.45 ± 0.01 bc	cohesive	31.15 ± 0.56 bc	poor flowability
MA75	1.39 ± 0.03 c	cohesive	27.84 ± 1.79 c	poor flowability
IN25	1.59 ± 0.04 a	cohesive	37.26 ± 1.58 a	poor flowability
IN50	1.45 ± 0.03 bc	cohesive	30.82 ± 1.65 bc	poor flowability
IN75	1.36 ± 0.08 c	cohesive	26.57 ± 4.16 c	poor flowability
CH5	1.45 ± 0.06 bc	cohesive	31.09 ± 2.99 bc	poor flowability
CH10	1.46 ± 0.06 bc	cohesive	31.53 ± 2.95 bc	poor flowability
CH15	1.36 ± 0.13 c	cohesive	26.03 ± 7.54 c	poor flowability

[a]Means in the same column with the same letter are not significantly different (P ≥ 0.05); [d]Values in brackets indicate the percentage (m/m) of polymer in the formulation

Table A.3

Average degradation rate constants (K) and adjusted coefficient of determination (R^2_{adj}) of the zero order, first order, second order and fractional conversion models fitted to the experimental data of aspalathin content as monitored for green rooibos extract (GRE), and GRE microencapsulated with maltodextrin (MA25, MA50, MA75), inulin (IN25, IN50 and IN75) and chitosan (CH5, CH10, CH15) exposed to accelerated storage conditions (40°C/75% RH) for 96 h

Formulation	R^2_{adj}			
	Zero order model[a]	First order model[b]	Second order model[c]	Fractional conversion model[d]
GRE	0.8726	0.8917	0.9094	0.9877
MA25[e]	0.8094	0.8256	0.8413	0.9360
MA50	0.7793	0.7924	0.8052	0.8917
MA75	0.7378	0.7616	0.7854	0.9436
IN25	0.8280	0.8493	0.8702	0.9930
IN50	0.8681	0.8841	0.8994	0.9815
IN75	0.8934	0.9054	0.9156	0.9348
CH5	0.7149	0.7400	0.7658	0.9754
CH10	0.7524	0.7810	0.8094	0.9661
CH15	0.7285	0.7558	0.7833	0.9647

[a]Zero order model: $C = C_0 - Kt$; [b]First-order model : $C = C_0\exp(-Kt)$; [c]Second-order model: $C = C_0/(1 + C_0Kt)$; [d]Fractional conversion model: $C = C_\infty + (C_0-C_\infty)\exp(-Kt)$ where C is aspalathin content (g/100 g extract, d.b.), C_0 is initial aspalathin content (g/100 g extract, d.b.), t is the time in minutes and C_∞ the stable fraction of aspalathin (g/100 g extract, d.b.); [e]Values in brackets indicate the percentage (m/m) of polymer in the formulation

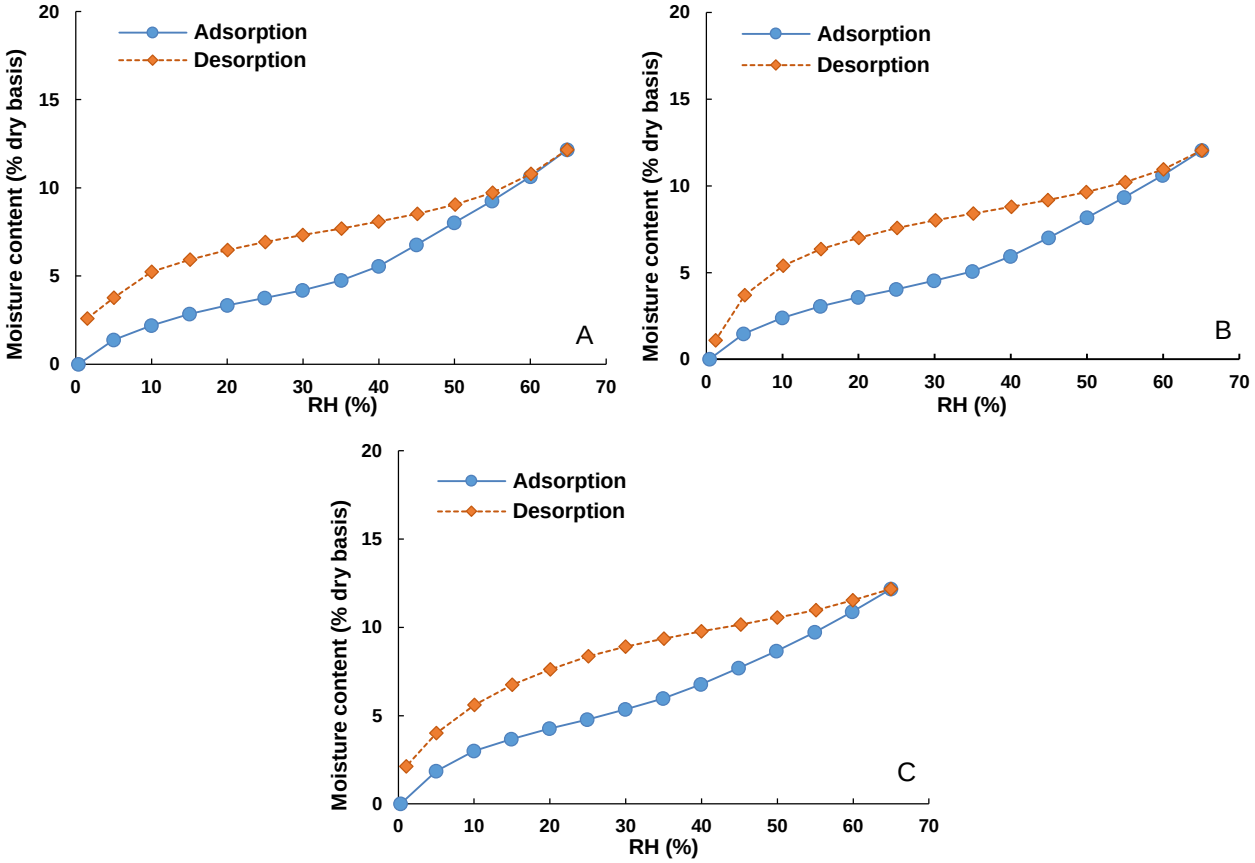

Fig. A.1 Moisture sorption and desorption isotherms obtained at 25 °C for green rooibos extract (GRE) microencapsulated with maltodextrin: (A) MA25, (B) MA50 and (C) MA75. Values indicate the percentage (m/m) of polymer in the formulation.

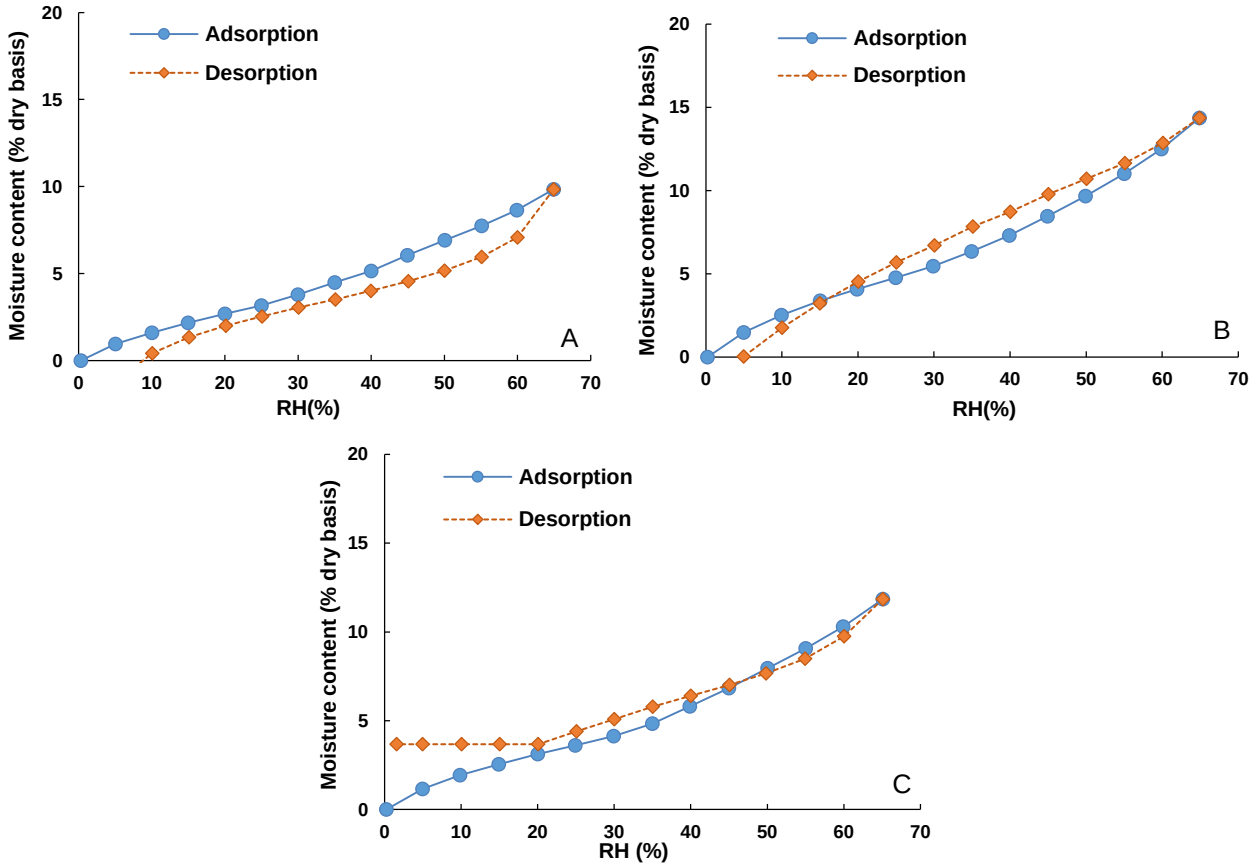

Fig. A.2 Moisture sorption and desorption isotherms obtained at 25 °C for green rooibos extract (GRE) microencapsulated with chitosan: (A) CH5, (B) CH10 and (C) CH15. Values indicate the percentage (m/m) of polymer in the formulation.

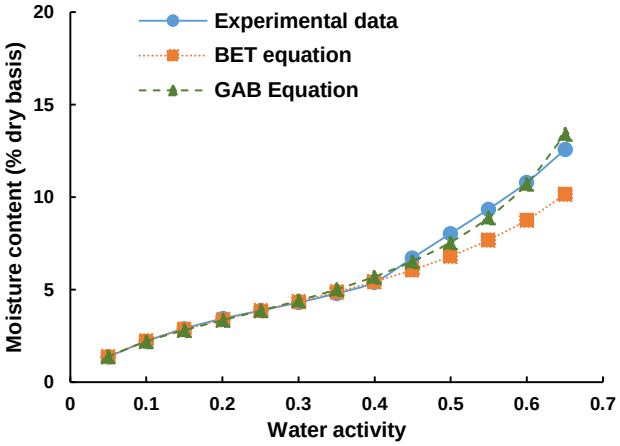

Fig. A.3 Moisture sorption isotherm obtained at 25°C for the green rooibos extract (GRE) fitted with GAB and BET models.

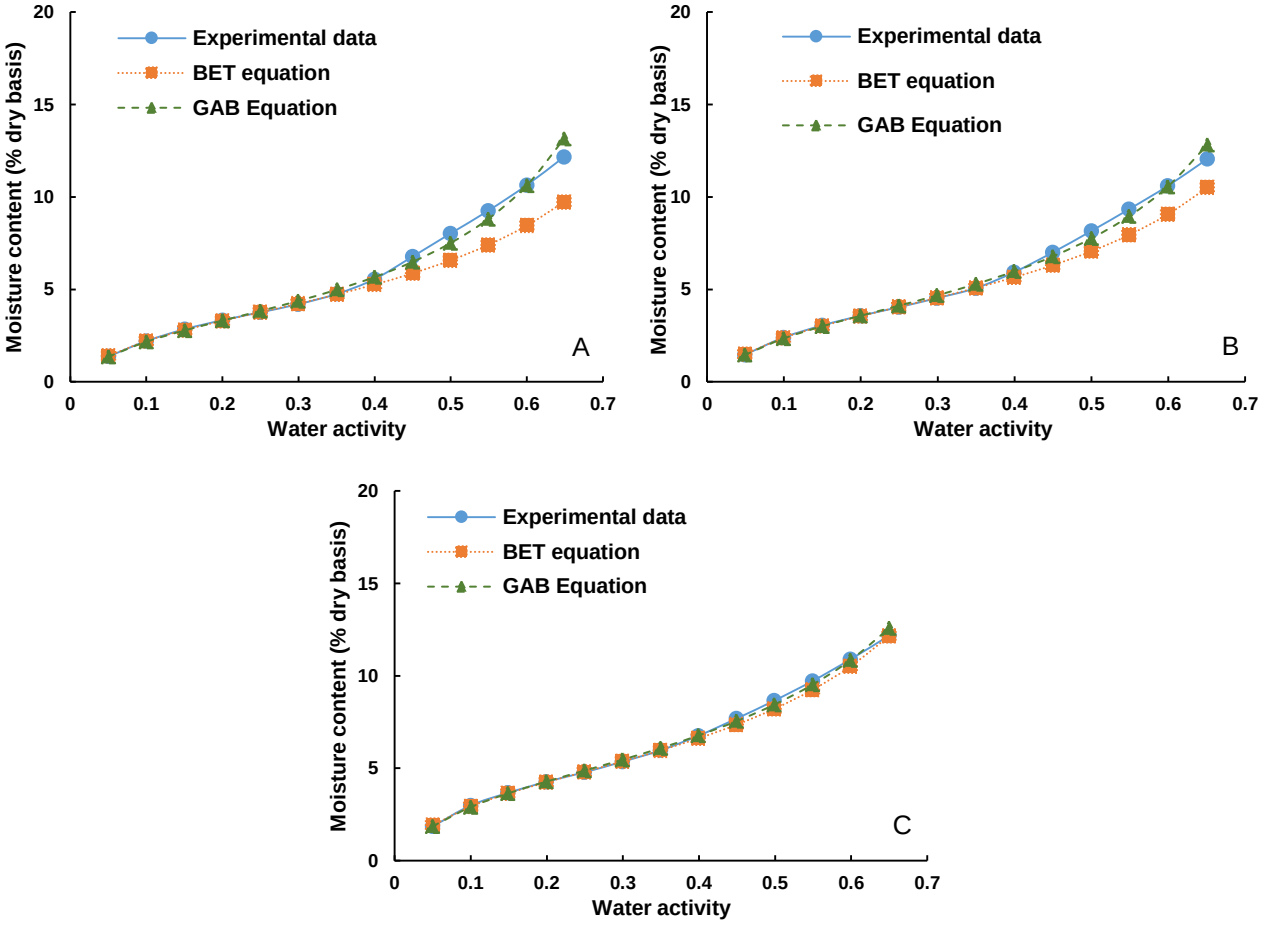

Fig. A.4 Moisture sorption isotherms obtained at 25°C for green rooibos extract (GRE) microencapsulated with maltodextrin: (A) MA25, (B) MA50 and (C) MA75 fitted with the GAB and BET models. Values indicate the percentage (m/m) of polymer in the formulation.

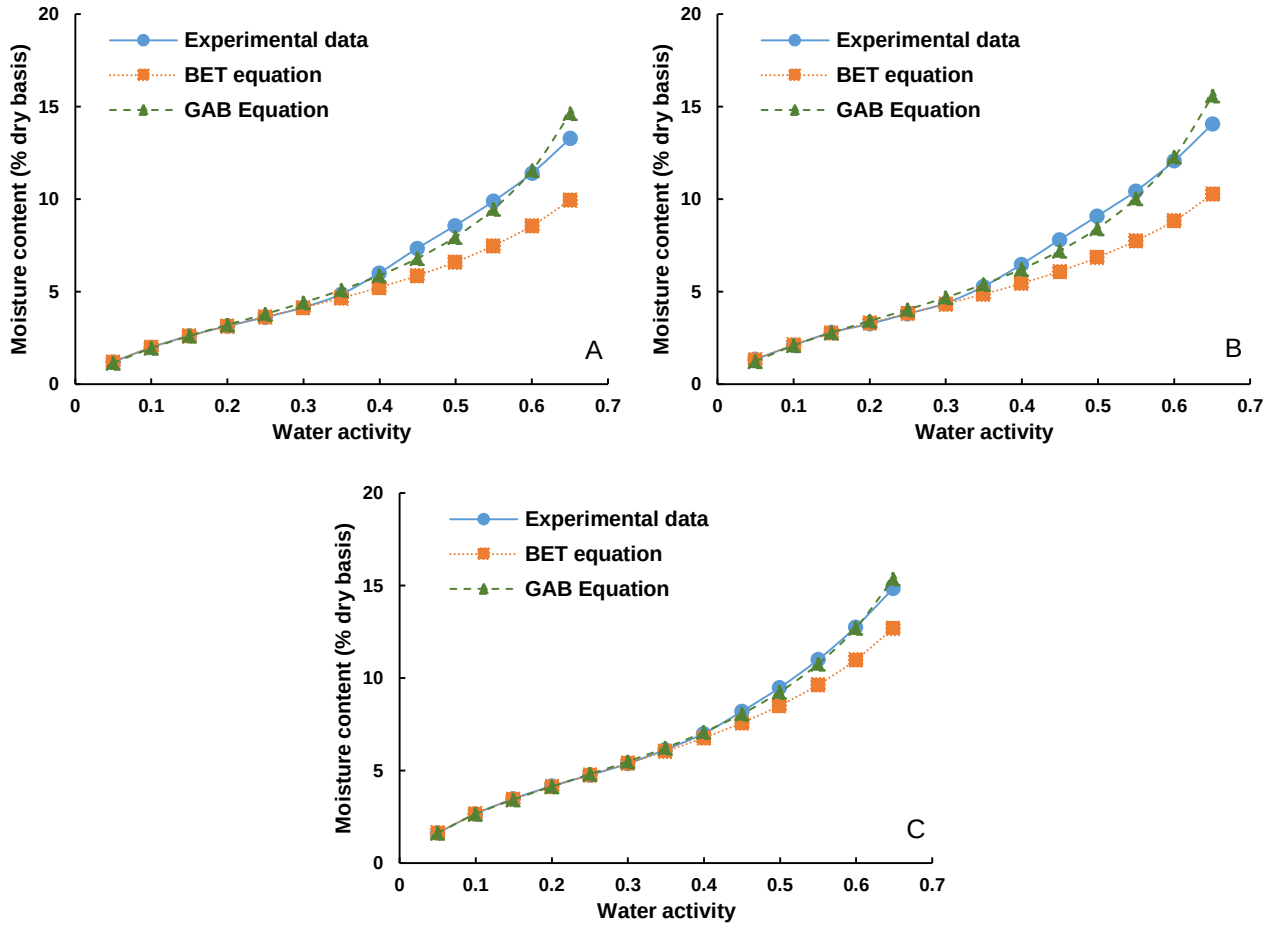

Fig. A.5 Moisture sorption isotherms obtained at 25°C for green rooibos extract (GRE) microencapsulated with inulin: (A) IN25, (B) IN50 and (C) IN75 fitted with the GAB and BET models. Values indicate the percentage (m/m) of polymer in the formulation.

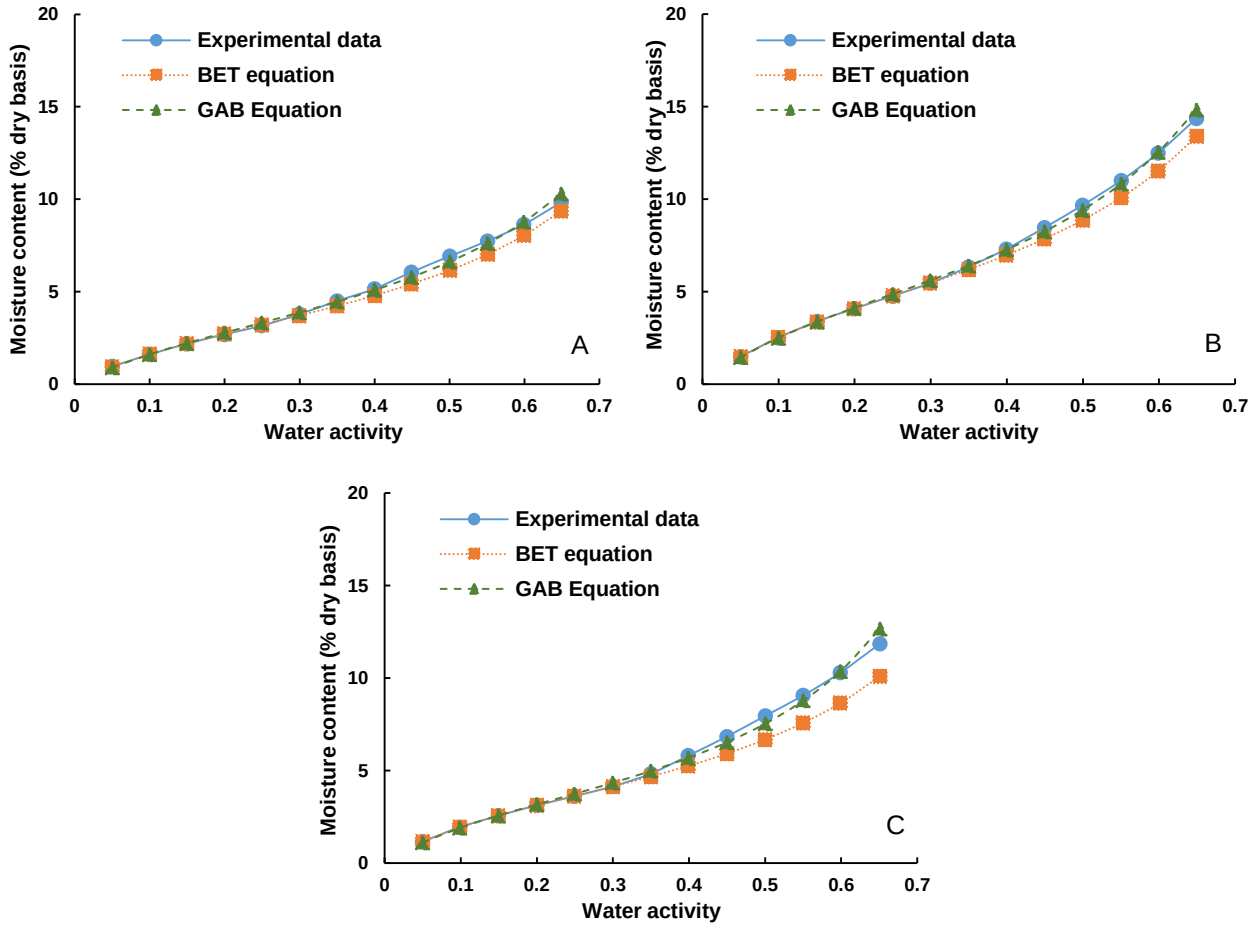

Fig. A.6 Moisture sorption isotherms obtained at 25 °C for green rooibos extract (GRE) microencapsulated with chitosan: (A) CH5, (B) CH10 and (C) CH15 fitted with the GAB and BET models. Values indicate the percentage (m/m) of polymer in the formulation.

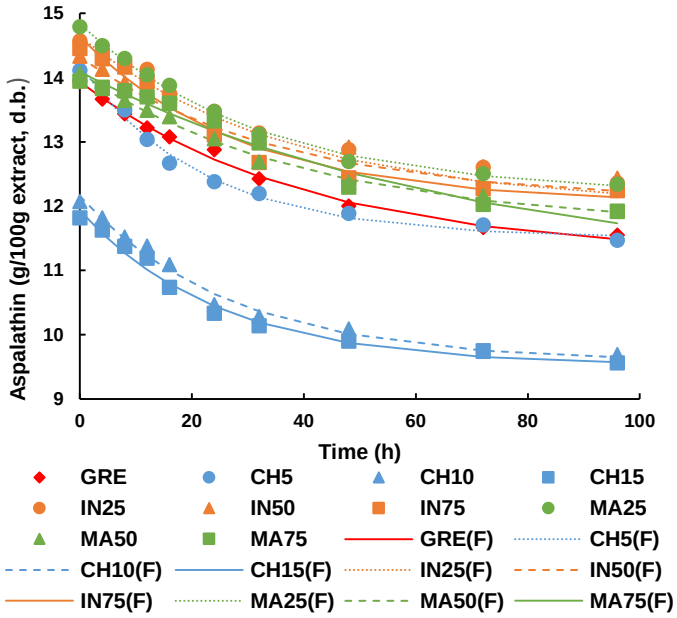

Fig. A.7 Fractional conversion kinetic fitting (indicated by (F)) and experimental data for green rooibos extract (GRE) and GRE microencapsulated with maltodextrin (MA25, MA50 and MA75), inulin (IN25, IN50, IN75) and chitosan (CH5, CH10 and CH15) as a function of storage time at accelerated storage conditions (40°C/75% RH). Values in brackets indicate the percentage (m/m) of polymer in the formulation.

Chapter 4

Shelf-life stability of ready-to-use iced tea powder formulations containing microencapsulated green rooibos extract – effect of common food ingredients and packaging materials

ABSTRACT

The aim of the study was to formulate a shelf-stable green rooibos iced tea powdered product. The effect of common food ingredients (sucrose, xylitol, citric acid and ascorbic acid) and microencapsulation of green rooibos extract with inulin on the physicochemical and dihydrochalcone stability of the formulated powder were investigated for 5 months in semi-permeable packaging and 12 months in impermeable packaging stored at 30 and 40 °C, 65% relative humidity. Pre-screening of the powders revealed minor incompatibilities between ingredients according to isothermal microcalorimetry and high hygroscopicity. Visual inspection revealed clumping and darkening of the formulations after storage, with the effect more pronounced for samples stored at 40 °C in the semi-permeable sachets. Visual changes were correlated to changes in the particulate morphology as imaged with scanning electron microscopy and minor changes in the solid state revealed by X-ray powder diffraction and differential scanning calorimetry. Higher first order reaction rate constants and extent of aspalathin and nothofagin degradation indicated the negative effect of storage at the higher temperature and an increase in moisture content of the formulated powders on phenolic stability. Furthermore, the formulations that contained crystalline ingredients, especially acids, showed decreased chemical stability compared to the green rooibos extract and microencapsulated green rooibos extract. A significant change in the sensory profile of the powders when reconstituted to iced tea solutions were also observed under these extreme conditions. The sensory profile changed to be more similar to that of fermented rooibos. Overall the study indicated that green rooibos powders require storage at lower temperatures (≤ 30 °C) and protection against moisture uptake in order to be shelf-stable and deliver a product with high dihydrochalcone content.

4.1 Introduction

The development of functional food has gained interest in the last decade primarily as a result of its being one of the major categories of the health and wellness market (Khan, Grigor, Winger & Win, 2013). Functional beverages, in particular, offer an excellent means of delivering nutrients and bioactive compounds in a convenient format (Corbo, Bevilacqua, Petruzzi, Casanova & Sinigaglia, 2014). The search for new bioactive compounds, specifically natural, phenolic rich sources and the utilisation of these as nutraceutical ingredients in food products, is rapidly expanding (Bigliardi & Galati, 2013).

In **Chapter 3**, it was shown that inulin (IN), a functional ingredient itself (Dehghan, Gargari & Jafar-Abadi, 2014), is a suitable encapsulating agent for green rooibos extract (GRE) as it not only improved particle morphology and water activity (a_w) of the powder, but also aspalathin retention during spray-drying, similar to that of encapsulation with maltodextrin. Miller, De Beer, Aucamp, Malherbe & Joubert (2018) also showed improved wettability of a similar green rooibos extract-inulin powder, an important factor considering that the product must be reconstituted in water for consumption. Due to its low kilojoule content (65–75% less) (Shoaib *et al.*, 2016), inulin is preferred to maltodextrin, a carbohydrate that is rapidly digested, contributing to increase in postprandial blood glucose levels. This is important in the context of the functionality of aspalathin in relation to diabetes and obesity (Johnson *et al.*, 2018). However, the use of a nutraceutical ingredient, such as aspalathin, in functional beverages poses a challenge due to its sensitivity towards environmental factors. De Beer, Joubert, Viljoen & Manley (2011) demonstrated that extensive aspalathin losses (<80% remaining) occurred during 3 months storage at 25 °C for ready-to-drink (RTD) green rooibos iced teas. In contrast, powdered iced tea formulations, packaged in a single-serve format, could offer both convenience and most likely improved stability of aspalathin due to the low a_w of the powder.

Whilst inulin is compatible with GRE as shown in **Chapter 3**, interaction of other ingredients, although in powder form, could affect stability and shelf-life of the product. Commercially formulated iced tea products generally contain several types of food ingredients and additives such as ascorbic acid, citric acid, fruit juices and chelating agents, amongst others (Chen, Zhu, Tsang & Huang, 2001; Ferruzzi, 2010). Complex formulations such as these can result in a range of physical and chemical interactions, making it essential to consider these effects prior to final formulation and during storage in order to deliver a quality product (Jones & Jew, 2007). Compatibility of ingredients is not a given, as found for catechins in green tea powder (Ortiz, Ferruzzi, Taylor & Mauer, 2008) and phenolic compounds in green honeybush iced tea powders (De Beer *et al.*, 2018), which both showed increased chemical and physical instability with the addition of ingredients such as citric and ascorbic acid. Sucrose is normally used as sweetener of iced tea beverages, including rooibos. To formulate an iced tea powder suitable for diabetics, an alternative sweetener must be used. Xylitol is not

only a suitable sweetener for consumption by diabetics, with its metabolism independent of insulin, but is also considered a prebiotic as reviewed by Ur-Rehman, Mushtaq, Zahoor, Jamil & Murtaza (2015). Furthermore, it has a sweetening power equivalent to sucrose, but has one third of the energy value of sucrose (Ur-Rehman *et al.*, 2015). It should be noted, however, that consumption of xylitol could cause physiological responses (i.e. diarrhoea). Although not recommended for use in beverages, use in coffee and tea, considered to be self-restricted, is condoned as gastrointestinal side effects are negligible (Makinen, 2016). While taking cognisance of the limitation in terms of xylitol consumption, for the purpose of this study, no attempts were made to investigate other sweeteners.

The objectives of the current study were to determine the effect of ingredients on the physical and chemical shelf-life stability of a single-serve green rooibos powdered product containing inulin-microencapsulated GRE as nutraceutical ingredient, suitable for consumption by diabetics. Moisture sorption isotherms and isothermal microcalorimetry compatibility studies were performed to pre-screen the formulations for possible interactions and instabilities. The powdered rooibos formulations were stored at 30°C/65% RH or 40°C/65% RH, in semi-permeable packaging for 5 months and impermeable packaging for 12 months. The aspalathin content, moisture content (MC), a_w, physical appearance, changes in crystalline structure and thermal properties were monitored throughout to test for overall stability during storage. Descriptive sensory analysis (DSA) of a formulation which had poor physical and chemical stability was used to elucidate if changes during storage would have an effect on the sensory profile.

4.2 Materials and methods

4.2.1 Materials

Authentic reference standards for high-performance liquid chromatography (HPLC) analysis, HPLC solvents, water purification systems, IN and GRE are described in **Chapter 3** (section 3.2.1 and 3.2.2). Food grade citric acid monohydrate and ascorbic acid were obtained from Cape Food Ingredients (Westlake, South Africa), xylitol was obtained from Warren Chemicals (Cape Town, South Africa) and sucrose (white sugar, Huletts, Cape Town, South Africa) was purchased from a local supermarket.

4.2.2 Spray-drying and microencapsulation

Spray-drying of GRE and a GRE-IN mixture in a 1:1 (m/m) ratio (IN50) was done on Büchi B-290 mini spray-drier (Büchi Labortechnik AG, Flawil, Switzerland) as described in **Chapter 3** (section 3.2.3).

4.2.3 Preparation of green rooibos powders

A total of 7 formulations, including the controls, GRE and IN50, were prepared. IN50 was used as the rooibos nutraceutical ingredient in all the formulations (Table 4.1). The ratio of the various ingredients were based on a RTD iced tea formulation containing 1.75 g rooibos extract, 60 g sucrose, 1.2 g citric acid and 0.2 g ascorbic acid per liter (Joubert, Viljoen, De Beer & Manley, 2009; Joubert *et al.*, 2010). The amount of xylitol, used instead of sucrose, was adapted in order to maintain a constant final mass of 63.17 g/L powder for F3 to F7 and 1.75 g/L GRE or 3.5 g/L IN50. All the ingredients, except IN50,were ground separately to a fine powder using a Fritsch GmbH Pulverisette ball mill (Idar-Oberstein, Germany) whereafter the powder was sieved to ensure a small particle size (< 210 µm; Endecotts Ltd., London, England). IN50 and the food ingredients were mixed by a tumbling action, using a glass mixing vessel attached to the rotary driving mechanism of a rotary evaporator (Büchi Labortechnik AG).

Table 4.1

Components (%) of green rooibos powders containing GRE[a] or IN50[b] as the nutraceutical ingredient and various food grade ingredients including sugar or xylitol and acids

	Formulations						
Ingredient	GRE	IN50	F[c]3	F4	F5	F6	F7
GRE	100.00	0.00	0.00	0.00	0.00	0.00	0.00
IN50	0	100.00	5.54	5.54	5.54	5.54	5.54
Sucrose	0.00	0.00	94.46	0.00	0.00	0.00	0.00
Xylitol	0.00	0.00	0.00	94.46	92.58	94.15	92.26
Ascorbic acid	0.00	0.00	0.00	0.00	0.00	0.31	0.31
Citric acid	0.00	0.00	0.00	0.00	1.89	0.00	1.89
Total (%)	100.00	100.00	100.00	100.00	100.00	100.00	100.00

[a]Spray-dried green rooibos extract; [b]Green rooibos extract encapsulated with inulin in 1:1 ratio (m/m) by spray-drying; [c]Formulation

4.2.4 Storage stability testing and kinetic modelling of aspalathin and nothofagin degradation

Each formulation was weighed (*ca.* 500 mg) into sachets and glass vials. The sachets, produced from 12 µm metalised polyethylene terephthalate (MET/PET) film and a 50 µm linear low density polyethylene (LLDPE) film attached with a layer of adhesive) are semi-permeable (0.4% transmission of moisture vapour measured as g/m^2 in 24 h (Anonymous, 2018), while the sealed glass vials (5 mL amber screw cap vials, tightly sealed with PTFE caps) simulated impermeable packaging as would be provided by three layer (e.g. polyester film/aluminium foil/LDPE) type sachets with minimal to no transmission of moisture vapour (0.01%) (Anonymous, 2018). Storage conditions were set at 30 °C/65% RH and 40 °C/65% RH in temperature and humidity controlled cabinets (SMC Scientific Manufacturing cc., Table View, South Africa). The viewing windows of the cabinets were blocked with non-transparent material to eliminate the effect of light. Three

separate replicates (n = 3) of each formulation (n = 7), packed in both the sachets and vials, were added for each sampling time point (n = 9) at the different storage conditions (n = 2). Samples stored in the sachets were removed weekly for the first three intervals and thereafter monthly up to 5 months. Samples stored in the vials were removed at monthly intervals up to 6 months and every 3 months thereafter up to 12 months.

The phenolic content of the powder formulations were monitored quantitatively throughout the storage by HPLC-diode array detection (DAD) according to a method previously reported (Walters, De Villiers, Joubert & De Beer, 2017). The dihydrochalcones, aspalathin and nothofagin, were used as marker compounds to track stability. Various regression models were fitted to the data and the first order model (Van Boekel, 2008; Wibowo, Grauwet, Gedefa, Hendrickx & Van Loey, 2015) selected to quantify the effect of storage on the dihydrochalcone content in terms of degradation rate and final content in the formulation (Eq. 4.1):

$$C = C_0 e^{-Kt} \quad (4.1)$$

where C is aspalathin/nothofagin content (g/100 g extract, dry basis (d.b.)), C_0 is initial aspalathin/nothofagin content (g/100 g extract, d.b.), t is the time in months and K is the reaction rate constant.

4.2.5 Physicochemical analysis

For pre-screening of the powder formulations, moisture sorption isotherms (MSI's), MC and a_w were determined. Isothermal microcalcorimetry was used to detect incompatibilities between IN50 and the other ingredients. X-ray powder diffraction (XRPD) and differential scanning calorimetry (DSC) were used to analyse the food ingredients and the formulations before and after storage. Particle morphology of the powder formulations was determined by scanning electron microscopy (SEM) imaging before and after storage. All experimental and instrument details are described in **Chapter 3**, sections 3.2.4.2–3.2.4.3 and 3.2.4.5–3.2.4.8.

4.2.6 Descriptive sensory analysis

DSA was used to establish the effect of storage on the sensory profile of the formulation showing major physical and chemical changes during storage.

4.2.6.1 Reference standards

The reference samples for panel training included green rooibos plant material (Rooibos Ltd, Clanwilliam, South Africa), semi-fermented rooibos plant material (green rooibos plant material fermented for 1 h at 37°C and dried at 40°C for 16 h) and fermented rooibos plant material (Rooibos Ltd, Clanwilliam, South Africa), extracted with deionised water (3 g/mL) at 93°C for 40 min based on Miller, De Beer & Joubert (2017). The

extracts were allowed to cool overnight and served at ambient temperature (± 21°C) during the respective training sessions. The range of rooibos reference samples was chosen to represent the full spectrum of aroma attributes that associate with the reconstituted green rooibos powders and oxidised rooibos. Additionally, xylitol (58 g/L deionised water) was used as a reference standard for 'synthetic' sweet aftertaste and citric acid (1.2 g/L deionised water) for sour taste.

4.2.6.2 Reconstituted green rooibos iced tea samples

F5 containing IN50, xylitol and citric acid was prepared, packed in sachets and vials and stored at 30°C and 40°C/65% RH for 1 month as previously described (sections 4.2.3 and 4.2.4). A sample that was not stored was freshly prepared on each day of the testing and served as control. Six repetitions of each formulation were prepared and stored. Prior to training and testing, the powder formulations were reconstituted in deionised water at 63 g/L and *ca.* 70 mL served in standard ISO wine tasting glasses covered with a plastic lid at ambient temperature (± 21°C).

4.2.6.3 Training and testing phases

The panel consisting of 12 female judges with extensive training in descriptive sensory analysis (DSA) developed a standard profiling technique During five one-hour training sessions, the panel came to a consensus on the range of orthonasal aroma, retronasal aroma, taste, mouthfeel and aftertaste descriptors (Table 4.2) illustrating the sensory profile of the respective samples. The rooibos lexicon developed by Koch, Muller, Joubert, Rijst & Næs (2012) was used as basis and definitions were adjusted where necessary.

The full sample set (n = 5) was tested during each session, with 2 sessions per day over 3 days. All the testing sessions were conducted in individual tasting booths. Samples were labelled with three-digit codes and presented in a complete randomised order, specific to each panellist. The sample not subjected to storage was additionally served as a control sample and labelled as such for each panellist. The relevant attributes were scored on an unstructured scale from 0 (not detected) to 100 (extremely high intensity) for each sample. Scoring data were captured with Compusense® *five* software (Compusense, Guelph, Canada). The data of all the panellists were subjected to statistical analysis (section 4.2.7.2) to test panel reliability.

4.2.6.4 pH and objective colour measurement

The pH of each sample was measured using a Crison GLP 21 pH meter (Crison Instruments SA, South Africa), standardised with buffer references (pH 7 ± 0.01 and pH 4 ± 0.01 at 25°C). CIE L*a*b* objective colour measurements of the solutions were performed using a Konica Minolta CM-5 spectrophotometer (Osaka,

Japan). L*, a* and b* values of the reconstituted iced tea powders were measured in transmittance mode in 10 mm plastic cuvettes (Greiner Bio-one, Monroe, USA). Auto-calibration was achieved with a black calibration plate (0% calibration) and a cuvette filled with deionised water (100% calibration). The difference in colour (ΔE) of samples before and after storage was calculated using Eq. 4.2:

$$\Delta E = \sqrt{(L_2^* - L_1^*)^2 + (a_2^* - a_1^*)^2 + (b_2^* - b_1^*)^2} \quad (4.2)$$

where subscript 1 and 2 refer to values before and after storage, respectively.

Table 4.2

Sensory attributes used during descriptive analysis of reconstituted green rooibos powder formulation F5[a] before and after storage for 1 month at 30°C/65% RH and 40°C/65% RH in sealed glass vials and semi-permeable sachets

Attributes	Descriptions
Rooibos-woody aroma	Aromatics associated with dry bushes, stems and twigs of fermented rooibos herbal tea
Apple aroma	Sweet aromatics associated with apple pie or cooked apples
Fruity-sweet aroma	Aromatics associated with sweet/sour smell of non-specific fruit
Honey aroma	Aromatics associated with fragrance of fynbos honey or *Alyssum* blossoms
Hay dried grass aroma	Slightly sweet aroma associated with dried grass or hay
Grainy aroma	Aroma of grains, porridge or dog pellets
Seaweed aroma	Aromatics associated with seaweed lying in the sun, fishy aroma/flavour of omega-3 oil
Rubber-putty-like aroma	Aromatics associated with Band-aid®, rubber or putty
Dusty aroma	Earthy aromatics associated with dry dirt roads
Sweet taste	Fundamental taste of sucrose
Sour taste	Fundamental taste of citric acid
Bitter taste	Fundamental taste of caffeine
Astringent mouthfeel	Dry puckering feeling/sensation on the tongue and other mouth surfaces
Synthetic sweet aftertaste	A lingering, synthetic sweet taste

[a]Contains green rooibos extract microencapsulated with inulin in a 1:1 ratio (m/m), xylitol and citric acid

4.2.7 Statistical procedures

4.2.7.1 Rooibos powder and stability data analysis

The experimental design employed in the study was completely random with three independently replicated experiments for each formulation, namely GRE, IN50, F3, F4, F5, F6 and F7. Univariate analysis of variance (ANOVA) was performed on all observed variables to compare the formulations, using the GLM (General Linear Models) procedure of SAS software (Version 9.4; SAS Institute Inc, Cary, USA).

For assessment of dihydrochalcone stability during shelf-life trials, aspalathin and nothofagin contents were determined for samples subjected to different storage times. Non-linear regression analysis with time as independent variable was performed to describe aspalathin and nothofagin degradation over time, using the

NLIN procedure of SAS. Zero, first, second order and fractional conversion regression models were fitted for each experimental replicate. The regression parameters obtained for the first order regression model were used as input for ANOVA to test for the formulation effect on the model parameters. A split-plot analysis of variance with sample formulation as main plot factor and time as sub-plot factor was performed. Data were tested for normality using the Shapiro-Wilk test. Fisher's least significant difference (LSD) was calculated at the 5% level to compare means. $P < 0.05\%$ was considered significant.

4.2.7.2 Sensory analysis data

In a similar fashion, ANOVA, the Shapiro-Wilk test and Fisher's LSD were conducted using the DSA data representing 5 samples (F5 stored under different conditions), 12 judges and 6 replicate sessions. Principal component analysis (PCA), based on the correlation matrix, was also conducted using XLStat software (Addinsoft, France) to visualise and elucidate the relationships between the samples and their attributes (Næs, Brockhoff & Tomic, 2010).

4.3 Results and discussion

4.3.1 Selection of ingredients

Formulation of the green rooibos iced tea powders containing inulin-microencapsulated GRE as the nutraceutical ingredient was guided by the common food ingredients present in RTD fermented (Joubert *et al.*, 2009) and green (Joubert *et al.*, 2010) rooibos iced teas such as a sweetener, citric acid as major acidifier and ascorbic acid as antioxidant. The xylitol content in F5–F7 was slightly varied to accommodate the small quantities of citric acid and ascorbic acid, while keeping the amount of IN50 and thus also GRE constant in the formulated powders.

Xylitol was used as an alternative sweetener to sucrose in accordance with the strategy of the National Department of Health to reduce excessive sugar intake by the South African population in an effort to reduce obesity (Benade & Essop, 2017). Polyols such as xylitol have become increasingly important in the food, nutraceutical and pharmaceutical industries due to their lower energy value compared to sucrose (10.0 vs 16.7 kJ/g), but nearly similar sweetness (Islam, 2011). Gastrointestinal disturbances caused by xylitol have been shown. However, consumption of 20 g xylitol in a single oral bolus dose in a liquid, such as 330 mL of iced tea, is not expected to lead to gastrointestinal disturbances according to Storey, Lee, Bornet & Brouns (2007). In addition, for the α-glucosidase inhibition of green rooibos to be effective, the beverage should be consumed with a meal, further reducing gastrointestinal disturbance (Makinen, 2016). Another consideration when

incorporating a substance such as xylitol into a food formulation is the necessity to investigate its effect on the stability of the active ingredient compared to sucrose (Talja & Roos, 2001). One formulation (F3) contained sugar instead of xylitol and no citric or ascorbic acid to allow direct comparison with xylitol (F4) (Table 4.1).

4.3.1.1 Compatibility of food ingredients with IN50

Isothermal microcalorimetry was used to assess the compatibility of the ingredients in the formulated powders, where differences in the heat flow indicated incompatibility and interaction between ingredients (Chadha & Bhandari, 2004). The difference between the average interaction heat flow values as obtained from the iced tea powder formulations and theoretical non-interaction curve as obtained from the individual ingredients was used to indicate possible incompatibilities between IN50 and other ingredients (expressed as interaction average heat flow error; Table 4.3 and Supplementary material, Fig. B.1). All the interaction values were below 10 µW/g which, as a rule of thumb, indicates a low possibility of incompatibility and interaction of ingredients (Schmitt, Peck, Sun & Geoffroy, 2001). The interaction heat flow errors for F3 and F5–7 (3.13 to 4.85 µW/g) were very similar and slightly lower for F4 (1.29 µW/g), which contained only IN50 and xylitol. These results indicated a mixture of IN50 and xylitol will be the most compatible and stable during storage, while addition of citric acid and ascorbic acid could decrease the physical stability of the formulation.

Table 4.3

Interaction average heat flow values and errors obtained from isothermal microcalorimetry for green rooibos powders

Formulations	Interaction average heat flow (µW/g) (absolute values)[a]	Interaction average heat flow error (µW/g) (absolute values)[b]
F3[c]	3.65	4.90
F4[d]	0.90	1.29
F5[e]	4.10	4.85
F6[f]	1.38	3.13
F7[g]	1.23	3.45

[a]Heat flow of actual rooibos powder formulations measured at 40 °C; [b]Difference between the heat flow of actual the rooibos powders and the theoretical zero interaction curve of the ingredients; [c]Formulation 3 (IN50 and sucrose); [d]Formulation 4 (IN50 and xylitol); [e]Formulation 5 (IN50, xylitol and citric acid); [f]Formulation 6 (IN50, xylitol and ascorbic acid); [g]Formulation 7 (IN50, xylitol, citric acid and ascorbic acid); IN50 - green rooibos extract microencapsulated in 1:1 (m/m) ratio with inulin

4.3.1.2 MSI's

MSI's were used to describe the relationship between the MC and a_w of the formulations. The MSI's could be classified as type II isotherms typical of food products as described by Brunauer, Deming & Teller (1940) (Fig. 4.1). Type II isotherms were also observed for the amorphous spray-dried powders in **Chapter 3**. Addition of deliquescent crystalline ingredients (sucrose, xylitol and acidifiers) to the amorphous IN50 did not change the isotherm type, but changed its MSI. The addition of crystalline sugar or xylitol to IN50 substantially reduced

the MC (up to 10 x) of the powder at the same a_w, as well as reduced the hysteresis loop (F3 and F4). Little difference in the MSI's could be seen between powders containing sucrose (F3) or xylitol (F4). The addition of ascorbic acid (F6) had little effect on the MSI of F4, whereas the addition of citric acid increased the hysteresis loop and moisture uptake (F5 and F7).

Crystalline substances have highly ordered structures that restrict molecular mobility and minimise free volume between molecules, allowing only minimal water uptake on the surface when kept below deliquescence RH (RH_0) (Thorat *et al.*, 2017), explaining the substantially lower MC's for F3–F7 compared to IN50 alone. Hysteresis arises from physical changes in the powders, which expose new sites able to absorb moisture as the a_w decreases in the desorption curve (Caurie, 2007). Hysteresis can be used as a measure of food quality (Caurie, 2007), as it indicates that exposure to moisture will result in permanent physical changes (Al-Muhtaseb, McMinn & Magee, 2002; Raji & Ojediran, 2011) and affect shelf-life stability. As per this explanation, the addition of sucrose and xylitol will have a positive effect on the shelf-life of IN50, whereas the addition of citric acid will affect the shelf-life negatively. The effects of citric acid monohydrate, as used in this study is discussed in later sections.

Additionally, a sharp increase in adsorption was observed for F5 and F7 at *ca.* 50% RH, evident of deliquescence (Salameh, Mauer & Taylor, 2006) and a lower RH_0 compared to IN50 and the other formulations which do not show clear evidence of deliquescence in the experimental RH range. Lowering of RH_0 is not uncommon for certain combinations of crystalline and amorphous ingredients (Salameh & Taylor, 2006b; Kwok, Mauer & Taylor, 2010; Allan & Mauer, 2016) and usually results in earlier onset of unwanted chemical and physical changes as water is more rapidly absorbed after RH_0 is reached (Hiatt, Taylor & Mauer, 2011).

The MSI adsorption data were fitted to the Guggenheim-Anderson-de Boer (GAB) and Brunauer-Emmet-Teller (BET) adsorption models. The BET model is only valid for $0.05 < a_w < 0.35$ (Al-Muhtaseb *et al.*, 2002) and was therefore only fitted for a_w levels ≤ 0.3 (Table 4.4 and Supplementary material Fig. B.2). Over these low a_w levels the BET model provided a better fit than the GAB model. The calculated monolayer moisture content values (M_0) were between 0.23–0.26% (d.b.), and were lower than the actual a_w (0.29–0.33) values of the formulations (Table 4.4). M_0 values were higher than a_w values of GRE and IN50 (Data pertaining to GRE and IN50 are available in **Chapter 3**, section 3.3.4). The M_0 values provide an indication of water strongly bound to the hydrophilic surface sites (Gabas, Telis, Sobral & Telis-Romero, 2007) and when higher than the a_w, water is more available for chemical reactions and will most likely adversely affect the stability of the product (De Souza, Thomazini, Balieiro & Fávaro-Trindade, 2015). For a shelf-stable product, the MC must be lower than the predicted M_0 (Labuza & Altunakar, 2007). This is not the case for the iced tea powders F3 to F7,

indicating potential instability during storage due to the ingredients. Practically, these results emphasises the importance of protection against changes in humidity during storage and handling of the powders.

Table 4.4

Moisture content (MC), water activity (a_w) and parameters for Guggenheim-Anderson-de Boer (GAB) and Brunauer-Emmet-Teller (BET) models fitted to moisture adsorption data obtained at 25°C for green rooibos powders

Formulation	MC[a]	a_w[b]	Parameters of GAB model				Parameters of BET model		
			M_0[c]	C[d]	K[d]	R^2	M_0	C	R^2
F3[f]	0.657 ± 0.035 a[e]	0.290 ± 0.013 b	0.178	11.11	1.05	0.7799	0.224	7.09	0.9743
F4[g]	0.347 ± 0.035 b	0.323 ± 0.011 a	0.148	12.54	1.41	0.7745	0.263	5.47	0.9733
F5[h]	0.487 ± 0.012 ab	0.321 ± 0.010 a	0.154	11.67	1.41	0.7877	0.244	6.69	0.9955
F6[i]	0.515 ± 0.012 ab	0.322 ± 0.022 a	0.184	11.09	1.15	0.7989	0.240	7.42	0.9721
F7[j]	0.593 ± 0.016 a	0.333 ± 0.004 a	0.154	10.00	1.41	0.7287	0.255	5.65	0.9849

[a]Moisture content (% d.b.); [b]Water activity measured at 25°C; [c]M_0 = monolayer moisture content (% d.b.); [d]C and K = constants in BET and/or GAB adsorption model; [e]Means in the same column with the same letter are not significantly different ($P \geq 0.05$); [f]Formulation 3 (IN50 and sucrose); [g]Formulation 4 (IN50 and xylitol); [h]Formulation 5 (IN50, xylitol and citric acid); [i]Formulation 6 (IN50, xylitol and ascorbic acid); [j]Formulation 7 (IN50, xylitol, citric acid and ascorbic acid); IN50 – green rooibos extract microencapsulated with inulin in 1:1 (m/m) ratio

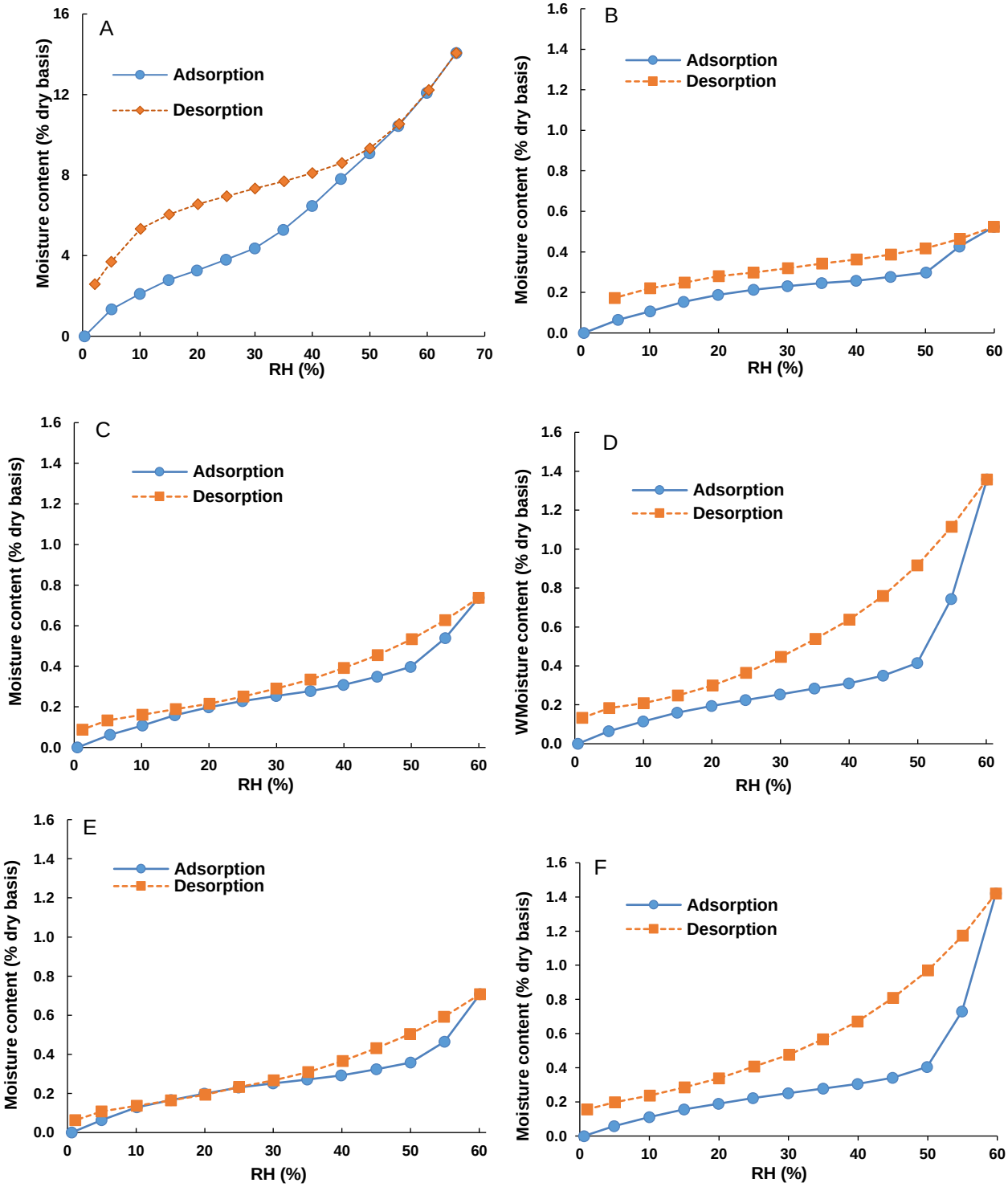

Fig. 4.1 Moisture adsorption and desorption isotherms of green rooibos powders at 25 °C: (A) IN50 (green rooibos extract microencapsulated with inulin in 1:1 (m/m) ratio), (B) F3 (IN50 and sucrose), (C) F4 (IN50 and xylitol), (D) F5 (IN50, xylitol and citric acid), (E) F6 (IN50, xylitol and ascorbic acid) and (F) F7 (IN50, xylitol, ascorbic and citric acid).

4.3.2 Physical changes of powder formulations during storage

GRE, subjected to shelf-life stability trials at 30 and 40 °C (65% RH), showed clumping and slight discoloration after 12 months when stored in glass vials. Discolouration was extensive after 5 months when

GRE was stored in semi-permeable sachets at 40 °C/65% RH (Table 4.5). Clumping of IN50 also occurred, but discolouration of the powder was slightly less, most likely due to the "dilution" effect of IN. The change in physical appearance of GRE and IN50 stored in the sachets was accompanied by a complete collapse of the particulate morphology into a sheet-like morphology (Fig. 4.2) and a significant increase in moisture content (Fig. 4.3), partially responsible for the drastic change in physical appearance. Additionally, IN50 showed evidence of crystallisation as evident from the sharp peaks on the X-ray powder diffractogram (Fig. 4.4).

Of interest is the effect of the other food ingredients as they affected the extent to which changes in the physical appearance of the powder occurred (Table 4.5). Powders packed in the glass vials showed no or little obvious physical changes after 12 months, irrespective of storage temperature (Table 4.5). F5 and F7, the only formulations that contained citric acid showed some evidence of discolouration (browning) and clumping when stored at 40 °C. No increase in the MC of the powder was observed, as would be expected for an impermeable packaging material, except for a slight increase which occurred in the first month of storage (Supplementary material, Fig. B.3). This increase could be attributed to equilibration reached between moisture trapped in the head space of the vials and the powders.

The appearance of the powders packed in semi-permeable sachets, especially when stored at 40 °C, changed substantially (Table 4.5) and the SEM images revealed the formation of large and distorted particles (Fig. 4.2), evident after only 5 months. Replacement of sugar (F3) with xylitol (F4) resulted in clumping and slight browning, as well as higher MC (1.04% vs 1.25%) and a_w (0.48 vs 0.54) values after 5 months at 40 °C, respectively (Fig. 4.3). This was to be expected, given their respective MSI's where exposure to 60% RH produced powders with MC's of 0.52% and 0.73% when sugar (F3) and xylitol (F4), respectively, were added to IN50 (Fig. 4.1). Addition of citric acid resulted in more pronounced browning and clumping (F5 and F7). Not only were the prominent changes observed for F5 accelerated by the higher storage temperature, but its large hysteresis loop (Fig. 4.1) and a significant increase in MC (from 0.49% to 3.58%) and a_w (0.32 to 0.79) (Fig. 4.3) over 5 months at 40 °C indicated lower stability (Caurie, 2007). Addition of ascorbic acid to the IN50 and xylitol mixture (F6) minimally decreased the slight discolouration observed for F4, thus offering some protection to polyphenols (e.g. aspalathin) against oxidative browning. The final MC after 5 months at 40 °C were similar for F6 and F4 (1.25% vs 1.26%, Fig. 4.3) as predicted by very similar MSI's (Fig. 4.1).

Natural extracts, such as GRE, are prone to oxidation and hydrolysis that result in colour changes (Cortés-Rojas & Oliveira, 2012). Heinrich, Willenberg & Glomb (2012) showed that aspalathin in solution under oxidative conditions forms a brown product, explaining the darkening of some of the powders. These colour changes were attributed to dibenzofurans formed by non-enzymatic oxidation of aspalathin. The colour change was most pronounced for GRE and IN50 that contain ≥ 50% GRE. These type of reactions are often

accelerated by the presence of moisture and temperature (Bott, Labuza & Oliveira, 2010), which explains the extreme changes in colour and formation of clumps observed for the formulations stored at 40 °C in the semi-permeable sachets compared to the sealed glass vials. However, the oxidation process can be slowed by the addition of antioxidants such as ascorbic acid, as shown by slightly less discolouration of F6 compared to F4. Furthermore, citric acid monohydrate is thermodynamically unstable at relatively low temperature and humidity (25 °C, < 65% RH) and is deliquescent in higher RH environments, where the transition from monohydrate to anhydrous citric acid occurs at *ca.* 36.3 °C (Sun, 2009; Apelblat, 2014). Thus, the addition of citric acid could introduce more moisture and higher instability as demonstrated for F5 and F7.

The observed visual changes of the powders stored in the sachets and at the higher temperature were highlighted by fusing, enlargement and more irregular shaped particles attributed to hydration (Sun, 2009) (Fig. 4.2). Combining and disappearance of peaks in the XRPD diffractograms of F3–F7 (Fig. 4.4) and the occurrence of crystallisation of IN50 for the samples stored in the sachets at 40 °C further support physical changes. Additionally, changes in peak shape and intensities in the DSC thermograms (Fig. 4.5) indicate subtle changes in the molecular rearrangement of IN50 and crystal structures of F3–F7. In the case of amorphous materials such as IN50, moisture acts as a plasticiser, leading to increased molecular mobility and lowering of the glass transition temperature (T_g), which results in crystallisation as excess adsorbed water is desorbed during storage (Bott *et al.*, 2010; Saffari & Langrish, 2014). In the case of deliquescent crystalline formulations (F3–F7), the powders have the ability to partially dissolve and recrystallize, which results in the formation of co-crystal structures (Jayasankar, Good & Rodríguez-Hornedo, 2007), distorted crystal structures (Lafontaine, Sanselme, Cartigny, Cardinael & Coquerel, 2012; Tham, Wang, Yeoh & Zhou, 2016) and the formation of liquid bridges between crystals (Salameh & Taylor, 2006a; Stoklosa, Lipasek, Taylor & Mauer, 2012). The rate of these effects is increased at higher temperatures and in the presence of moisture when more energy is available for molecular motion (Wahl *et al.*, 2008; Mauer & Taylor, 2010; Tham *et al.*, 2016).

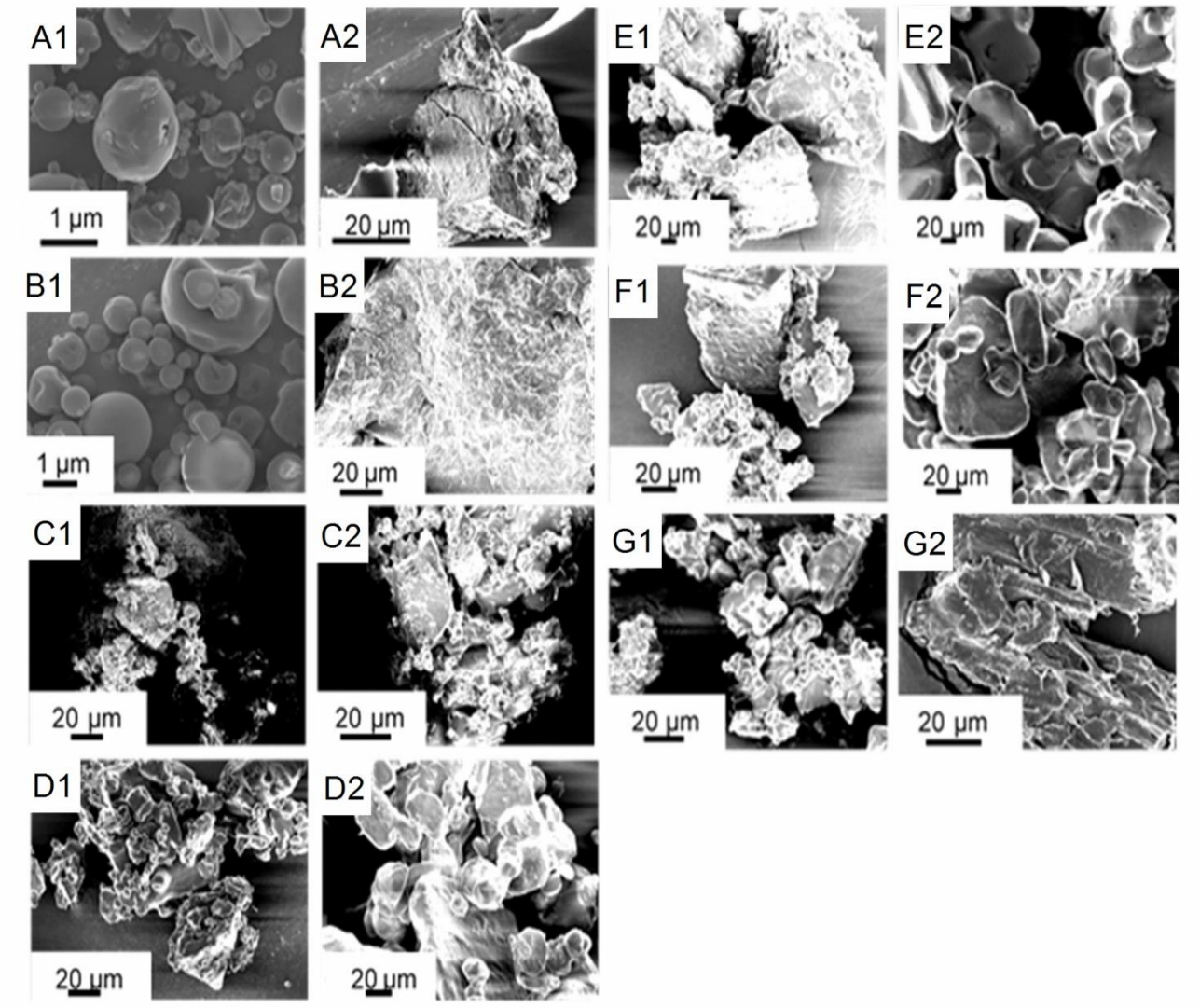

Fig. 4.2 SEM images of green rooibos powders: (A) green rooibos extract (GRE), (B) GRE microencapsulated with inulin in 1:1 ratio (m/m) (IN50) and formulations (C) F3 (IN50 and sucrose), (D) F4 (IN50 and xylitol), (E) F5 (IN50, xylitol and citric acid) and (F) F6 (IN50, xylitol and ascorbic acid), (G) F7 (IN50, xylitol, citric acid and ascorbic acid) (1) before storage and (2) after storage at 40 °C/65% RH for 5 months in semi-permeable sachets.

Table 4.5

Change in visual appearance of the green rooibos powders before and after storage at 30°C/65% and 40°C/65% RH for 12 months in sealed glass vials and 5 months in semi-permeable sachets

Formulation	Before storage	After storage			
		Vials (12 months)		Sachets (5 months)	
		30°C	40°C	30°C	40°C
GRE[a]					
IN50[b]					
F3[c]					
F4[d]					
F5[e]					
F6[f]					
F7[g]					

[a]Green rooibos extract; [B]GRE microencapsulated with inulin in 1:1 ratio (m/m); [c]Formulation 3 (IN50 and sucrose); [d]Formulation 4 (IN50 and xylitol); [e]Formulation 5 (IN50, xylitol and citric acid); [f]Formulation 6 (IN50, xylitol and ascorbic acid); [g]Formulation 7(IN50, xylitol, citric acid and ascorbic acid)

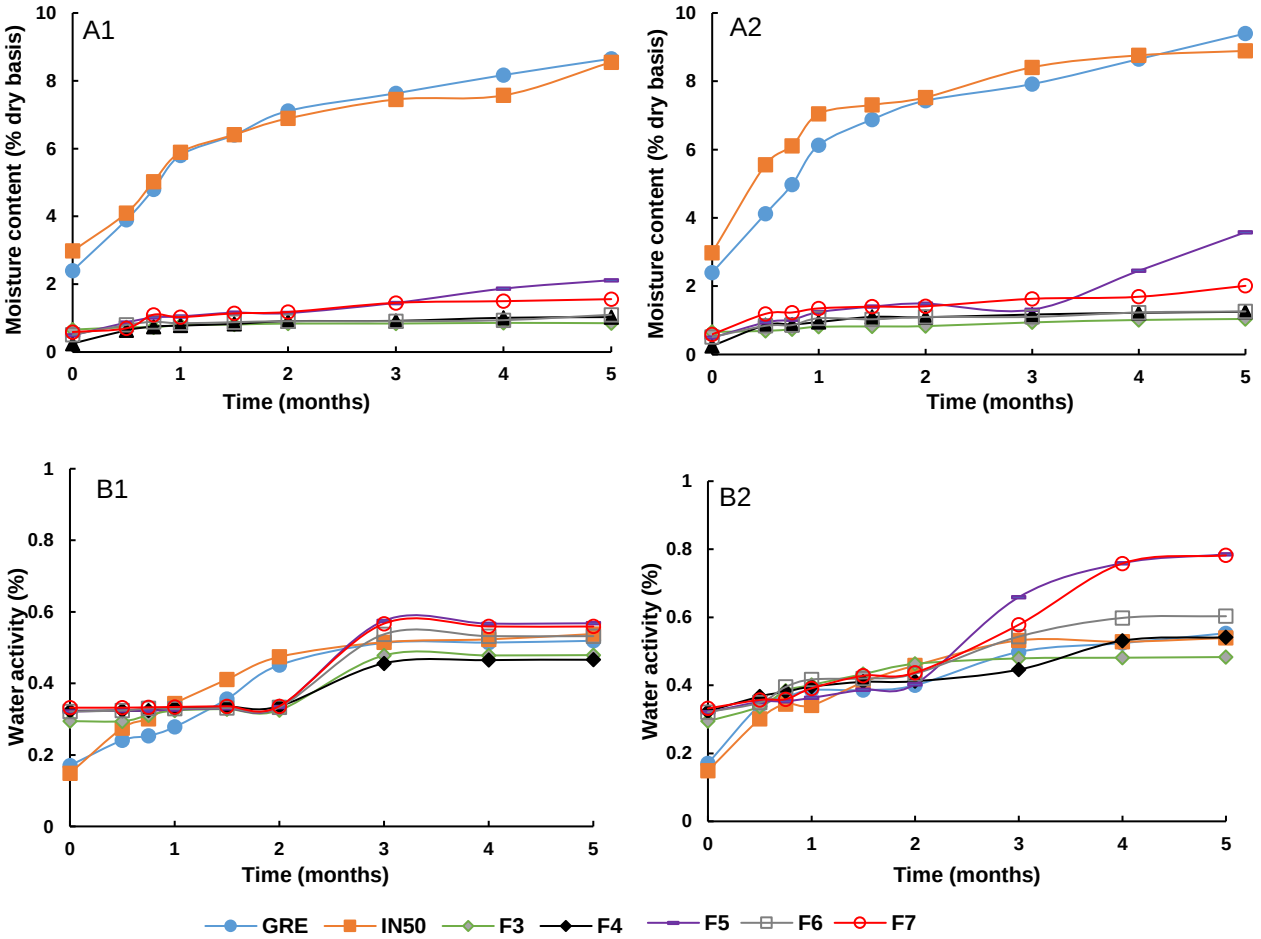

Fig. 4.3 Moisture content (A) and water activity (B) of green rooibos powders: green rooibos extract (GRE), GRE microencapsulated with inulin in 1:1 ratio (m/m) (IN50), F3 (IN50 and sucrose), F4 (IN50 and xylitol), F5 (IN50, xylitol and citric acid), F6 (IN50, xylitol and ascorbic acid) and F7 (IN50, xylitol, ascorbic acid and citric acid), during storage at (1) 30°C/65% RH and (2) 40°C/65% RH for 5 months in semi-permeable sachets.

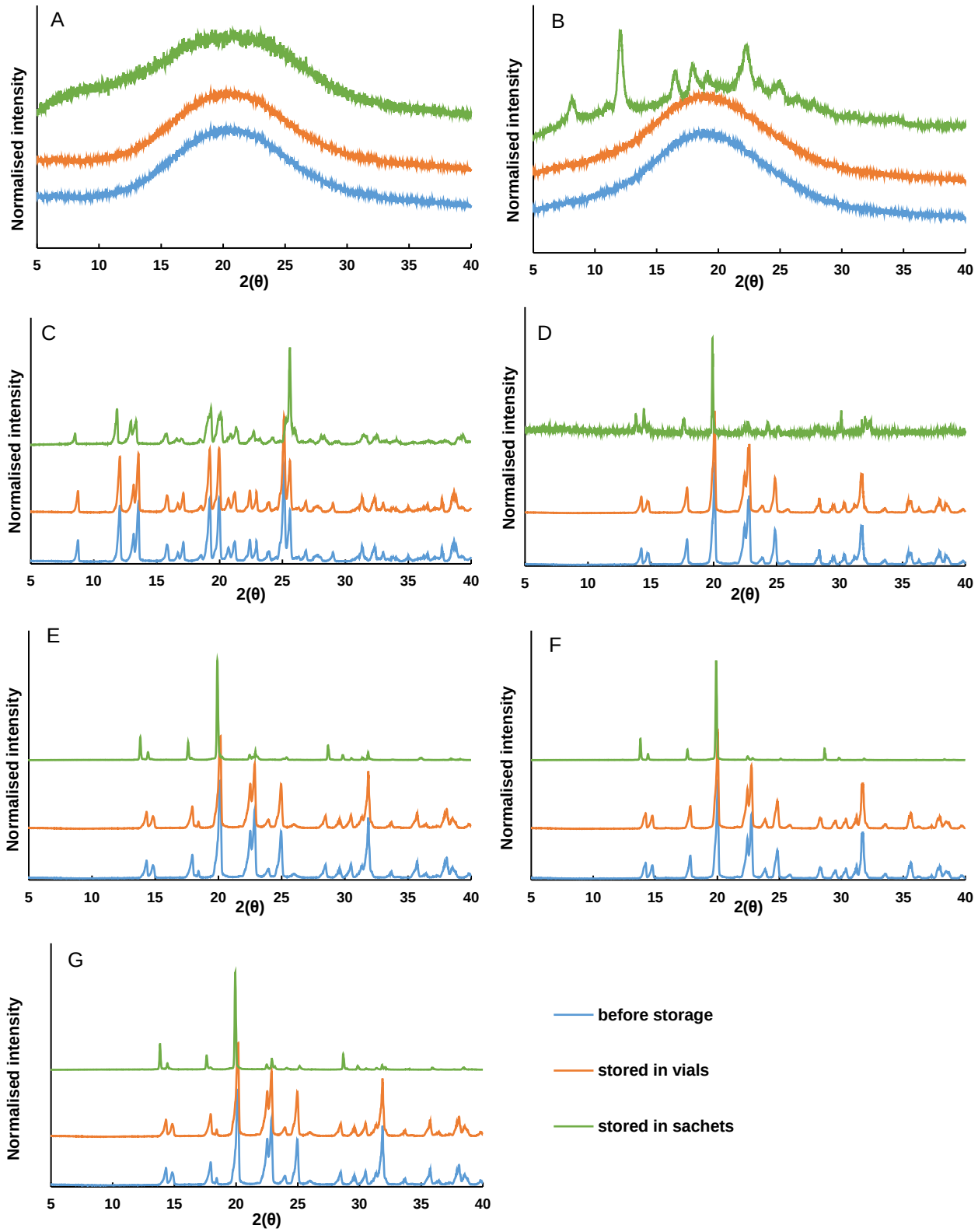

Fig. 4.4 X-ray powder diffractograms of green rooibos powders: (A) green rooibos extract (GRE), (B) GRE microencapsulated with inulin in 1:1 ratio (m/m) (IN50), (C) F3 (IN50 and sucrose), (D) F4 (IN50 and xylitol), (E) F5 (IN50, xylitol and citric acid), (F) F6 (IN50, xylitol and ascorbic acid) and (G) F7 (IN50, xylitol, ascorbic and citric acid), before storage and after storage at 40 °C/65% RH for 12 months in glass vials and 5 months in semi-permeable sachets.

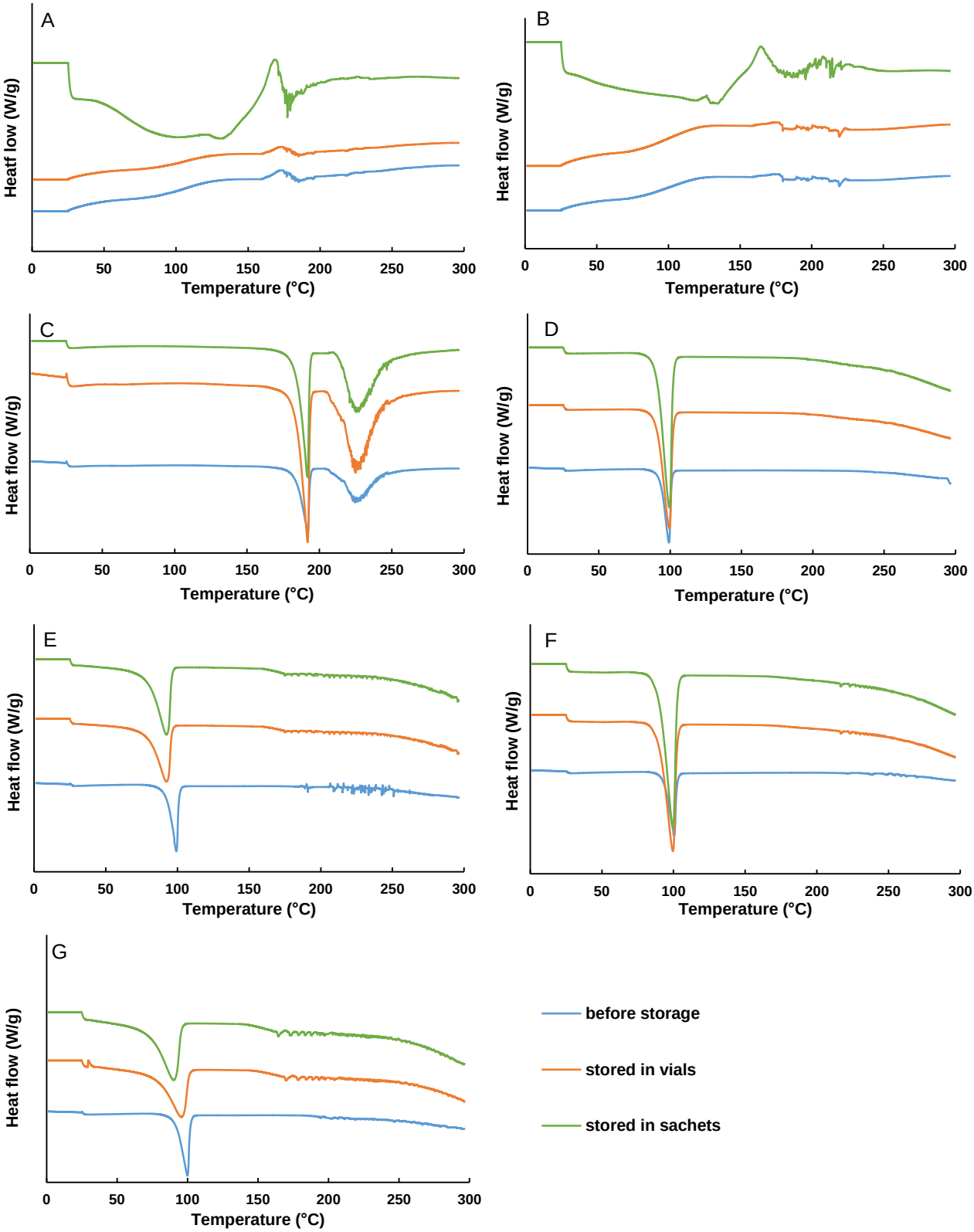

Fig. 4.5 Differential scanning calorimetry thermograms of green rooibos powders: (A) green rooibos extract (GRE), (B) GRE microencapsulated with inulin in 1:1 ratio (m/m) (IN50), (C) F3 (IN50 and sucrose), (D) F4 (IN50 and xylitol), (E) F5 (IN50, xylitol and citric acid), (F) F6 (IN50, xylitol and ascorbic acid) and (G) F7 (IN50, xylitol, ascorbic and citric acid), before storage and after storage at 40°C/65% RH for 12 months in glass vials and 5 months in semi-permeable sachets.

4.3.3 Chemical stability and kinetic modelling of the degradation of dihydrochalcones, aspalathin and nothofagin

The change in aspalathin content as a function of storage time was modelled using zero order, first order, second order and fractional conversion models. All these models showed a reasonable fit, where superiority of the model was dependent on the specific formulation as indicated by adjusted coefficients of determination (R^2_{adj}) values of between 0.6678 and 0.9805 (Table B.1). Even though slightly superior R^2_{adjs} were observed for the fractional conversion model, the predicted equilibrium aspalathin content values were below zero, which is practically impossible. This could likely be due to a too short storage period. In light of this, the reaction rate constants were determined based on the first order model, a reaction kinetics model commonly utilised for the degradation of phenolic compounds. Examples are De Paepe *et al.* (2014), who investigated dihydrochalcones in cloudy apple juice and Beelders, De Beer & Joubert (2015), who investigated xanthones and benzophenones in *Cyclopia genistoides*. The effects of storage temperature, packaging materials, microencapsulation and ingredients on the stability of aspalathin were established according to reaction rate constants and extent of aspalathin degradation (Table 4.6 and Fig. 4.6). The small extent of aspalathin degradation (<10%) observed for GRE (except GRE stored at 40 °C in the sachets and vials) and IN50 resulted in a poor fit of the kinetic models and will thus not be discussed with regard to reaction kinetics.

Additionally, nothofagin content, as the other major dihydrochalcone in GRE, was modelled using first order reaction kinetics. The decrease in nothofagin and the reaction rate constants (Supplementary material Fig. B.4 and Table B.2) were comparable to those of aspalathin. The catechol group on the B-ring of aspalathin did not significantly increase its degradation compared to nothofagin with a single OH-group on the B-ring. The discussion will therefore be based on the results obtained for aspalathin.

The extent of aspalathin degradation and degradation rate constants were significantly higher when the formulations were stored at 40 °C than at 30 °C (Table 4.6 and Fig. 4.6). As an example, the extent of aspalathin degradation in the powders ranged from 6.66–50.62% and 9.67–90.31% for the samples stored in glass vials for 12 months at 30 °C and 40 °C, respectively. Furthermore, the semi-permeable sachets showed more aspalathin degradation over 5 months compared to the vials over 5 months at 30 °C and 40 °C (Table 4.6). This indicated higher instability of aspalathin in the semi-permeable sachets, as for the more drastic physical changes in the appearance of the powders (Table 4.5) and higher reaction rates in most cases (except F3 and F4 stored at 30 °C and F5 stored at 40 °C). The discrepancies in reaction rates could be attributed to other variables having a larger effect than addition of moisture through the semi-permeable sachets.

In addition to the effects of temperature and packaging, the effects of the different ingredients are of interest as they significantly affected the physical stability of the formulations (Table 4.5 and section 4.3.2). In all cases,

except powders stored in vials at 30 °C which showed no significant difference, a significant decrease ($P < 0.05$) in aspalathin degradation was observed after microencapsulation of GRE with inulin (IN50) compared to GRE (Table 4.6). In **Chapter 3** (section 3.3.6), less aspalathin loss was noted after microencapsulation with inulin for samples stored at 40 °C/75% RH for 96 h. Thus, results for the current study indicate that microencapsulation of GRE with inulin does indeed decrease aspalathin degradation during storage. The extent of aspalathin degradation for the GRE and IN50 was significantly lower compared to formulations F3–F7, which contained additional crystalline ingredients (Table 4.6). Furthermore, in all cases, except powders stored in sachets at 30 °C, the replacement of sucrose (F3) by xylitol (F4) resulted in significantly more aspalathin degradation. Aspalathin degradation in sachets stored at 40 °C was 39.78% for F3 and 61.51% for F4 after 5 months. In the vials stored at 40 °C it was 34.00% for F3 and 40.84% for F4 after 5 months (Table 4.6). The reaction rate constants showed similar trends. The addition of citric acid to the IN50 and xylitol powder formulation (F5) resulted in increased aspalathin instability in all cases, except during storage in the sachets at 40 °C, as shown by the extent of aspalathin degradation and reaction rate constants. The addition of ascorbic acid (F6) showed similar results with decreased aspalathin stability except for the powders stored in the vials at 30 °C, which showed no significant difference to F4. Generally, as expected, the combination of the citric and ascorbic acid also showed decreased aspalathin stability compared to F4.

The increase in aspalathin degradation with an increase in temperature is typical for phenolics as previously shown for dihydrochalcones in cloudy apple juice (De Paepe *et al.*, 2014), epigallocatechin gallate (EGCG) powder (Li, Taylor & Mauer, 2014) and xanthones and benzophenones in honeybush plant material (Beelders *et al.*, 2015). The general higher instability of aspalathin for the powders stored in the semi-permeable sachets could be due to higher moisture content, as confirmed by significant increases in MC and a_w for all the formulations (Fig. 4.3). The negative effect of exposure to high RH on phenolic stability and specifically aspalathin is not uncommon, and has been shown for EGCG powders (Li *et al.*, 2014) and flavone *C*-glycosides (Bott *et al.*, 2010).

The effect of microencapsulation and the addition of crystalline ingredients become more complicated to understand as also indicated by Ortiz, Kestur, Taylor & Mauer (2009). Generally, higher physical and chemical instability has been reported for blends of deliquescent crystalline and amorphous ingredients compared to individual amorphous components (Thorat *et al.*, 2017). For example, Ortiz *et al.* (2009) found that the addition of citric acid to amorphous green tea powders resulted in a decrease in physical and chemical stability. Similarly, De Beer *et al.* (2018) found a decrease in xanthone stability with the addition of ascorbic and citric acid to honeybush powders. Generally, the trend in the current study also seem to indicate that addition of

acidifiers result in higher aspalathin instability, however, this was not always the case. Citric acid monohydrate, as used in the current study, has the tendency to dehydrate under various storage conditions (Apelblat, 2014). In the sealed glass vials, this dehydration most probably resulted in wetting of the powders, explaining the decreased stability of F5. However, in the sachets at 40 °C where the powders were already exposed to moisture and large amounts of water was absorbed from the storage cabinet environment (65% RH), the extra moisture produced by the citric acid was probably negligible and affected the aspalathin stability to a lesser extent. Ascorbic acid is generally added to food formulations as an antioxidant with the aim to decrease chemical degradation as shown for aspalathin in RTD iced tea (Joubert *et al.*, 2010) . However, results of the present study and a study by Ortiz *et al.* (2009) showed that the effect of ascorbic acid on powder stability is more complex.

Table 4.6

Aspalathin degradation (%) and degradation rate constants (K) of the first order model[a] fitted to the experimental data representing aspalathin degradation in green rooibos powders during storage at 30 °C/65 % and 40°C/65 % RH for 12 months in glass vials and 5 months in semi-permeable sachets

	Sealed glass vials						Semi-permeable sachets			
	30°C/65% RH			40°C/65% RH			30°C/65% RH		40°C/65% RH	
	Decrease (%) after 5 months	Decrease (%) after 12 months	K (month^{-1})	Decrease (%) after 5 months	% change after 12 months	K (month^{-1})	Decrease (%) after 5 months	K (month^{-1})	Decrease (%) after 5 months	K (month^{-1})
GRE[b]	3.60 ± 0.51 c[c]	6.66 ± 1.25 d	N/A[d]	6.21 ± 0.54 d	17.77 ± 0.78 f	0.0187 ± 0.0031 e	4.92 ±1.08 e	N/A	18.51 ±1.23 f	0.0354 ± 0.0032 e
IN50[e]	1.85 ± 1.57 c	7.27 ± 0.33 d	N/A	3.68 ± 0.38 d	9.67 ± 0.43 g	N/A	0.30 ± 0.72 f	N/A	4.39 ± 0.68 g	N/A
F3[f]	15.31 ± 1.48 b	17.74 ± 1.58 c	0.0161 ± 0.0029 c	34.00 ± 2.00 c	50.08 ± 1.00 e	0.0690 ± 0.0054 d	25.23 ± 2.13 c	0.0438 ± 0.0075 b	39.78 ± 2.81 e	0.0904 ± 0.0183 d
F4[g]	12.06 ± 2.93 b	34.28 ± 2.98 b	0.0406 ± 0.0015 b	40.84 ± 2.31 b	76.88 ± 0.56 d	0.1137 ± 0.0066 c	21.01 ± 2.12 d	0.0353 ± 0.0051b	61.51 ± 0.75 c	0.1489 ± 0.0138 b
F5[h]	11.89 ± 2.58 b	50.62 ± 2.34 a	0.0559 ± 0.0059 a	41.65 ± 1.49 b	87.10 ± 0.53 b	0.1398 ± 0.0032 b	29.86 ± 1.94 b	0.0479 ± 0.0123 b	50.23 ± 2.36 d	0.1143 ± 0.0057 c
F6[i]	27.44 ± 1.35 a	34.96 ± 2.74 b	0.0404 ± 0.0026 b	54.05 ± 1.34 a	85.48 ± 0.67 c	0.1556 ± 0.0041 a	41.21 ± 2.61 a	0.0879 ± 0.0105 a	82.09 ± 1.12 a	0.2829 ± 0.0099 a
F7[j]	25.85 ± 3.61 a	36.80 ± 2.98 b	0.0401 ± 0.0039 b	54.22 ± 5.30 a	90.31 ± 0.39 a	0.1578 ± 0.0120 a	41.92 ± 1.35 a	0.0870 ± 0.0108 a	66.98 ± 2.68 b	0.1673 ± 0.0030 b

[a]First order model: $C = C_0 \exp(-Kt)$, where C is aspalathin (g/100 g extract, d.b. data not shown), C_0 is initial aspalathin (g/100 g extract, d.b. data not shown), t is the time in months and K is the reaction rate constant; [b]Green rooibos extract; [c]Means in the same column with the same letter are not significantly different ($P \geq 0.05$); [d]Less than 10% change in aspalathin content observed – not suitable for kinetic modelling; [e]GRE microencapsulated with inulin in 1:1 ratio (m/m); [f]Formulation 3 (IN50 and sucrose); [g]Formulation 4 (IN50 and xylitol); [h]Formulation 5 (IN50, xylitol and citric acid); [i]Formulation 6 (IN50, xylitol and ascorbic acid); [j]Formulation 7 (IN50, xylitol, citric acid and ascorbic acid)

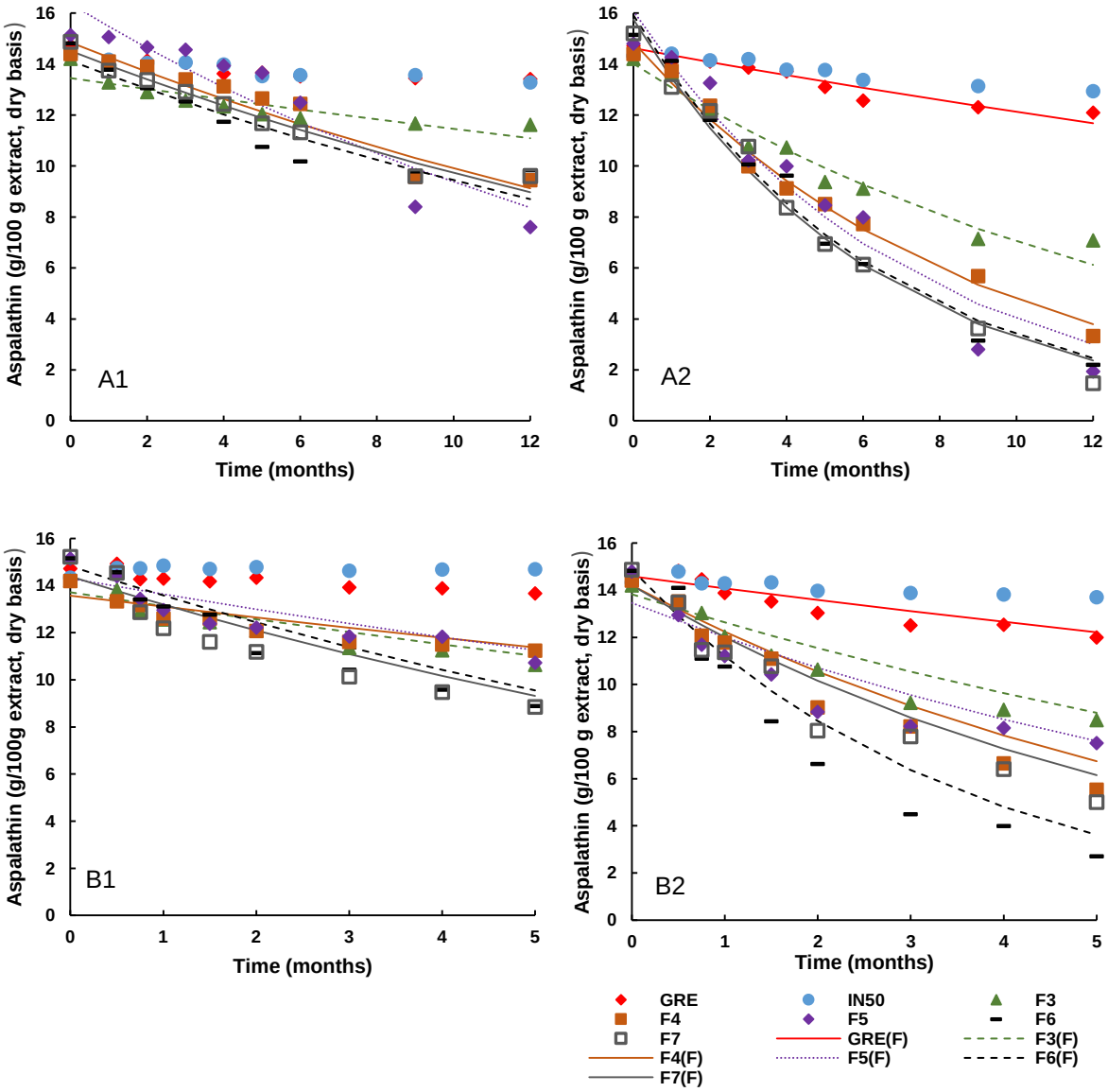

Fig. 4.6 First order kinetic fitting (indicated by (F), solid and broken lines) and experimental data (markers only) for aspalathin degradation in green rooibos powders as a function of storage time: green rooibos extract (GRE), GRE microencapsulated with inulin in 1:1 ratio (m/m) (IN50), F3 (IN50 and sucrose), F4 (IN50 and xylitol), F5 (IN50, xylitol and citric acid), F6 (IN50, xylitol and ascorbic acid) and F7 (IN50, xylitol, ascorbic acid and citric acid), during storage at (1) 30°C/65% RH and (2) 40°C/65% RH for (A) 12 months in sealed glass vials and (B) 5 months in semi-permeable sachets. Aspalathin degradation (<10%) not suitable for kinetic modelling.

4.3.4 Change in sensory profile of formulation 5 during storage

Given the physicochemical changes observed for F5 (Table 4.5) during storage, it was of interest to determine whether noticeable sensory changes also took place. For a quick screening, samples were stored for 1 month at 30°C/65% RH and 40°C/65% RH in sealed vials and semi-permeable sachets.

The PCA bi-plot (Fig. 4.7) shows the association of samples with the aroma attributes tested orthonasally and retronasally. The first two principal components, PC1 (F1) and PC2 (F2), explain 76.03% of the variance.

Samples stored in the sachets at 40 °C are separated from the other samples on PC1, while samples stored in vials at 40 °C separated from the control and samples stored at 30 °C on PC2. Samples stored in sachets at 40 °C associated with the positive aroma attributes, i.e. 'rooibos-woody', 'honey', 'apple', 'apricot' and 'fruity-sweet'. These attributes are typical of fermented rooibos tea (Koch *et al.*, 2012; Jolley, Van der Rijst, Joubert & Muller, 2017). The other samples either associated with 'rubber-putty' (F5 in vials at 40 °C) or with 'hay dried grass', 'seaweed' and 'grainy'. Apart from 'hay dried grass' (Jolley *et al.*, 2017), the attributes 'seaweed' and 'grainy' could be considered atypical. Jolley *et al.* (2017) noted that the intensity of the aroma attribute 'hay dried grass' should be low in good quality fermented rooibos tea. Viljoen *et al.* (2017) showed that consumers preferred typical 'rooibos-woody' attributes, while the presence of 'hay-like' attributes did not reduce preference, even though associated with lower quality.

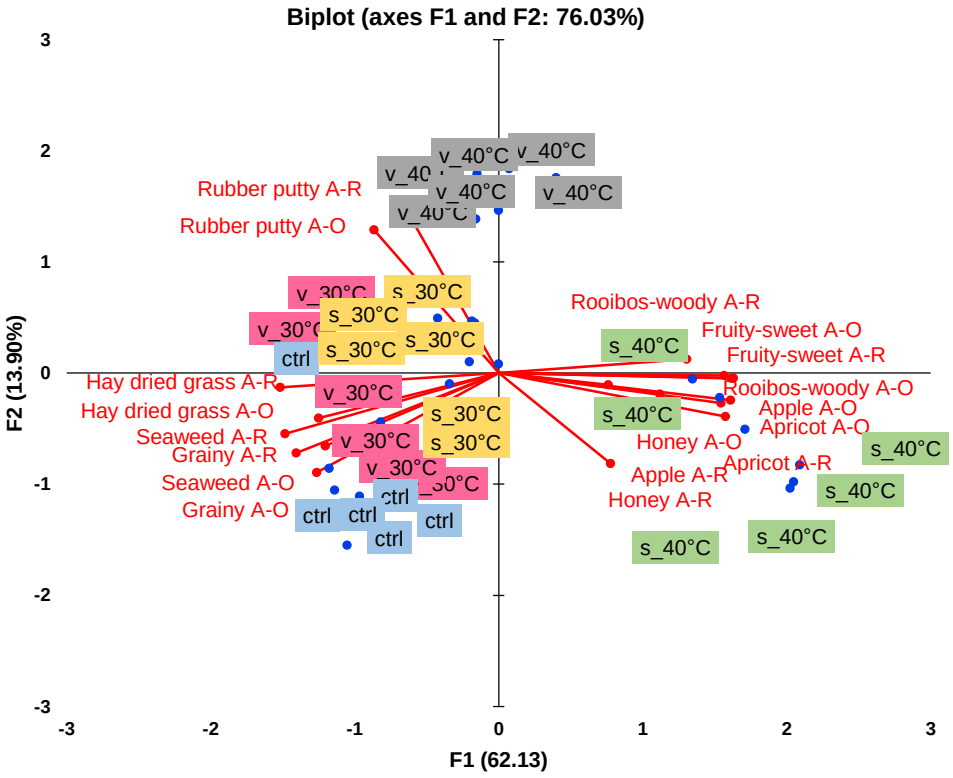

Fig. 4.7 Principal component analysis (PCA) bi-plot showing the position of selected sensory attributes (orthonasal (A-O) and retronasal (A-R) aroma) in relation to formulation 5 reconstituted in water (green rooibos extract microencapsulated with inulin in 1:1 ratio (m/m), xylitol and citric acid), before storage (control, ctrl) and stored at 30 °C/65% RH and 40 °C/65% RH for 1 month in sealed glass vials (v) and in semi-permeable sachets (s).

For further elucidation of results, the mean intensities of the positive and negative aroma attributes, tested orthonasally and retronasally (Fig. 4.8), as well as that of taste, astringency (mouthfeel) and 'synthetic' sweet aftertaste (Fig. 4.9), were considered. As the results indicate that the aroma attributes tested orthonasally and

retronasally followed similar trends, the discussion henceforth will focus on the aroma attributes tested orthonasally. 'Rooibos-woody', a sensory attribute typically associated with fermented ("oxidised") rooibos tea (Jolley *et al.*, 2017), was barely perceptible (< 5 on a 100-point scale), while 'honey' intensity was also very low (< 10). Both these attributes could thus be considered to be negligible when considering the sensory profile of the reconstituted green rooibos powders (Fig. 4.8). The positive aroma attributes 'apricot', 'apple' and 'fruity-sweet' were present in intensity levels > 10, especially in samples stored in the sachets at 40 °C. The higher storage temperature of 40 °C, compared to 30 °C, and the moisture uptake during storage (due to the use of semi-permeable sachets) promoted the development of these three aroma attributes typically associated with fermented rooibos tea and lessened the development of the negative aroma attributes 'grainy' and 'seaweed'. Interestingly, a significantly higher intensity for 'rubber-putty' like aroma was observed for samples stored in vials at 40 °C, most probably as a result of the prevention of moisture uptake during storage (Fig. 4.8). This effect was observed to a lesser extent at 30 °C for samples stored in vials. Only minor changes in the intensities, but no clear trend were observed for the basic taste attributes (sweet and sour taste), the mouthfeel attribute astringency and also for the lingering attribute 'synthetic' sweet aftertaste (Fig. 4.9). This aftertaste is typically linked to xylitol as noted during the training sessions. The major impact of storage on the sensory profile of F5 was therefore on its aroma characteristics.

The change in the sensory profile of F5 during storage was also accompanied by a change in the colour of the powders when reconstituted in water for consumption (Table 4.7). The pH values of all the solutions were the same (pH 2.88–2.89). The colour parameters for samples stored in the sachets at 40 °C differed the most from those of the control (Table 4.5). The changes in L*, a*, b*, C* and h* values of the solutions were consistent with the browning observed for the powders, which can be associated with the oxidation of rooibos phenolic compounds (Heinrich *et al.*, 2012).

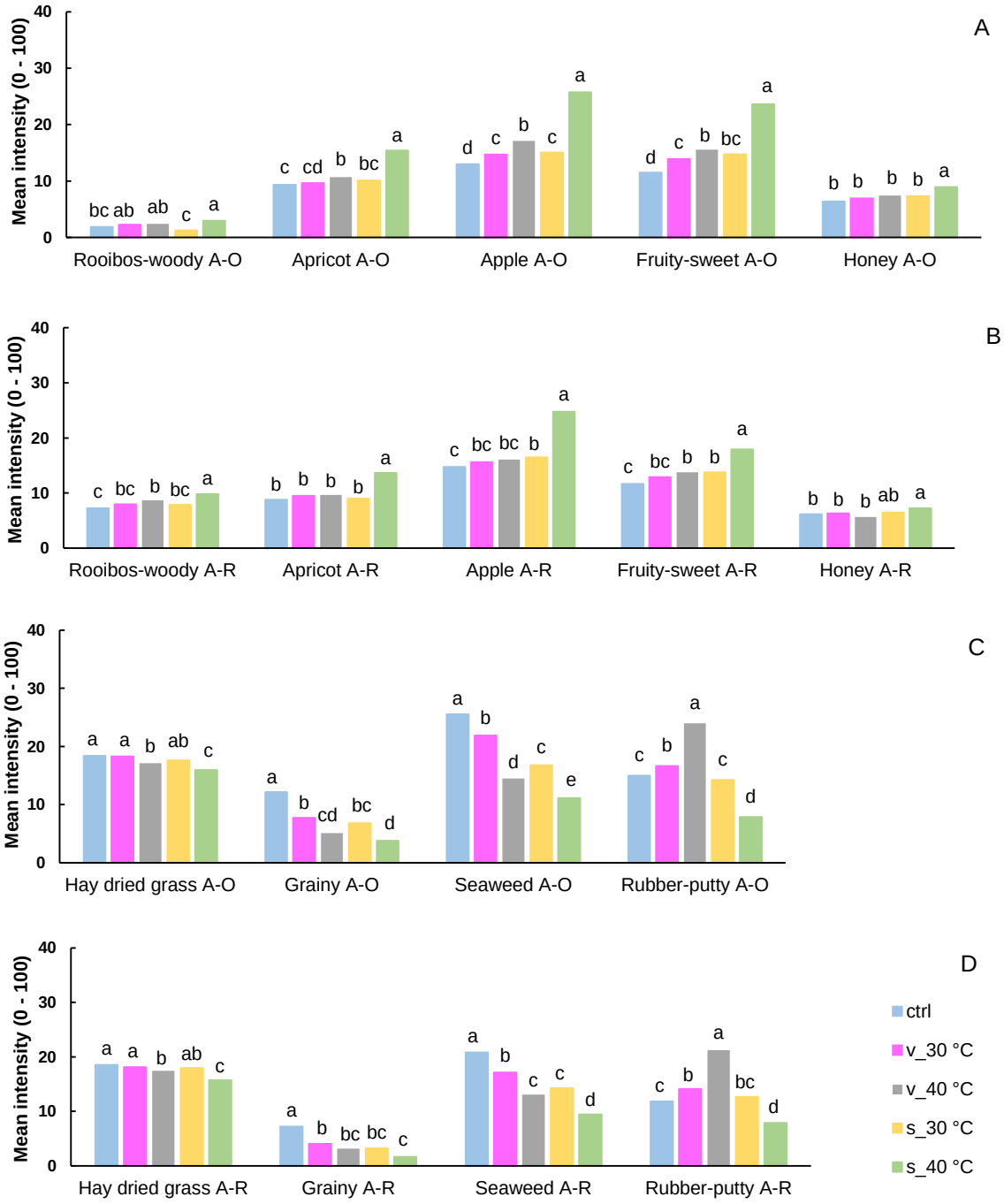

Fig. 4.8 Mean intensities of the positive (A) orthonasal (A-O) and (B) retronasal (A-R) aroma attributes, as well the negative (C) orthonasal (A-O) and (D) retronasal (A-R) aroma attributes for formulation 5 reconstituted in water (green rooibos extract microencapsulated with inulin in 1:1 ratio (m/m), xylitol and citric acid), before storage (control, ctrl) and stored for 1 month at 30°C/65% RH and 40°C/65% RH in sealed glass vials (v) and semi-permeable sachets (s). Means with different letters, within a sensory attribute, differ significantly ($P \leq 0.05$).

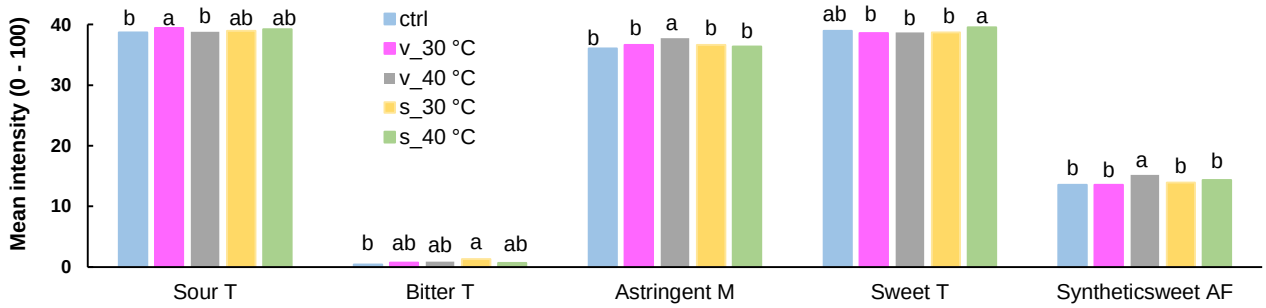

Fig. 4.9 Mean intensities of the taste (T), mouthfeel (M) and aftertaste (AF) attributes for formulation 5 reconstituted in water (green rooibos extract microencapsulated with inulin in 1:1 ratio (m/m), xylitol and citric acid), before storage (control, ctrl) and stored for 1 month at 30 °C/65% RH and 40 °C/65% RH in sealed glass vials (v) and semi-permeable sachets (s). Means with different letters, within a sensory attribute, differ significantly ($P \leq 0.05$).

Table 4.7

Colour measurements (L*a*b*) and calculated chroma (C*), hue (h) and difference in colour (ΔE) for formulation 5[a] reconstituted in water (63 g powder/L) before storage (control, ctrl) and after storage at 30°C/65% RH and 40°C/65% RH for 1 month in glass sealed vials (v) and semi-permeable sachets (s)

Storage condition	L*	a*	b*	C*	h	ΔE
ctrl	54.48 ± 0.79 b[b]	4.81 ± 0.18 e	24.96 ± 0.28 e	25.15 ± 0.28 e	78.97 ± 0.40 a	0.00 ± 0.00 e
s_30°C	55.83 ± 0.56 a	5.54 ± 0.31 c	27.65 ± 0.24 c	28.20 ± 0.27 c	78.68 ± 0.57 ab	3.39 ± 0.32 c
s_40°C	51.01 ± 0.50 d	9.93 ± 0.15 a	36.04 ± 0.18 a	37.38 ± 0.20 a	74.60 ± 0.19 d	12.93 ± 0.27 a
v_30°C	54.24 ± 0.54 b	5.22 ± 0.11 d	25.27 ± 0.35 d	25.80 ± 0.36 d	78.32 ± 0.11 b	0.88 ± 0.42 d
v_40°C	53.53 ± 0.41 c	6.83 ± 0.25 b	28.33 ± 0.50 b	29.04 ± 0.51 b	77.33 ± 0.44 c	4.10 ± 0.56 b

[a]Contains green rooibos extract microencapsulated with inulin in 1:1 ratio (m/m), xylitol and citric acid; [b]Means in the same column with the same letter are not significantly different ($P \geq 0.05$)

4.4 Conclusions

The shelf-life stability of pre-formulated, single serve iced tea powder products is crucial as this will determine their physical properties, retention of the bioactive compounds in the nutraceutical ingredient and even sensory profiles. The addition of xylitol instead of sugar provided an advantage by lowering the kilojoule value of the powders, however, xylitol significantly increased the rate of dihydrochalcone degradation, indicating that a compromise would have to be made between stability and energy value, or an alternative low kJ sweetener should be investigated. The addition of citric acid monohydrate and ascorbic acid also resulted in overall decreased stability of the formulated powder with regard to increased dihydrochalcone degradation and physical changes. These effects were most pronounced for citric acid and the samples stored at the higher temperature (40 °C) in the semi-permeable sachets. Thus, in order to produce stable iced tea powders, ingredients should be selected carefully, avoiding thermodynamically unstable crystalline ingredients already containing moisture such as citric acid monohydrate. Protection against moisture uptake and a low storage temperature of 30 °C would prolong product shelf-life of the range of green rooibos powder formulations

investigated. From a sensory perspective, changes for the samples stored in the sachets at the higher temperature 40°C resulted in a sensory profile related to fermented rooibos tea, which has a higher consumer preference. However, shelf-life stable iced tea powders should preferably not undergo any sensory changes during storage to ensure consistency of products.

4.5 References

Al-Muhtaseb, A. H., McMinn, W. A. M. & Magee, T. R. A. (2002). Moisture sorption isotherm characteristics of food products: A review. *Food and Bioproducts Processing,* 80, 118–128.

Allan, M. & Mauer, L. J. (2016). Comparison of methods for determining the deliquescence points of single crystalline ingredients and blends. *Food Chemistry,* 195, 29–38.

Anonymous (2018). Flexifoil packaging: Barrier properties of films. URL http://www.flexifoilpackaging.com/barrier-properties-films. Accessed 4 June 2018.

Apelblat, A. (2014). Properties of citric acid and its solutions. In: *Citric Acid*. Pp. 13–141. Switzerland: Springer International Publishing.

Beelders, T., De Beer, D. & Joubert, E. (2015). Thermal degradation kinetics modeling of benzophenones and xanthones during high-temperature oxidation of *Cyclopia genistoides* (L.) Vent. plant material. *Journal of Agricultural and Food Chemistry,* 63, 5518–5527.

Benade, J. & Essop, M. F. (2017). Introduction of "sugar tax" in South Africa: Placebo or panacea to curb the onset of cardio-metabolic diseases? *SAHeart,* 3, 148–153.

Bigliardi, B. & Galati, F. (2013). Innovation trends in the food industry: The case of functional foods. *Trends in Food Science & Technology,* 31, 118–129.

Bott, R. F., Labuza, T. P. & Oliveira, W. P. (2010). Stability testing of spray- and spouted bed-dried extracts of *Passiflora alata*. *Drying Technology,* 28, 1255–1265.

Brunauer, S., Deming, L. S. & Teller, E. (1940). On a theory of Van der Waals adsorption of gases. *Journal of the American Chemical Society,* 62, 1723–1732.

Caurie, M. (2007). Hysteresis phenomenon in foods. *International Journal of Food Science & Technology,* 42, 45–49.

Chadha, R. & Bhandari, S. (2004). Drug–excipient compatibility screening — Role of thermoanalytical and spectroscopic techniques. *Journal of Pharmaceutical and Biomedical Analysis,* 87, 82–97.

Chen, Z.-Y., Zhu, Q. Y., Tsang, D. & Huang, Y. (2001). Degradation of green tea catechins in tea drinks. *Journal of Agricultural and Food Chemistry,* 49, 477–482.

Corbo, M. R., Bevilacqua, A., Petruzzi, L., Casanova, F. P. & Sinigaglia, M. (2014). Functional beverages: The emerging side of functional foods. *Comprehensive Reviews in Food Science and Food Safety,* 13, 1192–1206.

Cortés-Rojas, D. F. & Oliveira, W. P. (2012). Physicochemical properties of phytopharmaceutical preparations as affected by drying methods and carriers. *Drying Technology,* 30, 921–934.

De Beer, D., Joubert, E., Viljoen, M. & Manley, M. (2011). Enhancing aspalathin stability in rooibos (*Aspalathus linearis*) ready-to-drink iced teas during storage: the role of nano-emulsification and beverage ingredients, citric and ascorbic acids. *Journal of the Science of Food and Agriculture,* 92, 274–282.

De Beer, D., Pauck, C. E., Aucamp, M., Liebenberg, W., Stieger, N., Van der Rijst, M. & Joubert, E. (2018). Phenolic and physicochemical stability of a functional beverage powder mixture during storage: effect of the microencapsulant inulin and food ingredients. *Journal of the Science of Food and Agriculture,* 98, 2925–2934.

De Paepe, D., Valkenborg, D., Coudijzer, K., Noten, B., Servaes, K., De Loose, M., Voorspoels, S., Diels, L. & Van Droogenbroeck, B. (2014). Thermal degradation of cloudy apple juice phenolic constituents. *Food Chemistry,* 162, 176–185.

De Souza, V. B., Thomazini, M., Balieiro, J. C. & Fávaro-Trindade, C. S. (2015). Effect of spray drying on the physicochemical properties and color stability of the powdered pigment obtained from vinification byproducts of the Bordo grape (*Vitis labrusca*). *Food and Bioproducts Processing,* 93, 39–50.

Dehghan, P., Gargari, B. P. & Jafar-Abadi, M. A. (2014). Oligofructose-enriched inulin improves some inflammatory markers and metabolic endotoxemia in women with type 2 diabetes mellitus: a randomized controlled clinical trial. *Nutrition,* 30, 418–423.

Ferruzzi, M. G. (2010). The influence of beverage composition on delivery of phenolic compounds from coffee and tea. *Physiology & Behavior,* 100, 33–41.

Gabas, A. L., Telis, V. R. N., Sobral, P. J. A. & Telis-Romero, J. (2007). Effect of maltodextrin and arabic gum in water vapor sorption thermodynamic properties of vacuum dried pineapple pulp powder. *Journal of Food Engineering,* 82, 246–252.

Heinrich, T., Willenberg, I. & Glomb, M. A. (2012). Chemistry of color formation during rooibos fermentation. *Journal of Agricultural and Food Chemistry,* 60, 5221–5228.

Hiatt, A. N., Taylor, L. S. & Mauer, L. J. (2011). Effects of co-formulation of amorphous maltodextrin and deliquescent sodium ascorbate on moisture sorption and stability. *International Journal of Food Properties,* 14, 726–740.

Islam, M. S. (2011). Effects of xylitol as a sugar substitute on diabetes-related parameters in nondiabetic rats. *Journal of Medicinal Food,* 14, 505–511.

Jayasankar, A., Good, D. J. & Rodríguez-Hornedo, N. (2007). Mechanisms by which moisture generates cocrystals. *Molecular Pharmaceutics,* 4, 360–372.

Johnson, R., De Beer, D., Dludla, P. V., Ferreira, D., Muller, C. J. F. & Joubert, E. (2018). Aspalathin from rooibos (*Aspalathus linearis*): A bioactive *C*-glucosyl dihydrochalcone with potential to target the metabolic syndrome. *Planta Medica,* 84, 568–583.

Jolley, B., Van der Rijst, M., Joubert, E. & Muller, M. (2017). Sensory profile of rooibos originating from the Western and Northern Cape governed by production year and development of rooibos aroma wheel. *South African Journal of Botany,* 110, 161–166.

Jones, P. J. & Jew, S. (2007). Functional food development: concept to reality. *Trends in Food Science & Technology,* 18, 387–390.

Joubert, E., Viljoen, M., De Beer, D., Malherbe, C. J., Brand, D. J. & Manley, M. (2010). Use of green rooibos (*Aspalathus linearis*) extract and water-soluble nanomicelles of green rooibos extract encapsulated with ascorbic acid for enhanced aspalathin content in ready-to-drink iced teas. *Journal of Agricultural and Food Chemistry,* 58, 10965–10971.

Joubert, E., Viljoen, M., De Beer, D. & Manley, M. (2009). Effect of heat on aspalathin, iso-orientin, and orientin contents and color of fermented rooibos (*Aspalathus linearis*) iced tea. *Journal of Agricultural and Food Chemistry,* 57, 4204–4211.

Khan, R. S., Grigor, J., Winger, R. & Win, A. (2013). Functional food product development – Opportunities and challenges for food manufacturers. *Trends in Food Science & Technology,* 30, 27–37.

Koch, I. S., Muller, M., Joubert, E., Rijst, M. V. d. & Næs, T. (2012). Sensory characterization of rooibos tea and the development of a rooibos sensory wheel and lexicon. *Food Research International,* 46, 217–228.

Kwok, K., Mauer, L. J. & Taylor, L. S. (2010). Kinetics of moisture-induced hydrolysis in powder blends stored at and below the deliquescence relative humidity: Investigation of sucrose-citric acid mixtures. *Journal of Agricultural and Food Chemistry,* 58, 11716–11724.

Labuza, T. P. & Altunakar, L. (2007). Water activity prediction and moisture sorption isotherms. In: *Water Activity in Foods*. Pp. 109–154. Iowa: Blackwell Publishing Ltd.

Lafontaine, A., Sanselme, M., Cartigny, Y., Cardinael, P. & Coquerel, G. (2012). Characterization of the transition between the monohydrate and the anhydrous citric acid. *Journal of Thermal Analysis and Calorimetry,* 112, 307–315.

Li, N., Taylor, L. S. & Mauer, L. J. (2014). The physical and chemical stability of amorphous (−)-epi-gallocatechin gallate: Effects of water vapor sorption and storage temperature. *Food Research International,* 58, 112–123.

Makinen, K. K. (2016). Gastrointestinal disturbances associated with the consumption of sugar alcohols with special consideration of xylitol: Scientific review and instructions for dentists and other health-care professionals. *International Journal of Dentistry,* 2016, 5967–5907.

Mauer, L. J. & Taylor, L. S. (2010). Deliquescence of pharmaceutical systems. *Pharmaceutical Development and Technology,* 15, 582–594.

Miller, N., De Beer, D., Aucamp, M., Malherbe, C. J. & Joubert, E. (2018). Inulin as microencapsulating agent improves physicochemical properties of spray-dried aspalathin-rich green rooibos (*Aspalathus linearis*) extract with α-glucosidase inhibitory activity. *Journal of Functional Foods,* 48, 400–409.

Miller, N., De Beer, D. & Joubert, E. (2017). Minimising variation in aspalathin content of aqueous green rooibos extract: optimising extraction and identifying critical material attributes. *Journal of the Science of Food and Agriculture,* 97, 4937–4942.

Næs, T., Brockhoff, P. B. & Tomic, O. (2010). Quality Control of Sensory Profile Data. In: *Statistics for sensory and sonsumer science*. New York USA: John Wiley & Sons, Ltd.

Ortiz, J., Ferruzzi, M. G., Taylor, L. S. & Mauer, L. J. (2008). Interaction of environmental moisture with powdered green tea formulations: effect on catechin chemical stability. *Journal of Agricultural and Food Chemistry,* 56, 4068–4077.

Ortiz, J., Kestur, U. S., Taylor, L. S. & Mauer, L. J. (2009). Interaction of environmental moisture with powdered green tea formulations: relationship between catechin stability and moisture-induced phase transformations. *Journal of Agricultural and Food Chemistry,* 57, 4691–4697.

Raji, A. O. & Ojediran, J. O. (2011). Moisture sorption isotherms of two varieties of millet. *Food and Bioproducts Processing,* 89, 178–184.

Saffari, M. & Langrish, T. (2014). Effect of lactic acid in-process crystallization of lactose/protein powders during spray drying. *Journal of Food Engineering,* 137, 88–94.

Salameh, A. K., Mauer, L. J. & Taylor, L. S. (2006). Deliquescence lowering in food ingredient mixtures. *Journal of Food Science,* 71, E10–E16.

Salameh, A. K. & Taylor, L. S. (2006a). Deliquescence-induced caking in binary powder blends. *Pharmaceutical Development and Technology,* 11, 453–464.

Salameh, A. K. & Taylor, L. S. (2006b). Role of deliquescence lowering in enhancing chemical reactivity in physical mixtures. *The Journal of Physical Chemistry B,* 110, 10190–10196.

Schmitt, E. A., Peck, K., Sun, Y. & Geoffroy, J. (2001). Rapid, practical and predictive excipient compatibility screening using isothermal microcalorimetry. *Thermochimica Acta,* 380, 175–183.

Shoaib, M., Shehzad, A., Omar, M., Rakha, A., Raza, H., Sharif, H. R., Shakeel, A., Ansari, A. & Niazi, S. (2016). Inulin: Properties, health benefits and food applications. *Carbohydrate Polymers,* 147, 444–454.

Stoklosa, A. M., Lipasek, R. A., Taylor, L. S. & Mauer, L. J. (2012). Effects of storage conditions, formulation, and particle size on moisture sorption and flowability of powders: A study of deliquescent ingredient blends. *Food Research International,* 49, 783–791.

Storey, D., Lee, A., Bornet, F. & Brouns, F. (2007). Gastrointestinal tolerance of erythritol and xylitol ingested in a liquid. *European Journal of Clinical Nutrition,* 61, 349–354.

Sun, C. (2009). Improving powder flow properties of citric acid by crystal hydration. *Journal of Pharmaceutical Sciences,* 98, 1744–1749.

Talja, R. A. & Roos, Y. H. (2001). Phase and state transition effect on dielectric, mechanical and thermal properties of polyols. *Thermochimica Acta,* 380, 109–121.

Tham, T. W. Y., Wang, C., Yeoh, A. T. H. & Zhou, W. (2016). Moisture sorption isotherm and caking properties of infant formulas. *Journal of Food Engineering,* 175, 117–126.

Thorat, A., Marrs, K. N., Ghorab, M. K., Meunier, V., Forny, L., Taylor, L. S. & Mauer, L. J. (2017). Moisture-mediated interactions between amorphous maltodextrins and crystalline fructose. *Journal of Food Science,* 82, 1142–1156.

Ur-Rehman, S., Mushtaq, Z., Zahoor, T., Jamil, A. & Murtaza, M. A. (2015). Xylitol: a review on bioproduction, application, health benefits, and related safety issues. *Critical Reviews in Food Science and Nutrition,* 55, 1514–1528.

Van Boekel, M. A. J. S. (2008). Kinetic modeling of reactions in foods. Boca Raton: CRC Press.

Viljoen, M., Muller, M., De Beer, D. & Joubert, E. (2017). Identification of broad-based sensory attributes driving consumer preference of ready-to-drink rooibos iced tea with increased aspalathin content. *South African Journal of Botany,* 110, 177-183.

Wahl, M., Bröckel, U., Brendel, L., Feise, H. J., Weigl, B., Röck, M. & Schwedes, J. (2008). Understanding powder caking: Predicting caking strength from individual particle contacts. *Powder Technology,* 188, 147–152.

Walters, N. A., De Villiers, A., Joubert, E. & De Beer, D. (2017). Improved HPLC method for rooibos phenolics targeting changes due to fermentation. *Journal of Food Composition and Analysis,* 55, 20–29.

Wibowo, S., Grauwet, T., Gedefa, G. B., Hendrickx, M. & Van Loey, A. (2015). Quality changes of pasteurised mango juice during storage. Part II: Kinetic modelling of the shelf-life markers. *Food Research International,* 78, 410–423.

SUPPLEMENTARY MATERIAL CHAPTER 4_ADDENDUM B

Table B.1

The adjusted coefficient of determination (R^2_{adj}) between average measured and estimated aspalathin content of green rooibos powders stored at 30°C/65 % RH and 40°C/65 % RH for 12 months in sealed glass vials and 5 months in semi-permeable sachets. Data were fitted to for zero order, first order, second order and fractional conversion (based on first order) models

Storage condition		Formulation	R^2_{adj}			
			Zero order[a]	First order[b]	Second order[c]	Fractional conversion[d]
Vials	30°C	GRE[e]	N/A	N/A	N/A	N/A
		IN50[f]	N/A	N/A	N/A	N/A
		F3[g]	0.6678	0.6968	0.7267	0.9546
		F4[h]	0.9348	0.9414	0.9323	0.9324
		F5[i]	0.8760	0.8229	0.7590	0.8549
		F6[j]	0.7602	0.8235	0.8765	0.9412
		F7[k]	0.8997	0.9280	0.9418	0.9481
	40°C	GRE	0.7972	0.8166	0.8339	0.8769
		IN50	N/A	N/A	N/A	N/A
		F3	0.8601	0.9270	0.9515	0.9524
		F4	0.9405	0.9754	0.9370	0.9749
		F5	0.9474	0.9273	0.8375	0.9531
		F6	0.9219	0.9759	0.9081	0.9784
		F7	0.9364	0.9722	0.8999	0.9805
Sachets	30°C	GRE	N/A	N/A	N/A	N/A
		IN50	N/A	N/A	N/A	N/A
		F3	0.8097	0.8206	0.8302	0.8681
		F4	0.8220	0.8366	0.8506	0.9135
		F5	0.7396	0.7578	0.7759	0.8683
		F6	0.9435	0.9574	0.9617	0.9612
		F7	0.8361	0.8646	0.8880	0.9108
	40°C	GRE	0.8670	0.8805	0.8922	0.9141
		IN50	N/A	N/A	N/A	N/A
		F3	0.9005	0.9271	0.9427	0.9412
		F4	0.9584	0.9655	0.9512	0.9678
		F5	0.8200	0.8786	0.9275	0.9692
		F6	0.9134	0.9751	0.9529	0.9725
		F7	0.9231	0.9493	0.9500	0.9428

[a]Zero order model: $C = C_0 - Kt$; [b]First-order model : $C = C_0 \exp(-Kt)$; [c]Second-order model: $C = C_0/(1 + C_0 Kt)$; [d]Fractional conversion model: $C_\infty + (C_0 - C_\infty) * \exp(-K*t)$ where C is aspalathin (g/100 g extract, d.b.), C_0 is initial aspalathin (g/100 g extract, d.b.), t is the time in minutes and C_∞ the stable fraction of aspalathin (g/100 g extract, d.b.); [e]Green rooibos extract; [f]GRE microencapsulated with inulin in 1:1 ratio (m/m); [g]Formulation 3 (IN50 and sucrose); [h]Formulation 4 (IN50 and xylitol); [i]Formulation 5 (IN50, xylitol and citric acid); [j]Formulation 6 (IN50, xylitol and ascorbic acid); [k]Formulation 7(IN50, xylitol, citric acid and ascorbic acid)

Table B.2

Nothofagin degradation (%) and average degradation rate constants (K) of the first order model[a] fitted to the experimental data representing nothofagin degradation in green rooibos powders during storage at 30°C,/65 % RH and 40°C/65 % RH for 12 months in glass vials and 5 months in semi-permeable sachets

	Sealed glass vials						Semi-permeable sachets					
	30°C/65% RH			40°C/65% RH			30°C/65% RH			40°C/65% RH		
	Decrease (%) after 12 months	K (month^{-1})	R^2_{adj}	Decrease (%) after 12 months	K (month^{-1})	R^2_{adj}	Decrease (%) after 5 months	K (month^{-1})	R^2_{adj}	Decrease (%) after 5 months	K (month^{-1})	R^2_{adj}
GRE[b]	8.33 ± 0.56 d[c]	N/A[d]	N/A	20.17 ± 1.92 d	0.0203 ± 0.0020 e	0.9164	5.34 ± 1.40 e	N/A	N/A	17.34 ± 2.19 f	0.0349 ± 0.0026 f	0.8434
IN50[e]	10.24 ± 0.86 d	N/A	N/A	12.11 ± 1.60 d	N/A	N/A	0.36 ± 0.51 f	N/A	N/A	3.33 ± 0.35 g	N/A	N/A
F3[f]	18.91 ± 1.85 c	0.0168 ± 0.0004c	0.6901	48.88 ± 1.21 c	0.0689 ± 0.0023 d	0.9453	24.05 ± 2.11 c	0.0468 ± 0.0133 bc	0.8171	37.62 ± 6.24 e	0.0865 ± 0.0093 e	0.9026
F4[g]	36.03 ± 3.28 b	0.0377 ± 0.0021 b	0.8641	76.36 ± 0.63 b	0.1127 ± 0.0034 c	0.9816	19.90 ± 3.30 d	0.0382 ± 0.0062 c	0.6979	59.46 ± 1.30 c	0.1425 ± 0.0047 c	0.9484
F5[h]	48.49 ± 2.88 a	0.0578 ± 0.0096 a	0.9095	88.12 ± 0.62 b	0.1448 ± 0.0022 b	0.9357	29.08 ± 3.00 b	0.0592 ± 0.0053 b	0.7822	47.73 ± 3.34 d	0.1144 ± 0.0053 d	0.8308
F6[i]	35.74 ± 3.50 b	0.0409 ± 0.0048 b	0.7896	85.25 ± 0.46 a	0.1525 ± 0.0028 a	0.9786	39.65 ± 4.30 a	0.0823 ± 0.0091 a	0.9327	80.20 ± 2.22 a	0.2691 ± 0.0080 a	0.9560
F7[j]	33.73 ± 3.25 b	0.0345 ± 0.0029 b	0.8754	90.73 ± 0.73 a	0.1557 ± 0.0017 a	0.9802	40.79 ± 2.08 a	0.0829 ± 0.0073 a	0.8619	66.04 ± 1.88 b	0.1739 ± 0.0071 b	0.9300

[a]First order model : $C = C_0 \exp(-Kt)$, where C is nothofagin (g/100 g extract, d.b. data not shown), C_0 is initial nothofagin (g/100 g extract, d.b. data not shown), t is the time in months and K is the reaction rate constant; [b]Green rooibos extract; [c]Means in the same column with the same letter are not significantly different ($P \geq 0.05$); [d]Less than 10% change in nothofagin content observed – not suitable for kinetic modelling; [e]GRE microencapsulated with inulin in 1:1 ratio (m/m); [f]Formulation 3 (IN50 and sucrose); [g]Formulation 4 (IN50 and xylitol); [h]Formulation 5 (IN50, xylitol and citric acid); [i]Formulation 6 (IN50, xylitol and ascorbic acid); [j]Formulation 7 (IN50, xylitol, citric acid and ascorbic acid)

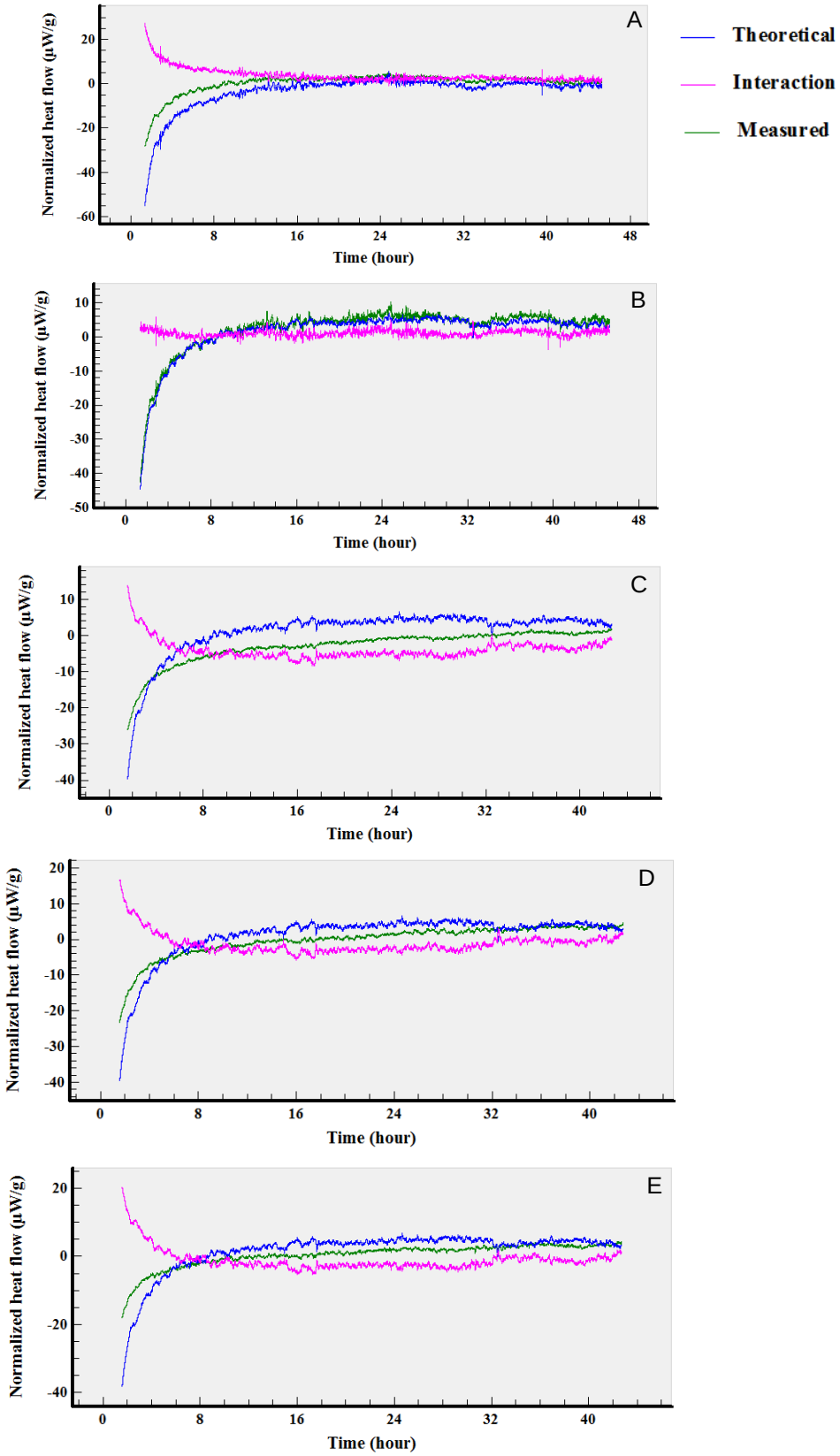

Fig. B.1 Measured, theoretical (as calculated from individual ingredients) and interaction heat flow of green rooibos powders: (A) F3 ((green rooibos extract microencapsulated with inulin in 1:1 ratio (m/m) (IN50) and sucrose), (B) F4 (IN50 and xylitol), (C) F5 (IN50, xylitol and citric acid), (D) F6 (IN50, xylitol and ascorbic acid) and (E) F7 (IN50, xylitol, ascorbic and citric acid).

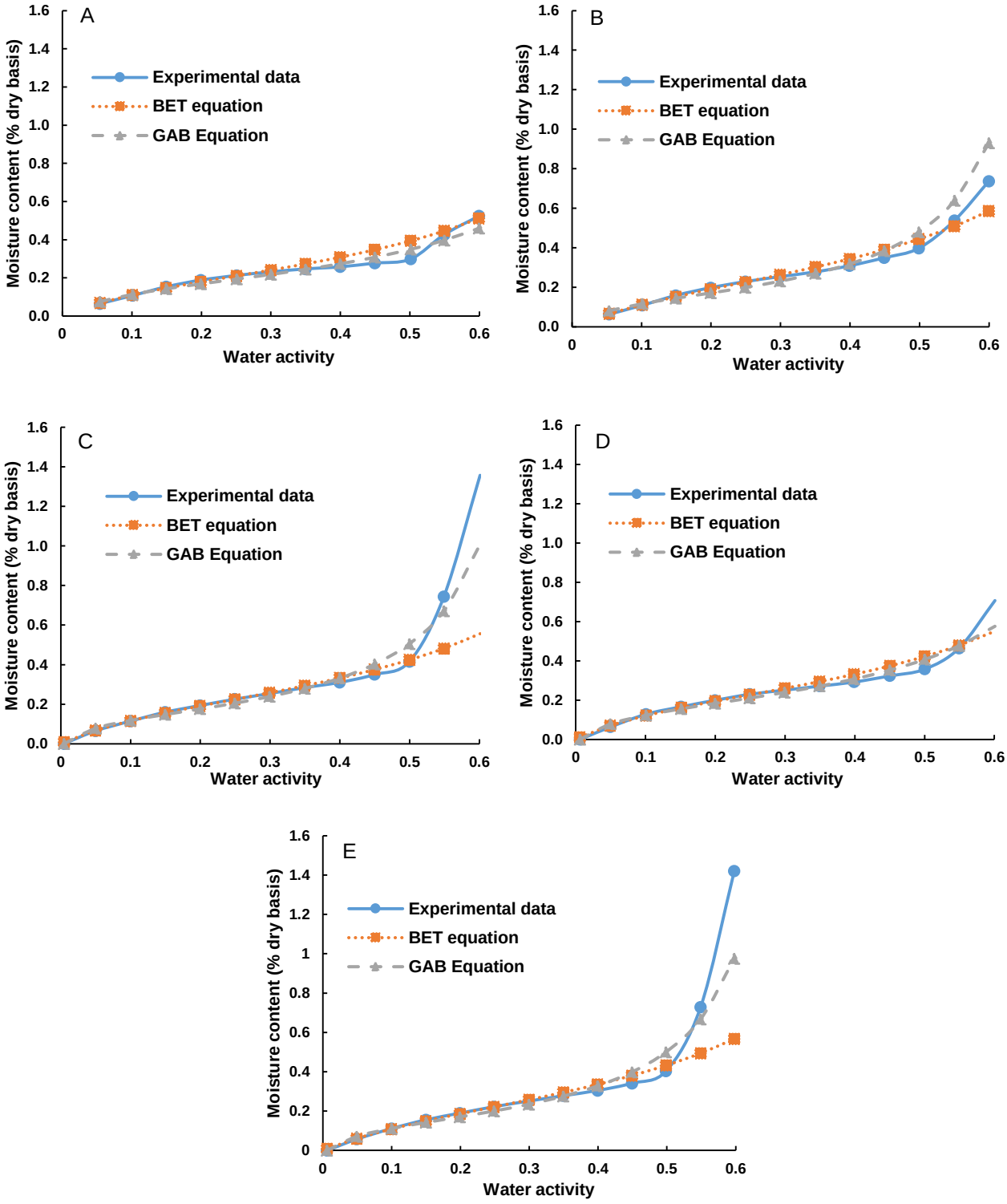

Fig. B.2 Moisture sorption isotherms of green rooibos powders at 25 °C: (A) F3 (green rooibos extract microencapsulated with inulin in 1:1 ratio (m/m) (IN50) and sucrose), (B) F4 (IN50 and xylitol), (C) F5 (IN50, xylitol and citric acid) and (D) F6 (IN50, xylitol and ascorbic acid) and (E) F7 (IN50, xylitol and ascorbic and citric acid) fitted with Brunauer-Emmet-Teller (BET) and Guggenhein-Anderson-de Boer (GAB) model.

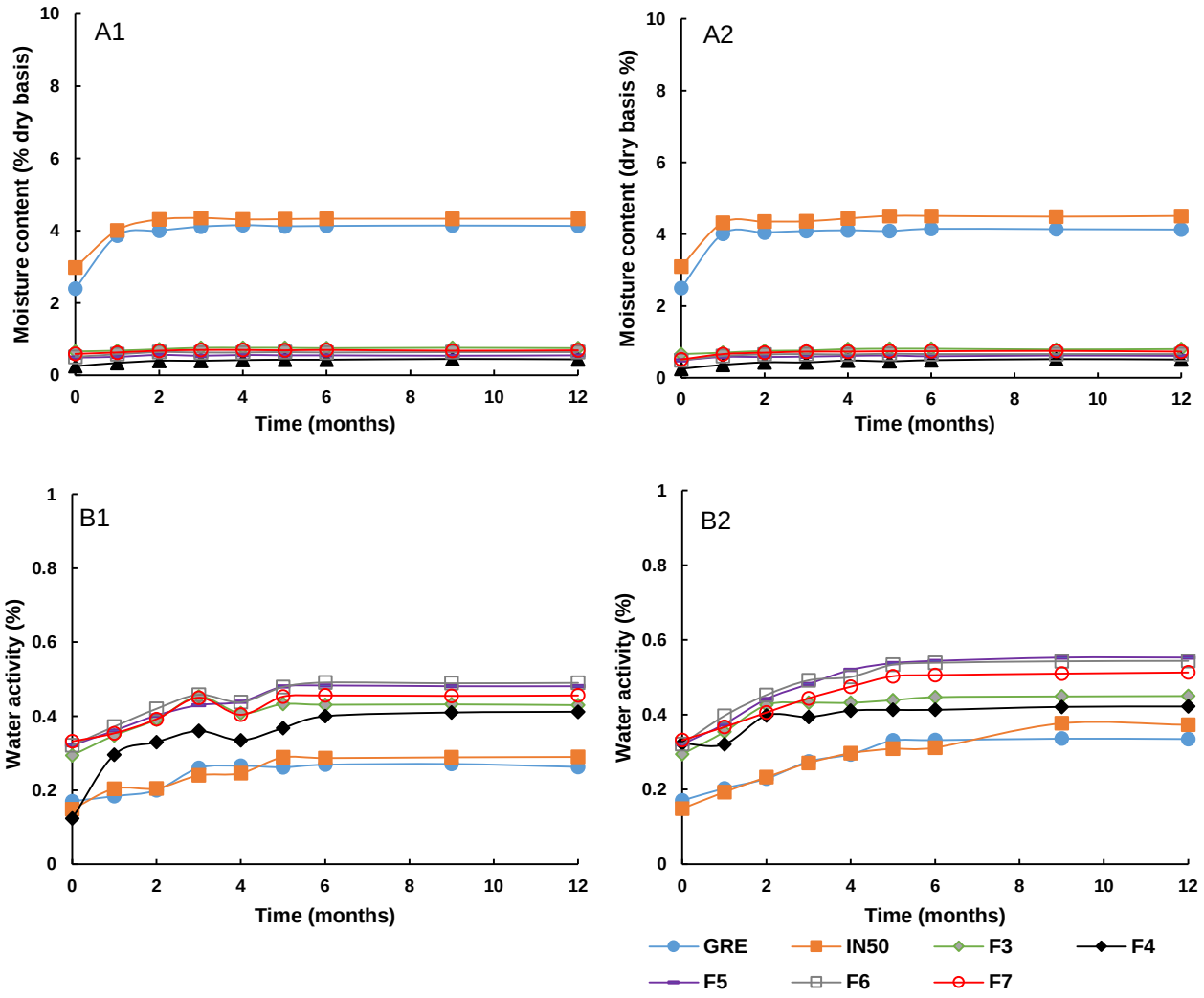

Fig. B.3 Moisture content (A) and water activity (B) of green rooibos powders: green rooibos extract (GRE), GRE microencapsulated with inulin in 1:1 ratio (m/m) (IN50), F3 (IN50 and sucrose), F4 (IN50 and xylitol), F5 (IN50, xylitol and citric acid), F6 (IN50, xylitol and ascorbic acid) and F7 (IN50, xylitol, ascorbic acid and citric acid) throughout storage at (1) 30°C/65% RH and (2) 40°C/65% RH for 12 months in sealed glass vials.

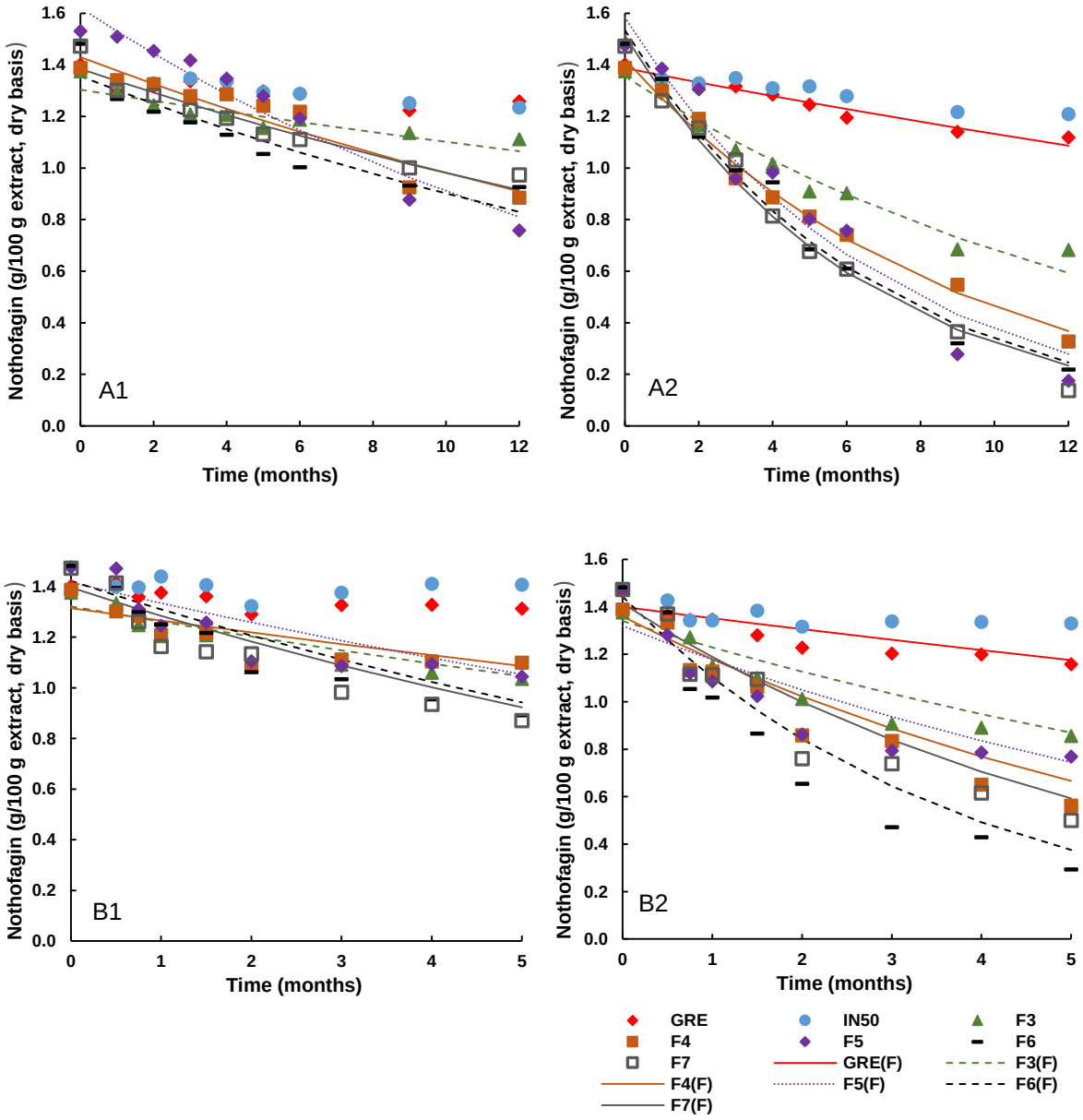

Fig. B.4 First order kinetic fitting (indicated by (F)) and experimental data of nothofagin degradation in green rooibos powders as a function of storage time: green rooibos extract (GRE), GRE microencapsulated with inulin in 1:1 ratio (m/m) (IN50), F3 (IN50 and sucrose), F4 (IN50 and xylitol), F5 (IN50, xylitol and citric acid), F6 (IN50, xylitol and ascorbic acid) and F7 (IN50, xylitol, ascorbic acid and citric acid), throughout storage at (1) 30°C/65% RH and (2) 40°C/65% RH for (A) 12 months in sealed glass vials and (B) 5 months in and semi-permeable sachets.

Chapter 5

Evaluation of conventional methods and electrospraying for nanoencapsulation of an aspalathin-rich fraction prepared from green rooibos with natural and synthetic polymers

*Published in *Food Chemistry*

DECLARATION BY THE CANDIDATE

With regard to *Chapter 5 (Pp. 164–189)*, the nature and scope of my contribution were as follows:

Nature of contribution	Extent of contribution (%)
Conducted all experimental work and data interpretation. Wrote the entire manuscript and edited the document in its entirety.	70%

The following co-authors have contributed to *Chapter 5 (Pp. 164–189)*:

Name	e-mail address	Nature of contribution	Extent of contribution (%)
Prof Dalene de Beer	DBeerD@arc.agric.za	Assisted in editing the document in its entirety	10%
Ms Marieta van der Rijst	VanDerRijstM@arc.agric.za	Advice and assistance with statistical analysis	5%
Prof Marique Aucamp	maucamp@uwc.ac.za	Isothermal microcalorimetry analyses and assistance with data interpretation	5%
Prof Elizabeth Joubert	JoubertL@arc.agric.za	Assisted in editing and contextualisation of the document in its entirety	10%

Signature of candidate: **Declaration with signature in possession of candidate and supervisor*	**Date**

DECLARATION BY CO-AUTHORS

The undersigned hereby confirm that:

1. the declaration above accurately reflects the nature and extent of the contributions of the candidate and the co-authors to *Chapter 5 (Pp. 164–189)*,
2. no other authors contributed to *Chapter 5 (Pp. 164–189)*, besides those specified above, and
3. potential conflicts of interest have been revealed to all interested parties and that the necessary arrangements have been made to use the material in *Chapter 5 (Pp. 164–189)* of this dissertation.

Signature	Institutional affiliation	Date
Prof Dalene de Beer	Plant Bioactives Group, Post-Harvest & Agro-Processing Technologies, Agricultural Research Council (ARC), Infruitec-Nietvoorbij	
Ms Marieta van der Rijst	Biometry Unit, Agricultural Research Council (ARC), Infruitec-Nietvoorbij	
Prof Marique Aucamp	School of Pharmacy, University of the Western Cape, Bellville, 7535, South Africa	
Prof Elizabeth Joubert	Plant Bioactives Group, Post-Harvest & Agro-Processing Technologies, Agricultural Research Council (ARC), Infruitec-Nietvoorbij	

ABSTRACT

The aim of the study was to identify a suitable polymer and method to produce a nanoparticulate nutraceutical food ingredient containing the bioactive hydrophilic dihydrochalcone, aspalathin. Polymers investigated included both natural (chitosan and lecithin) and synthetic (poly(lactide-co-glycolide) and a poly(methacrylic acid-co-methyl methacrylate) polymers, (Eudragit S100®, ES100)). Nanoencapsulation was achieved by a suitable conventional method and electrospraying for each polymer. All the particles were < 1.1 µm. Electrospraying produced more favourable results than the conventional methods for the synthetic polymers, resulting in spherical particles with higher encapsulation efficiencies (EE > 50%) and loading capacities (LC > 10%). The conventional methods performed better than electrospraying when using the natural polymers. An *in vitro* release study revealed biphasic aspalathin release profiles at pH 7.4 with ES100 electrosprayed nanoparticles having the slowest release rate (1.67 h^{-1}). Overall, these nanoparticles showed the most favourable combination of parameters for production of a nutraceutical food ingredient containing high amounts of aspalathin.

5.1 Introduction

Formulation of a powdered green rooibos nutraceutical ingredient produced by microencapsulation with inulin and addition of this ingredient to powder iced tea formulations improved stability of aspalathin, however, significant aspalathin losses due to hygroscopicity of the formulation were still apparent (**Chapter 3 and 4**). In an attempt to further address its stability, nanoencapsulation was investigated. In addition, efficient delivery of aspalathin, into the gastrointestinal tract (GIT), as is the case with various polyphenols, remains a challenge (Uzzan, Nechrebeki & Labuza, 2007; Braithwaite *et al.*, 2014). In some instances, nanoencapsulation of the bioactive compound could overcome these challenges (Ezhilarasi, Karthik, Chhanwal & Anandharamakrishnan, 2013).

Nanoencapsulation involves the encapsulation of a substance in nano-sized packages by absorption, incorporation, chemical interactions or dispersion (Anandharamakrishnan, 2014). It provides an attractive option for the reformulation of nutraceutical food ingredients as it could improve processability, shelf-life stability, thermal stability and solubility (Ezhilarasi *et al.*, 2013). Moreover, nanoencapsulation can also be used for the delivery of poorly bioavailable bioactive compounds in nutraceutical food ingredients as it can increase their absorption in cellular structures due to favourable particle shape, size, and surface properties. These properties enable nanoparticles to increase the solubilisation potential, alter absorption pathways by changing the rate and site of release, influence gastrointestinal dispersion and prevent premature metabolic degradation of a bioactive compound (Bilia, Isacchi, Righeschi, Guccione & Bergonzi, 2014). In the last two decades, nanoencapsulation have been applied to polyphenols and other food ingredients with varying levels of success although such studies have mainly focused on compounds that are poorly water-soluble. Different conventional encapsulation techniques include emulsion type systems, direct polymerisation methods and ionic/covalent interactions, amongst others (Anandharamakrishnan, 2014). One-step electrospraying processing, on the other hand, results in higher encapsulation efficiency and omits the use of extreme temperatures and vacuums. Furthermore, electrospraying is especially useful for hydrophilic bioactive compounds where leaching of the bioactive compound into the surrounding aqueous environment is a problem during conventional nanoencapsulation (Zamani, Prabhakaran & Ramakrishna, 2013). A range of natural and synthetic polymers are employed for nanoencapsulation. Natural encapsulating materials include polymers such as chitosan, alginates, cyclodextrins and phospholipids, amongst others (Hu, Liu, Zhang & Zeng, 2017). Synthetic polymers include biodegradable esters such as poly(lactide-co-glycolide) (PLGA), poly-Ɛ-caprolactone (PCL) and methacrylate polymers (Anandharamakrishnan, 2014). Studies directly comparing a range of methods or materials for a specific bioactive ingredient or compound are limited, making it difficult to establish which method/material is superior for a specific bioactive compound.

To date, investigation of the use of nanoencapsulated rooibos extract is limited to its application in a ready-to-drink rooibos beverage (De Beer, Joubert, Viljoen & Manley, 2011; Joubert *et al.*, 2010). An aspalathin-enriched green rooibos extract encapsulated together with ascorbic acid in a polyoxyethylene sorbitan monolaurate (Tween 20 emulsifier) shell improved the thermal and storage stability of aspalathin when in a beverage compared to the non-encapsulated extract, although shelf-life was still limited.

As a first step towards a nanoencapsulated nutraceutical ingredient for a functional beverage with a standardised aspalathin content, the present study evaluated two natural biodegradable (chitosan and lecithin) and two synthetic (poly(methacrylic acid-co-methyl methacrylate) copolymer, Eudragit S100® (ES100) and biodegradable PLGA) polymers for their suitability to produce nanoparticles loaded with an aspalathin-rich fraction prepared from green rooibos (*ca.* 40% aspalathin; GRAF). For each polymer a suitable conventional wet encapsulation method (i.e. ionic gelation for chitosan, thin-film hydration for lecithin liposomes, nanoprecipitation of ES100 and water-oil-water emulsion for PLGA), as well as electrospraying was compared. The polymers were chosen based on their properties, with all exhibiting sustained release (Liang *et al.*, 2011; Adibkia *et al.*, 2011; Zhang, Nie & Wang, 2013; Jahangiri *et al.*, 2014), which could aid in the protection of aspalathin in food formulations and in the gastrointestinal tract. In conjunction with this, the ES100 polymer has a targeted release profile at pH values above 7 (Akhgari *et al.*, 2017), which is ideal as aspalathin has been shown to be absorbed in the small intestines (Kreuz, Joubert, Waldmann & Ternes, 2008). Chitosan exhibits mucoadhesive properties (Liang *et al.*, 2011), which could help with the absorption of the poorly absorbed flavonoids found in GRAF (Muller *et al.*, 2018). The resulting nanoparticles were characterised based on process yield, encapsulation efficiency (EE), loading capacity (LC), zeta potential, particle morphology, compatibility of GRAF with the polymers, as well as thermal, chemical and crystal properties. The *in vitro* release profiles of aspalathin from selected nanoparticles were determined for additional characterisation and evaluation of the suitability of the polymers and methods.

5.2 Materials and methods

5.2.1 Chemicals

Poly(lactide-co-glycolide) (PLGA, Resomer RG 504 H) and Eudragit S100 (ES100, methacrylate acid copolymer) were obtained from Evonik Industries (Darmstadt, Germany). Warren Chemicals (Cape Town, South Africa) kindly donated food grade egg lecithin. Medium molecular mass (200–800 cps in 1% acetic acid) chitosan, poly(vinyl alcohol) (PVA, MW 31,000–50,000, 98–99% hydrolysed), cholesterol from sheep wool, sodium triphosphate pentabasic (TPP), dimethyl sulfoxide (DMSO), *n*-butanol (*n*-BuOH), anhydrous

dichloromethane (DCM), anhydrous chloroform ($CHCl_3$), anhydrous dimethylformamide (DMF), phosphate buffered saline tablets (PBS), hydrochloric acid (HCl) and ascorbic acid were obtained from Sigma Aldrich (St Louis, USA). High-performance liquid chromatography (HPLC) grade methanol (MeOH) and acetonitrile, glacial acetic acid and potassium acetate were obtained from Merck (Darmstadt, Germany). Deionised water prepared using an Elix water purification system was further purified to HPLC grade using a Milli-Q Academic water purification system from Merck. Aspalathin used as authentic reference standard (> 95% purity, HPLC-mass spectroscopy and -diode array detection (DAD)) was obtained from the South African Medical Research Council (SAMRC, Cape Town, South Africa).

5.2.2 Preparation of GRAF

GRAF, containing *ca.* 40% aspalathin, was prepared from green rooibos plant material as described previously (De Beer *et al.*, 2015). Briefly, a hot water extract was prepared at 93°C for 30 min using a plant material to water ratio of 1:10. The extract was filtered (Whatman nr 4 filter paper) and aliquots subjected to liquid-liquid fractionation using *n*-BuOH. The *n*-BuOH fractions were collected, evaporated under vacuum and the residue suspended in a small volume of water to allow freeze-drying.

5.2.3 Conventional wet nanoencapsulation

5.2.3.1 Chitosan-TPP nanoparticles

GRAF-chitosan-TPP nanoparticles (Ch-TPP) were synthesised by the ionic gelation method as demonstrated by Calvo, Remunan-Lopez, Vila-Jato & Alonso (1997). Chitosan (1.5 mg/mL) and GRAF were dissolved together by sonication (1 min, 80 W (50/60 HZ)) in aqueous acetic acid (1%, v/v) at a 1:4 (m/m) ratio. TPP (1.5 mg/mL), dissolved in deionised water, and the chitosan/GRAF solution were mixed to obtain a 5:2 (m/m) ratio of TPP:chitosan. The mixture was stirred on a magnetic stirrer for 60 min. Nanoparticles were collected by centrifugation (13680 $\times g$ for 10 min at 15°C) and washed twice with distilled water to remove non-encapsulated GRAF and organic solvents. An aliquot of the nanoparticle dispersion was freeze-dried in preparation for physicochemical analysis.

5.2.3.2 Lecithin liposomes

GRAF-lecithin liposomes (Li-TFH) were synthesised by the thin-film hydration method as proposed by Lu, Li & Jiang (2011) with minor modifications. Egg lecithin (400 mg/mL) and cholesterol (100 mg/mL) were dissolved in 10 mL $CHCl_3$ and GRAF in an equal volume of aqueous DMSO (10%, v/v) at a 1:4 (m/m)

GRAF:lipid ratio. The solution was sonicated in an ultrasonic bath at 250 W (44 KHz) for 10 min and evaporated under vacuum at 40 °C. The film was allowed to dry overnight and rehydrated with deionised water (20 mL) before further sonication for 10 min, followed by centrifugation as described for Ch-TPP nanoparticles.

5.2.3.3 PLGA nanoparticles

GRAF-PLGA nanoparticles (PLGA-WOW) were prepared by the water-in-oil-in-water (W/O/W) emulsion method as proposed by Srivastava *et al.* (2013) with minor modifications. GRAF (40 mg/mL) was dissolved in an aqueous DMSO solution (10%, v/v) and added to rapidly stirred (1000 rpm) PLGA (50 mg/mL) dissolved in DCM. The mixture was allowed to stir for 2 h. The ratio of aqueous solution to organic solvent was kept constant at 1:4 (v/v). The secondary emulsion was formed by adding 25 mL of the primary emulsion to 40 mL of a rapidly stirred aqueous PVA solution (1%, m/v). The solution was allowed to stir for a further 18 h which resulted in solid nanoparticles as the DCM evaporated. The particles were collected by centrifugation as described for Ch-TPP nanoparticles.

5.2.3.4 ES100 nanoparticles

GRAF-ES100 nanoparticles (ES100-NP) were prepared by the nanoprecipitation technique as previously demonstrated by Wu *et al.* (2008) with minor modifications. ES100 (20 mg/mL) and GRAF (5 mg/mL) were dissolved in MeOH by sonication (1 min, 80 W (50/60 HZ)). This solution mixture was added slowly in a dropwise fashion to a rapidly stirred aqueous PVA solution (1%, m/v). The ratio of aqueous solution to MeOH was kept constant at 20:1. Particle formation was instantaneous and followed by centrifugation as described for Ch-TPP nanoparticles.

5.2.4 Electrospray nanoencapsulation

Electrospraying conditions were kept constant, following preliminary experiments to select conditions producing Taylor cone formation, no dripping and SEM confirmation of particle formation. A plastic syringe (1 mL) with a stainless steel needle (20 gauge, 0.9 mm i.d.) containing the polymer solution was mounted on a Genie Plus metered syringe pump (Kent Scientific, Connecticut, USA), set at 4 µL/min. This was placed opposite a charged collector plate with a tip-to-collector distance of 15 cm. The collector plate and needle were connected to a high-voltage supply (Stellenbosch University Electrical Engineering Department, South Africa) with a summative voltage of 20 kV.

The concentrations and solvents of the feed solutions were selected to suit each polymer system. Chitosan (1%, m/m) was dissolved in 2% acetic acid (v/v), lecithin in $CHCl_3$ (15%, m/m), PLGA in DMF (7.5%, m/m) and

ES100 in MeOH (1%, m/m). GRAF was added to the feed solution at a ratio of 1:4 (m/m) with the polymer prior to electrospraying. The resulting particles were designated Ch-Espray, Li-Espray, ES100-Espray and PLGA-Espray.

5.2.5 Characterisation of nanoparticles

5.2.5.1 Process yield

The process yield, determined gravimetrically, was calculated as the mass of nanoparticles obtained, expressed as a percentage of the sum of the mass of GRAF and polymers added during nanoparticle preparation.

5.2.5.2 Encapsulation efficiency (EE) and loading capacity (LC)

The EE was determined in terms of aspalathin content (as the marker compound). An aliquot of each type of nanoparticle (*ca.* 1 mg/mL) was suspended in 10% (v/v) aqueous DMSO containing 10% (m/v) ascorbic acid to prevent oxidation of aspalathin and sonicated (ultrasonic bath, 250 W, 44 kHz) for 60 min to allow disintegration of the particles and full release of GRAF. After centrifugation (7690 × *g* at 15 °C for 10 min), the supernatant was analysed using HPLC with diode array detection (DAD) as described by De Beer *et al.* (2015). The EE (%) represents the encapsulated aspalathin (g) calculated as a percentage of the amount of aspalathin (g) initially added to the nanoparticle preparation. The LC (%) was calculated by expressing the encapsulated aspalathin (g) as a percentage of the mass of the nanoparticles (g). The loading capacity was adjusted to represent GRAF by taking into account the percentage of aspalathin in GRAF.

5.2.5.3 Scanning and scanning transmission electron microscopy (SEM and STEM), differential scanning calorimetry (DSC), X-ray powder diffraction (XRPD) and isothermal microcalorimetry

Imaging of the GRAF-loaded nanoparticles was accomplished using SEM and STEM. Thermograms and diffractograms of GRAF, polymers and nanoparticles were recorded with DSC and XRPD, respectively. Heat flow curves of GRAF, the blank polymer nanoparticles and GRAF-loaded nanoparticles obtained from isothermal microcalorimetry were used to calculate the interaction average heat flow error (µW/g). Experimental details, sample preparation and data processing are described in **Chapter 3**, section 3.2.4.2 (SEM and STEM), 3.2.4.5–3.2.4.6 (XRPD and DSC) and 3.2.4.8 (isothermal microcalorimetry).

5.2.5.4 Measurement of particle size, particle size distribution and zeta potential

Photo correlation spectroscopy (Zetasizer Nanoseries 2590, Malvern Instruments, England) was used to measure the particle size and the particle size distribution expressed as the polydispersity index (PDI). The zeta potential was calculated from the electrophoretic mobility of the particles in solution. Dry nanoparticles were suspended in distilled water (1 mg/mL) and measurements were repeated three times with each measurement consisting of four scans at 25 °C.

5.2.5.5 Fourier transform infrared (FTIR)

A Thermo-Scientific Nicolet iS10 Smart iTR instrument and Omnic software (Massachusetts, USA) were used to obtain FTIR spectra of GRAF, the polymers and nanoparticles. Measurements were done in attenuated total reflectance (ATR) mode with a resolution of 4 cm^{-1} and an average number of 64 scans over the wavenumber range of 450–4500 cm^{-1}.

5.2.5.6 In vitro release studies

Selected nanoparticles (Ch-TPP, Li-TFH, ES100-Espray, PLGA-Espray, *ca.* 20 mg) were suspended in 30 mL of PBS (pH 7.4) and incubated at 37 °C under gentle magnetic stirring (150 rpm). Additionally, the release profile of ES100 electrosprayed nanoparticles were investigated at pH 4 (potassium acetate buffer adjusted with HCl). Ascorbic acid (10%, m/v) was added to the buffer solutions to prevent degradation of the phenolic compounds. At predetermined intervals, 1 mL aliquots were removed and replaced by 1 mL fresh buffer to maintain sink conditions. The samples were centrifuged (7690 × *g* at 15 °C for 10 min) and the supernatants analysed using HPLC-DAD as described in section 5.2.5.2. After 8 h, the samples were sonicated (ultrasonic bath, 250 W, 44 kHz) for 1 h to determine the total amount of aspalathin remaining in the nanoparticles.

Various regression models were fitted on the data and the Gompertz model (Eq. 5.1) selected (highest adjusted coefficient of determination (R^2_{adj})) to characterise the release of aspalathin from the nanoparticles suspended in solution (Costa & Lobo, 2001):

$$Asp(t) = Asp_{max} e^{-e^{-k(t-t_{lag})}} \quad (5.1)$$

where $Asp(t)$ is the percentage aspalathin dissolved at time *t*, Asp_{max} is the maximum percentage of dissolved aspalathin, *k* is the release rate constant (h^{-1}) and t_{lag} is the inflection time point (h).

The mean dissolution time (MDT) (Eq. 5.2) was also calculated from the raw data using the following equation (Costa & Lobo, 2001):

$$MDT = \frac{\sum_{i=1}^{n} t_{mid} \Delta Asp}{\sum_{i=1}^{n} \Delta Asp} \quad (5.2)$$

where *n* is the number of time intervals, *i* is the interval number, t_{mid} is time at midpoint between two time intervals t_i and t_{i-1}, where *i-1* is the previous interval number to *i* and ΔAsp is the additional percentage of aspalathin dissolved between t_i and t_{i-1}.

5.2.6 Statistical analysis

The experimental design was completely random with three independently replicated experiments for each of the nanoparticle systems, namely Ch-TPP, Ch-Espray, Li-TFH, Li-Espray, ES100-NP, ES100-Espray, PLGA-WOW and PLGA-Espray. Univariate Analysis of Variance (ANOVA), using the GLM (General Linear Models) procedure of SAS software (Version 9.4; SAS Institute Inc, Cary, USA), was performed on all measured variables to compare the systems,.

For the *in vitro* release study, aspalathin release at different time intervals was observed for each experimental replicate. These observations over time were combined in a split-plot ANOVA with nanoparticle system as main plot factor and time as sub-plot factor. Regression analysis with time as independent variable was also performed for each experimental replicate to describe aspalathin release patterns over time, using the NLIN procedure of SAS. Regression parameters obtained for the Gompertz model were used as input in an ANOVA for the nanoparticle types.

The Shapiro-Wilk test was performed on the data to test for normality. Fisher's least significant difference (LSD) was calculated at the 5% level to compare means. $P < 0.05\%$ was considered significant.

5.3. Results and discussion

5.3.1 Evaluation of GRAF-loaded nanoparticles

Two natural and two synthetic polymeric encapsulating materials were investigated for suitability to prepare GRAF-loaded nanoparticles. Each polymer was processed using two methods, i.e. conventional wet nanoparticle formation and electrospraying. Amongst the particle characteristics, the particle morphology, size and EE were considered to be the most important parameters.

5.3.1.1 Process yield, EE and LC

The process yields were all > 70%, except for the chitosan nanoparticles, which showed yields of 18.1% and 57.9% for electrospraying and ionic gelation, respectively (Table 5.1). The low yield for electrospraying could be attributed to the high conductivity of the polymer solution as a result of the amine groups that

complicates the electrospraying process, as well as the viscous nature of dissolved chitosan (Duan, Dong, Yuan & Yao, 2004).

The EE is a good measure of the success of the encapsulation. Varying results were obtained, depending on the combination of polymer and method (Table 5.1). The two synthetic polymers, ES100 and PLGA, showed significantly higher EE values for the electrospraying method (55.4% and 50.8%, respectively) compared to the conventional encapsulation methods (1.6% and 1.2%, respectively). The reverse was observed for the natural polymers, chitosan and lecithin, i.e. high EE values were obtained for conventional encapsulation methods (31.1% and 86.8%, respectively) compared to electrospraying (4.4% and 74.4%, respectively). The solubility of the bioactive compound in the matrix and solvent used to dissolve the polymeric material largely determined the EE and LC of the conventional methods (Kumari, Yadav, Pakade, Singh & Yadav, 2010). In the case of hydrophilic bioactive compounds, such as aspalathin, leaching of the compound into the surrounding medium due to lack of interaction between the hydrophilic compound and the hydrophobic polymeric materials is not uncommon. This could explain the low EE for GRAF in the synthetic polymers processed by the conventional encapsulation methods. On the other hand, the natural polymeric materials allow for interaction between the polymer and aspalathin during conventional processing as chitosan is also hydrophilic (Arulmozhi, Pandian & Mirunalini, 2013) and liposomes possess a hydrophilic core (Fang & Bhandari, 2010). Studies on green tea phenolic compounds and nutraceutical extracts similarly found that for conventional processing methods (e.g. emulsions, nanoprecipitation, ionic gelation, etc.), natural polymers tend to achieve higher encapsulation efficiencies compared to synthetic polymers (Sanna *et al.*, 2015). In the case of the synthetic polymers showing higher EE values for electrospraying, even though there are no or minimal interactions between aspalathin and the synthetic polymers, there is limited opportunity of leaching of GRAF, as the solidification and solvent evaporation occur in a single step (Zamani *et al.*, 2013).

The LC will ultimately determine the product dose of the nanoparticles, which preferably needs to be minimised for cost and biological implications. The LC of the particles produced by conventional processing methods varied from 0.2% to 20.0% and from 1.0% to 17.1% for electrospraying, with lecithin liposomes having the highest LC (Table 5.1). These range of LC values is not uncommon for other reported nanoparticle systems. Loading capacities of 5.7% were reported for curcumin-PLGA (Xie *et al.*, 2011), 3.0–6.2% for hesperetin-lipid (Fathi, Varshosaz, Mohebbi & Shahidi, 2012) and 8.0–16.0% for green tea-chitosan (Liang *et al.*, 2011) nanoparticles.

5.3.1.2 Particle morphology, size, distribution and zeta potential

The SEM (Fig. 5.1) images of the GRAF-loaded nanoparticles showed a range of morphologies. No distinction between GRAF and the polymer phases could be made from the selected STEM images (Supplementary C.1), possibly due to similar elements in the polymers and extracts. Morphologically favourable (i.e. smooth, spherical, un-clumped particles) particles were formed when using natural polymers, chitosan and lecithin, with conventional methods and synthetic polymers, ES100 and PLGA, when electrosprayed. Such particles have better *in vitro* distribution, absorption and also general handleability (Bilia *et al.*, 2014). Electrospraying of the natural polymers resulted in irregular and fused nanoparticles. Particle formation by electrospraying is affected by various factors, where in the present study all factors were kept constant except the polymer concentration and solvent. Thus, differences in the particle morphologies can be attributed to the conductivity of the polymer in solution and the boiling point of the solvent (Torres-Giner, Wilkanowicz, Melendez-Rodriguez & Lagaron, 2017).

Particle sizes and particle size distribution (expressed as the PDI) were determined by photo correlation spectroscopy and expressed as the average of mean values (Table 5.1). The chitosan particles prepared by ionic gelation had the smallest average size (128 nm), followed by the electrosprayed ES100 (189 nm). Lecithin, when electrosprayed, resulted in very large particles > 1000 nm, which is consistent with the SEM images (Fig. 5.1) and other studies that showed undefined and clumped particle morphologies (Yu, Yang, Wang & Tian, 2012). Generally, the synthetic polymers formed GRAF-loaded nanoparticles with smaller diameters when electrosprayed, whereas the conventional encapsulation techniques produced GRAF-loaded nanoparticles with smaller diameters when using natural polymers.

The PDI provides a measure of the dispersity of the particle sizes in solution, whth PDI values of 0.0 to 0.1 classified as monodisperse, 0.1 to 0.7 moderately polydisperse and from 0.7 to 1.0 broadly polydisperse (Stetefeld, McKenna & Patel, 2016). All the PDI values were > 0.4, indicating a polydisperse distribution (Table 5.1). This is also shown by the distribution graphs obtained from the SEM images (Supplementary material, Fig. C.2). Particles with these types of distributions have a greater tendency to aggregate and sediment in solution (Wyatt, 2014).

The zeta potential is a measure of the charge potential on the surface of the particles. A higher absolute zeta potential and surface charge represent higher repulsion forces between particles and theoretically higher stability (Fathi *et al.*, 2012). The zeta potential values for the nanoparticles made with the same polymer were very similar even when using different processing methods, indicating that the zeta potential is largely dependent on the characteristics of the polymer itself (Table 5.1). GRAF-loaded ES100 electrosprayed nanoparticles had the highest absolute zeta potential (44.3 mV). The GRAF-loaded chitosan nanoparticles

had the lowest absolute zeta potential, but it was the only system with a positive potential, indicating its mucoadhesive nature, which could enhance absorption of the particles. The intestinal mucosa are dominated by negatively charged compounds and thus slightly positively charged particles pass more efficiently through the cell membranes (Berscht, Nies, Liebendörfer & Kreuter, 1994).

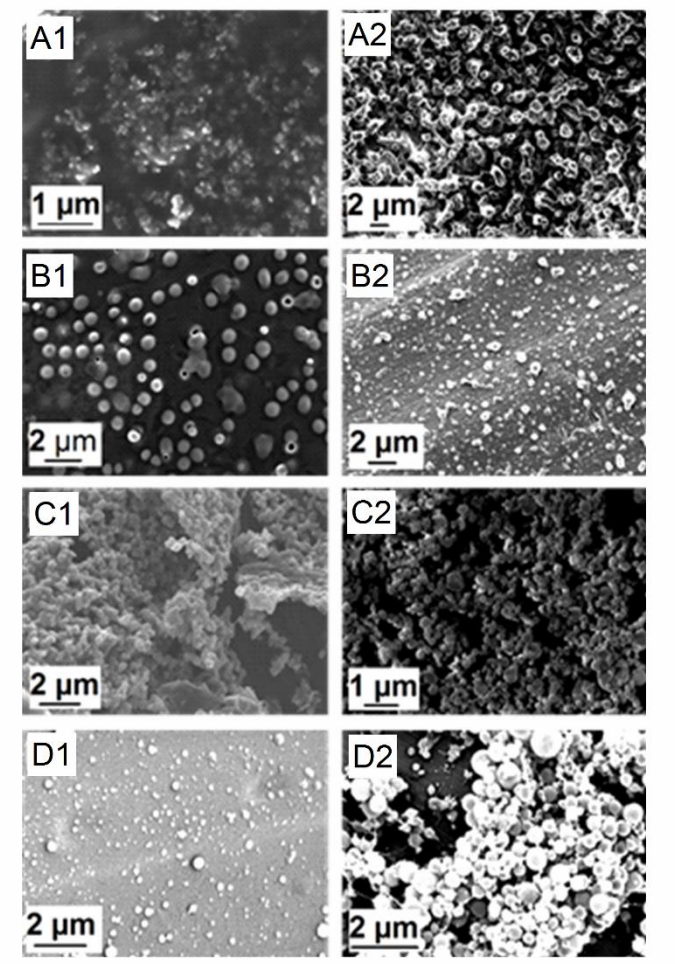

Fig. 5.1 Scanning electron microscope images of nanoparticles loaded with an aspalathin-rich fraction from green rooibos prepared using: (A) lecithin, (B) chitosan, (C) Eudragit S100 (ES100) and (D) poly(lactide-co-glycolide) (PLGA) synthesised by (1) conventional methods and (2) electrospraying.

.

Table 5.1

Summary of the process yield, encapsulation efficiency (EE), loading capacity (LC), particle size, zeta potential and polydispersity index (PDI) for the nanoparticles containing an aspalathin-rich fraction prepared from green rooibos prepared using different polymers and encapsulation methods.

Polymer	Method	Nanoparticle system	Yield (%)	EE (%)	LC (%)	Particle size (nm)	PDI	Zeta potential (mV)
chitosan	conventional	Ch-TPP[a]	57.9 ± 1.9 e[b]	31.1 ± 0.2 e	7.1	128 ± 15 f	0.81 ± 0.21 ab	13.4 ± 0.3 a
	electrospray	Ch-Espray[c]	18.1 ± 0.9 f	4.4 ± 0.0 f	1.0	334 ± 42 c	0.65 ± 0.31 abc	12.2 ± 0.4 a
lecithin	conventional	Li-TFH[d]	73.9 ± 2.2 c	86.8 ± 0.1 a	20.0	332 ± 16 c	0.41 ± 0.09 c	−37.3 ± 2.2 d
	electrospray	Li-Espray[e]	70.3 ± 2.9 d	74.4 ± 0.4 b	17.1	1093 ± 33 a	0.92 ± 0.13 a	−35.6 ± 0.6 cd
ES100	conventional	ES100-NP[f]	79.4 ± 0.9 a	1.6 ± 0.0 g	0.3	247 ± 15 d	0.72 ± 0.16 ab	−37.2 ± 0.2 d
	electrospray	ES100-Espray[g]	77.9 ± 0.7 ab	55.4 ± 0.1 c	12.7	190 ± 2 e	0.53 ± 0.14 bc	−44.3 ± 0.2 e
PLGA	conventional	PLGA-WOW[h]	77.6 ± 1.9 ab	1.2 ± 0.0 h	0.2	414 ± 9 b	0.76 ± 0.09 ab	−32.9 ± 1.5 bc
	electrospray	PLGA-Espray[i]	75.7 ± 1.2 bc	50.8 ± 0.0 d	10.2	333 ± 25 c	0.55 ± 0.17 bc	−31.6 ± 3.3 b

[a]Chitosan-tripolyphosphate nanoparticles prepared by ionic gelation; [b]Means in the same column with the same letter are not significantly different ($P \geq 0.05$) [c]Chitosan nanoparticles prepared by electrospraying; [d]Lecithin nanoparticles prepared by thin film hydration method; [e]Lecithin nanoparticles prepared by electrospraying; [f]Eudragit S100 nanoparticles prepared by nanoprecipitation method; [g]Eudragit S100 nanoparticles prepared by electrospraying; [h]Poly(lactide-co-glycolide) nanoparticles prepared by water-in-oil-water emulsion method; [i]Poly(lactide-co-glycolide) nanoparticles prepared by electrospraying.

5.3.2 XRPD, DSC and FTIR analyses of selected nanoparticles

Ch-TPP, Li-TFH, PLGA-Espray and ES100-Espray were selected for further analyses as these nanoparticle systems had the most favourable combination of properties, including yield, EE, LC and particle size. XRPD, DSC and FTIR analyses were performed in order to determine the physical state of the four selected GRAF-loaded nanoparticles and possible interactions of GRAF constituents with the polymers (chitosan, lecithin, PLGA and ES100).

DSC thermograms (Fig. 5.2) of the polymers, nanoparticles and GRAF displayed a weak endothermic signal between 30 and 80 °C, which is indicative of water loss (Dudhani & Kosaraju, 2010). The polymers and GRAF showed no distinct crystalline melting peaks, indicating their amorphous nature (Jahangiri *et al.*, 2014). However, broad phase transitions were visible for the polymers. The DSC thermograms for the GRAF-loaded nanoparticles were different compared to those of the polymers, indicating that GRAF was incorporated into the polymeric matrix preventing the normal organisation of the polymeric chains (Jahangiri *et al.*, 2014).

XRPD diffractograms (Fig. 5.3) confirmed that all polymers, nanoparticles and GRAF were amorphous, evident from the typical 'halo' and flat patterns, as also demonstrated for curcumin encapsulated in PLGA (Xie *et al.*, 2011) and Naproxen encapsulated in Eudragit (Adibkia *et al.*, 2011). Minimal evidence of amorphous 'halo' patterns were evident after incorporation of GRAF into the nanoparticles, indicating a 'dilution effect', most clearly shown by the flat diffractograms of Ch-TPP and ES100-Espray nanoparticles. The inclusion of GRAF had no significant effect on the amorphous structure of the polymers and no crystallisation occurred evident from the absence of sharp peaks (Adibkia *et al.*, 2011).

FTIR (Fig. 5.4) is a useful tool to investigate possible chemical and physical interactions between the polymers and GRAF constituents. When comparing the polymers with the GRAF-loaded nanoparticles, the spectra for the Li-TFH and PLGA-Espray nanoparticles appear to be identical to those of the respective polymers, i.e. lecithin and PLGA, indicating that GRAF is possibly encapsulated inside the polymer matrix and not on the surface (Sanna *et al.*, 2015). The spectra of the ES100-Espray nanoparticles showed the addition of a broad OH peak between 3000–3600 cm^{-1} and a sharp C=O peak at 1615 cm^{-1}, also evident in the GRAF spectrum and attributed to the flavonoids present. The spectrum of GRAF-loaded Ch-TPP nanoparticles also showed a faint indication of the OH functionality at 3000-3600 cm^{-1}, but not the C=O peak. These additional peaks in the spectra of the nanoparticles are evidence of the presence of GRAF on the surface of the nanoparticles (Sanna *et al.*, 2015).

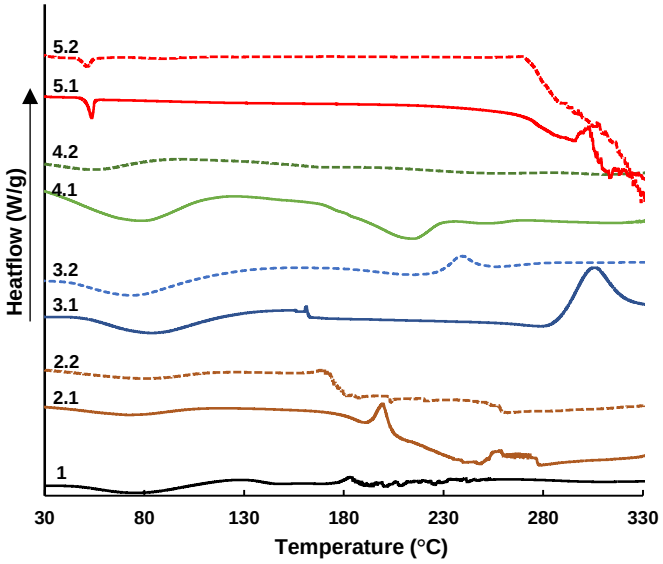

Fig. 5.2 Differential scanning calorimetry thermograms of an aspalathin-rich fraction prepared from green rooibos (1), lecithin (2.1), chitosan (3.1), Eudragit S100 (ES100) (4.1) and poly(lactide-co-glycolide) (PLGA) (5.1), as well as nanoparticles processed by conventional methods, namely lecithin-thin film hydration (Li-TFH) (2.2) and chitosan-tripolyphosphate (Ch-TPP) (3.2), and by electrospraying, namely Eudragit S100 (ES100-Espray) (4.2) and poly(lactide-co-glycolide) (PLGA-Espray) (5.2).

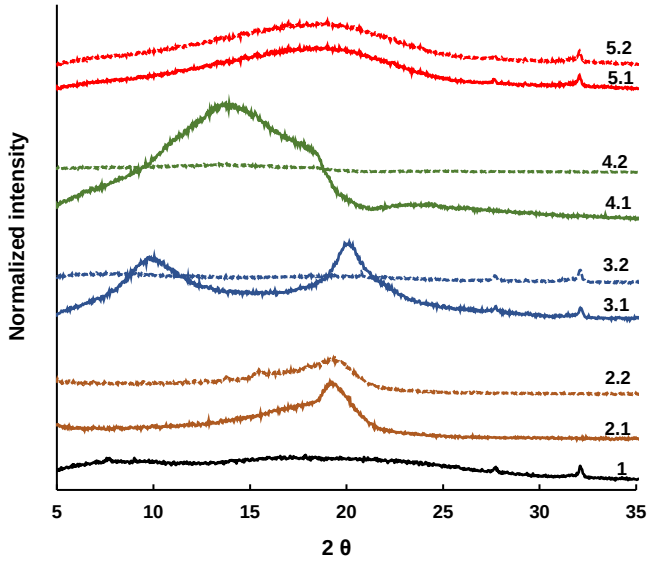

Fig. 5.3 X-ray powder diffractograms of an aspalathin-rich fraction prepared from green rooibos (1), lecithin (2.1), chitosan (3.1), Eudragit S100 (ES100) (4.1) and poly(lactide-co-glycolide) (PLGA) (5.1), as well as nanoparticles processed by conventional methods, namely lecithin-thin film hydration (Li-TFH) (2.2) and chitosan-tripolyphosphate (Ch-TPP) (3.2), and by electrospraying, namely Eudragit S100 (ES100-Espray) (4.2) and poly(lactide-co-glycolide) (PLGA-Espray) (5.2).

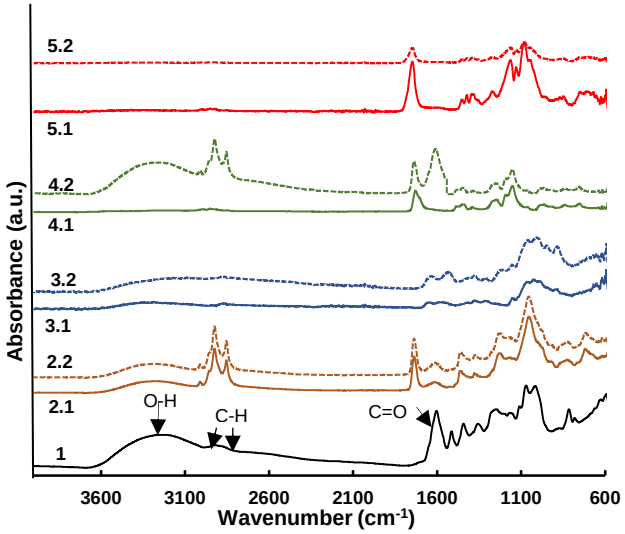

Fig. 5.4 Fourier transform infrared spectra of an aspalathin-rich fraction prepared from green rooibos (1), lecithin (2.1), chitosan (3.1), Eudragit S100 (ES100) (4.1) and poly(lactide-co-glycolide) (PLGA) (5.1), as well as nanoparticles processed by conventional methods, namely lecithin-thin film hydration (Li-TFH) (2.2) and chitosan-tripolyphosphate (Ch-TPP) (3.2), and by electrospraying, namely Eudragit S100 (ES100-Espray) (4.2) and poly(lactide-co-glycolide) (PLGA-Espray) (5.2).

5.3.3 Compatibility of GRAF with polymers

The heat flow error, representing the difference between the average interaction heat flow values obtained from the GRAF nanoparticles and theoretical non-interaction curve (obtained for the blank polymer nanoparticles and GRAF) were used to evaluate possible incompatibilities between GRAF and the polymers. The interaction average heat flow errors (Table 5.2 and supplementary material Fig. C.3) were much higher for chitosan (7885.10 µW/g) and slightly higher for lecithin systems (22.84 µW/g) than for ES100 (4.46 µW/g) and PLGA systems (3.25 µW/g). Thus, the natural polymer systems have a higher possibility for interaction between GRAF and the polymer during storage, which might cause instabilities during storage and prevent long-term storage. It is important to note that the average interaction heat flow error values are very small, implying a very low degree of incompatibility. A precise cause of instability cannot be identified as the heat flow curves are non-specific and are a summary of all the reactions that take place under the specified conditions (Chadha & Bhandari, 2004).

Table 5.2

Interaction average heat flow values obtained from isothermal microcalorimetry for nanoparticles loaded with an aspalathin-rich fraction prepared from green rooibos

Formulation	Interaction average heat flow (µW/g) (absolute values)	Interaction average heat flow error (µW/g) (absolute values)
Ch-Tpp[a]	174.70	7885.10
Li-Tfh[b]	17.05	22.84
ES100-Espray[c]	3.63	3.25
PLGA-Espray[d]	2.56	4.46

[a]Chitosan-tripolyphosphate nanoparticles prepared by ionic gelation; [b]Lecithin nanoparticles prepared by thin film hydration method; [c]Eudragit S100 nanoparticles prepared by electrospraying; [d]Poly(lactide-co-glycolide) nanoparticles prepared by electrospraying.

5.3.4 In vitro release kinetics

The release of aspalathin from the nanoparticles was investigated under physiological conditions (pH 7.4 at 37°C). The behaviour of the nanoparticles at this pH is of interest, as the colonic region is one of the most feasible sites for absorption of polyphenols such as aspalathin (Hu *et al.*, 2017). Fig. 5.5 shows the release profiles of aspalathin from the four selected GRAF-loaded nanoparticles over 8 h at pH 7.4. The curves of the respective nanoparticles showed biphasic release profiles for aspalathin, consisting of a rapid release phase, followed by plateauing. This can be explained by the non-uniform distribution of GRAF in the particles (Zhang *et al.*, 2018). The release after the first sampling interval (15 min), classified as the burst release (Table 5.3), is attributed to GRAF adsorbed to the particle surface (Kumari *et al.*, 2010), while the second phase could be explained by GRAF trapped in the polymer matrix (Sanna *et al.*, 2015).

In order to assess and compare the release profiles, a number of mathematical models were fitted, with the Gompertz model providing the best fit (R^2_{adj} > 0.9536, Supplementary material, Table C.1) for most of the nanoparticles. In addition, model-independent and model-dependent parameters were calculated (Table 5.3). PLGA-Espray particles showed a large burst release with an average of 57.7% of the aspalathin released in the first 15 min, attributed to loosely absorbed GRAF due to minimal interaction. Ch-TPP and Li-TFH showed much lower burst releases of 9.9% and 13.4%, respectively, while the ES100-Espray particles showed a minimal burst release of only 1.4%. Even though burst release is generally explained by the release of GRAF from the particle surface as discussed above, various other factors such as the swelling capability, targeted release profile and interaction between the polymer and GRAF have an effect. For example, even though the FTIR (Fig.5.4) indicated that GRAF is most likely encapsulated on the surface of the ES100 particles, the lower burst release is most likely governed by its targeted release profile and swelling rate rather than the position of GRAF.

The MDT is a measure of the time required for a bioactive compound to be released into solution (Podczeck, 1993). All the nanoparticles, except ES100-Espray, resulted in MDT values of less than 63 min. The ES100-

Espray particles had an MDT of 104 min, corresponding to a slower release profile than that of the other nanoparticles. The release rate constant calculated for these nanoparticles was the lowest (1.67 h^{-1}), followed by the natural polymeric nanoparticles, Ch-TPP (2.51 h^{-1}) and Li-TFH (3.40 h^{-1}), and finally PLGA-Espray (6.58 h^{-1}). Sustained, controlled or targeted release obtained with nanoencapsulation can aid in the protection of bioactive compounds as the compound of interest spends more time in the particle before being exposed to the aqueous environment in the digestive system (Hu *et al.*, 2017).

The specific bioactive compound-polymer combination and encapsulation method are likely to affect the release profile. The interactions of the bioactive compound and polymer, as well as the ratio of compound trapped versus adsorbed to the surface of the nanoparticles will also have an effect (Adibkia *et al.*, 2011). ES100 is classified as an enteric polymer and swells above pH 7 (Akhgari *et al.*, 2017). The swelling of the polymer matrix may retard the release of surface adsorbed GRAF. The natural polymeric systems are of hydrophilic nature and will swell in the aqueous alkaline environment of the gut, allowing water to penetrate the nanoparticles, solubilise aspalathin within and result in its release.

The release of aspalathin from ES100-Espray particles was also investigated at a pH of 4 to determine whether aspalathin will be released in an aqueous environment such as a ready-to-drink iced tea beverage (Fig. 5.5 and Table 5.3). Even though a smaller burst release (0.8%) and longer MDT (119 min) were obtained compared to pH 7.4, the particles showed a significantly higher release rate (2.23 h^{-1}) compared to ES100-Espray at pH 7.4. These values and the large amount of aspalathin released in the acidic media after 8 h (75%) could be attributed to the high solubility of aspalathin in aqueous buffer solution. Similar results were found by (Akhgari *et al.* (2017)) who showed unexpected high release of Indomethacin, with high water solubility, from Eudragit polymers at pH values below its targeted pH.

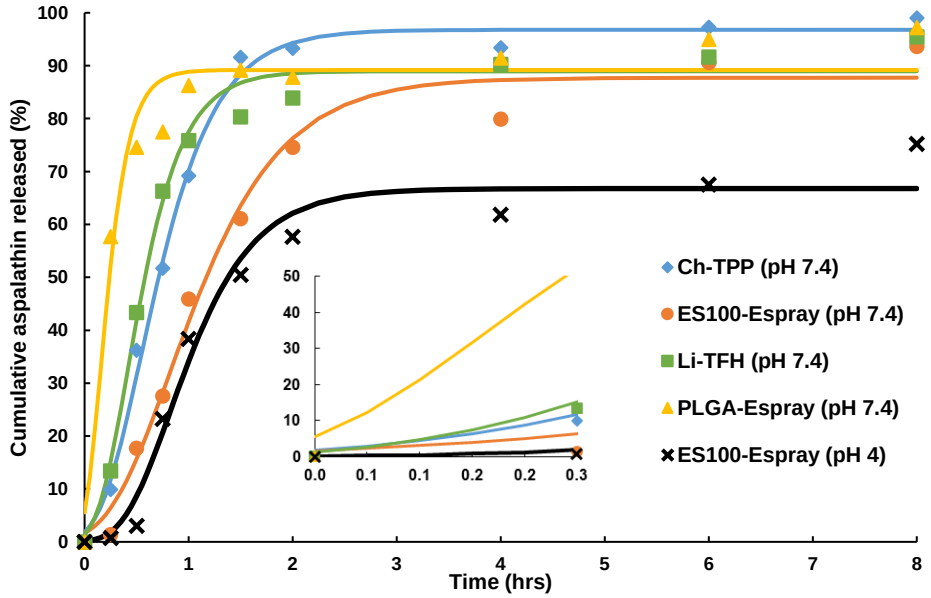

Fig. 5.5 *In vitro* release profiles (markers represent measured data and solid lines a fitted Gompertz model) of aspalathin from nanoparticles loaded with an aspalathin-rich fraction prepared from green rooibos processed by conventional methods (chitosan-tripolyphosphate (Ch-TPP) and lecithin-thin film hydration (Li-TFH) and by electrospraying (Eudragit (ES100-Espray) and poly(lactide-co-glycolide) (PLGA-Espray)) in phosphate-buffered saline (pH 7.4) at 37°C over 8 h. Addtionally, release profile of ES100-espray particles in acetate buffer (pH 4).

Table 5.3

Model-independent and model-dependent parameters comparing the *in vitro* release profiles of aspalathin from nanoparticles loaded with an aspalathin-rich fraction prepared from green rooibos

Nanoparticles	pH	Model independent parameters			Model dependent parameters [a]	
		Burst release [b] (%)	Total release [c] (%)	Mean dissolution time (MDT) (min)	R^2_{adj}	Release rate (h^{-1})
Ch-TPP[d]	7.4	9.9 ± 0.1 c[e]	99.1 ± 1.0 a	60 ± 3 c	0.9943	2.51 ± 0.07 c
Li-TFH[f]		13.4 ± 0.1 b	95.5 ± 1.7 bc	63 ± 1 c	0.9859	3.40 ± 0.03 b
ES100-Espray[g]		1.4 ± 0.0 d	93.7 ± 2.5 c	103 ± 8 b	0.9848	1.67 ± 0.07 e
PLGA-Espray[h]		57.7 ± 0.1 a	97.2 ± 0.8 ab	42 ± 3 d	0.9563	6.58 ± 0.16 a
ES100-Espray[i]	4	0.8 ± 0.0 e	75.23 ± 0.4 d	119 ± 3 a	0.9736	2.23 ± 0.23 d

[a]Data fitted to the Gompertz model; [b]% of aspalathin released in the first 15 min; [c]% of aspalathin released after 8 h ; [d]Chitosan-tripolyphosphate nanoparticles prepared by ionic gelation; [e] Means in the same column with the same letter are not significantly different ($P \geq 0.05$); [f]Lecithin nanoparticles prepared by thin film hydration method; [g]Eudragit S100 nanoparticles prepared by electrospraying; [h]Poly(lactide-co-glycolide) nanoparticles prepared by electrospraying.

5.4. Conclusions

Nanoencapsulation was demonstrated to be an effective technique to produce nanoparticles loaded with an aspalathin-rich fraction prepared from green rooibos. This was achieved with polymers approved by the Food and Drug Administration, suitable for use in food and controlled release formulations. Overall, nanoencapsulation of GRAF with Eudragit ES100® using electrospraying showed the most favourable

nanoparticle characteristics, i.e. high EE and LC, small particle size, high zeta potential and a controlled slow release profile. The hypothesis that electrospraying using a synthetic polymer would be most effective was thus supported by the results obtained. Further work needed includes stability testing in a relevant food formulation.

5.5 References

Adibkia, K., Javadzadeh, Y., Dastmalchi, S., Mohammadi, G., Niri, F. K. & Alaei-Beirami, M. (2011). Naproxen-Eudragit® RS100 nanoparticles: Preparation and physicochemical characterization. *Colloids and Surfaces B: Biointerfaces,* 83, 155–159.

Akhgari, A., Heshmati, Z., Garekani, H. A., Sadeghi, F., Sabbagh, A., Makhmalzadeh, B. S. & Nokhodchi, A. (2017). Indomethacin electrospun nanofibers for colonic drug delivery: *In vitro* dissolution studies. *Colloids and Surfaces B: Biointerfaces,* 152, 29–35.

Anandharamakrishnan, C. (2014). Techniques for nanoencapsulation of food ingredients. Pp. 1–89. New York: Springer.

Arulmozhi, V., Pandian, K. & Mirunalini, S. (2013). Ellagic acid encapsulated chitosan nanoparticles for drug delivery system in human oral cancer cell line (KB). *Colloids and Surfaces B: Biointerfaces,* 110, 313–320.

Berscht, P. C., Nies, B., Liebendörfer, A. & Kreuter, J. (1994). Incorporation of basic fibroblast growth factor into kethylpyrrolidinone chitosan fleeces and determination of the in vitro release characteristics. *Biomaterials,* 15, 593–600.

Bilia, A. R., Isacchi, B., Righeschi, C., Guccione, C. & Bergonzi, M. C. (2014). Flavonoids loaded in nanocarriers: an opportunity to increase oral bioavailability and bioefficacy. *Food and Nutrition Sciences,* 5, 1212–1327.

Braithwaite, M. C., Tyagi, C., Tomar, L. K., Kumar, P., Choonara, Y. E. & Pillay, V. (2014). Nutraceutical-based therapeutics and formulation strategies augmenting their efficiency to complement modern medicine: An overview. *Journal of Functional Foods,* 6, 82–99.

Calvo, P., Remunan-Lopez, C., Vila-Jato, J. L. & Alonso, M. J. (1997). Novel hydrophilic chitosan–polyethylene oxide nanoparticles as protein carriers. *Journal of Applied Polymer Science,* 63, 125-132.

Chadha, R. & Bhandari, S. (2004). Drug–excipient compatibility screening — Role of thermoanalytical and spectroscopic techniques. *Journal of Pharmaceutical and Biomedical Analysis,* 87, 82–97.

Costa, P. & Lobo, J. M. S. (2001). Modeling and comparison of dissolution profiles. *European Journal of Pharmaceutical Sciences,* 13, 123-133.

De Beer, D., Joubert, E., Viljoen, M. & Manley, M. (2011). Enhancing aspalathin stability in rooibos (*Aspalathus linearis*) ready-to-drink iced teas during storage: the role of nano-emulsification and beverage ingredients, citric and ascorbic acids. *Journal of the Science of Food and Agriculture,* 92, 274–282.

De Beer, D., Malherbe, C. J., Beelders, T., Willenburg, E. L., Brand, D. J. & Joubert, E. (2015). Isolation of aspalathin and nothofagin from rooibos (*Aspalathus linearis*) using high-performance countercurrent chromatography: Sample loading and compound stability considerations. *Journal of Chromatography A,* 1381, 29–36.

Duan, B., Dong, C., Yuan, X. & Yao, K. (2004). Electrospinning of chitosan solutions in acetic acid with poly(ethylene oxide). *Journal of Biomaterials Science, Polymer Edition,* 15, 797-811.

Dudhani, A. R. & Kosaraju, S. L. (2010). Bioadhesive chitosan nanoparticles: Preparation and characterization. *Carbohydrate Polymers,* 81, 243-251.

Ezhilarasi, P. N., Karthik, P., Chhanwal, N. & Anandharamakrishnan, C. (2013). Nanoencapsulation techniques for food bioactive components: A review. *Food and Bioprocess Technology,* 6, 628–647.

Fang, Z. & Bhandari, B. (2010). Encapsulation of polyphenols - A review. *Trends in Food Science & Technology,* 21, 510–523.

Fathi, M., Varshosaz, J., Mohebbi, M. & Shahidi, F. (2012). Hesperetin-loaded solid lipid nanoparticles and nanostructure lipid carriers for food fortification: Preparation, characterization, and modeling. *Food and Bioprocess Technology,* 6, 1464–1475.

Hu, B., Liu, X., Zhang, C. & Zeng, X. (2017). Food macromolecule based nanodelivery systems for enhancing the bioavailability of polyphenols. *Journal of Food and Drug Analysis,* 25, 3-15.

Jahangiri, A., Davaran, S., Fayyazi, B., Tanhaei, A., Payab, S. & Adibkia, K. (2014). Application of electrospraying as a one-step method for the fabrication of triamcinolone acetonide-PLGA nanofibers and nanobeads. *Colloids and Surfaces B: Biointerfaces,* 123, 219–224.

Joubert, E., Viljoen, M., De Beer, D., Malherbe, C. J., Brand, D. J. & Manley, M. (2010). Use of green rooibos (*Aspalathus linearis*) extract and water-soluble nanomicelles of green rooibos extract encapsulated with ascorbic acid for enhanced aspalathin content in ready-to-drink iced teas. *Journal of Agricultural and Food Chemistry,* 58, 10965–10971.

Kreuz, S., Joubert, E., Waldmann, K. & Ternes, W. (2008). Aspalathin, a flavonoid in *Aspalathus linearis* (rooibos), is absorbed by pig intestine as a *C*-glycoside. *Nutrition Research,* 28, 690–701.

Kumari, A., Yadav, S. K., Pakade, Y. B., Singh, B. & Yadav, S. C. (2010). Development of biodegradable nanoparticles for delivery of quercetin. *Colloids and Surfaces B: Biointerfaces,* 80, 184–192.

Liang, J., Li, F., Fang, Y., Yang, W., An, X., Zhao, L., Xin, Z., Cao, L. & Hu, Q. (2011). Synthesis, characterization and cytotoxicity studies of chitosan-coated tea polyphenols nanoparticles. *Colloids and Surfaces B: Biointerfaces,* 82, 297–301.

Lu, Q., Li, D. C. & Jiang, J. G. (2011). Preparation of a tea polyphenol nanoliposome system and its physicochemical properties. *Journal of Agricultural and Food Chemistry,* 59, 13004–13011.

Muller, C. J. F., Malherbe, C. J., Chellan, N., Yagasaki, K., Miura, Y. & Joubert, E. (2018). Potential of rooibos, its major *C*-glucosyl flavonoids, and *Z*-2-(β-D-glucopyranosyloxy)-3-phenylpropenoic acid in prevention of metabolic syndrome. *Critical Reviews in Food Science and Nutrition,* 58, 227–246.

Podczeck, F. (1993). Comparison of in vitro dissolution profiles by calculating mean dissolution time (MDT) or mean residence time (MRT). *International Journal of Pharmaceutics,* 97, 93–100.

Sanna, V., Lubinu, G., Madau, P., Pala, N., Nurra, S., Mariani, A. & Sechi, M. (2015). Polymeric nanoparticles encapsulating white tea extract for nutraceutical application. *Journal of Agricultural and Food Chemistry,* 63, 2026–2032.

Srivastava, A. K., Bhatnagar, P., Singh, M., Mishra, S., Kumar, P., Shukla, Y. & Gupta, K. C. (2013). Synthesis of PLGA nanoparticles of tea polyphenols and their strong in vivo protective effect against chemically induced DNA damage. *International Journal of Nanomedicine,* 8, 1451–1462.

Stetefeld, J., McKenna, S. A. & Patel, T. R. (2016). Dynamic light scattering: a practical guide and applications in biomedical sciences. *Biophysical Reviews,* 8, 409–427.

Torres-Giner, S., Wilkanowicz, S., Melendez-Rodriguez, B. & Lagaron, J. M. (2017). Nanoencapsulation of *Aloe vera* in synthetic and naturally occurring polymers by electrohydrodynamic processing of interest in food technology and bioactive packaging. *Journal of Agricultural and Food Chemistry,* 65, 4439–4448.

Uzzan, M., Nechrebeki, J. & Labuza, T. P. (2007). Thermal and storage stability of nutraceuticals in a milk beverage dietary supplement. *Journal of Food Science,* 72, E109–E114.

Wu, T. H., Yen, F. L., Lin, L. T., Tsai, T. R., Lin, C. C. & Cham, T. M. (2008). Preparation, physicochemical characterization, and antioxidant effects of quercetin nanoparticles. *International Journal of Pharmaceutics,* 346, 160–168.

Wyatt, P. J. (2014). Measurement of special nanoparticle structures by light scattering. *Analytical Chemistry,* 86, 7171–7183.

Xie, X., Tao, Q., Zou, Y., Zhang, F., Guo, M., Wang, Y., Wang, H., Zhou, Q. & Yu, S. (2011). PLGA nanoparticles improve the oral bioavailability of curcumin in rats: Characterizations and mechanisms. *Journal of Agricultural and Food Chemistry,* 59, 9280–9289.

Yu, D.-G., Yang, J.-H., Wang, X. & Tian, F. (2012). Liposomes self-assembled from electrosprayed composite microparticles. *Nanotechnology,* 23, 1–8.

Zamani, M., Prabhakaran, M. P. & Ramakrishna, S. (2013). Advances in drug delivery via electrospun and electrosprayed nanomaterials. *International Journal of Nanomedicine,* 8, 2997–3017.

Zhang, H., Qin, H., Li, L., Zhou, X., Wang, W. & Kan, C. (2018). Preparation and characterization of controlled-release avermectin/castor oil-based polyurethane nanoemulsions. *Journal of Agricultural and Food Chemistry,* 66, 6552–6560.

Zhang, J., Nie, S. & Wang, S. (2013). Nanoencapsulation enhances epigallocatechin-3-gallate stability and its antiatherogenic bioactivities in macrophages. *Journal of Agricultural and Food Chemistry,* 61, 9200–9209.

SUPPLEMENTARY MATERIAL CHAPTER 5_ADDENDUM C

Table C.1

Adjusted coefficient of determination (R^2_{adj}) values for alternative kinetic models[a] of aspalathin release from nanoparticles loaded with an aspalathin-rich fraction prepared from green rooibos

Formulations	pH	R^2_{adj}				
		Sigmoid[f]	Logistic[g]	Mitscherlich[h]	Growth[i]	Gompertz[j]
Ch-Tpp[b]	7.4	0.9894	0.9929	0.9683	0.9921	0.9943
Li-Tfh[c]		0.9781	0.9849	0.9712	0.9814	0.9859
ES100-Espray[d]		0.9741	0.9849	0.9708	0.9798	0.9848
PLGA-Espray[e]		0.9388	0.9479	0.9797	0.9422	0.9563
ES100-Espray[d]	4	0.9608	0.9716	0.9375	0.9705	0.9736

[a]Models selected with release rate as variable; [b]Chitosan-tripolyphosphate nanoparticles prepared by ionic gelation; [c]Lecithin nanoparticles prepared by thin film hydration method; [d]Eudragit S100 nanoparticles prepared by electrospraying; [e]Poly(lactide-co-glycolide) nanoparticles prepared by electrospraying; [f]Sigmoid: $Asp(t) = Asp_{max}/(1 + e^{(-(t-tlag)/k)}$;

[g]Logistic: $Asp(t) = Asp_{max}/(1 + \left(\frac{t+1}{t_{lag}}\right)^{(-k)}$); [h]Mitscherlich: $Asp(t) = Asp_{max}(1 - e^{(-k(t))})$;

[i]Growth: $Asp(t) = Asp_{max}\left(1 - e(-k(t)^2)\right)$; [j]Gompertz: $Asp(t) = Asp_{max}e^{-e^{-k(t-t_{lag})}}$

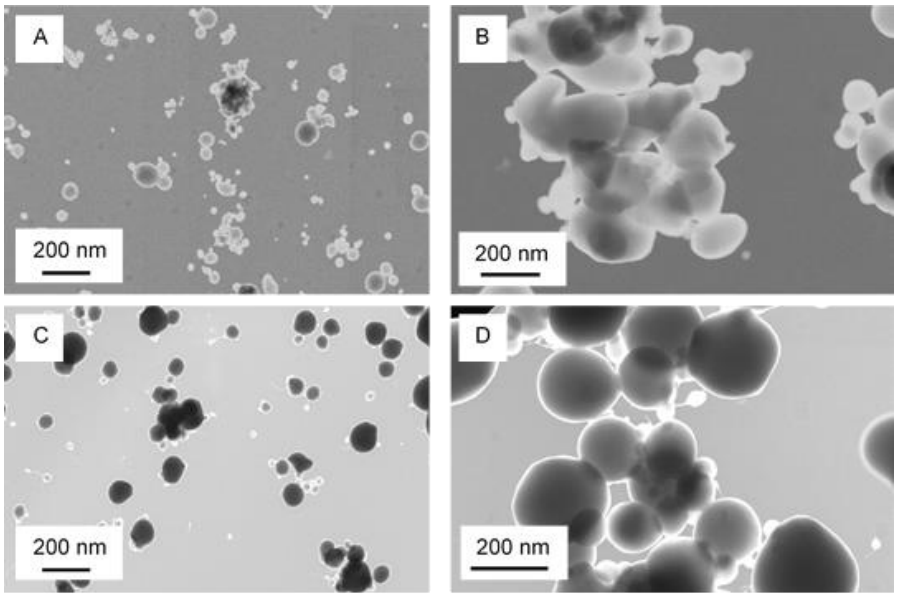

Fig. C.1 Scanning electron microscope images of nanoparticles loaded with an aspalathin-rich fraction from green rooibos: (A) Lecithin nanoparticles prepared by thin film hydration, (B) Chitosan-tripolyphosphate nanoparticles prepared by ionic gelation, (C) Eudragit S100 and (D) poly(lactide-co-glycolide) nanoparticles prepared by electrospraying.

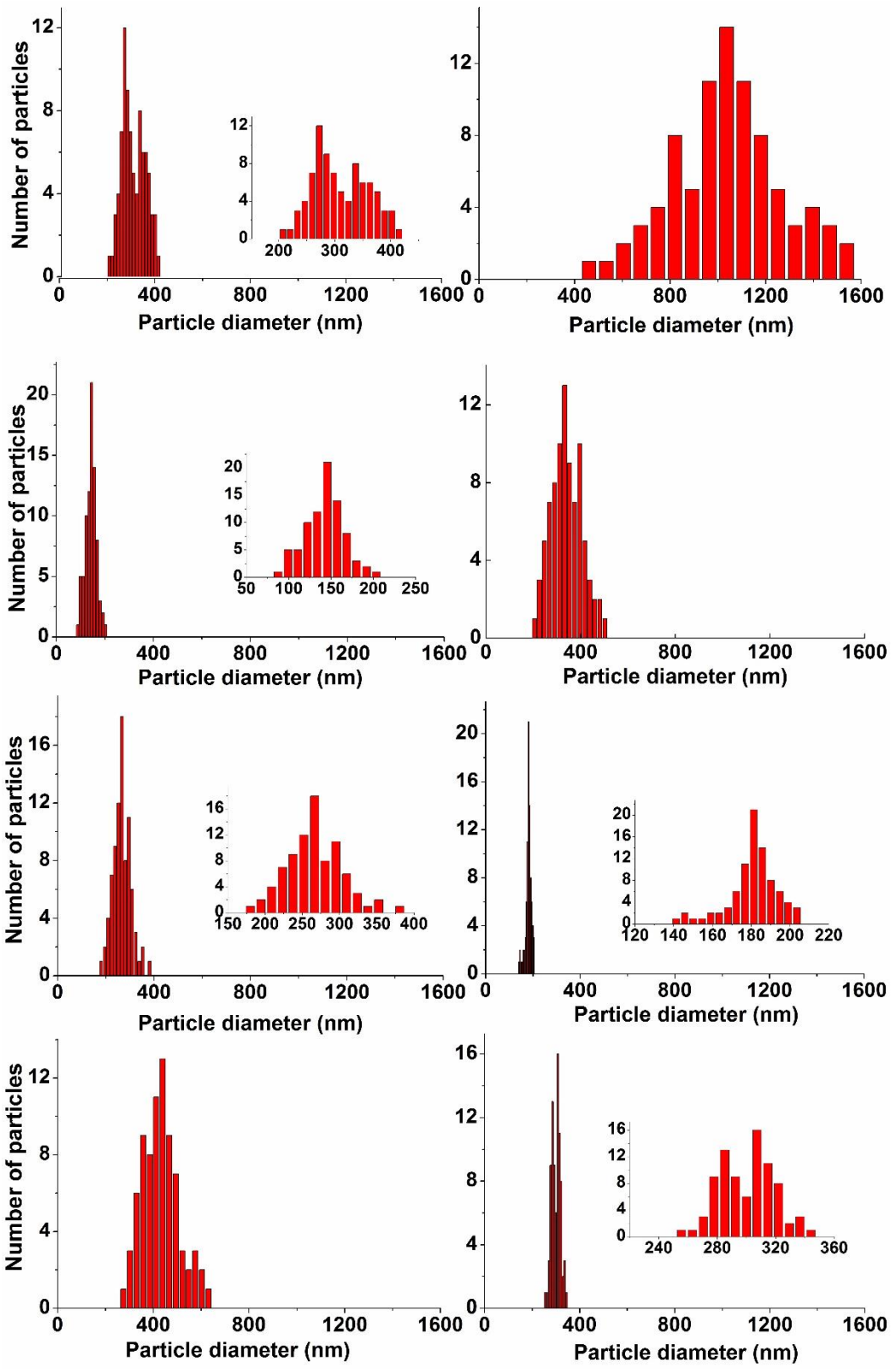

Fig. C.2 Particle size distribution of nanoparticles loaded with an aspalathin-rich fraction prepared from green rooibos prepared using: (A) lecithin, (B) chitosan, (C) Eudragit S100 (ES100) and (D) poly(lactide-co-glycolide) (PLGA) synthesised by (1) conventional methods and (2) electrospraying. Particle diameters were measured with with AxioVision 4.4 software (3 images × 30 measurements).

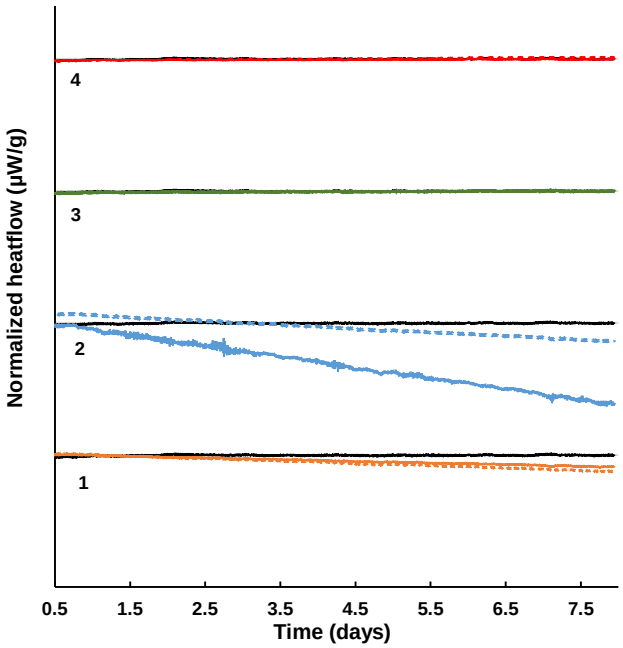

Fig. C.3 Heat flow curves obtained from isothermal calorimetry at 40 °C for aspalathin-rich fraction prepared from green rooibos (solid black line), loaded nanoparticles (dotted coloured lines) and blank nanoparticles (solid coloured lines) for: lecithin systems (1), chitosan systems (2), poly(lactide-co-glycolide) (PLGA) (3) and (Eudragit (ES100) systems (4).

Chapter 6

Optimisation of electrospraying for nanoencapsulation of an aspalathin-rich fraction from green rooibos in a pH-responsive enteric polymer

ABSTRACT

The aim of the study was to optimise electrospraying conditions for the nanoencapsulation of an aspalathin-rich fraction prepared from green rooibos (GRAF; 40% aspalathin, m/m). Eudragit S100 (ES100), a synthetic poly(methacrylic acid-co-methyl methacrylate) polymer with a targeted release profile at pH 7, was used to encapsulate the fraction to improve orogastrointestinal stability of aspalathin. Experimental conditions were varied according to a central composite design, with ES100 concentration (1–6%, m/m), GRAF concentration (5–25%, m/m relative to polymer concentration) and voltage (10–25 kV) as nanoencapsulation parameters and particle size (nm), polydispersity index, product yield (%), encapsulation efficiency (EE, %) and loading capacity (LC, %) as responses. Selected ranges of process parameters based on the optimisation were as follows: ES100 concentration (5–6%, m/m), GRAF concentration (17–19%, m/m relative to ES100 concentration) and voltage (22–25 kV). Additional experiments showed good correlation between predicted and experimental outcomes for selected responses, with yields varying between 78.2–78.3%, EE between 73.9–77.4% and LC between 10.4–12.2%. The selected conditions were subsequently applied to nanoencapsulate pure aspalathin. Nanoencapsulation of aspalathin resulted in similar yield, EE, LC, particle size and particle morphologies to those of nanoencapsulated GRAF. The nanoparticles were further evaluated for stability and release of aspalathin at fixed pH-time combinations, simulating the pH and residence/transit time at various locations of the orogastrointestinal tract. Nanoencapsulation significantly decreased aspalathin degradation when the pH was below the targeted release pH of the polymer. Pure aspalathin was less stable than when present in the extract, indicating that the extract matrix offered some protection against degradation. The parallel artificial membrane permeability assay and the Caco-2 monolayer model indicated no or minimal changes in the permeability of aspalathin after nanoencapsulation with the hydrophobic polymer. Passive transcellular and paracellular transport of aspalathin through the intestinal membrane would therefore not improve with nanoencapsulation using Eudragit S100.

6.1 Introduction

Chapter 5 describes the evaluation of two natural and two synthetic polymers for their suitability to produce nanoparticles loaded with an aspalathin-rich fraction prepared from green rooibos (40% aspalathin m/m; GRAF). Conventional techniques and electrospraying were used to prepare nanoparticles. Electrospraying of GRAF with the food and drug administration (FDA) approved, pH-responsive carrier, poly(methacrylic acid-co-methyl methacrylate) polymer (Eudragit S100 (ES100)) (Yoshida, Lai, Kwon & Sako, 2013) produced nanoparticles having a combination of the most favourable properties in terms of particle size, zeta potential, encapsulation efficiency (EE), loading capacity (LC) and sustained release profile. Another consideration for selection of this polymer is its targeted enteric release profile (pH > 7) (McGinity & Felton, 2008), since the small intestine (pH 6.0–7.4) is the most likely site of absorption and biotransformation of aspalathin (Kreuz, Joubert, Waldmann & Ternes, 2008).

Given the positive results obtained with electrospraying for the production of GRAF-loaded ES100 nanoparticles, optimisation of the process was the next step. Process parameters (ES100 concentration, voltage and GRAF concentration) were varied according to a central composite design (CCD), as this experimental design has the advantage of requiring a relative small number of experiments for optimisation (Bezerra, Santelli, Oliveira, Villar & Escaleira, 2008). The nanoparticles were evaluated in terms of particle size, polydispersity index (PDI), product yield, EE and LC as responses. The product yield is related to the cost and scale-up potential of nanoencapsulation by electrospraying, as higher yields relate to a more efficient process. The particle size and PDI affect the absorption of nanoparticles in the gastrointestinal tract. A higher intracellular uptake can be achieved since smaller uniform particles, i.e. nanoparticles (diameter < 1000 nm) tend to absorb better than microparticles (diameter > 1000 nm) (McClements & Rao, 2011). A smaller PDI which relates to more uniform particles is also important for predictable properties and absorption of nanoparticles (Knop, Hoogenboom, Fischer & Schubert, 2010). Lower dosages would be required for nanoparticles that contain more aspalathin, thus higher LC and EE would be advantages.

The optimum process parameters were subsequently employed to encapsulate pure aspalathin with the same synthetic co-polymer. Both GRAF- and aspalathin-loaded nanoparticles were evaluated with regard to aspalathin stability and release at fixed pH-time combinations based on orogastrointestinal pH and residence/transit times. Membrane permeability was assessed using the parallel artificial membrane permeability assay (PAMPA) and the Caco-2 monolayer model to elucidate the effect of nanoencapsulation on intestinal absorption of aspalathin.

6.2 Material and Methods

6.2.1 Chemicals and reagents

ES100, poly(methacrylic acid-co-methyl methacrylate) with a 1:2 carboxyl/ester ratio was obtained from Evonik Industries (Darmstadt, Germany). Potassium acetate ($KC_2H_3O_2$), potassium phosphate (KH_2PO_4), hydrochloric acid (HCl), phosphate buffered saline tablets (PBS), *n*-butanol (*n*-BuOH), high performance liquid chromatography (HPLC)-grade acetonitrile, dimethyl sulfoxide (DMSO), caffeine (purity > 95%), analytical grade ascorbic acid, calcium chloride ($CaCl_2$), Lucifer yellow (LY) and Hanks Balanced Salt Solution (HBSS) were obtained from Sigma Aldrich (St Louis, MO, USA). Formic acid and rutin (purity > 95%) were obtained from Merck (Darmstadt, Germany). Deionised water prepared using an Elix water purification system was further purified to HPLC grade using a Milli-Q Academic water purification system from Merck. Aspalathin (> 95% purity, HPLC-mass spectroscopy and -diode array detection (DAD)) used as authentic reference standard for HPLC-DAD quantification were obtained from the South African Medical Research Council (SAMRC, Cape Town, South Africa). GRAF (40% aspalathin) was prepared as described in **Chapter 5,** section 5.2.2, according to De Beer *et al.* (2015). Aspalathin (> 95% purity, HPLC-DAD) for nanoencapsulation, isolated from green rooibos, was obtained from the Agricultural Research Council of South Africa (Infruitec-Nietvoorbij, Stellenbosch, South Africa).

6.2.2 Optimisation of nanoencapsulation of GRAF with ES100 (ES100-GRAF) by electrospraying and nanoencapsulation of aspalathin with ES100 (ES100-ASP)

An CCD experimental design, consisting of 20 experimental runs, which included 6 star points, 8 factorial points and 6 central points performed in triplicate in a randomised order, was used for optimisation (Table 6.1). The coded and de-coded values of the independent parameters were selected based on results of preliminary experiments. These parameters included ES100 concentration (1, 2, 4, 5 and 6% (m/m); X_1), voltage (10, 13, 18, 22 and 25 kV; X_2) and GRAF concentration (5, 9, 15, 21 and 25% (m/m relative to ES100); X_3). The responses were particle size (nm), PDI, product yield (%), EE (%) and LC (%). Nanoparticle formation was confirmed by scanning electron microscopy imaging (SEM) of the particles produced at four design points (1 factorial, 2 star and 1 central). Experimental data from the CCD were fitted to the following second order polynomial equation and regression coefficients were calculated:

$$Y = \beta_0 + \beta_1 X_1 + \beta_2 X_2 + \beta_3 X_3 + \beta_{11} X_1^2 + \beta_{22} X_2^2 + \beta_{33} X_3^2 + \beta_{12} X_1 X_2 + \beta_{13} X_1 X_3 + \beta_{23} X_2 X_3 \quad (6.1)$$

where β_0 is the intercept, β_1, β_2 and β_3 the linear coefficients, β_{11}, β_{22} and β_{33} the squared coefficients, β_{12}, β_{13} and β_{23} the interaction coefficients, X_1, X_2 and X_3 the process parameters to be optimised and Y is the predicted response.

In order to test the validity of the models, electrospraying of ES100-GRAF was done at the combination of minimum (ES100 (4%, m/m); GRAF (17%, m/m relative to ES100) and voltage (22 kV)) and maximum (ES100 (5%, m/m); GRAF (19%, m/m relative to ES100) and voltage (25 kV)) values of the selected optimum range for the three process parameters were subsequently performed in triplicate. Pure aspalathin was encapsulated with ES100 using the combination of maximum levels selected for each process parameter.

The electrospraying set-up is described in **Chapter 5**, section 5.2.4. The stainless steel needle size (20 gauge, 0.9 mm i.d.) and feed flow rate (4 µL/min) were kept constant. The formed nanoparticles were allowed to completely dry in a fume hood for 24 h after electrospraying.

6.2.3 Evaluation of process

Product yield was determined gravimetrically and expressed as a percentage of the sum of the mass of GRAF and ES100 in the feed solution used for nanoparticle preparation. EE was calculated by expressing the encapsulated aspalathin (g) as a percentage of aspalathin (g) initially added to the nanoparticle preparation, whereas LC was calculated by expressing the encapsulated aspalathin (g) as a percentage of the mass of the nanoparticles (g). Aspalathin was quantified by HPLC- DAD (De Beer *et al.*, 2015). Particle size and PDI were determined by photo correlation spectroscopy and particle imaging using SEM. All experimental and instrument details are described in **Chapter 5**, sections 5.2.5.1-5.2.5.4.

6.2.4 Orogastrointestinal pH stability and release studies

Orogastrointestinal pH stability of pure aspalathin and when present in the extract matrix (GRAF) and nanoparticles (ES100-ASP and ES100-GRAF) was determined by suspending/dissolving the samples (*ca.* 15 mg) in 20 mL of each buffer (0.2 M KH_2PO_4 (pH 6.8); 0.1 M KH_2PO_4 (pH 2); 0.1 M $KC_2H_3O_2$ (pH 4) and 0.2 M KH_2PO_4 (pH 7)); adjusted with HCl to obtain desired pH). The samples were incubated at 37 °C in screw-cap vials, placed in temperature-controlled heating blocks (Stuart, Bibby Scientific Limited, Stone, UK) and incubated for a fixed period at each pH to simulate pH and residence/transit time (pH 6.8, 5 min; pH 2, 120 min; and pH 7, 120 min) in the orogastrointestinal tract (Versantvoort, Oomen, Van de Kamp, Rompelberg & Sips, 2005). Samples were also subjected to pH 4 for 60 min to simulate elevated gastric pH after a meal (Gardner, Ciociola & Robinson, 2002). After the degradation experiments, aliquots of the nanoparticles were

disintegrated by sonication (ultrasonic bath, 250 W, 44 kHz) for 60 min. The degradation of aspalathin from ES100-GRAF and ES100-ASP was calculated by expressing the amount of aspalathin present after degradation and sonication as a percentage of the initial aspalathin content of the nanoparticles.

The same conditions were used to monitor the release of aspalathin from ES100-GRAF and ES100-ASP under gentle magnetic stirring (150 rpm) in a jacketed glass beaker at 37 °C. In this case, ascorbic acid (10%, m/v) was added to the buffer solutions to prevent aspalathin degradation during the release experiments.

The release of aspalathin from ES100-GRAF and ES100-ASP were calculated by expressing the amount of aspalathin released into the stirring solution as a percentage of the initial aspalathin content of the nanoparticles.

6.2.5 Parallel artificial membrane permeability assay (PAMPA)

The assay was carried out in a Corning Gentest™ pre-coated PAMPA plate system (Discovery Labware Inc., MA, USA) consisting of a 96 well insert system with a PVDF filter plate, pre-coated with lipids, and a matched donor and acceptor plate. Stock solutions of aspalathin, caffeine (high permeability marker) and rutin (low permeability marker) were made up in DMSO and further diluted with PBS to 5% (v/v) DMSO working solutions (compounds at 200 µM). The GRAF working solution was similarly prepared, while ES100-GRAF and ES100-ASP were directly suspended in PBS containing 5% (v/v) DMSO. The samples were briefly vortexed in their respective solutions to ensure proper dispersion of the nanoparticles. GRAF, ES100-GRAF and ES100-ASP concentrations were prepared to deliver 200 µM aspalathin. Working solutions of the samples (300 µL) were added to separate donor wells and PBS (200 µL) was added to the each of the acceptor wells. The acceptor plate was carefully lowered onto the donor plate, ensuring contact between the liquid in the donor wells and the lipid membrane. The plate was covered and incubated at room temperature (22 °C) for 16 h, while mildly shaken (400 rpm), using a microplate shaker (Eppendorf MixMate®, Hamburg, Germany). After incubation, the samples were sonicated as described in section 6.2.4. Aspalathin (pure aspalathin and aspalathin from GRAF, ES100-GRAF and ES100-ASP), rutin and caffeine from the donor and acceptor compartments were quantified using HPLC-DAD (De Beer *et al.*, 2015).

Permeability (P_e, cm/s) of the compounds was calculated using Equation 6.2 and 6.3 (Piazzini *et al.*, 2017) as stipulated by the instruction manual for the Corning Gentest™ pre-coated PAMPA plate system:

$$C_{equilibrium} = \frac{[C_d(t)\times V_d + C_A(t)\times V_a]}{(V_d \times V_a)} \quad (6.2)$$

$$P_e = \frac{-\ln[1-\frac{C_A(t)}{C_{equilibrium}}]}{A\times(\frac{1}{V_d}+\frac{1}{V_A})\times t} \quad (6.3)$$

where $C_d(t)$ is the compound concentration (mM) in the donor well at time t, $C_A(t)$ is the compound concentration (mM) in the acceptor well at time t, V_d is the donor well volume (0.3 mL), V_A is the acceptor well volume (0.2 mL), A is the filter area (0.3 cm^2) and t is the incubation time.

6.2.6 Caco-2 monolayer model

Stock solutions of pure aspalathin (5.4 mg/mL), GRAF (14.3 mg/mL), ES100-GRAF (106.4 mg/mL), ES100-ASP (39.2 mg/mL) and caffeine (4.0 mg/mL, high permeability marker) were made up in 40% (v/v) DMSO. Directly after preparation of the stock solutions, ES100-GRAF and ES100-ASP stocks were diluted with HBSS (pH 6.0) to *ca.* 3.6% (v/v) DMSO, to allow proper dispersion of the nanoparticles. Prior to analysis, all stock solutions were further diluted with HBSS (pH 6.0), containing LY (100 mM) and $CaCl_2$ (0.535 mM), to obtain working solutions, prepared to deliver 150 µM aspalathin or caffeine. The additional HBSS added to the nanoparticle stock solutions was accounted for during the preparation of the final working solutions.

Caco-2 cells were cultured, prepared and equilibrated prior to transport experiments as previously reported by Bowles *et al.* (2017) for apical-to-basolateral compartment studies. The trans-epithelial electrical resistance (TEER) values across the wells were determined to be >300 Ω prior to experiments and permeability of LY was <3% during experiments, which confirmed intact and robust monolayers. Following equilibration and removal of the transport medium, 1.5 mL of each working HBSS working solution (pH 6.0) containing caffeine, aspalathin, GRAF, ES100-GRAF or ES100-ASP was added to separate wells of the apical compartment and 2.4 mL HBSS (pH 7.4) was added to the basolateral compartment. At each time interval (0.0, 0.5, 1.0 and 2.0 h) aliquots (1.2 mL) were withdrawn from the basolateral compartment and replaced by 1.2 mL fresh buffer to maintain sink conditions. At 2.0 h, an aliquot (1.2 mL) was also withdrawn from each well of the apical compartment. Cell free samples of the formulations were also included as a control and to determine aspalathin degradation after 2 h. After incubation the sampled aliquots were divided in 350 µL aliquots, 35 µL 10% (m/v) ascorbic acid added and frozen with liquid nitrogen. Prior to HPLC-DAD quantification, the samples were sonicated as described in section 6.2.4. Apparent permeability (P_{app}, cm/s) of the compounds was calculated using Eq. 6.4 (Artursson & Karlsson, 1991):

$$P_{app} = \frac{\Delta Q}{\Delta t} \times \frac{1}{A \times C_0} \qquad (6.4)$$

where $\Delta Q/\Delta t$ is the permeability rate as determined from the appearance of compound in the basolateral compartment, C_0 is the initial concentration in the apical compartment (µM) and A is the surface area across which transport occurs (4.52 cm^2).

6.2.7 Statistical analysis

Statistica 13.0 (Statsoft Southern Africa, Sandton, South Africa) was used to analyse all data generated by CCD. The statistical significance and suitability of the regression model, its factors and their interactions were determined at the 5% probability level ($P < 0.05$) using Univariate Analysis of Variance (ANOVA). Standardised Pareto charts were constructed to illustrate the significant effects obtained from the ANOVA for the different responses. The fitting efficiency of the data to the model was evaluated by calculating the coefficient and adjusted coefficient of determination (R^2 and R^2_{adj}) and the significance of lack-of-fit (LOF). The regression functions generated for selected responses were graphically illustrated as two-dimensional contour and three-dimensional response surface plots. Multi-response desirability profiling was used to determine optimal nanoencapsulation parameters. To calculate the overall desirability (D), each response value was converted to a dimensionless value (d) ranging from 0 (undesirable/unacceptable response) to 1 (very desirable/optimum response). D is calculated as the geometric mean of the individual desirability values and an algorithm used to maximise the set of variable values (Ferreira *et al.*, 2007b; Ferreira, Silva, Luna, Lago & Senna, 2007a). Least significant difference of the Student's t-test ($P = 0.05$) was calculated to compare treatment means where significant differences were found ($P < 0.05$). Levene's test was used to test for treatment homogeneity of variance. In instances where variances were not equal, a weighted analysis of variance was used for the combined analyses. The Shapiro-Wilk test was performed on the standardised residuals from the models to assess for normal distribution of the data.

The experimental design of the orogastrointestinal stability, PAMPA and Caco-2 experiments was completely random with three independent replicates for each of the samples. ANOVA was performed on all observed variables to determine whether transport was significant, using the GLM (General Linear Models) procedure of SAS software (Version 9.4; SAS Institute Inc, Cary, USA). The Shapiro-Wilk test was performed on the data to test for normality. Fisher's least significant difference was calculated at the 5% level to compare means where $P < 0.05$ was considered significant.

6.3 Results and discussion

6.3.1 Optimisation of nanoencapsulation of GRAF by electrospraying

The results for the measured responses of the CCD experiments, i.e. particle size, PDI, product yield, EE and LC are summarised in Table 6.1. Particle size varied between 183 and 260 nm and their nanoscale size (diameter < 1000 nm) was confirmed by SEM images of particles produced at the conditions representing a

factorial point, two star points and a central point (Fig. 6.1). Product yield varied between 60.3 and 83.7%, EE between 20.5 and 81.8%, LC between 1.0 and 14.9%, and PDI between 0.35 and 0.74.

Table 6.1

Process parameters levels (coded and de-coded ES100[a] concentration, voltage and GRAF[b] concentration) and responses (particle diameter, PDI[c], yield, EE[d] and LC[e]) of a central composite design for the nanoencapsulation of GRAF with ES100 by electrospraying

Run number	Process parameters (independent variables)						Responses				
	coded levels			de-coded levels							
	X_1 ES100	X_2 Voltage	X_3 GRAF	ES100 (%, m/m)	Voltage (kV)	GRAF (%, m/m)[f]	Diameter (nm)	PDI	Yield (%)	EE (%)	LC (%)
1 (F)[g]	−1	−1	−1	2	13	9	205	0.38	67.2	27.9	2.2
2 (F)	−1	−1	1	2	13	21	206	0.67	63.8	54.3	9.9
3 (F)	−1	1	−1	2	22	9	194	0.35	69.5	41.7	3.3
4 (F)	−1	1	1	2	22	21	194	0.63	65.9	70.0	12.8
5 (F)	1	−1	−1	5	13	9	221	0.55	80.5	32.4	2.5
6 (F)	1	−1	1	5	13	21	239	0.55	76.3	73.9	14.9
7 (F)	1	1	−1	5	22	9	232	0.38	83.7	41.4	2.5
8 (F)	1	1	1	5	22	21	188	0.68	75.9	81.8	13.5
9 (S)[h]	−1.68	0	0	1	18	15	183	0.51	60.3	41.5	5.4
10 (S)	1.68	0	0	6	18	15	260	0.50	82.4	56.9	7.4
11 (S)	0	−1.68	0	4	10	15	232	0.50	72.5	48.6	6.3
12 (S)	0	1.68	0	4	25	15	213	0.46	78.3	69.1	9.0
13 (S)	0	0	−1.68	4	18	5	219	0.37	77.8	20.5	1.0
14 (S)	0	0	1.68	4	18	25	222	0.74	70.9	55.3	12
15 (C)[i]	0	0	0	4	18	15	222	0.54	74.3	54.1	7.1
16 (C)	0	0	0	4	18	15	222	0.54	75.5	54.8	7.2
17 (C)	0	0	0	4	18	15	223	0.46	76.0	55.9	7.3
18 (C)	0	0	0	4	18	15	223	0.49	74.0	54.8	7.1
19 (C)	0	0	0	4	18	15	220	0.48	74.6	53.8	7.1
20 (C)	0	0	0	4	18	15	220	0.48	75.1	54.5	7.1

[a]Eudragit S100 polymer; [b]Aspalathin-rich fraction prepared from green rooibos; [c]Polydispersity index; [d]Encapsulation efficiency; [e]Loading capacity; [f]GRAF concentration relative to ES100 concentration; [g]Factorial design point; [h]Star point; [i]Central point

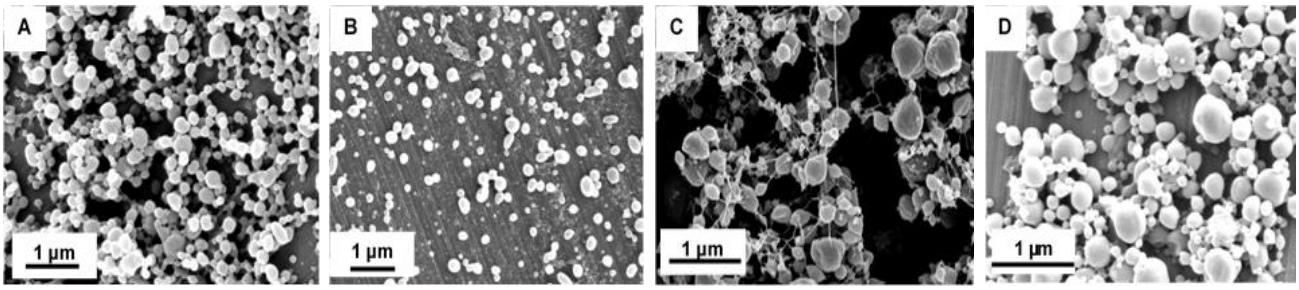

Fig. 6.1 SEM images of electrosprayed Eudragit S100 (ES100) nanoparticles loaded with an aspalathin-rich fraction prepared from green rooibos (GRAF): (A) Run 4 (factorial point), (B) Run 9 (star point), (C) Run 10 (star point), and (D) Run 17 (central point).

Pareto charts provide information regarding the significance of different nanoencapsulation parameters on the individual measured responses, as well as those parameters having the greatest effect. Fig. 6.2 shows the standardised Pareto charts generated for particle size, PDI, EE, LC and yield. The linear effect of ES100 concentration (%, m/m) was the most significant parameter for particle size and yield, whereas the GRAF concentration (%, m/m relative to ES100) was the most significant parameter for PDI, EE and LC. Additionally, voltage was observed to have a significant positive effect on EE and LC and a significant negative effect on the particle size. The GRAF concentration (%, m/m relative to ES100) had a significant negative effect on the yield. Given these effects, a compromise might have to be made between optimum yield and optimum EE, LC and PDI where GRAF concentration had the largest positive effect. Furthermore, various interaction parameters were also significant for the response factors. The interaction of ES100 concentration and voltage (2L × 3L) had a significant negative effect on the particle size, whereas the interaction of ES100 and GRAF concentration (1L × 3L) had a significant positive effect on EE and LC. These effects indicate that throughout the experimental range, certain combinations of these parameters will result in an opposite effect than expected for the individual process parameters.

The data were used to generate prediction models to investigate the effect of process parameters on selected responses (the complete set of response values and ANOVA results are available in supplementary material, Table D.1). The fit of the models was evaluated in terms of R^2_{adj} and LOF (Table 6.2) (Granato, Grevink, Zielinski, Nunes & van Ruth, 2014; Da Conceição, Da Costa, Da Rocha Filho, Pereira-Filho & Zamian, 2015). All the models (0.7956–0.9869), except the particle size model (0.5404), showed reasonable predictability based on R^2_{adj} values, with the model for yield showing the best fit with highest R^2_{adj} and non-significant LOF. The significant LOF for EE, LC and particle size indicated poor fit, however, the high R^2_{adj} values for LC and EE outweighed the significant LOF values. Further optimisation did not include particle size due to the significant LOF and low R^2_{adj} value for this parameter. The poor predictability could be due to errors in particle size measurements or due to too little variation in particle size in the chosen experimental range. The PDI values (0.33 to 0.74) indicated that all the nanoparticles were polydisperse, implying a large variation in particle sizes. Even though this is not favourable for reliable absorption of nanoparticles in the gut, optimisation of PDI is futile within the current experimental range as all operating conditions will result in polydisperse particles and thus will not be further considered. Thus, the final optimisation was based on EE, LC and yield.

Combined response surface and contour plots for EE, LC and yield (Fig. 6.3) visually depict the relationship between nanoencapsulation parameters and a response. An optimal response for EE (red/darker area > 68%)

and LC (red/darker area > 9%) is indicated in the ranges of 3–7% for ES100 concentration (m/m) and 16–26% for GRAF concentration (m/m relative to ES100) and 22–26 kV, where higher LC is more prevalent at the higher end of the GRAF concentration range. Interaction parameter of ES100 and GRAF concentration is visible as shown by the curvature of the plot for EE, and to a lesser extent for LC. An optimal response for yield (red/darker area > 74%) is indicated in the ranges of 3–7% for ES100 concentration (m/m), 1–12% for GRAF concentration (m/m, relative to ES100) and 18–26 kV. Voltage and GRAF concentration had minimal effect on yield, even though both were indicated as significant on the Pareto charts. Although the surface response plots indicate feasible ranges for the process parameters, no clear optimum point could be obtained from the plots due to the fact that the optimum point most likely does not fall within the experimental region (Bezerra *et al.*, 2008).

Table 6.2

Coefficients of determination (R^2), adjusted coefficient of determination (R^2_{adj}) and lack-of-fit (LOF) for the polynomial regression for the response factors (particle size, PDI[a], yield, EE[b] and LC[c]) based on the process parameters (ES100[d] concentration, voltage and GRAF[e] concentration) of a central composite design for the nanoencapsulation of GRAF with ES100 by electrospraying

Response model	R^2	R^2_{adj}	LOF
Particle size (nm)	0.7582	0.5406	0.000013
PDI	0.8924	0.7956	0.109611
EE (%)	0.9360	0.8785	0.000048
LC (%)	0.9527	0.9106	0.000003
Yield (%)	0.9750	0.9869	0.193476

[a]Polydispersity index; [b]Encapsulation efficiency; [c]Loading capacity; [d]Eudragit S100 polymer; [e]Aspalathin-rich fraction prepared from green rooibos

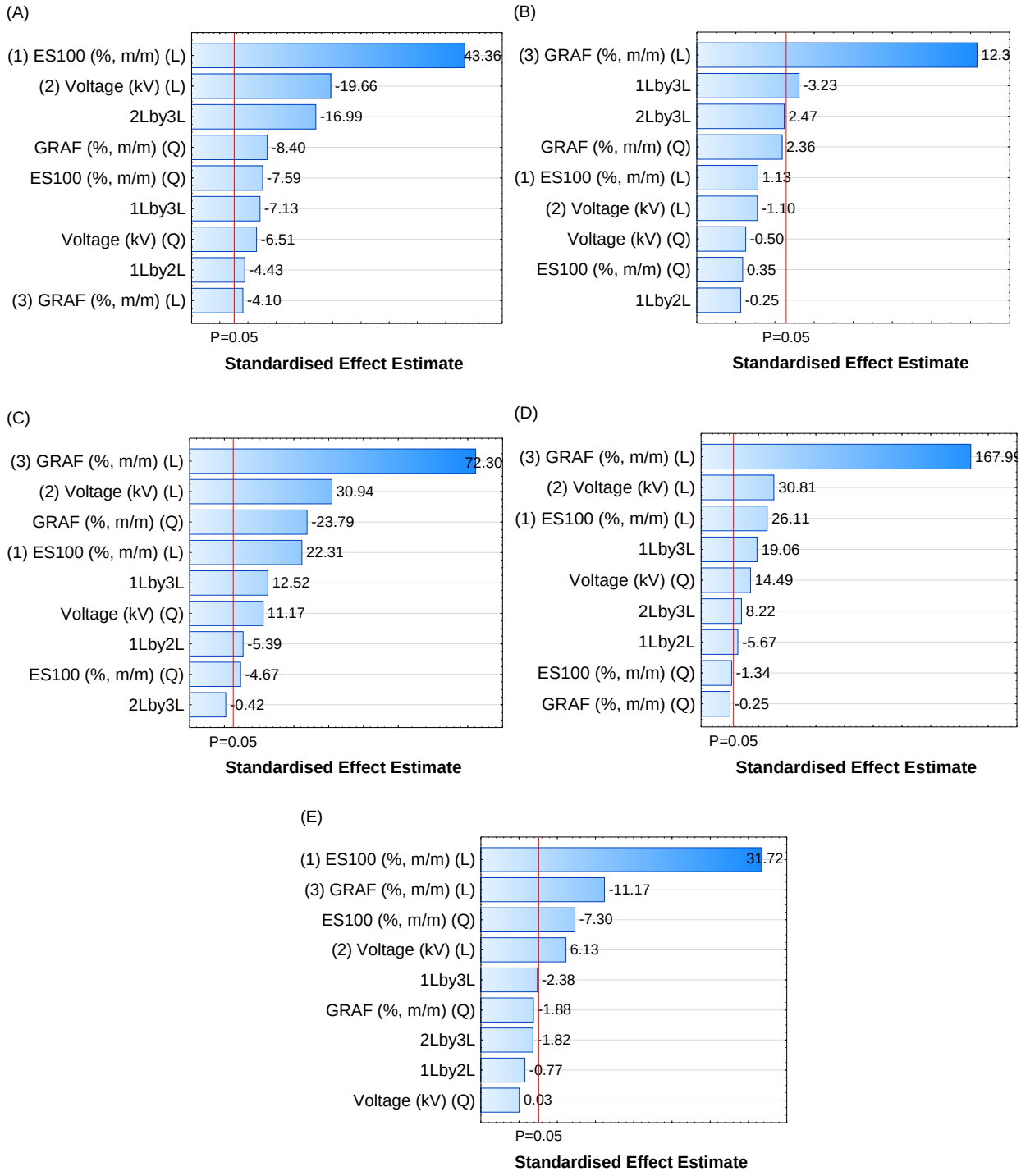

Fig. 6.2 Standardised Pareto charts showing linear (L), quadratic (Q) and interaction effects of the Eudragit S100 (ES100) concentration (%, m/m), voltage (kV) and concentration of aspalathin-rich fraction prepared from green rooibos (GRAF) (%, m/m relative to ES100) for: (A) particle size, (B) polydispersity index, (C) encapsulation efficiency, (D) loading capacity and (E) yield. Process parameters and interactions crossing the red line were considered significant ($P < 0.05$).

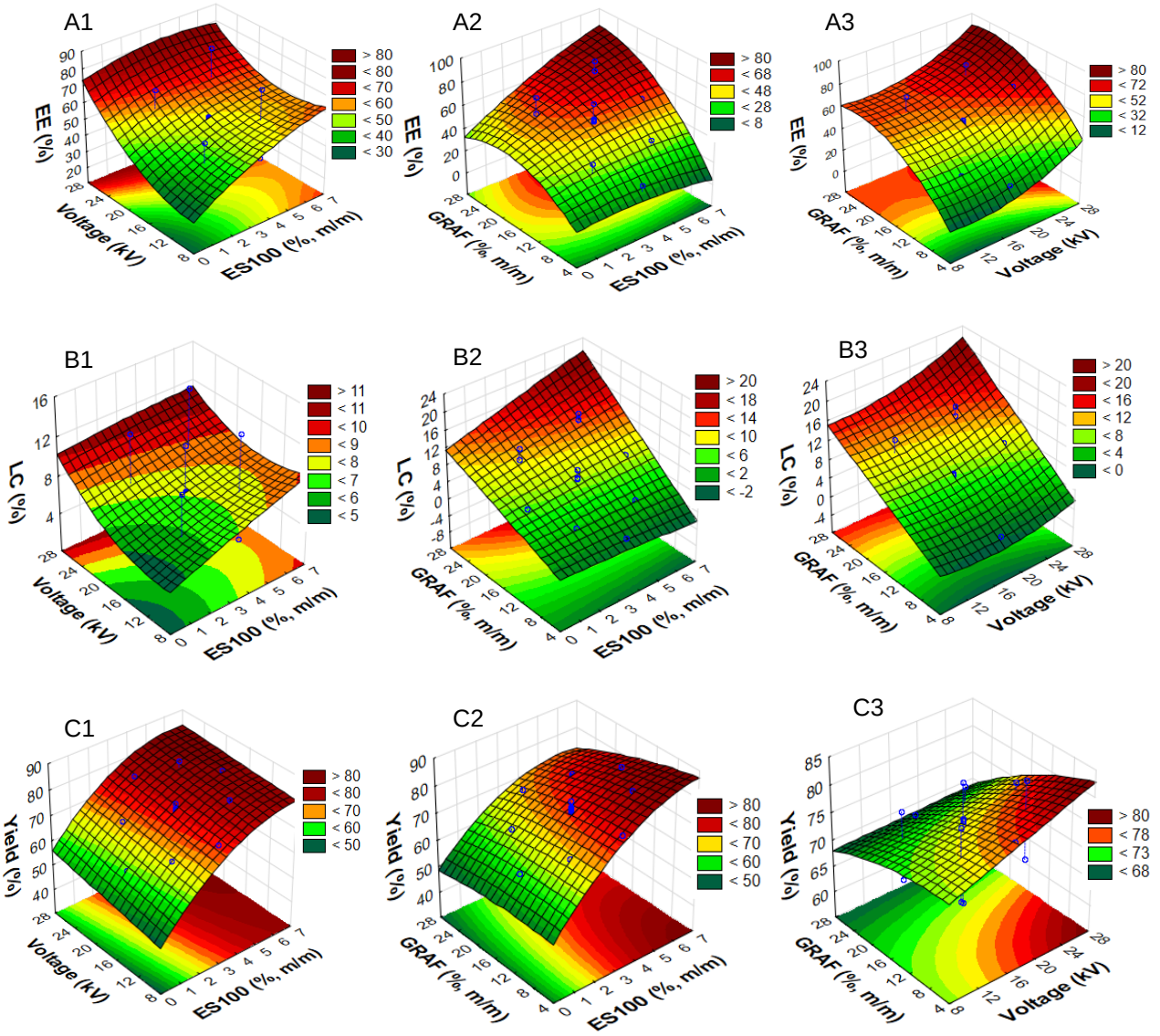

Fig. 6.3 Combined response surface and contour plots showing effects of: (1) Eudragit S100 (ES100) concentration (%, m/m) and voltage (kV); (2) ES100 concentration (%, m/m) and concentration of aspalathin-rich fraction prepared from green rooibos (GRAF) (%, m/m relative to ES100), and lastly (3) GRAF concentration (%; m/m) and voltage (kV) on the (A) encapsulation efficiency (EE), (B) loading capacity (LC) and (C) yield.

6.3.1.1 Multiresponse desirability profiling, predicted and experimental outcomes at selected optimum process parameters and nanoencapsulation of pure aspalathin

Multiresponse desirability profiling was utilised to determine optimum levels of process parameters. Optimum levels of the selected process parameters for desired EE, LC and yield were at ES100 concentration of 6% (m/m), a GRAF concentration of 19% (m/m relative to ES100) and a voltage of 25 kV (Fig. 6.4). However, the optimal value for ES100 concentration was not practically feasible as thin fibres connecting the particles were observed at 6% (m/m). Therefore, 5% (m/m) was selected as practical optimum for ES100 concentration as no fibres were formed. High polymer concentrations allow for more chain entanglements during flight

(Ruiter, Alexander, Rose & Segal, 2017) resulting in electrospinning rather than electrospraying. For a more flexible approach, a small range for each process parameter was selected, taking into account optimal values and practical considerations (Table 6.3).

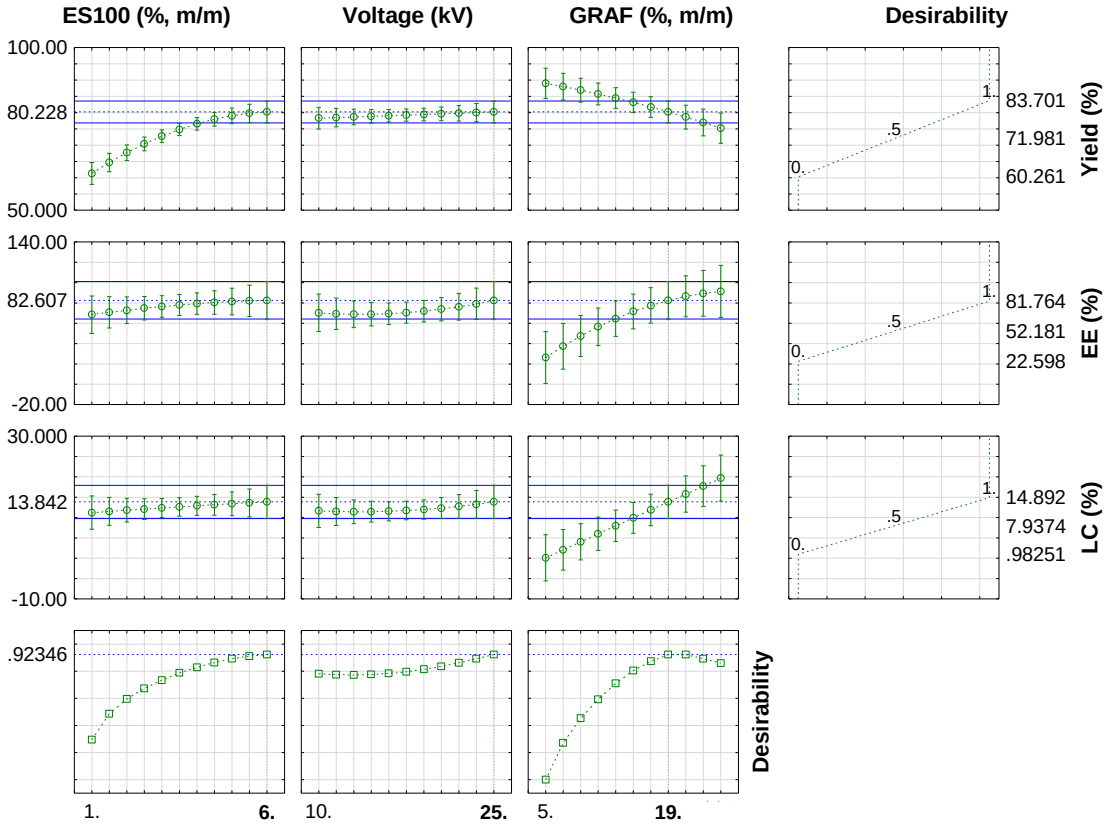

Fig. 6.4 Multiresponse desirability profiles for encapsulation efficiency (EE), loading capacity (LC) and yield (%), as affected by the Eudragit S100 (ES100) concentration (%, m/m), voltage (kV) and concentration of aspalathin-rich fraction prepared from green rooibos (GRAF) (%, m/m relative to ES100). Dashed red lines indicate optimum values.

The predictability of the model was tested by two additional experiments for the combination of minimum (ES100 (4%, m/m); GRAF (17%, m/m relative to ES100) and voltage (22 kV)) and maximum (ES100 (5%, m/m); GRAF (19%, m/m relative to ES100) and voltage (25 kV)) values selected for the three process parameters. In addition to this, pure aspalathin was encapsulated using the combination of maximum values to produce ES100-ASP nanoparticles. The experimentally obtained responses for ES100-GRAF nanoparticles were similar to the predicted values (as calculated by substituting the values for the process parameters into the appropriate polynomial equation (Eq. 6.1)). Encapsulation of pure aspalathin resulted in slightly higher yield and LC than predicted by the model (Table 6.4). Additionally, nanoparticles produced at the critical maximum and minimum process parameters were also evaluated with regard to particle properties that were not optimised. The SEM images (Fig. 6.5) showed smooth, unfused particles for the nanoparticles loaded with

GRAF and aspalathin. The particle sizes for ES100-GRAF (189 and 210 nm) and ES100-ASP (194 nm), as well as the PDI for ES100-GRAF (0.48 and 0.51) and ES100-ASP (0.45), also fell into acceptable ranges (Table 6.4).

Table 6.3

Selected optimum ranges based on optimal values of ES100[a] concentration, voltage and GRAF[b] concentration for the nanoencapsulation of GRAF with ES100 by electrospraying

Parameter	Minimum	Maximum
ES100 concentration (%, m/m)	4	5
Voltage (kV)	22	25
GRAF concentration (%, m/m)[c]	17	19

[a]Eudragit S100 polymer; [b]Aspalathin-rich fraction prepared from green rooibos; [c]GRAF concentration relative to ES100

Table 6.4

Predicted and experimental response (yield, EE[a], LC[b], particle size and PDI[c]) at selected optimum conditions for the nanoencapsulation of GRAF[d] and aspalathin with ES100[e] by electrospraying

Response	Combined minimum values for selected parameters[f]		Combined maximum values for selected process parameters[g]		
	Predicted response	Experimental response for ES100-GRAF[h]	Predicted response	Experimental response for ES100-GRAF	Experimental response for ES100-ASP[i]
Yield (%)	77.0	78.2 ± 4.5	78.8	78.3 ± 3.1	80.0 ± 1.4
EE (%)	68.3	73.9 ± 3.0	78.9	77.4 ± 3.5	78.5 ± 1.7
LC (%)	10.0	10.4 ± 0.4	12.9	12.2 ± 0.5	13.8 ± 0.3
Size (nm)	-	189 ± 4	-	210 ± 1	194 ± 3
PDI	-	0.48 ± 0.14	-	0.51 ± 0.09	0.45 ± 0.11

[a]Encapsulation efficiency; [b]Loading capacity; [c]Polydispersity index; [d]Aspalathin-rich fraction prepared from green rooibos; [e]Eudragit S100 polymer; [f]ES100 (4%, m/m), GRAF (17%, m/m relative to ES100) and voltage (22 kV); [g]ES100 (5%, m/m), GRAF (19%, m/m relative to ES100) and voltage (25 kV); [h]ES100 electrosprayed nanoparticles loaded with GRAF; [i]ES100 electrosprayed nanoparticles loaded with aspalathin

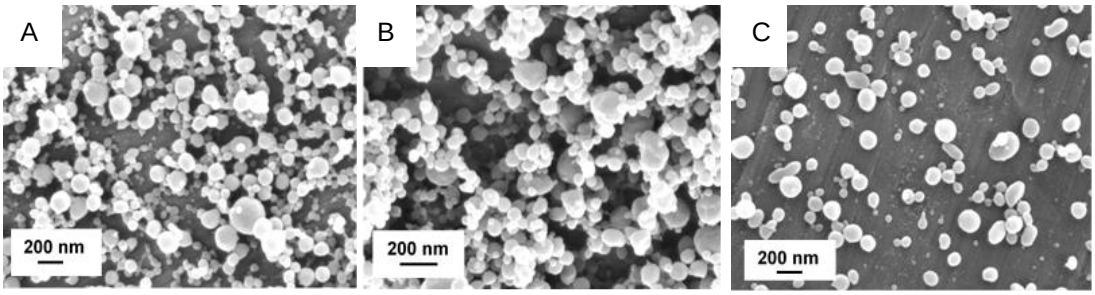

Fig. 6.5 SEM images of electrosprayed Eudragit S100 (ES100) nanoparticles loaded with aspalathin-enriched fraction of green rooibos extract (GRAF) at: (A) minimum and (B) maximum optimum process parameters, and (C) electrosprayed Eudragit S100 (ES100) nanoparticles loaded with aspalathin.

6.3.2. Orogastrointestinal pH stability and release

The total quantity of ingested bioactive compound does not always reflect the quantity available for absorption (Rein *et al.*, 2013). Many polyphenols are pH-sensitive, as was also demonstrated for aspalathin

(De Beer, Joubert, Viljoen & Manley, 2011; Bowles *et al.*, 2017). Furthermore, ES100 has a pH triggered targeted release profile (McGinity & Felton, 2008) and will thus be greatly affected by changes in the pH *in vivo*. The pH and residence times for stability tests were chosen based on studies by Versantvoort *et al.* (2005), whilst omitting the digestive fluids. Table 6.5 summarises the data for the orogastrointestinal pH stability of aspalathin (expressed as aspalathin degradation) and its release from the nanoparticles when subjected to four different pH-time combinations (pH 6.8, 5 min; pH 2, 120 min; pH 4, 60 min and pH 7, 120 min).

The stability of aspalathin was greatly affected by pH (Table 6.5) as is evident from experiments for pH-time combinations with the same time period, i.e. substantially higher aspalathin degradation was observed at pH 7 (52.6–58.6%) compared to pH 2 (1.4–13.2%) over 120 min. Little degradation of aspalathin was observed at pH 6.8 due to the short exposure time, in spite of the high pH. In all cases except pH 7, pure aspalathin was the most prone to degradation. When present in the extract matrix (GRAF) aspalathin was less susceptible to degradation. Even at pH 2, degradation of pure aspalathin was 13.2% compared to 3.8% when in GRAF. Furthermore, ES100-GRAF and ES100-ASP showed significantly less aspalathin degradation than GRAF and aspalathin, except at pH 7, as the polymer would release aspalathin and thus offer no protection. The highest degree of protection offered by nanoencapsulation was shown at pH 2.

Previous studies showed a higher degree of degradation of phenolic compounds at pH 7 and above compared to lower pH values. For instance, an increase in degradation of neohesperidin dihydrochalcone in model solutions (Canales, Borrego & Lindley, 1993) and green tea polyphenols (Komatsu *et al.*, 1993; Li, Taylor, Ferruzzi & Mauer, 2012) was observed above pH 7. The instability of pure compounds compared to when in an extract matrix, as demonstrated for aspalathin, is also not uncommon. Volf, Ignat, Neamtu & Popa (2014) found more degradation of catechin, gallic acid and vanillic acid in model solutions compared to vegetal extracts which contained these polyphenols. Furthermore, nanoencapsulation protected both pure aspalathin and aspalathin in GRAF. The highest aspalathin stability was therefore observed for ES100-GRAF, the result of the combined effect of the matrix and encapsulation with the pH-responsive polymer. The protective effect of nanoencapsulation of polyphenols has been previously shown by Singh *et al.* (2015) for epigallocatechin-3-gallate (EGCG) encapsulated with PLGA, by Hong *et al.* (2014) for EGCG encapsulated with chitosan and polyaspartic acid and by Sanna *et al.* (2015) for white tea extract encapsulated with poly(caprolactone) (PCL) and alginate.

Considering the release of aspalathin from the nanoparticles, more than 50% was released at pH 7 (53.9–58.5%), while minimal release was observed at pH 2 (11.8–12.6%) over 120 min (Table 6.5). This was expected as ES100 has a targeted release profile at pH 7 and above (McGinity & Felton, 2008; Akhgari

et al., 2017). However, as much as 42.8% and 48.2% of aspalathin was released from ES100-GRAF and ES100-ASP, respectively, when these nanoparticles were subjected to pH 4 for 60 min. These results indicate that even though the polymer has a targeted release profile at pH 7, some swelling and thus release is likely more prevalent at pH 4 compared to a very low pH of 2. Aspalathin was dispersed in the polymer and thus has the ability to diffuse through the polymer. The extent of aspalathin release differed slightly between the nanoencapsulated pure aspalathin and GRAF, where in most cases (except pH 2) the pure aspalathin showed more release, indicating that the release was governed by slightly different solubility and interaction parameters.

Theoretically, large quantities of aspalathin will not be available for permeation and absorption in the small intestine target region, as a significant percentage of aspalathin is lost due to degradation and release, especially in the intestines. Nanoencapsulation with ES100 by electrospraying was shown to increase the quantity of aspalathin that would theoretically reach the target area. This is achieved by creating a more stable environment inside the nanoparticles and by a degree of targeted release.

Table 6.5

Degradation of aspalathin (%), aspalathin when present in GRAF[a], GRAF and aspalathin nanoencapsulated with ES100[b] and aspalathin release from GRAF and aspalathin nanoencapsulated with ES100 by electropsraying as a function of pH-time combinations

		pH-time combinations based on orogastrointestinal tract			
	Formulation/compound	Oral	Gastric	Postprandial gastric	Intestinal
		6.8 (5 min)[c]	2 (120 min)	4 (60 min)	7 (120 min)
Degradation (%)	GRAF	3.5 ± 0.2 c[d]	3.8 ± 0.8 c	3.5 ± 0.4 c	53.4 ± 0.8 a
	ES100-GRAF[e]	1.4 ± 0.9 d	1.4 ± 0.3 d	1.6 ± 0.1 d	52.6 ± 4.5 a
	Aspalathin	13.9 ± 1.2 a	13.2 ± 0.9 a	12.5 ± 2.5 a	58.6 ± 2.6 a
	ES100-ASP[f]	7.5 ± 1.2 b	5.6 ± 0.2 b	6.6 ± 0.3 b	55.6 ± 3.3 a
Release (%)	ES100-GRAF	6.1 ± 0.8	12.6 ± 2.4	42.8 ± 1.6	53.9 ± 2.5
	ES100-ASP	12.9 ± 0.3	11.8 ± 0.5	48.2 ± 2.8	58.5 ± 3.9

[a]Aspalathin-rich fraction prepared from green rooibos; [b]Eudragit S100 polymer; [c]pH followed by time in brackets; [d]Means in the same column with the same letter is not significantly different (P ≥ 0.05); [e]ES100 electrosprayed nanoparticles loaded with GRAF; [f]ES100 electrosprayed nanoparticles loaded with aspalathin

6.3.3 Assessing membrane permeation of aspalathin

PAMPA and Caco-2 monolayer models were used as *in vitro* methods to determine whether nanoencapsulation of aspalathin could improve its intestinal absorption. PAMPA is useful to measure the effective permeability of compounds through the membrane as a result of passive transcellular diffusion (Kansy, Senner & Gubernator, 1998). By using a specific composition for the artificial membrane, absorption through the gastrointestinal tract can be simulated (Wexler *et al.*, 2005). The Caco-2 monolayer, derived from human colon adenocarcinoma, has been used widely as an *in vitro* model of absorption by intestinal epithelial

cells. It can thus be used to study different routes of absorption (Artursson, Palm & Luthman, 2001). Previously, Bowles et al. (2017) showed that aspalathin is not actively transported by the glucose transporters, leading to the conclusion that it presumably passes the monolayer through the water-filled pores of the paracellular pathway, given that aspalathin is a hydrophylic compound. With aspalathin encapsulated by ES100, imparting a more hydrophobic character, and the nano-size of the particles, an increase in absorption via the transmembrane route would be expected. The P_e and P_{app} values for aspalathin as obtained from PAMPA and Caco-2 monolayer models, respectively, are summarised in Table 6.6. In the PAMPA assay, caffeine and rutin served as high and low permeability markers, respectively (Konczol *et al.*, 2013), to ensure the data obtained were reliable. Caffeine had a high P_e, whereas no P_e could be accurately determined for rutin, due to its low permeability. The high P_{app} of caffeine (4.2×10^{-5} cm/s), TEER values >300 Ω and <3% passage of LY indicated reliability of the Caco-2 model and intact, robust cell layers. Low P_e ($\leq 0.28 \times 10^{-7}$ cm/s) and P_{app} ($\leq 0.68 \times 10^{-6}$ cm/s) values were observed for pure aspalathin and aspalathin present in GRAF, ES100-GRAF and ES100-ASP, indicating poor permeability. Active or paracellular transport are indicated when permeability obtained from PAMPA << Caco-2 (Kerns *et al.*, 2004). Neither the presence of the extract matrix nor nanoencapsulation had any significant effect on aspalathin absorption, nor could any trend be observed.

Previously Bowles *et al.* (2017) demonstrated that pure aspalathin and aspalathin present in a green rooibos extract were both poorly absorbed in the Caco-2 model, similar to results of the current study. The low permeability of pure aspalathin, and when present in the extract matrix (GRAF), was expected due to its low lipophilicity and chemical structure, also noted by Bowles *et al.* (2017). The similar permeability values for aspalathin and aspalathin from GRAF, irrespective of nanoencapsulation, could potentially be due to swelling of the polymer at pH 7 resulting in large polymer aggregates and clogging of the lipid membrane, preventing an increase in permeability. In addition, the large PDI could also affect the absorption negatively. Mesallati, Umerska, Paluch & Tajber (2017) found decreased permeability when Eudragit L100, similar to Eudragit S100, but with a targeted release at lower pH (Patel, Prajapati & Patel, 2007), was added to ciproflaxin for similar reasons. However, a recent review highlighted the importance of phenolic compounds to the gut microbiota, rather than the human host (Ercolini & Fogliano, 2018), indicating the usefulness of rooibos nanoparticles with a targeted enteric delivery and passage, even though no increase in permeability was achieved.

Table 6.6

P_e[a] and P_{app}[b] of aspalathin when present in GRAF[c], GRAF and aspalathin nanoencapsulated with ES100[d], as well as caffeine and rutin

Formulation/compound	P_e x 10^{-7} (cm/s)	P_{app} x 10^{-6} (cm/s)
Aspalathin	0.38 ± 0.09 b	0.96 ± 0.22 b
GRAF	0.81 ± 0.64 b	0.68 ± 0.07 b
ES100-GRAF[f]	0.28 ± 0.15 b	0.71 ± 0.29 b
ES100-ASP[g]	0.41 ± 0.17 b	0.73 ± 0.24 b
Caffeine[h]	89.47 ± 19.8 a	42.04 ± 0.79 a
Rutin[i]	Nq[j]	-

[a]Effective permeability values obtained from parallel artificial membrane permeability assay carried out for 16 h at 22°C; [b]Apparent permeability values obtained apical to basolateral transport in Caco-2 cell model over 2 h. [c]Aspalathin-rich fraction prepared from green rooibos; [d]Eudragit S100 polymer; [e]Means in the same column with the same letter are not significantly different (P ≥ 0.05); [f]ES100 electrosprayed nanoparticles loaded with GRAF; [g]Eudragit S100 electrosprayed nanoparticles loaded with aspalathin; [h]Caffeine representing a high permeability marker; [i]Rutin representing a low permeability marker; [j]Compound concentration in acceptor compartment was too small to quantify

6.4 Conclusions

Nanoencapsulation of an aspalathin-rich fraction prepared from green rooibos and pure aspalathin with Eudragit S100 polymer by electrospraying was successful, with the formation of nanosized particles achieving reasonable encapsulation efficiency, loading capacity and process yield. The central composite design used offered a quick and verifiable method to obtain optimum conditions. Nanoencapsulation offered protection against aspalathin degradation at lower pH values, due to minimal release by the polymer, indicating the value of using a targeted release polymer. Pure aspalathin and nanoencapsulated pure aspalathin proved to be less stable than the nanoencapsulated aspalathin-rich fraction prepared from green rooibos or the fraction alone, indicating that a compromise would have to be made between stability of the nutraceutical formulation and the dosage. However, nanoencapsulation with ES100 offers a method to ensure that higher aspalathin concentrations reach the target area, which already lowers the required dosage. No increase in passive permeation was achieved for the nanoencapsulated rooibos extract and aspalathin, maintaining the low permeability values for aspalathin. However, minimal permeation in combination with targeted enteric delivery could be useful to the gut microbiota.

6.5 References

Akhgari, A., Heshmati, Z., Garekani, H. A., Sadeghi, F., Sabbagh, A., Makhmalzadeh, B. S. & Nokhodchi, A. (2017). Indomethacin electrospun nanofibers for colonic drug delivery: *In vitro* dissolution studies. *Colloids and Surfaces B: Biointerfaces,* 152, 29–35.

Artursson, P. & Karlsson, J. (1991). Correlation between oral drug absorption in humans and apparent drug permeability coefficients in human intestinal epithelial (Caco-2) cells. *Biochemical and Biophysical Research Communications,* 175, 880–885.

Artursson, P., Palm , K. & Luthman, K. (2001). Caco-2 monolayers in experimental and theoretical predictions of drug transport. *Advanced Drug Delivery Reviews,* 46, 27–43.

Bezerra, M. A., Santelli, R. E., Oliveira, E. P., Villar, L. S. & Escaleira, L. A. (2008). Response surface methodology (RSM) as a tool for optimization in analytical chemistry. *Talanta,* 76, 965–977.

Bowles, S., Joubert, E., De Beer, D., Louw, J., Brunschwig, C., Njoroge, M., Lawrence, N., Wiesner, L., Chibale, K. & Muller, C. (2017). Intestinal transport characteristics and metabolism of *C*-glucosyl dihydrochalcone, aspalathin. *Molecules,* 22, 554–569.

Canales, I., Borrego, F. & Lindley, M. G. (1993). Neohesperidin dihydrochalcone stability in aqueous buffer solutions. *Journal of Food Science,* 57, 589–591.

Da Conceição, L. R. V., Da Costa, C. E. F., Da Rocha Filho, G. N., Pereira-Filho, E. R. & Zamian, F. R. (2015). Ethanolysis optimisation of Jupati (*Raphia taedigera* Mart.) oil to biodiesel using response surface methodology. *Journal of the Brazilian Chemical Society,* 26, 1321–1330.

De Beer, D., Joubert, E., Viljoen, M. & Manley, M. (2011). Enhancing aspalathin stability in rooibos (*Aspalathus linearis*) ready-to-drink iced teas during storage: the role of nano-emulsification and beverage ingredients, citric and ascorbic acids. *Journal of the Science of Food and Agriculture,* 92, 274–282.

De Beer, D., Malherbe, C. J., Beelders, T., Willenburg, E. L., Brand, D. J. & Joubert, E. (2015). Isolation of aspalathin and nothofagin from rooibos (*Aspalathus linearis*) using high-performance countercurrent chromatography: Sample loading and compound stability considerations. *Journal of Chromatography A,* 1381, 29–36.

Ercolini, D. & Fogliano, V. (2018). Food design to feed human gut microbiota. *Journal of Agricultural and Food Chemistry,* 66, 3754–3758.

Ferreira, F. B. A., Silva, F. L. G., Luna, A. S., Lago, D. C. B. & Senna, L. F. (2007a). Response surface modeling and optimization to study the influence of deposition parameters on the electrodeposition of Cu–Zn alloys in citrate medium. *Journal of Applied Electrochemistry,* 37, 473–481.

Ferreira, S. L., Bruns, R. E., Ferreira, H. S., Matos, G. D., David, J. M., Brandao, G. C., Da Silva, E. G., Portugal, L. A., Dos Reis, P. S., Souza, A. S. & Dos Santos, W. N. (2007b). Box-Behnken design: an alternative for the optimization of analytical methods. *Analytica Chimica Acta,* 597, 179–186.

Gardner, J. D., Ciociola, A. A. & Robinson, M. (2002). Measurement of meal-stimulated gastric acid secretion by *in vivo* gastric autotitration. *Journal of Applied Physiology,* 92, 427–434.

Granato, D., Grevink, R., Zielinski, A. A., Nunes, D. S. & van Ruth, S. M. (2014). Analytical strategy coupled with response surface methodology to maximize the extraction of antioxidants from ternary mixtures of green, yellow, and red teas (*Camellia sinensis var. sinensis*). *Journal of Agricultural and Food Chemistry,* 62, 10283–10296.

Hong, Z., Xu, Y., Yin, J. F., Jin, J., Jiang, Y. & Du, Q. (2014). Improving the effectiveness of (-)-epigallocatechin gallate (EGCG) against rabbit atherosclerosis by EGCG-loaded nanoparticles prepared from chitosan and polyaspartic acid. *Journal of Agricultural and Food Chemistry,* 62, 12603–12609.

Kansy, M., Senner, F. & Gubernator, K. (1998). Physicochemical high throughput screening: parallel artificial membrane permeation assay in the description of passive absorption processes. *Journal of Medicinal Chemistry,* 7, 1007–1010.

Kerns, E. H., Di, L., Petusky, S., Farris, M., Ley, R. & Jupp, P. (2004). Combined application of parallel artificial membrane permeability assay and Caco-2 permeability assays in drug discovery. *Journal of Pharmaceutical Sciences,* 93.

Knop, K., Hoogenboom, R., Fischer, D. & Schubert, U. S. (2010). Poly(ethylene glycol) in drug delivery: Pros and cons as well as potential alternatives. *Angewandte Chemie International Edition,* 49, 6288–6308.

Komatsu, Y., Suematsu, S., Hisanobu, Y., Saigo, H., Matsuda, R. & Hara, K. (1993). Effects of pH and temperature on reaction kinetics of catechins in green tea infusion. *Bioscience, Biotechnology, and Biochemistry,* 57, 907–910.

Konczol, A., Muller, J., Foldes, E., Beni, Z., Vegh, K., Kery, A. & Balogh, G. T. (2013). Applicability of a blood-brain barrier specific artificial membrane permeability assay at the early stage of natural product-based CNS drug discovery. *Journal of Natural Products,* 76, 655–663.

Kreuz, S., Joubert, E., Waldmann, K. & Ternes, W. (2008). Aspalathin, a flavonoid in *Aspalathus linearis* (rooibos), is absorbed by pig intestine as a *C*-glycoside. *Nutrition Research,* 28, 690–701.

Li, N., Taylor, L. S., Ferruzzi, M. G. & Mauer, L. J. (2012). Kinetic study of catechin stability: Effects of pH, concentration, and temperature. *Journal of Agricultural and Food Chemistry,* 60, 12531–12539.

McClements, D. J. & Rao, J. (2011). Food-grade nanoemulsions: Formulation, fabrication, properties, performance, biological fate, and potential toxicity. *Critical Reviews in Food Science and Nutrition,* 51, 285–330.

McGinity, J. W. & Felton, L. A. (2008). Aqueous polymeric coatings for pharmaceutical dosage forms. Pp. 1–475. Florida: CRC Press.

Mesallati, H., Umerska, A., Paluch, K. J. & Tajber, L. (2017). Amorphous polymeric drug salts as ionic solid dispersion forms of ciprofloxacin. *Molecular Pharmaceutics,* 14, 2209–2223.

Patel, V. M., Prajapati, B. G. & Patel, M. M. (2007). Effect of hydrophilic polymers on buccoadhesive Eudragit patches of propranolol hydrochloride using factorial design. *AAPS PharmSciTech,* 8, E1–E8.

Piazzini, V., Rosseti, C., Bigagli, E., Luceri, C., Bilia, A. R. & Bergonzi, M. C. (2017). Prediction of permeation and cellular transport of *Silybum marianum* extract formulated in a nanoemulsion by using PAMPA and Caco-2 cell models. *Planta Medica,* 83, 1184–1193.

Rein, M. J., Renouf, M., Cruz-Hernandez, C., Actis-Goretta, L., Thakkar, S. K. & Da Silva Pinto, M. (2013). Bioavailability of bioactive food compounds: a challenging journey to bioefficacy. *British Journal of Clinical Pharmacology,* 75, 588–602.

Ruiter, F. A. A., Alexander, C., Rose, F. & Segal, J. I. (2017). A design of experiments approach to identify the influencing parameters that determine poly-D,L-lactic acid (PDLLA) electrospun scaffold morphologies. *Biomedical Materials,* 12, 1–11.

Sanna, V., Lubinu, G., Madau, P., Pala, N., Nurra, S., Mariani, A. & Sechi, M. (2015). Polymeric nanoparticles encapsulating white tea extract for nutraceutical application. *Journal of Agricultural and Food Chemistry,* 63, 2026–2032.

Singh, M., Bhatnagar, P., Mishra, S., Kumar, P., Shukla, Y. & Gupta, K. C. (2015). PLGA-encapsulated tea polyphenols enhance the chemotherapeutic efficacy of cisplatin against human cancer cells and mice bearing Ehrlich ascites carcinoma. *International Journal of Nanomedicine,* 10, 6789–809.

Versantvoort, C. H. M., Oomen, A. G., Van de Kamp, E., Rompelberg, C. J. M. & Sips, A. J. A. M. (2005). Applicability of an *in vitro* digestion model in assessing the bioaccessibility of mycotoxins from food. *Food and Chemical Toxicology,* 43, 31–40.

Volf, I., Ignat, I., Neamtu, M. & Popa, V. (2014). Thermal stability, antioxidant activity, and photo-oxidation of natural polyphenols. *Chemical Papers,* 68, 121–129.

Wexler, D. S., Gao, L., Anderson, F., Ow, A., Nadasdi, L., McAlorum, A., Urfer, R. & Huang, S. G. (2005). Linking solubility and permeability assays for maximum throughput and reproducibility. *Journal of Biomolecular Screening,* 10, 383–390.

Yoshida, T., Lai, T. C., Kwon, G. S. & Sako, K. (2013). pH- and ion-sensitive polymers for drug delivery. *Expert Opinion on Drug Delivery,* 10, 1497–513.

SUPPLEMENTARY MATERIAL CHAPTER 6_ADDENDUM D

Table D. 1

ANOVA results of polynomial regression for the response factors (particle size, PDI[a], yield, EE[b] and LC[c]) based on the process parameters (ES100[d] concentration, voltage and GRAF[e] concentration) of a central composite design for the nanoencapsulation of GRAF with ES100 by electrospraying

Parameter	Regr Coeff.[f]	SS[g]	DF[h]	MS[i]	F	P
Particle size (nm) model						
Intercept	33.289					
(1) ES100 concentration (%, m/m)	29.593	3212.846	1	3212.846	1880.201	0.000000
ES100 concentration (%, m/m) (Q)[j]	-1.183	98.482	1	98.482	57.633	0.000630
(2) Voltage (kV) (L)[k]	7.911	660.412	1	660.412	386.482	0.000006
Voltage (kV) (Q)	-0.112	72.497	1	72.497	42.426	0.001275
(3) GRAF concentration (%, m/m)[l]	8.697	28.733	1	28.733	16.815	0.009349
GRAF concentration (%, m/m) (Q)	-0.081	120.454	1	120.454	70.491	0.000393
1L x 2L	-0.308	33.483	1	33.483	19.595	0.006850
1L x3L	-0.372	86.900	1	86.900	50.855	0.000842
2L x 3L	-0.296	493.503	1	493.503	288.805	0.000013
Lack of Fit		1509.332	5	301.866	176.656	0.000013
Pure Error		8.544	5	1.709		
Total SS		6277.742	19			
R^2						0.75821
R^2_{adj}						0.5406
PDI (%) model						
Intercept	0.345338					
(1) ES100 concentration (%, m/m)	0.070310	0.001451	1	0.001451	1.275	0.310030
ES100 concentration (%, m/m) (Q)	0.001412	0.000140	1	0.000140	0.123	0.739872
(2) Voltage (kV) (L)	-0.009469	0.001380	1	0.001380	1.213	0.320982
Voltage (kV) (Q)	-0.000225	0.000290	1	0.000290	0.254	0.635398
(3) GRAF concentration (%, m/m)	-0.003102	0.172815	1	0.172815	151.876	0.000062
GRAF concentration (%, m/m) (Q)	0.000593	0.006339	1	0.006339	5.571	0.064722
1L x 2L	-0.000453	0.000072	1	0.000072	0.063	0.811402
1L x3L	-0.004356	0.011858	1	0.011858	10.421	0.023252
2L x 3L	0.001113	0.006962	1	0.006962	6.119	0.056284
Lack of Fit		0.018614	5	0.003723	3.272	0.109611
Pure Error		0.005689	5	0.001138		
Total SS		0.225847	19			
R^2						0.8924
R^2_{adj}						0.7956

Table D.1 Continued

EE (%) model						
Intercept	−11.070					
(1) ES100 concentration (%, m/m)	3.9629	260.602	1	260.602	497.875	0.000003
ES100 concentration (%, m/m) (Q)	−0.4025	11.402	1	11.402	21.784	0.005496
(2) Voltage (kV) (L)	−1.5972	501.180	1	501.180	957.494	0.000001
Voltage (kV) (Q)	0.1070	65.262	1	65.262	124.681	0.000101
(3) GRAF concentration (%, m/m)	5.0304	2735.994	1	2735.994	5227.060	0.000000
GRAF concentration (%, m/m) (Q)	−0.1282	296.127	1	296.127	565.744	0.000002
1L x 2L	−0.2080	15.216	1	15.216	29.070	0.002962
1L x3L	0.3623	82.030	1	82.030	156.717	0.000058
2L x 3L	−0.0041	0.094	1	0.094	0.180	0.689094
Lack of Fit		270.363	5	54.073	103.304	0.000048
Pure Error		2.617	5	0.523		
Total SS		4267.597	19			
R^2						0.93603
R^2_{adj}						0.87847
LC (%) model						
Intercept	1.682535					
(1) ES100 concentration (%, m/m)	−0.025127	6.0715	1	6.0715	681.79	0.000002
ES100 concentration (%, m/m) (Q)	−0.015105	0.0161	1	0.0161	1.80	0.237097
(2) Voltage (kV) (L)	−0.512748	8.4559	1	8.4559	949.55	0.000001
Voltage (kV) (Q)	0.018113	1.8699	1	1.8699	209.98	0.000028
(3) GRAF concentration (%, m/m)	0.293908	251.3054	1	251.3054	28220.02	0.000000
GRAF concentration (%, m/m) (Q)	−0.000175	0.0006	1	0.0006	0.06	0.812997
1L x 2L	−0.028547	0.2865	1	0.2865	32.17	0.002371
1L x3L	0.071931	3.2338	1	3.2338	363.14	0.000007
2L x 3L	0.010344	0.6019	1	0.6019	67.59	0.000434
Lack of Fit		13.3787	5	2.6757	300.47	0.000003
Pure Error		0.0445	5	0.0089		
Total SS		285.3365	19			
R^2						0.9527
R^2_{adj}						0.9106
Yield (%) model						
Intercept	40.228					
(1) ES100 concentration (%, m/m)	10.424	556.730	1	556.730	1006.420	0.000001
ES100 concentration (%, m/m) (Q)	−0.647	29.503	1	29.503	53.335	0.000754
(2) Voltage (kV) (L)	0.643	20.799	1	20.799	37.600	0.001675
Voltage (kV) (Q)	0.000	0.001	1	0.001	0.001	0.977034
(3) GRAF concentration (%, m/m)	0.498	68.960	1	68.960	124.663	0.000101
GRAF concentration (%, m/m) (Q)	−0.010	1.958	1	1.958	3.541	0.118621
1L x 2L	−0.031	0.327	1	0.327	0.591	0.476666
1L x3L	−0.071	3.140	1	3.140	5.676	0.062971
2L x 3L	−0.018	1.828	1	1.828	3.305	0.128736
Lack of Fit		6.304	5	1.260	2.279	0.193476
Pure Error		2.765	5	0.553		
Total SS		691.523	19			
R^2						0.97508
R^2_{adj}						0.98688

[a]Polydispersity index; [b]Encapsulation efficiency; [c]Loading capacity; [d]Eudragit S100 polymer; [e]Aspalathin-rich fraction prepared from green rooibos; [f]Regression coefficient; [g]Sum of squares; [h]Degrees of freedom; [i]Mean square; [j]Quadratic coefficient; [k]Linear coefficient; [l]GRAF concentration relative to ES100 concentration

Chapter 7

General discussion and conclusion

Aspalathin, a major dihydrochalcone naturally present in *Aspalathus linearis*, stimulates cellular mechanisms and physiological responses underlying its potential and that of aspalathin-rich extracts in the prevention of the metabolic syndrome (Johnson *et al.*, 2018; Muller *et al.*, 2018). The emergence of the nutraceutical market (Corbo, Bevilacqua, Petruzzi, Casanova & Sinigaglia, 2014) has also sparked interest in a condition-specific rooibos nutraceutical extract to exploit the beneficial effects of aspalathin. Traditionally, rooibos products comprised of herbal tea, and later also food ingredient extracts from oxidised (referred to as "fermented") plant material (Joubert & De Beer, 2011). Fermented rooibos plant material contains only 0.02–1.16% aspalathin. Green rooibos plant material contains significantly higher amounts of aspalathin (3.8–9.7%) (Joubert & Schulz, 2006), as the oxidation step in the production of the traditional, "fermented" product is excluded making green rooibos the product of choice for the manufacture of extracts, rich in aspalathin (Miller, De Beer & Joubert, 2017). In the present study a green rooibos extract (GRE), containing 14% aspalathin, was used for production of microencapsulated extract powder. Green rooibos leaves, due to their higher aspalathin content in relation to the stem (Miller *et al.*, 2017), were used to prepare a fraction containing 40% aspalathin (GRAF) by hot water extraction followed by *n*-butanol/water liquid-liquid fractionation. This fraction was used to prepare nanoparticles.

Delivery of aspalathin as part of the diet poses a problem as it is highly susceptible to oxidative changes, governed not only by the availability of oxygen, but factors such as light, moisture, temperature and pH also play a role (Koeppen & Roux, 1965; De Beer *et al.*, 2015). An investigation of the stability of aspalathin in ready-to-drink (RTD) rooibos iced teas confirmed poor aspalathin retention during heat treatment and storage (Joubert, Viljoen, De Beer & Manley, 2009; Joubert *et al.*, 2010; De Beer, Joubert, Viljoen & Manley, 2011). There is thus a need for a stable functional rooibos convenience product. Single-serve powder products, which have become increasingly popular due to increased convenience and portability, require powder with low water activity (a_w) and moisture content (MC), as well as good flowability and wettability. In the present study a green rooibos iced tea powder formulation was investigated in terms of the effect of microencapsulation, addition of common iced tea ingredients (sweetener, acidifier and antioxidant) and suitable convenience product packaging (e.g. single-serve sachets) on the stability and applicable physicochemical characteristics. In addition to microencapsulation, nanoencapsulation was investigated to produce a nutraceutical green rooibos ingredient in nanoparticle form.

As an initial step, microencapsulation was investigated in order to formulate a more stable green rooibos nutraceutical ingredient prior to addition to iced tea powders containing a sweetener, acidifier and antioxidant. Encapsulation could protect ingredients prone to degradation by sequestering them from the environment and

controlling their release (Gibbs, Kermasha, Alli & Mulligan, 1999; Augustin & Hemar, 2009; Nedovic, Kalusevic, Manojlovic, Levic & Bugarski, 2011).

Maltodextrin is widely used for microencapsulation of various food ingredients and natural extracts, as it is water-soluble, easy to use, readily available, inexpensive and has good coating properties (Gharsallaoui, Roudaut, Chambin, Voilley & Saurel, 2007). However, maltodextrin results in post-prandial glycaemia as it is metabolised into simple sugars (Hofman, Van Buul & Brouns, 2016), making it unsuitable for consumers with diabetes, one of the cluster of metabolic abnormalities characterising the metabolic syndrome (Johnson *et al.*, 2018). Thus, research is turning to alternative polymers for encapsulation of plant extracts. Miller, De Beer, Aucamp, Malherbe & Joubert (2018) investigated the use of inulin as an alternative to maltodextrin. Inulin is a non-digestible, low kilojoule fructan-type polysaccharide with various functional properties, including stimulation of the growth of beneficial intestinal bacteria and immune boosting properties (Kolida & Gibson, 2007; Shoaib *et al.*, 2016). Studies have linked the role of gut microbe health to various inflammatory metabolic disorders (Dehghan, Gargari & Jafar-Abadi, 2014), making inulin ideal for use in a green rooibos nutraceutical ingredient aimed at prevention of the metabolic syndrome.

Microencapsulation of a green rooibos extract with inulin (1:1, m/m) by spray-drying produced powders with >95% aspalathin retention, improved wettability and a_w compared to maltodextrin, important for dissolution of instant beverages and shelf-life stability, respectively. These promising results obtained by Miller *et al.* (2018) prompted further investigation (**Chapter 3**) by including chitosan, in addition to inulin and maltodextrin, and optimising encapsulation and aspalathin retention with regard to the polymer and GRE:polymer ratio. As with inulin, chitosan is also indigestible to humans. Furthermore, it has the ability to bind fat and cholesterol in the digestive tract, ideal for prevention of the metabolic syndrome (Yao & Chiang, 2006). However, chitosan is only soluble in weak acidic media. This results in high viscosity at low concentration, which proved to be a disadvantage in this study.

The present study not only confirmed that inulin is a superior alternative to maltodextrin, but that chitosan is unsuitable for encapsulation of GRE. Chitosan formulations resulted in lower yields and aspalathin retention than the other two polymers. Differences in trends observed for chitosan compared to maltodextrin and inulin were postulated to be an effect of the high viscosity and sticky nature of chitosan solutions. Spray-drying of GRE with inulin resulted in similar properties compared to spray-drying of GRE with maltodextrin. Firstly, most of the aspalathin was retained after spray-drying, which is one of the first pre-requisites for a green rooibos nutraceutical ingredient with high aspalathin content. The yield, which relates to the cost and efficiency of the process, and the MC and a_w, which relate to the stability of the powders, also fell into reasonable ranges. Thus,

inulin was confirmed to be a suitable encapsulating agent as it not only increased the value of the rooibos functional ingredient with its inherent health properties, but also the general powder characteristics of the microencapsulated extract. Based on isothermal microcalorimetry, employed to indicate possible incompatibility between polymers and GRE, as well as the possibility of state transformations when exposed to moisture, inulin used in a 1:1 ratio with GRE appeared to be more compatible and overall more stable. This is the first time that GRE:polymer ratio was optimised in terms of physicochemical properties. The stability of aspalatihin was subsequently determined under accelerated storage conditions (40 °C/75% (relative humidity) RH for 96 h). Aspalathin stability served as an additional criterion of the relative merits of the polymers. The mini-hygrostat system employed to expose the powders to a constant RH allowed the use of small quantities of the spray-dried powders and minimal experimental effort. In addition, accelerated stability testing allows for the extrapolating of data to normal, suitable shelf-life storage conditions, whilst minimising the duration of experiments (Aulton, 1996). All the powders showed >10% aspalathin degradation accompanied by substantial moisture uptake. This was not unexpected, given the results of the dynamic moisture sorption experiments, the amorphous nature of the powders and the presence of glucose, often associated with hygroscopicity in natural extracts. However, this emphasises that the hygroscopic nature of the powders should be carefully considered during production of the convenience iced tea powder product, as it is most likely a factor in the stability of aspalathin and overall stability of the product. Modelling of aspalathin degradation as a function of time was best predicted by the fractional conversion model based on first-order kinetics. Constants derived from kinetic modelling, i.e. degradation rate constants and equilibrium concentrations, are used to derive the basic kinetic information of active compounds, formulations or final products. Kinetic information and models can be utilised to predict and understand the chemical degradation during storage (Van Boekel, 1996; 2008) and is thus more valuable than conventional trial and error methods for stability prediction. The extent of aspalathin degradation, the predicted equilibrium aspalathin content and reaction rate constants of the extract encapsulated with chitosan (10 and 15%), indicated a significant decrease in aspalathin stability compared to the other formulations, whereas chitosan at 5% did not have the same effect. Firstly, these results not only confirmed that chitosan was unsuitable for the production of a microencapsulated green rooibos nutraceutical ingredient with high aspalathin content, but also that the level of chitosan plays a crucial role. The degradation rate constants for aspalathin in the extract microencapsulated with inulin and maltodextrin were not significantly different between treatments, however, significantly higher predicted equilibrium aspalathin content and less degradation of aspalathin (%) was observed for some of the inulin and maltodextrin formulations compared to GRE, but no clear pattern was evident for the level of these

polymers. The results from accelerated stability tests should be interpreted with caution, since degradation rates do not give the full picture in cases where fractional conversion occurs, i.e. degradation does not continue until zero concentration is reached. Another factor to be kept in mind is that accelerated stability tests hold the risk of resulting in reactions that do not usually occur under normal conditions (Aulton, 1996). The powders underwent deliquescence during storage at 75% RH, which, according to the moisture sorption isotherms, would most likely not have occurred at lower RH. Deliquescence could have rendered the immobilisation effect of microencapsulation obsolete, hence no differences were observed for the degradation rates of aspalathin when encapsulated with inulin and maltodextrin compared to aspalathin in GRE. While the accelerated stability tests provided a useful indication of aspalathin stability in the spray-dried powders and the effect of the microencapsulating polymers on its stability, the technique has limitations as discussed.

The next step was to determine the shelf-life stability of formulated rooibos iced tea products, containing the inulin-microencapsulated GRE (IN50) and other food ingredients used for production of rooibos iced tea, at 30 °C/65% RH and 40 °C/65% RH. This is the first study investigating the stability of rooibos iced tea powder formulations. Mixtures of IN50 with various ingredients were subjected to storage to elucidate their respective effects on product stability. The temperature/RH conditions were selected, guided by the South African climatic zone (zone II, Mediterranean, Subtropical) and International Council of Harmonisation (ICH), whilst maintaining a constant RH to allow for direct comparison of samples stored at different temperatures (Markens, 2009; EMEA, 2003). The different powders were stored in both semi-permeable and impermeable packaging. Sachets, produced from metallised polyethylene terephthalate (MET/PET) film and linear low density polyethylene (LLDPE) film were selected as the semi-permeable packaging (0.4% transmission of moisture vapour measured as g/m^2 in 24 h (Anonymous, 2018a)), while sealed glass vials (5 mL amber screw cap vials, tightly sealed) simulated impermeable packaging as would be provided by three layer (e.g. polyester film/aluminium foil/LDPE) sachets with minimal to no transmission of moisture vapour (0.01 %) (Anonymous, 2018a). Even though impermeable packaging is preferred for hygroscopic powders, semi-permeable packaging is generally more cost effective due to less materials required for their production. Storage was intended for 12 months, but storage of powders in the semi-permeable packaging was terminated after 5 months due to extensive browning and clumping of the powders under these conditions (**Chapter 4**). GRE microencapsulated with inulin in a 1:1 ratio (m/m) (IN50) was selected for this study as it had the lowest degree of incompatibility based on isothermal microcalorimetry. The investigation of stability was crucial as complex formulations containing common beverage ingredients such as sugars and organic acids, which are deliquescent crystalline materials, are very sensitive to moisture (Stoklosa, Lipasek, Taylor & Mauer, 2012).

This, in addition to interaction of ingredients with each other, could result in various unwanted reactions which could adversely affect the stability (Jones & Jew, 2007).

Xylitol, a naturally occurring sugar-alcohol, was used as it has a lower energy value compared to sucrose (10.0 vs 16.7 kJ/g) (Islam, 2011). In addition, xylitol is suitable for consumption by diabetics and has prebiotic effects as reviewed by Ur-Rehman, Mushtaq, Zahoor, Jamil & Murtaza (2015). This is ideal for the use in a functional iced tea formulation aimed at the prevention of the metabolic syndrome, in particular type 2 diabetes, also linked to obesity. Xylitol can, however, exert gastrointestinal disturbances and is not usually recommended for use in beverages (Makinen, 2016), but, as stated in **Chapter 4**, the consumption of 20 g xylitol, as would be delivered in a 330 mL serving (normal size of a can of carbonated drink), is not expected to cause gastrointestinal disturbances (Storey, Lee, Bornet & Brouns, 2007). The likeliness of this will be further reduced since, for efficient α-glucosidase inhibition by GRE (Miller *et al.*, 2018), the rooibos iced tea will be recommended for consumption with a meal in order to prevent spiking of post-prandial blood glucose levels (Makinen, 2016). However, its effect on the stability of the formulated powder product still required investigation. The addition of xylitol instead of sucrose significantly increased the rate of dihydrochalcone degradation (similar results obtained for aspalathin and its 3-deoxy derivative, nothofagin) in the shelf-life trials, indicating that a compromise would have to be made between stability and energy value. Xylitol was possibly not the best alternative for sucrose and other low energy sweeteners such as stevia should be investigated in future. Stevia is usually perceived with a significant bitter aftertaste. However, a honeybush iced tea formulation containing 40 g/L xylitol and 0.02 g/L stevia was accepted by an informal sensory panel (De Beer *et al.*, 2018), indicating that combinations of stevia and other sweeteners could be a viable option, which would further lessen the likelihood of gastrointestinal disturbances (13.2 g/330 mL vs 19.8 g/330 mL). Furthermore, Chranioti, Chanioti & Tzia (2016) showed that the bitter taste can be decreased by encapsulation. In addition to these considerations, stevia is perceived as being up to 200 times sweeter than xylitol or glucose (Torres, Raymundo & Sousa, 2013). This would completely change the ratio of ingredients in the formulation and subsequent effects of this would also have to be investigated. Furthermore, the shelf-life trials revealed higher aspalathin stability for IN50 than GRE, indicating that microencapsulation did indeed increase aspalathin stability under normal storage conditions, resolving any uncertainty of the results obtained with accelerated storage (**Chapter 3**). When IN50 is present in the formulated powder product containing other food ingredients, notably citric acid monohydrate, higher aspalathin instability, more discolouration and clumping were observed. The pronounced detrimental effect of citric acid monohydrate was likely due to its dehydration (Apelblat, 2014), increasing the moisture content of the other ingredients, accelerating physical and chemical changes. The

changes observed were accelerated at the higher temperature (40 °C vs 30 °C) and exposure to moisture as a result of the semi-permeability of the sachets, when the samples were stored at 65% RH. Changes in the aroma of the formulated product were also observed when samples were opened for analyses. A short storage trial was therefore executed to confirm this. The formulation containing IN50, xylitol and citric acid was stored for 1 month at 30 °C and 40 °C in both semi-permeable (sachets) and impermeable (sealed glass vials) packaging. Descriptive sensory analysis by a trained panel with extensive experience in sensory analysis of herbal teas, including rooibos, confirmed significant changes in the sensory profile of the powder when reconstituted to beverage strength (1.75 g extract/L). Storage in semi-permeable packaging resulted in the development of more favourable aroma attributes, such as the characteristic 'fruity-sweet' aroma associated with fermented rooibos tea (Koch, Muller, Joubert, Rijst & Næs, 2012; Jolley, Van der Rijst, Joubert & Muller, 2017). Viljoen, Muller, De Beer & Joubert (2017) found that South African consumers prefer rooibos iced teas with sensory attributes typical to fermented rooibos and dislike 'plant-like' attributes associated with green rooibos iced tea. However, as indicated in this study, the typical rooibos attributes are likely linked to a low aspalathin content and even though more acceptable to consumers, it is unacceptable for an iced tea formulation aimed at prevention of metabolic syndrome. Thus, instead of allowing the iced tea formulations to develop these typical aroma attributes of fermented rooibos tea, a formulation containing extracts of both fermented and green rooibos would be an option as found by Viljoen *et al.* (2017). The stability of such a mixture needs to be investigated as different matrix effects, discussed in a later section, could be relevant. In summary, these results indicated that in order to produce more stable rooibos iced tea powders, addition of thermodynamically unstable crystalline ingredients should be avoided if possible, while lower storage temperatures (30 °C) and minimal exposure to moisture (impermeable packaging) is of utmost importance.

This study provided valuable insight into the behaviour of GRE in iced tea powder formulations, interaction between ingredients and storage conditions required for optimum shelf-life. Furthermore, it confirmed that such a product is more stable, with respect to aspalathin, than RTD iced tea formulations. A study by De Beer *et al.* (2011) on green rooibos RTD formulations (*ca.* 20% aspalathin), containing similar ingredients, found that only 67% of aspalathin was retained after 8 weeks of storage at 25 °C, whereas in the current study up to 87% aspalathin could be retained in the dry powder iced tea formulations stored in impermeable packaging at 30 °C for 2 months (*ca*. 8 weeks). Even after 24 weeks 67% of aspalathin was retained in the most unstable formulation. However, ideally, formulations containing exactly the same extract and ingredients should be stored under the same conditions for direct comparison. Aspalathin degradation in a dry powder product can be further decreased by separating the powdered nutraceutical green rooibos ingredient (in this study, IN50)

from the crystalline ingredients, as the powders which contained crystalline ingredients showed significantly more aspalathin degradation (15.31–27.44%) compared to IN50 alone (1.85%), under the same storage conditions. Considering this, a type of packaging material such as the 'Gizmo Closure and Delivery System' (Anonymous, 2018b) where IN50 is stored in the bottle cap and the crystalline iced tea ingredients are in solution in the bottle itself, but only mixed with IN50 upon opening of the bottle, would be ideal for retaining as much as possible aspalathin. This would enable the production of a rooibos RTD iced tea containing high levels of aspalathin.

Nanoencapsulation was investigated as an alternative and more specialised approach for the production of an encapsulated rooibos nutraceutical extract. Even though micro- and nanoencapsulation both rely on encapsulation, they differ not only in particle characteristics and the technical aspects of production, but usually also in the end use of the encapsulated extract. In addition to stability, nanoencapsulation of GRE with specialised polymers could also address the stability of aspalathin as it passes through the gastrointestinal tract (GIT) and its absorption in the gut (Bilia, Isacchi, Righeschi, Guccione & Bergonzi, 2014).

Even though nanoencapsulation has various advantages, loading capacities for bioactive compounds are usually low, for example 5.7% for curcumin-PLGA particles (Xie *et al.*, 2011), 3.0–6.2% for hesperetin-lipid based particles (Fathi, Varshosaz, Mohebbi & Shahidi, 2012) and 8.0–16.0% for green tea-chitosan nanoparticles. (Liang *et al.*, 2011). In order to compensate for this, an aspalathin-rich fraction from green rooibos (GRAF, 40% aspalathin) was utilised instead of GRE to increase the loading of aspalathin in the nanoparticles. Higher loading capacities are not only required for lower dosages in the final product, but also to lower the amount of polymer in the final product due to limits set by the Food and Drug Administration (FDA) regulations, consumer acceptance and cost implications.

A number of polymers and methods were investigated for production of nanoencapsulated GRAF (**Chapter 5**)**.** Different polymers and methods for nanoencapsulation are seldom directly compared in the same study, often causing difficulty to select an optimum method/material combination for a specific bioactive. Two natural and two synthetic biodegradable polymers were selected based on their properties, the desired outcomes for the GRAF-loaded nanoparticles and their possible use in powdered iced tea formulations. All the selected polymers (chitosan, lecithin, poly(lactide-co-glycolide) (PLGA) and Eudragit S100 (ES100), a synthetic poly(methacrylic acid-co-methyl methacrylate) polymer) have sustained release profiles (Liang *et al.*, 2011; Adibkia *et al.*, 2011; Zhang, Nie & Wang, 2013; Jahangiri *et al.*, 2014), which could aid in the protection of aspalathin in the GIT as intended, but also during storage. For each polymer, a suitable conventional wet encapsulation method, which usually entails re-suspending the nanoparticles in an aqueous medium for

centrifugation and freeze-drying, was investigated. However, in literature these techniques are mostly applied to more hydrophobic extracts and compounds (Wang *et al.*, 2014). GRAF and aspalathin, being more hydrophilic, resulted in poor encapsulation, likely due to leaching into the surrounding aqueous medium. This effect was pronounced for the synthetic polymers due to lack of interaction between the hydrophilic compound and the hydrophobic polymers (Arulmozhi, Pandian & Mirunalini, 2013). In an effort to overcome this, electrospraying was investigated, which resulted in more efficient encapsulation. Electrospraying is a one step process, thus eliminating the possibility of leaching as the solidification and solvent evaporation occur in a single step (Zamani, Prabhakaran & Ramakrishna, 2013). Compared to conventional techniques, electrospraying requires very high voltages (10–40 kV), which might be viewed as a disadvantage due to operational costs. Currently electrospinned/sprayed products are employed in the biomedical industry as wound dressings, drug delivery vehicles as well as cell culture and tissue engineering scaffolds (Anonymous, 2018c).

Overall, GRAF-loaded ES100 electrosprayed nanoparticles had the best combination of properties, i.e. high encapsulation efficiency (EE) and product yield, which relates to the cost and efficiency of the process, high loading capacity (LC) (i.e. lower dosages required), small particle size and smooth, uniform particle morphology, which could help with the ease of absorption in the human body (Bilia *et al.*, 2014). In addition, ES100 is designed to have a targeted release profile at pH ≥ 7 (McGinity & Felton, 2008). This slow delayed release profile at pH 7.4 is ideal for delivery of aspalathin unchanged into the small intestine, the most likely site of absorption (Kreuz, Joubert, Waldmann & Ternes, 2008). Additionally, even though the targeted release profile of Eudragit was designed for GIT purposes, theoretically, GRAF should remain encapsulated at lower pH and thus is potentially suitable for fortification of rooibos RTD iced teas with pH < 4. In practice, this was not the case, as up to 75% of GRAF was released at pH 4 within 8 h, likely due to the hydrophilic nature of aspalathin, matrix type of encapsulation and some degree of swelling of the polymer at this pH. Another option would be to investigate alternative encapsulation techniques such as co-axial electrospraying, where the bioactive (core) is entrapped inside the polymer (shell), rather than dispersed in it (Zamani *et al.*, 2013).

Even though ES100 electrosprayed particles proved to have the best combination of properties, the electrospraying process is governed by various controllable process parameters. Thus, to ensure that the optimal particle properties were achieved, a quality-by-design (QbD) approach, employing a design of experiments and response surface methodology, was followed (**Chapter 6**)**.** Process parameters were varied according to a central composite design (CCD), which has the advantage of requiring a relatively small number of experiments for optimisation (Bezerra, Santelli, Oliveira, Villar & Escaleira, 2008). The responses measured

were the product yield, particle size, polydispersity index (PDI), EE and LC, but only the yield, EE and LC were optimised. Practically, it was futile to optimise the PDI, since all the particles within the experimental range could be classified as polydisperse (Stetefeld, McKenna & Patel, 2016). In addition, the polynomial regression equation showed a poor fit for particle size, due to the small range of particle sizes obtained. However, for the selected experimental range, all the particle sizes (<260 nm) were in the nanorange.

Additionally, pure aspalathin was also nanoencapsulated for the first time. A slightly higher loading capacity of pure aspalathin, 13.8% compared to 12.2 % for GRAF (equalling 5.9% aspalathin) was achieved when conditions were optimised. Increased aspalathin loading, due to purity, combined with a postulated increased *in vivo* stability and absorption, both advantages of nanoencapsulation (Xiao, Cao & Huang, 2017), would mean less nanoparticles are required to elicit an effect. Investigation of aspalathin stability when in nanoparticles subjected to different pH-time combinations specific to the orogastrointestinal tract indicated that the nanoparticles could possibly improve aspalathin stability in the GIT tract, resulting in more aspalathin reaching the small intestines and colon. Interestingly, nanoencapsulated pure aspalathin was less stable than when aspalathin was present in the extract, likely due to matrix effects as previously demonstrated for various polyphenols in vegetal extracts from spruce bark and grape seeds (Volf, Ignat, Neamtu & Popa, 2014). This indicated that a compromise would have to be made between the dosage and stability during delivery. Formulations with higher aspalathin content and thus dosage efficiency should be subjected to *in vivo* tests to confirm efficacy and elucidate any adverse effects. Van der Merwe, De Beer, Joubert & Gelderblom (2015) showed in two sub-chronic studies of 28 days and 90 days in rats that fortification of their feed with an aspalathin-enriched green rooibos extract (18% aspalathin) resulted in altered expression of antioxidant related genes and subtle disruption of liver function. Abrahams, Samodien, Lilly, Joubert & Gelderblom (2018) using the same extract found expression of genes involved in energy, alcohol and steroid metabolism in the liver to be modulated. Their *in vitro* study in rat hepatocytes demonstrated a dose dependent effect. These studies imply that the dose and duration of exposure to polyphenol-enriched extracts should be carefully monitored.

No change in the passive permeability of aspalathin according to the parallel artificial membrane permeability assay (PAMPA) was achieved by nanoencapsulation, implying that even though more aspalathin will reach the gut if nanoencapsulated, intestinal absorption due to passive membrane diffusion will not be increased compared to pure aspalathin or aspalathin present in GRAF. Given the nanoscale of the particles, and the hydrophobic nature of both the encapsulating polymer and membrane (structured phospholipid layers), an increase in passive permeability was expected. However, other factors such as the large PDI and swelling

of the polymer at pH 7 could also likely prevent absorption, emphasising the many considerations in such a delivery design. The PAMPA model only provides information on the passive permeability of a bioactive compound. The effect of nanoencapsulation of aspalathin and GRAF using ES100 was therefore also determined using the Caco-2 intestinal model, as this includes both passive and active permeability (Chen, 2008). However, no increase was achieved for the apparent permeability of pure aspalathin and GRAF when nanoencapsulated, showing that nanoencapsulation also did not improve the active permeability of aspalathin. A recent review highlighted the important role of phenolic compounds in the composition of the gut microbiome, indicating that intestinal absorption is not always required for health benefits (Ercolini & Fogliano, 2018). Thus, rooibos/aspalathin nanoparticles with a targeted delivery to the gut, as prepared in the current study, could be more significant if utilised for this aim. However, further testing in this direction would be required.

The study successfully increased the stability of aspalathin by microencapsulation in order to produce a green rooibos nutraceutical ingredient. The study indicated that delivery in a dry, powder form is essential to achieve long-term shelf-life for aspalathin in green rooibos iced powders, presenting a challenge to the food industry for commercialization. Advanced packaging options such as the patented 'Gizmo Closure and Delivery System' (Anonymous, 2018b), where the functional ingredient is released from a modified bottle cap into the solution when the cap is turned, could also be considered. It not only has the advantage of delivering the dry powder, but ingredients that could accelerate degradation of aspalathin could be added to the solution while the nutraceutical ingredient is stored dry in the cap.

Nanoencapsulation with a targeted release polymer offered a method to not only produce a powdered green rooibos nutraceutical ingredient, but also increase stability under simulated GIT conditions. Various studies have shown increased stability of polyphenols when in nanoparticles, as reviewed by Ezhilarasi, Karthik, Chhanwal & Anandharamakrishnan (2013). Future investigations should include the storage stability of the GRAF loaded nanoparticles with regard to temperature and moisture. In addition, the *in vivo* effects of GRAF loaded nanoparticles with increased GIT stability and higher aspalathin content should be investigated in terms of α-glucosidase inhibition (Miller *et al.*, 2018), ability to enhance glucose uptake (Johnson et al., 2018) and modulation of the gut microbiota, amongst others. Other options for future work could be to investigate the fortification of a microencapsulated green rooibos iced tea powder with aspalathin nanoparticles, as this could potentially increase the aspalathin dosage, stability, and gastrointestinal stability simultaneously.

References

Abrahams, S., Samodien, S., Lilly, M., Joubert, E. & Gelderblom, W. (2018). Differential modulation of gene expression encoding hepatic and renal xenobiotic metabolizing enzymes by an aspalathin-enriched rooibos extract and aspalathin. *Planta Medica*, DOI 10.1055/a-0656-7500.

Adibkia, K., Javadzadeh, Y., Dastmalchi, S., Mohammadi, G., Niri, F. K. & Alaei-Beirami, M. (2011). Naproxen-Eudragit® RS100 nanoparticles: Preparation and physicochemical characterization. *Colloids and Surfaces B: Biointerfaces,* 83, 155–159.

Anonymous (2018a). Flexifoil packaging: Barrier properties of films. URL http://www.flexifoilpackaging.com/barrier-properties-films. Accessed 04.06.18.

Anonymous (2018b). Gizmo packaging: Tea of a kind project. URL https://www.gizmoclosures.com/. Accessed 28.06.18.

Anonymous (2018c). Stellenbosch Nanofibre company homepage. URL https://sncfibers.com/. Accessed 20.07.18.

Apelblat, A. (2014). Properties of citric acid and its solutions. In: *Citric Acid*. Pp. 13–141. Switzerland: Springer International Publishing.

Arulmozhi, V., Pandian, K. & Mirunalini, S. (2013). Ellagic acid encapsulated chitosan nanoparticles for drug delivery system in human oral cancer cell line (KB). *Colloids and Surfaces B: Biointerfaces,* 110, 313–320.

Augustin, M. A. & Hemar, Y. (2009). Nano- and micro-structured assemblies for encapsulation of food ingredients. *Chemical Society Reviews,* 38, 902–912.

Aulton, M. E. (1996). Pharmaceutics: The science of dosage form design. Pp. 1–725. New York: Churchill Livingstone.

Bezerra, M. A., Santelli, R. E., Oliveira, E. P., Villar, L. S. & Escaleira, L. A. (2008). Response surface methodology (RSM) as a tool for optimization in analytical chemistry. *Talanta,* 76, 965–977.

Bilia, A. R., Isacchi, B., Righeschi, C., Guccione, C. & Bergonzi, M. C. (2014). Flavonoids loaded in nanocarriers: an opportunity to increase oral bioavailability and bioefficacy. *Food and Nutrition Sciences,* 5, 1212–1327.

Chen, X. K. (2008). PAMPA: Novel BD Gentest™ pre-coated PAMPA plate system with high Caco-2 and human absorption predictability. URL: https://www.bdbiosciences.com/documents/webinar_2008_08_PAMPA101.pdf. Accessed 17.10.17.

Chranioti, C., Chanioti, S. & Tzia, C. (2016). Comparison of spray, freeze and oven drying as a means of reducing bitter aftertaste of steviol glycosides (derived from *Stevia rebaudiana* Bertoni plant) – Evaluation of the final products. *Food Chemistry,* 190, 1151–1158.

Corbo, M. R., Bevilacqua, A., Petruzzi, L., Casanova, F. P. & Sinigaglia, M. (2014). Functional beverages: The emerging side of functional foods. *Comprehensive Reviews in Food Science and Food Safety,* 13, 1192–1206.

De Beer, D., Joubert, E., Viljoen, M. & Manley, M. (2011). Enhancing aspalathin stability in rooibos (*Aspalathus linearis*) ready-to-drink iced teas during storage: the role of nano-emulsification and beverage ingredients, citric and ascorbic acids. *Journal of the Science of Food and Agriculture,* 92, 274–282.

De Beer, D., Malherbe, C. J., Beelders, T., Willenburg, E. L., Brand, D. J. & Joubert, E. (2015). Isolation of aspalathin and nothofagin from rooibos (*Aspalathus linearis*) using high-performance countercurrent

chromatography: Sample loading and compound stability considerations. *Journal of Chromatography A,* 1381, 29–36.

De Beer, D., Pauck, C. E., Aucamp, M., Liebenberg, W., Stieger, N., Van der Rijst, M. & Joubert, E. (2018). Phenolic and physicochemical stability of a functional beverage powder mixture during storage: effect of the microencapsulant inulin and food ingredients. *Journal of the Science of Food and Agriculture,* 98, 2925–2934.

Dehghan, P., Gargari, B. P. & Jafar-Abadi, M. A. (2014). Oligofructose-enriched inulin improves some inflammatory markers and metabolic endotoxemia in women with type 2 diabetes mellitus: a randomized controlled clinical trial. *Nutrition,* 30, 418–423.

EMEA (2003). ICH Q1A Stability testing guidelines: Stability testing of new drug substances and products. URL http://www.ich.org/fileadmin/Public_Web_Site/ICH_Products/Guidelines/Quality/Q1A_R2/Step4/Q1A_R2__Guideline.pdf. Accessed 13.10.17.

Ercolini, D. & Fogliano, V. (2018). Food design to feed human gut microbiota. *Journal of Agricultural and Food Chemistry,* 66, 3754–3758.

Ezhilarasi, P. N., Karthik, P., Chhanwal, N. & Anandharamakrishnan, C. (2013). Nanoencapsulation techniques for food bioactive components: A review. *Food and Bioprocess Technology,* 6, 628–647.

Fathi, M., Varshosaz, J., Mohebbi, M. & Shahidi, F. (2012). Hesperetin-loaded solid lipid nanoparticles and nanostructure lipid carriers for food fortification: Preparation, characterization, and modeling. *Food and Bioprocess Technology,* 6, 1464–1475.

Gharsallaoui, A., Roudaut, G., Chambin, O., Voilley, A. & Saurel, R. (2007). Applications of spray-drying in microencapsulation of food ingredients: An overview. *Food Research International,* 40, 1107–1121.

Gibbs, B. F., Kermasha, S., Alli, I. & Mulligan, C. N. (1999). Encapsulation in the food industry: A review. *International Journal of Food Sciences and Nutrition,* 50, 213–224.

Hofman, D. L., Van Buul, V. J. & Brouns, F. J. P. H. (2016). Nutrition, health, and regulatory aspects of digestible maltodextrins. *Critical Reviews in Food Science and Nutrition,* 56, 2091–2100.

Islam, M. S. (2011). Effects of xylitol as a sugar substitute on diabetes-related parameters in nondiabetic rats. *Journal of Medicinal Food,* 14, 505–511.

Jahangiri, A., Davaran, S., Fayyazi, B., Tanhaei, A., Payab, S. & Adibkia, K. (2014). Application of electrospraying as a one-step method for the fabrication of triamcinolone acetonide-PLGA nanofibers and nanobeads. *Colloids and Surfaces B: Biointerfaces,* 123, 219–224.

Johnson, R., De Beer, D., Dludla, P. V., Ferreira, D., Muller, C. J. F. & Joubert, E. (2018). Aspalathin from rooibos (*Aspalathus linearis*): A bioactive *C*-glucosyl dihydrochalcone with potential to target the metabolic syndrome. *Plant Medica,* 84, 568–583.

Jolley, B., Van der Rijst, M., Joubert, E. & Muller, M. (2017). Sensory profile of rooibos originating from the Western and Northern Cape governed by production year and development of rooibos aroma wheel. *South African Journal of Botany,* 110, 161–166.

Jones, P. J. & Jew, S. (2007). Functional food development: concept to reality. *Trends in Food Science & Technology,* 18, 387–390.

Joubert, E. & De Beer, D. (2011). Rooibos (*Aspalathus linearis*) beyond the farm gate: From herbal tea to potential phytopharmaceutical. *South African Journal of Botany,* 77, 869–886.

Joubert, E. & Schulz, H. (2006). Production and quality aspects of rooibos tea and related products. A review. *Journal of Applied Botany and Food Quality,* 80, 138–144.

Joubert, E., Viljoen, M., De Beer, D., Malherbe, C. J., Brand, D. J. & Manley, M. (2010). Use of green rooibos (*Aspalathus linearis*) extract and water-soluble nanomicelles of green rooibos extract encapsulated with ascorbic acid for enhanced aspalathin content in ready-to-drink iced teas. *Journal of Agricultural and Food Chemistry,* 58, 10965–10971.

Joubert, E., Viljoen, M., De Beer, D. & Manley, M. (2009). Effect of heat on aspalathin, iso-orientin, and orientin contents and color of fermented rooibos (*Aspalathus linearis*) iced tea. *Journal of Agricultural and Food Chemistry,* 57, 4204–4211.

Koch, I. S., Muller, M., Joubert, E., Rijst, M. V. d. & Næs, T. (2012). Sensory characterization of rooibos tea and the development of a rooibos sensory wheel and lexicon. *Food Research International,* 46, 217–228.

Koeppen, B. H. & Roux, D. G. (1965). Aspalathin: a novel *C*-glycosyl flavonoid from *Aspalathus linearis*. *Tetrahedron Letters,* 6, 3497–3503.

Kolida, S. & Gibson, G. R. (2007). Prebiotic capacity of inulin-type fructans. *The Journal of Nutrition,* 137, 2503S–2506S.

Kreuz, S., Joubert, E., Waldmann, K. & Ternes, W. (2008). Aspalathin, a flavonoid in *Aspalathus linearis* (rooibos), is absorbed by pig intestine as a *C*-glycoside. *Nutrition Research,* 28, 690–701.

Liang, J., Li, F., Fang, Y., Yang, W., An, X., Zhao, L., Xin, Z., Cao, L. & Hu, Q. (2011). Synthesis, characterization and cytotoxicity studies of chitosan-coated tea polyphenols nanoparticles. *Colloids and Surfaces B: Biointerfaces,* 82, 297–301.

Makinen, K. K. (2016). Gastrointestinal disturbances associated with the consumption of sugar alcohols with special consideration of xylitol: Scientific review and instructions for dentists and other health-care professionals. *International Journal of Dentistry,* 2016, 5967–5907.

Markens, U. (2009). Stability studies-recent changes to climatic zone IV. URL http://www.sgs.com/~/media/Global/Documents/Technical%20Documents/SGS%20Stability%20Studies-EN-09.pdf. Accessed 13.10.17.

McGinity, J. W. & Felton, L. A. (2008). Aqueous polymeric coatings for pharmaceutical dosage forms. Pp. 1–475. Florida: CRC Press.

Miller, N., De Beer, D., Aucamp, M., Malherbe, C. J. & Joubert, E. (2018). Inulin as microencapsulating agent improves physicochemical properties of spray-dried aspalathin-rich green rooibos (*Aspalathus linearis*) extract with α-glucosidase inhibitory activity. *Journal of Functional Foods,* 48, 400–409.

Miller, N., De Beer, D. & Joubert, E. (2017). Minimising variation in aspalathin content of aqueous green rooibos extract: optimising extraction and identifying critical material attributes. *Journal of the Science of Food and Agriculture,* 97, 4937–4942.

Muller, C. J. F., Malherbe, C. J., Chellan, N., Yagasaki, K., Miura, Y. & Joubert, E. (2018). Potential of rooibos, its major *C*-glucosyl flavonoids, and *Z*-2-(β-D-glucopyranosyloxy)-3-phenylpropenoic acid in prevention of metabolic syndrome. *Critical Reviews in Food Science and Nutrition,* 58, 227–246.

Nedovic, V., Kalusevic, A., Manojlovic, V., Levic, S. & Bugarski, B. (2011). An overview of encapsulation technologies for food applications. *Procedia Food Science,* 1, 1806–1815.

Shoaib, M., Shehzad, A., Omar, M., Rakha, A., Raza, H., Sharif, H. R., Shakeel, A., Ansari, A. & Niazi, S. (2016). Inulin: Properties, health benefits and food applications. *Carbohydrate Polymers,* 147, 444–454.

Stetefeld, J., McKenna, S. A. & Patel, T. R. (2016). Dynamic light scattering: a practical guide and applications in biomedical sciences. *Biophysical Reviews,* 8, 409–427.

Stoklosa, A. M., Lipasek, R. A., Taylor, L. S. & Mauer, L. J. (2012). Effects of storage conditions, formulation, and particle size on moisture sorption and flowability of powders: A study of deliquescent ingredient blends. *Food Research International,* 49, 783–791.

Storey, D., Lee, A., Bornet, F. & Brouns, F. (2007). Gastrointestinal tolerance of erythritol and xylitol ingested in a liquid. *European Journal of Clinical Nutrition,* 61, 349–354.

Torres, M. D., Raymundo, A. & Sousa, I. (2013). Effect of sucrose, stevia and xylitol on rheological properties of gels from blends of chestnut and rice flours. *Carbohydrate Polymers,* 98, 249–256.

Ur-Rehman, S., Mushtaq, Z., Zahoor, T., Jamil, A. & Murtaza, M. A. (2015). Xylitol: a review on bioproduction, application, health benefits, and related safety issues. *Critical Reviews in Food Science and Nutrition,* 55, 1514–1528.

Van Boekel, M. A. J. S. (1996). Statistical aspects of kinetic modeling for food science problems. *Journal of Food Science,* 61, 477–486.

Van Boekel, M. A. J. S. (2008). Kinetic modeling of food quality: A critical review. *Comprehensive Reviews in Food Science and Food Safety,* 7, 144–158.

Van der Merwe, J. D., De Beer, D., Joubert, E. & Gelderblom, W. C. (2015). Short-term and sub-chronic dietary exposure to aspalathin-enriched green rooibos (*Aspalathus linearis*) extract affects rat liver function and antioxidant status. *Molecules,* 20, 22674–22690.

Viljoen, M., Muller, M., De Beer, D. & Joubert, E. (2017). Identification of broad-based sensory attributes driving consumer preference of ready-to-drink rooibos iced tea with increased aspalathin content. *South African Journal of Botany,* 110, 177-183.

Volf, I., Ignat, I., Neamtu, M. & Popa, V. (2014). Thermal stability, antioxidant activity, and photo-oxidation of natural polyphenols. *Chemical Papers,* 68, 121–129.

Wang, S., Su, R., Nie, S., Sun, M., Zhang, J., Wu, D. & Moustaid-Moussa, N. (2014). Application of nanotechnology in improving bioavailability and bioactivity of diet-derived phytochemicals. *Journal of Nutritional Biochemistry,* 25, 363-376.

Xiao, J., Cao, Y. & Huang, Q. (2017). Edible nanoencapsulation vehicles for oral delivery of phytochemicals: A perspective paper. *Journal of Agricultural and Food Chemistry,* 65, 6727–6735.

Xie, X., Tao, Q., Zou, Y., Zhang, F., Guo, M., Wang, Y., Wang, H., Zhou, Q. & Yu, S. (2011). PLGA nanoparticles improve the oral bioavailability of curcumin in rats: Characterizations and mechanisms. *Journal of Agricultural and Food Chemistry,* 59, 9280–9289.

Yao, H.-T. & Chiang, M.-T. (2006). Effect of chitosan on plasma lipids, hepatic lipids, and fecal bile acid in hamsters. *Journal of Food and Drug Analysis,* 14, 183–189.

Zamani, M., Prabhakaran, M. P. & Ramakrishna, S. (2013). Advances in drug delivery via electrospun and electrosprayed nanomaterials. *International Journal of Nanomedicine,* 8, 2997–3017.

Zhang, J., Nie, S. & Wang, S. (2013). Nanoencapsulation enhances epigallocatechin-3-gallate stability and its antiatherogenic bioactivities in macrophages. *Journal of Agricultural and Food Chemistry,* 61, 9200–9209.